Innovative Pharmaceutical Stabilization and Formulation Techniques for Protein Drugs

Dissertation

zur

Erlangung des Doktorgrades (Dr. rer. nat.)

der

Mathematisch-Naturwissenschaftlichen Fakultät

der

Rheinischen Friedrich-Wilhelms-Universität Bonn

vorgelegt von

Katharina Dauer

aus

Nastätten

Bonn 2023

Angefertigt mit Genehmigung der Mathematisch-Naturwissenschaftlichen
Fakultät der Rheinischen Friedrich-Wilhelms-Universität Bonn

1. Gutachter: Prof. Dr. Karl Gerhard Wagner
2. Gutachter: Prof. Dr. Alf Lamprecht

Tag der Promotion: 29.11.2023
Erscheinungsjahr: 2023

PUBLICATIONS

This dissertation is based on the previously published book chapter and articles listed below:

Book chapter:

- K. Dauer, J. Kozak, A. Lamprecht, K.G. Wagner*: Innovative Pharmaceutical Stabilization and Formulation Techniques for Protein Drugs and Their Influence on Sequence and Structure – Part: Process*, Springer, 2023

Articles (peer-review):

- K. Dauer, K. Kayser, F. Ellwanger, A. Overbeck, A. Kwade, H.P. Karbstein, K.G. Wagner: *Highly protein-loaded melt extrudates produced by small-scale ram and twin-screw extrusion - evaluation of extrusion process design on protein stability by experimental and numerical approaches,* International Journal of Pharmaceutics: X, 2023
  DOI: 10.1016/j.ijpx.2023.100196

- K. Dauer and K.G. Wagner: *Micro-scale Vacuum Compression Molding as a Predictive Screening Tool of Protein Integrity for Potential Hot-Melt Extrusion Processes*, Pharmaceutics, 2023, 15(3), 723
  DOI: 10.3390/pharmaceutics15030723

- K. Dauer, C. Werner, D. Lindenblatt, K.G. Wagner: *Impact of process stress on protein stability in highly-loaded solid protein/PEG formulations from small-scale melt extrusion*, International Journal of Pharmaceutics: X, 2022, 5, 100154
  DOI: 10.1016/j.ijpx.2022.100154

Further articles published and conference participations are listed below:

Articles (peer-review):

- Y.Y. Elsayed, T. Kühl, K. Dauer, A. Sayin, K.G. Wagner, D. Imhof: *Bioanalytical workflow for qualitative and quantitative assessment of hot-melt extruded lysozyme formulations*, ACS Omega, 2022, 7 (45), 40836-40843
  DOI: 10.1021/acsomega.2c03559

- Á. López Mármol, A. Denninger, A. Touzet, K. Dauer, T. Becker, F. Pöstges, Y. Pellequer, A. Lamprecht, K.G. Wagner: *The relevance of supersaturation and solubilization in the gastrointestinal tract for oral bioavailability: An in vitro vs. in vivo approach,* International Journal of Pharmaceutics, 2021, 603
  DOI: 10.1016/j.ijpharm.2021.120648.

- K. Dauer, W. Kamm, K. G. Wagner, S. Pfeiffer-Marek: *High-Throughput Screening for Colloidal Stability of Peptide Formulations using Dynamic and Static Light Scattering,* Molecular Pharmaceutics, 2021, 18, 5, 1939–1955
  DOI: 10.1021/acs.molpharmaceut.0c01028

- K. Dauer, W. Kamm, S. Pfeiffer-Marek, K. G. Wagner: *Microwell Plate-Based Dynamic Light Scattering as a High-Throughput Characterization Tool in Biopharmaceutical Development*, Pharmaceutics, 2021, 27;13(2),172
  DOI: 10.3390/pharmaceutics13020172

Abstracts (Conference participation):

- K. Dauer, and K. G. Wagner: *Impact of process stress on protein stability in highly-loaded solid protein/PEG formulations from small-scale melt extrusion,* DPhG International PhD Student / Postdoc Meeting, Bonn 2023
  (poster presentation)

- K. Dauer, and K.G. Wagner: *Solid-State Stabilization of Proteins in Highly-Loaded Melt Extrudates – Characterization of Protein Integrity*, AAPS 2022 PHarmSCi 360, Boston 2022
  (poster presentation)

- K. Dauer, and K.G. Wagner: *Investigation on the influence of small-scale ram and twin-screw extrusion on protein integrity*, APV Workshop on Protein Aggregation and Immunogenicity, Basel Area 2022
  (poster presentation)

- K. Dauer, and K.G. Wagner: *Protein integrity in highly loaded melt extrudates processed by small scale ram and twin-screw extrusion*, 13th World Meeting on Pharmaceutics, Biopharmaceutics and Pharmaceutical Technology, Rotterdam 2022
  (oral presentation)

- K. Dauer, S. Pfeiffer-Marek, W. Kamm, K. G. Wagner: *Application of Stability Screening Tools for Protein Formulation Development*, 12th World Meeting on Pharmaceutics, Biopharmaceutics and Pharmaceutical Technology, Online 2021
  (poster presentation)

- K. Dauer, S. Pfeiffer-Marek, W. Kamm, K. G. Wagner: *Biophysical characterization methods to assess the stability of formulated protein-based drugs*, DPhG-Annual Meeting, Heidelberg 2019
  (poster presentation)

TABLE OF CONTENT

LIST OF ABBREVIATIONS

%	percentage
°C	degrees Celsius
AA	amino acids
API	active pharmaceutical ingredient
ASD	amorphous solid dispersion
AUC	analytical ultracentrifugation
BSE	backscattered electron
BSA	bovine serum albumin
CD	circular dichroism
cIEF	capillary isoelectric focusing
CQA	critical quality attribute
CV	coefficient of variation
D	dimensional
DIA	dynamic image analysis
DLS	dynamic light scattering
DSC	differential scanning calorimetry
DSF	differential scanning fluorescence
EDX	energy-dispersive X-ray
EVA	ethylene-*co*-vinyl acetate
FD	freeze-drying
FIM	Flow imaging microscopy
FTIR	Fourier transform infrared
GIT	gastrointestinal tract
HEWL	hen egg white lysozyme
HME	hot-melt extrusion
HMWS	high molecular weight species

IEX	ion-exchange
i.m.	intramuscular
i.v.	intravenous
L/D	length to diameter ratio
LVR	linear viscoelastic range
MRT	mean residence time
MS	mass spectrometry
M_w	molecular weight
[PCL-PEG]-*b*-[PCL]	poly(ε-caprolactone-PEG)-*block*-poly(ε-caprolactone)
PEG	polyethylene glycol
PEO	polyethylene oxide
PLGA	Poly(D,L-lactic-*co*-glycolic acid)
rpm	revolutions per minute
RP-HPLC	reversed-phase high performance liquid chromatography
RTD	residence time distribution
s.c.	subcutaneous
SD	spray-drying
SDS-PAGE	sodium dodecyl sulfate polyacrylamide gel electrophoresis
SEC	size-exclusion chromatography
SEM	scanning electron microscopy
SFD	spray-freeze drying
SLI	solid lipid implant
SLS	static light scattering
SME	specific mechanical energy
ss	solid-state
T_c	collapse temperature
TSE	twin-screw extrusion

TTS	time-temperature superposition
USP	United States Pharmacopeia
VA	vinyl acetate
VCM	vacuum compression molding
w/w	weight by weight (%)

1 INTRODUCTION

The biopharmaceutical sector is steadily increasing, focusing on the development of peptide- and protein-based drugs into stable biopharmaceutical products for the medical treatment of especially severe and chronic diseases (e.g., cancer, multiple sclerosis, diabetes mellitus, migraine) [1]–[3]. Biopharmaceuticals are composed of either peptides, proteins, and glycoproteins or a combination of biomolecules, including (monoclonal) antibodies (mAbs), antibody-drug conjugates, recombinant proteins, nanobodies, enzymes, hormones, vaccines, and gene therapy products, etc. [4], [5]. Since 1986 to date, there are 621 FDA-licensed biologics products (U.S. Food and Drug Administration), including more than 250 recombinant therapeutic proteins or peptides for clinical use [6], [7]. The Boston Consulting Group showed in a position paper of 2022 that sales in biopharmaceutical products have achieved approximately EUR 17.8 billion in Germany, representing approximately one third of the entire pharmaceutical market. Moreover, 37 biopharmaceutical products were approved in Germany in 2022 [8]. However, the formulation and administration of pharmacologically relevant proteins and peptides has hitherto been mostly limited to the parenteral administration of solutions or liquid dosage forms by intravenous (i.v.), intramuscular (i.m.), or subcutaneous (s.c.) injection [9]. The parenteral application is often the only option due to a lack of protein stability in the gastro-intestinal tract (GIT) [10]. Once a protein reaches GIT e.g., by an oral application, the digestion of proteins begins in the stomach by the secretion of gastric juice. The gastric juice mainly consists of water, mucus, hydrochloric acid, and pepsin. The enzyme pepsin is responsible for breaking down the polypeptide chain of the protein into smaller chains of amino acids (AA) by N-terminal cleavage [11]. The oral delivery of peptide- and protein-based drugs faces thus an immense challenge, since the GIT acts as a physical and biochemical barrier for absorption of proteins resulting in low bioavailability of less than 1 to 2 % [12], [13]. Apart from bioavailability, the protein stability issues also need to be considered when evaluating alternative formulations and modes of administration. In particular, alternatives for the often painful parenteral route via non-invasive routes such as solids for peroral, nasal, transdermal administration, or inhalation would significantly expand or improve the therapeutic use and the compliance of protein-based drugs [14]–[16]. From a formulation point of view, many biologics are not stable in liquid formulations due to protein degradation resulting in a limited shelf life of the biopharmaceutical product even when the product is stored under refrigerated conditions [17]. Common protein degradation pathways

are further described in section 1.3. Exubera®, a rapid-acting insulin using a pulmonary inhaler for application was a marketed solid protein formulation [18], [19]. From a patient's point of view, solid protein formulations such as Exubera® offer a huge advantage when it came to storage of the biopharmaceutical product. In contrast to liquid formulations, Exubera® insulin blisters could be stored at room temperature for 12 months and did not need refrigeration as compared to the conventional insulin products on the market (e.g., liquid insulin in a pen, or pump for s.c. administration) [20]. These aspects highlight the need of solid protein formulations since alternative administration routes (e.g., oral, transdermal, nasal, pulmonary, etc.) provide the opportunity for long-term protein release and minimize the pain associated with multiple or daily s.c., i.m., or i.v. administration. At the same time solid biopharmaceutical products reduce storage and handling efforts in general and for the patients in daily life due to the improved stability in the solid state [20]–[22]. The spray-dried amorphous powder insulin formulation Exubera® was withdrawn from the US-market in 2007 after it was only available for a year mainly for commercial reasons [23]. Despite the withdrawal of a solid biopharmaceutical product like Exubera®, the development of alternative solid protein formulations (e.g., protein-loaded extrudates or implants) as well as encapsulation procedures that employ dehydrated protein powders due to improved protein stability remain of interest [24]. Conventional and promising techniques (e.g., by hot-melt extrusion (HME), spray-drying (SD), freeze-drying (FD), or spray-freeze drying (SFD)) for the production of solid protein- and peptide-based formulations are discussed in sections 1.4.2 and 1.5. A special focus is paid on the implementation of scalable formulation technologies for the production of solid dosage forms of proteins and peptides with enhanced protein stability [24]–[28].

1.1 ORDERS OF PROTEIN STRUCTURE

Proteins are large macromolecules comprising one or more AA chains that fold into various 3D structures to exert a specific biologic or enzymatic function [29]. This specific functionality of proteins is highly dependent on the conformational protein structure. The final conformational structure of a protein adopted by any polypeptide chain is generally determined by energetic considerations, namely when the free energy is minimized [30]. The specific protein structure is based on four levels: (i) primary, (ii) secondary, (iii) tertiary, and (iv) quaternary structure [31]. The primary structure of a protein is comprised of a linear AA chain, where AAs are linked together

through peptide bonds to form a polypeptide chain. The next higher order structure (i.e., secondary structure) is formed by the polypeptide chains that are stabilized by hydrogen bonds between the carbonyl oxygen atom (O) of one AA and the amino hydrogen atom (H) of another AA. These hydrogen bonds are responsible for the formation of alpha(α)-helices and beta(β)-sheets (Figure 1) [30]. In the case of an α-helix, the pattern of bonding pulls the polypeptide chain into a helical structure that looks like a curled ribbon, whereas a β-pleated sheet appears as a sheet-like structure held together by hydrogen bonds [32]. The tertiary structure defines the 3D shape of a protein and is based on interactions between the side chains of the polypeptide backbone (e.g., formation of disulfide bridges) [30]. Only some proteins show a quaternary structure (e.g., antibody molecules and hemoglobin), where two or more polypeptides may bond together [33], [34].

1.2 MODEL PROTEINS

Some popular proteins, peptides, or antibodies are available for pharmaceutical research and have emerged as models for the investigation on protein structure and function.

Insulin (M_w = 5.8 kDa) is a therapeutically relevant blood glucose-reducing peptide hormone for the treatment of insulin-dependent diabetes mellitus [35], consisting of two peptide chains (A- (21 AAs) and B-chain (30 AAs) that are covalently linked by two inter-chain disulfide bonds (A7-B7 and A20-B19) and one intra-chain linkage in the A-chain (A6-A11) (Figure 1A) [36]–[38]. The three disulfide bonds are essential for the specific overall structure and thus the receptor binding activity of insulin [36]. The secondary structure of an insulin monomer is composed of three α-helices, a short β-strand, and β-turns [38], [39]. Patients with the autoimmune disease type 1 diabetes mellitus or patients with type 2 diabetes mellitus when oral antidiabetic agents fail to provide adequate glycemic control, are dependent on the s.c. administration of insulin via injection, pen, or insulin pump [40], [41].

The compact globular protein **lysozyme** (14.3 kDa) consists of one polypeptide chain, 129 AAs and is cross-linked by four intramolecular disulfide bonds (Figure 1B) [42]. The secondary structure of lysozyme is composed of four α-helices, three β-sheet structures, a large amount of random coils and β-turns, and a short helical structure [43], [44]. Moreover, lysozyme is an ideal model for studying protein behavior due to its highly stable 3D structure [45]. Lysozyme is a bacteriolytic enzyme that cleaves

the β(1→4)-glycosidic bond between *N*-acetylmuramic acid (MurNAc) and *N*-acetyl-D-glucosamine (GlcNAc) in the polysaccharide that forms the backbone of bacterial cell walls [46]. Therefore, most lysozyme activity assays exploit this activity and are based on the *Micrococcus lysodeikticus* lysis and the decrease in optical density over time measured by turbidity [47].

Bovine serum albumin (BSA), which comprises a single-chain midsize globular protein composed of 583 AAs with a molecular weight of approximately 66.5 kDa, has been widely investigated as a model protein in several research fields [48]–[50]. The secondary structure of BSA consists of 67 % α-helical structures with 6 turns, and 8 disulfide bridges without any β-sheets (Figure 1C) [51], [52]. The native BSA is generally present in solution in the form of native monomers with small amounts of oligomers (i.e., dimers, trimers, etc.). Alteration in the ratio of monomer to dimer, or the occurrence of trimers or oligomers can be used for monitoring of process-related effects on the BSA structure integrity [53], [54].

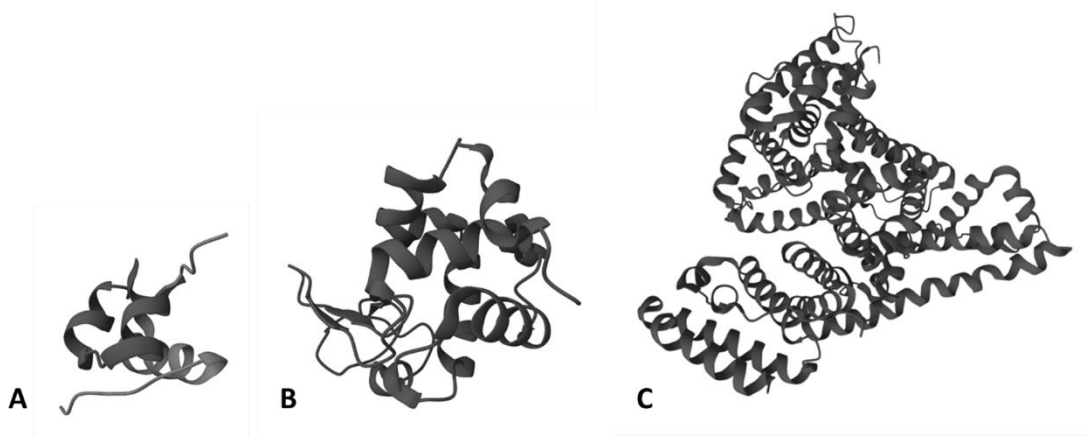

Figure 1 Crystal structures of **A** human insulin; **B** chicken egg white lysozyme; **C** bovine serum albumin.

1.3 ANALYTICAL CHARACTERIZATION AND PROTEIN STABILITY IN FORMULATION DEVELOPMENT AND DRUG DELIVERY

Liquid protein formulations exhibit generally a higher risk for degradation during the lifecycle of a biopharmaceutical product (e.g., manufacturing, formulation development, processing, storage, shipping, clinical use) compared to dried protein formulations [17], [55], [56]. This is mainly related due to the higher mobility of protein molecules in solution, protein-protein and protein-solvent interactions, and thus resulting in an increased probability of chemical reactions and physical instabilities [55], [57], [58]. Even in the solid state a protein can undergo spontaneous degradation

during formulation, manufacturing, storage, and clinical use [59], [60]. In general, degradation can be classified in chemical and physical instability [61] and remains the bottleneck for the formulation of protein-based therapeutics. Degradation pathways for protein-based drugs can involve chemical instability: oxidation, deamidation [62], [63], hydrolysis [64], isomerization [65], beta-elimination [62], racemization [65], and/or, disulfide exchange [66]), while physical instability presents itself via: denaturation, surface adsorption [62], fibrillation [17], [39], precipitation [62], fragmentation, and/or aggregation [62], [63], [67].

The most prominent physical protein instability is the formation of protein aggregates, subvisible, or even visible particles that seriously impacts the shelf life (protein stability) and protein functionality (safety, efficacy) [68]–[70]. Protein aggregates are formed between two or more monomers [71] while retaining their native structure or being miss- or unfolded and can occur at any point throughout the lifetime of a protein and even during administration of a biopharmaceutical product [17], [72]. The formed aggregates can lead to an increased solution viscosity [73]–[75], injection force [76] and thus show potential immunogenicity implications due to reports of undesired effects (e.g., formation of anti-drug antibodies in the organism) [61]. Hence, the control of any undefined aggregates in a protein formulation is essential prior to its parenteral administration [69]. Protein denaturation is also a commonly observed physical instability and is mainly caused by high temperature-induced changes of the protein secondary structure [51]. Thermal energy alters the intramolecular bonds of the protein, resulting in unfolding of the polypeptides. In the denatured state these weak interactions are disrupted, leading to the loss of the structures and the biological function [77].

The general aim of biopharmaceutical characterization is to identify critical process parameters and critical material attributes that are affecting the protein stability and thus the efficacy, purity, and safety of biopharmaceutical products, i.e., essential critical quality attributes (CQAs). The stability of peptide- and protein-based drugs and drug products can be negatively affected by: (i) temperature or mechanical stress, (ii) moisture, (iii) prolonged storage, (iv) denaturants, surfactants, preservatives, or other excipients, (v) organic solvents, (vi) oxygen, (vii) changes in pH levels, etc. [78]–[80]. Therefore, a well-established and characterized manufacturing process, effective in-process controls, and understanding the chemical and physical instabilities that can emerge throughout product processing are essential in

minimizing protein instabilities [61]. Any aberrations in the CQAs of biopharmaceutical products can be evaluated using various analytical and characterization methods.

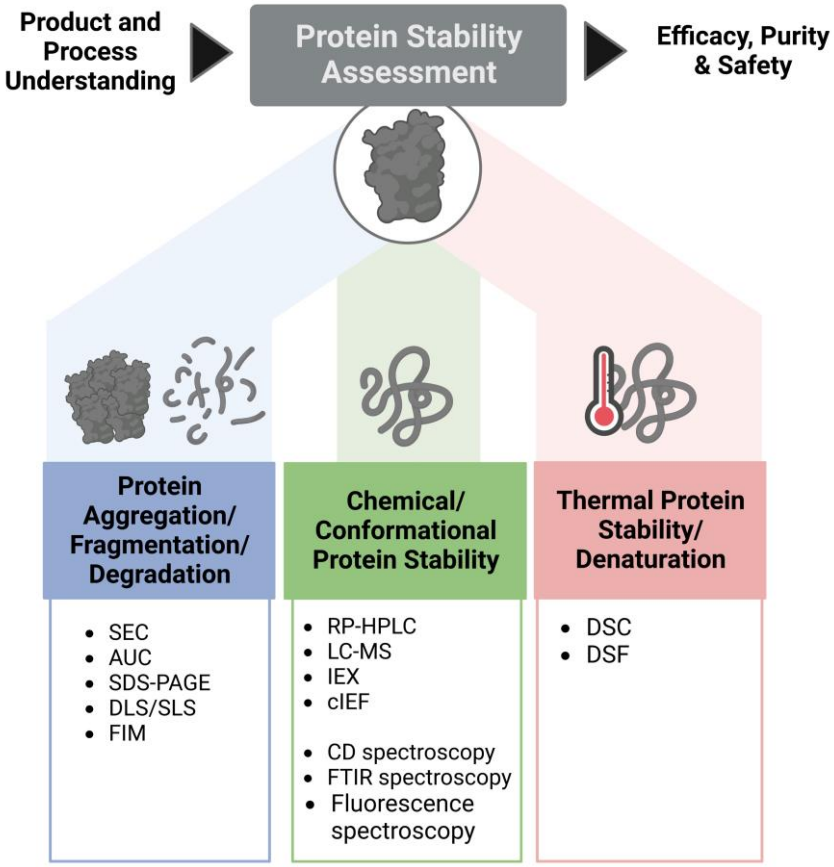

Figure 2 Overview on methods used to determine and assess protein stability: protein aggregation/ fragmentation/ degradation (blue), chemical/ conformational protein stability (green), and thermal protein stability/ denaturation (red).

The necessity for a rational analytical toolbox for determination and characterization of a protein (e.g., structural, biological, and physico-chemical characteristics) in various stages of formulation development is of crucial importance [17], [81]. Most of the analytical methods applied during protein formulation development studies focus on the investigation and characterization of proteins in solution or lyophilized proteins after their reconstitution [82]–[85]. Figure 2 shows orthogonal and complementary analytical techniques to assess product CQAs and to characterize protein aggregates, fragments, degradation products, the chemical, conformational and thermal protein stability, and protein denaturation behavior [60]. As protein degradation products or aggregates compromise the safety and efficacy of a therapeutic protein due to an enhanced risk of immunogenicity, monitoring and controlling protein stability is essential, especially in regard of aggregates and fragments [80], [86]. For this, size-exclusion chromatography (SEC), analytical ultracentrifugation (AUC), and SDS-

PAGE are used, particularly when the protein forms oligomers, or higher molecular weight species (HMWS) [87]–[89], while flow imaging microscopy (FIM) is available for studying the formation of micrometer-sized protein aggregates [90]–[92]. Dynamic and static light scattering (DLS/SLS) enables the detection of nanometer size protein aggregates [87], [88]. Methods for conformational analysis mainly includes circular dichroism (CD), Fourier transform infrared (FTIR), and intrinsic or extrinsic fluorescence spectroscopy [64], [88], [93]. Chromatographic methods such as reversed-phase (RP) HPLC/UPLC, (HPLC-)mass spectrometry, IEX chromatography and (capillary) isoelectric focusing (cIEF) can be used for the analysis of chemical changes, or chemical degradation products (impurities) [88], [94]. DSC (differential scanning calorimetry) and DSF (differential scanning fluorescence) are commonly used techniques for the evaluation of the thermal stability of a protein (e.g., unfolding temperature) [93], [95].

1.4 PROTEIN FORMULATION

The biopharmaceutical products are marketed either as liquid or solid dosage form and refrigerated storage (2 to 8 °C) of especially liquid protein formulations is a standard prerequisite [78], [96]. Protein stabilization in solution is often achieved by a mature combination of various formulation excipients and stabilizing agents [97]. These well-developed liquid formulations for a given protein are often a result of a material-, time-, and resources-demanding pre-development program [98]. Occasionally it is not feasible to develop a sufficiently stable, liquid protein formulation and the focused initial development strategy fails to meet the target product requirements [3]. Obligatory drug product-specification requirements for a liquid biopharmaceutical formulation in a vial include: (i) subvisible particles, (ii) visible particles, (iii) extractable volume, and (iv) sterility [99]. Since liquid protein formulations are more susceptible to protein instability mechanisms than in the dried state, it is recommended to use suitable drying techniques (Figure 3), such as FD, SD, or SFD for the immobilization of the protein molecules in a solid matrix system [27], [100], [101]. Despite, proteins in the solid state are consequently less prone to degradation, conventional solid protein formulations have to be mainly reconstituted by patients or medical staff to obtain an applicable product for parenteral administration routes like s.c., i.m., or i.v. injection [100], [102]. Alternative solid implantable devices or implants without the need of reconstitution prior administration are described in section 1.5.1.

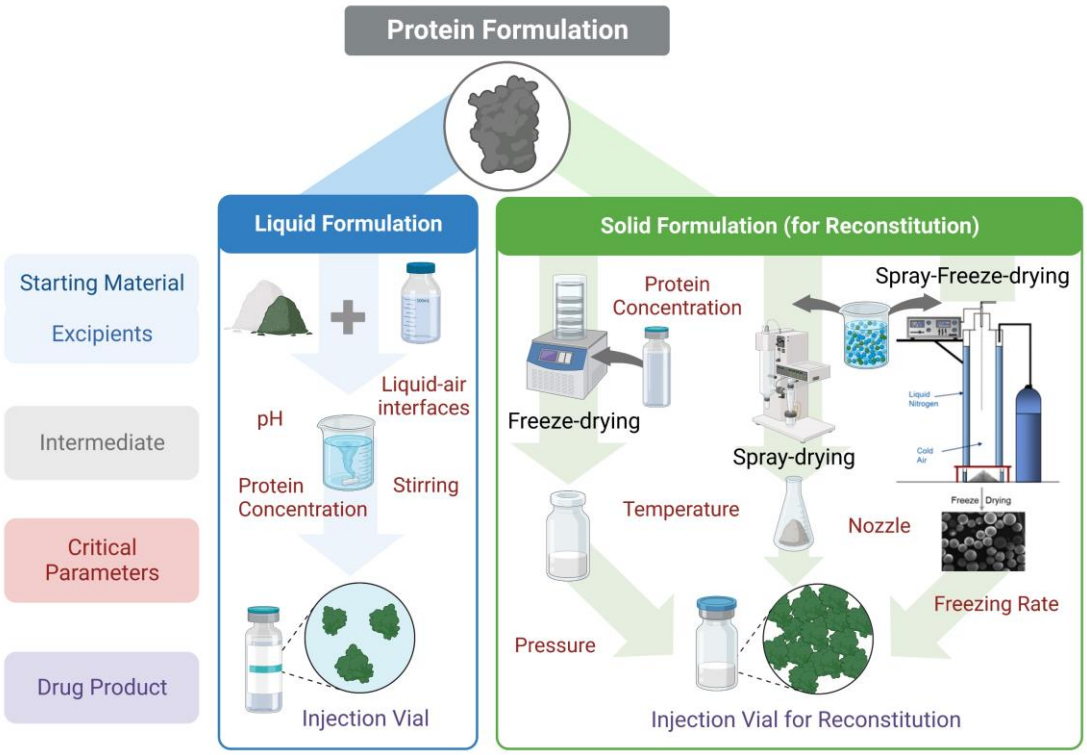

Figure 3 Schematic diagram of injectable, parenteral protein formulation development; procedure of liquid protein formulation development in blue and solid protein formulation development in green; critical parameters (red) affecting protein stability and drug product quality.

1.4.1 PROTEIN STABILIZATION IN LIQUID FORMULATIONS

In the case of liquid formulations, protein stabilization in solution can be achieved by addition of various excipients to the final formulation [56], [67]. As shown in Table 1, excipients are “pharmacologically non-active” substances which are added to formulations for a specific purpose (e.g., preservation, isotonization, enhancing stability or solubility, reducing viscosity and filling or dilution) [103], [104]. Possible excipients can range from simple buffer systems to more complex components such as preservatives, surfactants, and other stabilizing agents [67], [105].

Table 1 List of commonly used excipients in formulation development of liquid protein formulations

Category of excipient	Purpose	Excipient examples	References
Buffer systems	Maintaining acceptable formulation pH level	Acetic acid, Bis-tris, citrate, histidine, phosphate, succinate, TRIS	[67], [105]–[108]

Tonicity agents	Adjusting osmolality to physiologically acceptable levels (isotonic solutions)	Salts: sodium chloride, sodium sulfate Non-electrolytes: glycerol, mannitol	[58], [109]–[112]
Surfactants	Preventing aggregation and unwanted adsorption by surface tension reduction	Polysorbate 20, polysorbate 80, poloxamer 188	[113]–[118]
Preservatives	Ensuring sterility/ preventing microbial growth during shelf life	*m*-cresol, benzyl alcohol, phenol	[117], [119], [120]
Amino acids	Stabilizing proteins most likely by preferential exclusion	Arginine, histidine, lysine	[121]–[126]

Identifying the optimal formulation conditions for a designated protein or peptide candidate is often achieved by trial-and-error approaches during pre-development studies [127], [128]. A mechanistic understanding of how excipients work for a given protein candidate is often lacking and thus studying the interaction of excipients with proteins is the key to rational and successful stabilization of biopharmaceuticals [105], [110].

1.4.2 PROTEIN STABILIZATION IN SOLID FORMULATIONS

In comparison, liquid protein formulations typically exhibit a shelf life of 24 months, while the dried and mostly lyophilized protein formulations usually exhibit an extended shelf life of 36 to 48 months [3]. As water plays a crucial role in protein degradation and unfolding, the shelf life and thermal stability of proteins can be markedly enhanced by transformation from a liquid to a solid state due to vitrification and water replacement theory (Figure 4) [129]–[131]. Biopharmaceuticals are typically stored below their glass transition temperature (T_g) where the protein and other solutes are concentrated into a highly viscous amorphous, glassy matrix [132]. When a biopharmaceutical product is stored above its T_g (e.g., when a cooling system during transportation is defective, or when the T_g of the system is lowered to temperatures below the storage temperature by moisture transfer to the product) a collapse of the solid protein formulation can occur [133]. The mechanism of collapse upon processing or storage is described in more detail in section 1.4.2.2. Recently published studies have shown that the addition of polyols (e.g., glycerol and sorbitol) at low levels to protein formulations enhance the storage stability by reducing the local mobility of the

protein molecules, although polyols have often low T_gs and thus are expected to destabilize the protein by lowering the T_g of the matrix and increasing mobility [134], [135]. Excipients, such as polyols are thus promising protein stabilizers and offer the possibility to obtain ambient temperature storage stability where refrigeration is no longer required [134]. Circumventing the cold chain by developing solid protein formulations may thus significantly reduce the costs of storage and shipping, and improve the availability of biopharmaceutical products in tropical areas [136]. All drying technologies pursue the same target – removal of water. Removal of water can be performed using (i) an evaporation mechanism, (ii) evaporation and atomization pathways (e.g., in SD), or (iii) sublimation mechanisms (e.g., in FD or SFD) [101]. However, the applied drying technologies may introduce process-related degradation to the proteins including (i) aggregation, (ii) unfolding, (iii) denaturation, (iv) deamination, and (v) oxidation [134] and proteins can lose their structure and functionality upon exposure to (i) atomization, (ii) dehydration, (iii) thermal, (iv) freezing, (v) interfacial and/or (iv) shear stress during drying [101]. Upon removal of water, the protein requires stabilization by a rational selection of excipients to preserve the structural and functional protein integrity against process-induced degradation (Table 2).

Table 2 List of commonly used excipients as stabilizers during drying procedures in formulation development of solid protein formulations (modified from **[101]**)

Category of excipient	Purpose	Excipient examples	References
Buffer systems	Maintaining acceptable formulation pH level	Citrate, HEPES, phosphate	[134], [137]
Polyols	Water replacement, glassy state, control of collapse temperature, lyoprotectants, cryoprotectants	Mannitol, polyethylene glycol, sorbitol	[59], [134], [138]–[141]
Carboanhydrates		Dextran, fructose, glucose, lactose, maltose, sucrose, trehalose	
Surfactants	Preventing surface adsorption by interfacial stress reduction, preventing protein-protein interactions	Polysorbate 20, polysorbate 80	[82], [101], [142]–[144]

Polymers and Polysaccharides	Glassy state	Cyclodextrin, Na-carboxy methylcellulose, PLGA, polyvinylpyrrolidone (PVP)	[139], [145]–[147]
Amino acids	Water replacement, preventing protein-protein interactions	Alanine, arginine, glycine, histidine, leucine, phenylalanine	[134], [138], [147]

The “water replacement theory” (thermodynamic stabilization) and the “glassy matrix hypothesis” (kinetic stabilization) are the most common stabilization pathways (Figure 4) [101], [131]. The water replacement theory is based on the removal of water as reactant during drying and the substitution of solvent molecules by excipients with functional hydroxyl groups, such as carboanhydrates, polyols, or amino acids [59], [101]. The subsequent substitution of water molecules by excipient formed hydrogen bonds ensures the 3D protein structure (i.e., anhydrobiosis) [141]. The hydrogen bonds formed between protein and excipient molecules are responsible for an enhanced robustness of the protein against dehydration stress due to an increase of the free energy of unfolding by the hydrogen bonds and thus resulting in protein stabilization in the solid state [131], [148].

The second mechanism of protein stabilization in the solid state is based on the formation of an amorphous glass matrix (also called “vitrification”) [131]. Excipients such as polyols, polysaccharides, and polymers, can form a rigid, glassy matrix that acts like an envelope and presumably shields the protein from abiotic stresses [101]. The global mobility of protein molecules is drastically decreased due to an embedding of the molecules in the solid glassy matrix [141]. This protein immobilization results in a slowdown of potential protein-protein interactions, protein unfolding, or other degradations, and thus in an increased stability of the proteins [131], [134], [149].

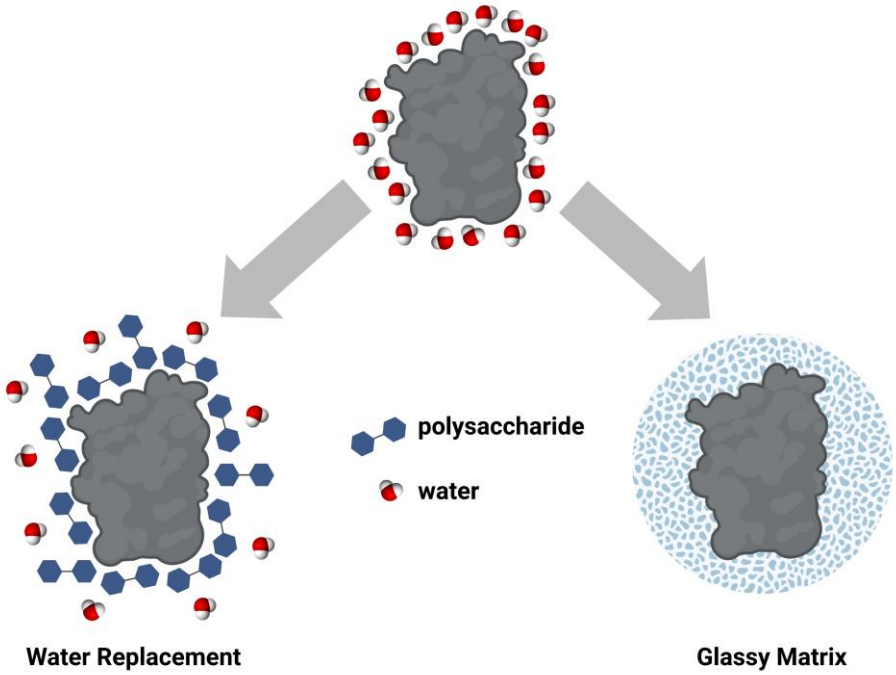

Figure 4 Theories of protein stabilization by excipients; left: Water is substituted during drying by excipients (water replacement theory); right: Excipients can form a glassy matrix around the protein (glassy matrix hypothesis/ vitrification).

1.4.2.1 SPRAY-DRYING (SD)

SD is a well-established continuous particle engineering process that has been successfully used to produce hollow particles with smooth or dimpled surfaces [150]. The SD process is generally divided into the following phases: (i) Liquid atomization, (ii) droplet drying, and (iii) powder particle separation [101]. In the case of protein formulation, SD enables rapid drying of a protein-excipient solution atomized in a nozzle, which is placed inside the drying chamber for forming fine droplets into a hot air stream [19], [146]. The end product – dried powder particles are separated from the hot air stream, typically using a cyclone (Figure 3) [101]. SD can be used as a beneficial single-step process leading to short processing times and thus enabling an application for the continuous manufacturing of biopharmaceutical products [146], [151]. Compared to FD, SD is a favored alternative due to its (i) evaporative cooling, (ii) lower energy consumption, (iii) good process control and scale-up opportunities, and (iv) lower operational costs [150]. The process controllability and adjustability is determined by the variability in (i) protein concentration, (ii) feeding flow rate, (iii) flow rate of hot air, and (vi) inlet temperature [101], [129]. The major drawbacks of commonly used techniques such as SD to formulate or encapsulate proteins in solid state in general are (i) the higher residual moisture of the powder particles, (ii) generated shear and temperature stress during spraying, and the (iii) exposure to

air-liquid interfaces [150]. The thermal stress (reported for inlet temperatures range from 70 to 220 °C [19], [152]–[154]) generated during SD and/or shear stress present at the outlet of the spray nozzle, may induce protein denaturation and aggregation and/or loss of activity [155]. On the one hand, excipients can be incorporated to stabilize the spray-dried protein and on the other hand to engineer the properties of the dry powder formulation (e.g., particle size, particle morphology, solubility) [101], [156]. The mechanism of stabilization of polysaccharides and polymers against the thermal stress generated during SD is based on the glassy matrix hypothesis and prevents exposure of the protein to the drying medium interface or hot atmosphere [101], [141], [155]. However, phase separation of polymers or the crystallization of other excipients and formulation components during SD may lead to denaturation or the formation of protein aggregation [157]–[159].

1.4.2.2 FREEZE-DRYING / LYOPHILIZATION (FD)

Lyophilization, also known as FD, is the most widely used drying technology for biomolecules such as a wide range of hormones, enzymes, vaccines, antibodies, gene therapy products, etc. [78], [101]. As shown in Figure 3 for a lab-scale FD cycle, glass vials containing the desired volume of the liquid protein formulation are partially plugged and loaded into the drying chamber of the freeze dryer. The subsequent lyophilization process typically consists of three major steps: (i) Freezing, (ii) primary drying, (iii) secondary drying, and an optional reconstitution step [160]. In general, the stability of freeze-dried proteins is improved by vitrification and water replacement [70], [161]. During freezing, the temperature of the solution in the partially stoppered vials is lowered [81]. Freezing of the sample leads to an immobilization of solution components due to the formation of an ice-crystal matrix [162]. Furthermore, the freezing step avoids foaming of the product when vacuum is applied by the followed primary drying step [129]. During primary drying, the ice will be removed from the frozen product by sublimation under vacuum [100]. During secondary drying, the temperature is increased to remove the absorbed water contained in the matrix by desorption to finally produce a dry product [129]. The dry product of a FD process is an intact, porous cake. Prior the application of a lyophilized biopharmaceutical product to a patient the dry powder cake has to be reconstituted into a solution by adding an appropriate solvent (mainly water for injection or saline) [163]. The United States Pharmacopeia (USP) defines the endpoint of a proper reconstitution procedure as the complete dissolution without any visible particulate or undissolved matter of the solid

cake after addition of the reconstitution liquid [164]. Lyophilization process parameters such as (i) freezing temperature and rate, (ii) drying temperature, and (iii) the formulation mainly affect the cake formation and properties and thus the reconstitution time of the FD cake [100]. A rapid reconstitution of protein lyophilizates is an important CQA [163]. However, compact lyophilization cakes, especially in the case of highly concentrated protein lyophilizates may require very long reconstitution times compared to free-flowing powders produced by alternative drying techniques such as SD, or SFD [165]. Hence, the required time for a thorough reconstitution can range from about 5 to more than 45 minutes and is dependent on process parameters and used excipients [163], [165]. Another advantage of freeze-dried proteins is the accurately dose, concentration and homogeneous distribution of the protein in the lyophilization cake [101]. Furthermore, FD enables controlling of the moisture content by adjusting the drying temperature and pressure and thus the freeze-dried proteins may contain 1 to 2 % of residual water after secondary drying [100], [166]. However, each step of the FD process entails the risk of damages of the protein structure due to induced (i) freezing, (ii) dehydration, and/or (iii) interfacial stress to the protein, (iv) changes in pH and ionic strength, or (v) ice crystal formation [17], [101]. In particular, the generated freezing and dehydration stress during FD may induce protein unfolding and the selection of excipients (e.g., cryoprotectants, and lyoprotectants) and process parameters, such as (i) freezing rate, (ii) protein concentration, (iii) cooling temperature, and (iv) drying pressure should be carefully considered to gain a stable, non-collapsed freeze-dried protein formulation [100], [101]. The collapse temperature (T_c) is a critical and the maximum acceptable product temperature during the primary drying step in FD [167], [168]. The solute system during primary drying remains amorphous and does not crystallize at the T_c and T_c is typically 1 to 3 °C above the T_g of the maximally freeze concentrated solution of an amorphous formulation [167], [169]. In the case of primary drying above the T_c, the lyophilization matrix begins to flow accompanied with a loss of structure in the dried region adjacent to the ice-vapor interface due to a glass transition in the amorphous product. The viscosity of the amorphous solute phase decreases as the temperature simultaneously increases resulting in a loss of the pore structure [167]. Such a collapse can occur either during the FD process or during subsequent storage and can negatively affect the cake appearance and stability of proteins due to high residual water [167], [169]. Therefore, it is of crucial importance to know the T_c of the designated formulation and to maintain the temperature of the product below the T_c

during the primary drying step [170]. Moreover, the T_c is highly dependent on the used type of excipient and the mass ratio of excipient-to-excipient and excipients-to-protein and drying above the T_c can lead to prolonged reconstitution times [101]. The use of crystalline bulking agents (e.g., mannitol and glycine) provides stable and fine cake structures, whereas formulations which contain only amorphous saccharides (e.g., sucrose), are prone to collapse upon the primary drying step [169]. This is contradicted by recently published works, that show that collapse during FD has no negative impacts on protein stability during storage at elevated temperatures when compared to non-collapsed cakes [171], [172], [133]. In some cases, defined collapse is even favored as due to well-conducted collapse drying, the same residual moisture as in elegantly dried cakes can be achieved [173]. Schersch et al. showed an improved long-term stability of protein formulations which were collapsed by using different amounts of excipients or by using different freeze-drying protocols [171], [172], [133]. FD can be generally time- and cost-consuming due to long processing times (i.e., two to three days) and the requirement of high energy resources, respectively [100]. In contrast, well conducted collapse drying can lead to an increased cake porosity and to significantly reduced primary drying times and energy costs due to the permission of higher vapor flow rates while the elegant cake structure can be maintained [174], [175]. In conclusion, FD is the gold standard for the production of solid protein formulations and the majority of marketed solid biopharmaceutical products are lyophilized (e.g., erythropoietin (NeoRecormon®), or mAbs such as Efalizumab (Raptiva®), Omalizumab (Xolair®), Mepolizumab (Nucala®)) [100], [163], [176].

1.4.2.3 SPRAY-FREEZE-DRYING (SFD)

SFD is besides FD and SD, another effective and versatile technique for converting protein solutions, or (nano)suspensions into dried particles [101]. SFD is a process that combines the advantages of SD (production of powder from liquids) with FD (i.e., heat-gentle drying, formation of highly porous rapidly dissolving product). The SFD process is divided into the following phases: (i) Droplet formation by spraying a solution through a nozzle, (ii) rapid freezing of liquids as fine droplets when sprayed into a chamber which is cooled down by cold air or liquid nitrogen, and (iii) freeze-drying of the frozen droplets by ice sublimation and thus final formation of dried particles [27], [177]. The (i) composition of the spray-solution or -suspension and use of excipients, (ii) the protein concentration, (iii) atomization and freezing rate, as well

as (iv) the temperature of the cryogenic liquid are decisive key parameters in determining the density and particle size distribution of SFD particles [178]. Compared to SD, the SFD results in porous and spherical microparticles with good flowability [101]. In contrast to the ultimately obtained dried cake in vials in case of lyophilization that require re-dissolution in an appropriate solvent before use, the produced microparticles by SFD enable a good and rapid reconstitution performance of the final product [177]. The combination of spraying of the liquid to fine droplets, freezing during descend, and freeze-drying gives the SFD product – microspheres in an achievable size range between 50 to 500 µm – some unique characteristics. Moreover, the SFD microparticles can be ideally used as a delivery platform enabling a large variety of therapeutic approaches that depend on the particle size (e.g., smallest SFD particles for pulmonary or nasal administration, or larger SFD particles for ophthalmic administration routes) [179]–[181]. SFD is a promising technique to produce free-flowing, rapidly-dissolving powder with narrow monomodal particle size distributions of small molecules or proteins for various therapeutic applications. The SFD was successfully applied in terms of an improved stability of processed model proteins (e.g., lysozyme, insulin, BSA, immunoglobulin G (IgG), calcitonin) [27], [28], [145], [182]–[184].

1.5 HOT-MELT EXTRUSION (HME)

The process of hot-melt extrusion (HME) is used in the pharmaceutical sector as continuous and robust manufacturing tool for the production of solid dosage forms and either focused on the development of new products or improving products already on the market [185], [186]. In the pharmaceutical industry, HME enables the formulation of poorly water-soluble small molecule drugs as so-called amorphous solid dispersions (ASD) with an improved solubility and bioavailability behavior of the active pharmaceutical ingredient (API) [186], [187]. Extrusion processes are classified in ram extrusion or screw extrusion [187]. Screw extruders can be divided in two general types: (i) Single-screw extruders (SSE) or (ii) twin-screw extruders (TSE), containing one or two rotating screws positioned inside a stationary barrel, respectively [186]. Furthermore, an extruder is basically composed of (i) a drive unit (motor), (ii) the stationary barrel, (iii) and the die [186]. In the HME process the drug-polymer-excipient mixture is intensively mixed at high shear rates induced by the extruder followed by melting, conveying and/or kneading producing extrudates of different shapes [187]. TSE provide the opportunity of dispersive and distributive

mixing [188], [189]. The powdered starting material is fed at constant feed-rate through a hopper into the feeding zone of the extruder barrel and transported to the subsequent zones by the turning motion of the screw along the barrel under pre-heating [190]. The temperature of the extruder barrel can be controlled by external heaters. This process of conveying introduces mixing and heat into the material through both external heaters and viscous heat dissipation [187]. The material flows through the barrel towards the die and experiences an unmolten, semi-molten, and molten state during processing [191]. In the case of ASD production, the crystalline drug is transformed into an amorphous state, dissolved or melted and dispersed in the surrounding stabilizing polymer matrix by applying thermal (i.e., extrusion temperatures of 130 to 160 °C) and mechanical (shear forces induced by screws) energy to a powdered material being processed [185], [192]. The fully molten material is discharged and cooled down resulting in respective extrudate strands (e.g., as drug delivery systems such as pellets, granules, implants, sustained release tablets) [193]. However, in the die zone of the extruder head pressure is developed, which is determined by several factors: (i) the molten blend viscosity, (ii) the flow rate of the molten blend, and (iii) the die temperature [194]. In general, HME processing offers various advantages for the manufacturing of solid dosage forms compared to other processing techniques. HME processing (i) is a solvent-free technique (e.g., without the use of organic solvents and thus eliminating time-consuming drying steps), (ii) can result in non-porous embedding of drugs at high loadings (up to 80 %) in polymeric matrices, (iii) eases the handling of highly potent APIs as it offers a closed system, (iv) requires no additional excipients such as surfactants or cryoprotectants, and (v) is scalable from lab- to pilot- to production-scale [195]–[198]. However, HME processing can exhibit also several limitations: (i) All formulation components must be thermally stable at the extrusion temperature during the short duration of the process, (ii) requirement of large batch sizes, which result in substantial amounts of drug substance and development costs, respectively, (iii) and it is a cost-intensive technology in terms of time, equipment, maintenance, and cleaning [187], [192], [199].

During ram extrusion, the powdered starting material is introduced into a pre-heated cylindrical barrel. After a melting time a driving piston pressurizes the molten material through the die and transforms the blend into the desired shape [25].

1.5.1 HOT-MELT EXTRUSION PRODUCTS WITH SUSTAINED RELEASE PROPERTIES

Some HME products with sustained-release properties are approved and can be administered via s.c., i.m., intravitreal (IVT) injection, etc. (Figure 5) [200], [201]. Conjunctival inserts (Ozurdex® as implant and Lacrisert® as tablet) are inserted into the intravitreal region by a surgery or are placed in the inferior or superior conjunctival fornix, respectively [201]. The inner arm implant Implanon® is a single-rod progestin-only contraceptive implant inserted subcutaneously using a special applicator [202]. The sustained release of the contraceptive etonogestrel incorporated in the non-biodegradable polymer EVA (ethylene-vinyl acetate) is then controlled for three years, after which the implant requires removal by a minor surgery [200]. The intravaginal ring (IVR) NuvaRing® is a co-extrudate composed of an inner core of EVA and the contraceptives etonogestrel and ethylvinyl estradiol [203]. The outer membrane is also composed of EVA but with a different VA content and thus enables a controlled release of the contraceptives over 21 days [204]. The NuvaRing® is self-administered once a month for contraception protection and thus does not require surgical intervention for removal [205]. Estring® is another hormonal IVR based on polydimethylsiloxane and is left in place for three months for the treatment of urogenital atrophy [206].

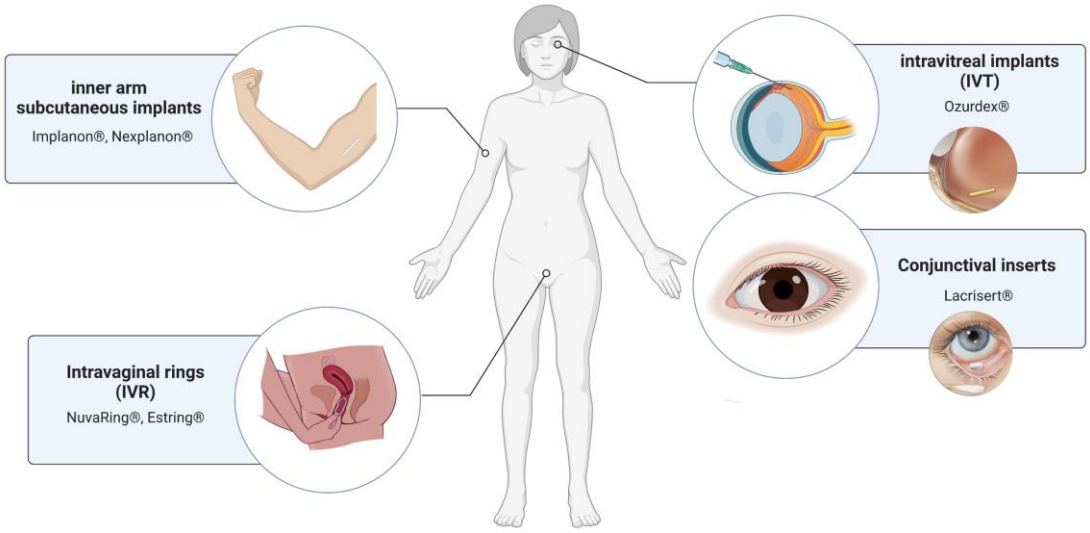

Figure 5 Overview on sites of FDA-approved implantable devices or implants; modified from **[200]** and **[201]**.

1.5.2 HOT-MELT EXTRUSION IN PROTEIN FORMULATION DEVELOPMENT

Nowadays, there is an increasing awareness to use HME for the production of solid protein formulations. Research in this field is continuing to expand the benefits of HME processing to sensitive biomolecules, such as peptides and proteins [185]. For

instance, HME processing can be used as protein solid-state stabilization approach or for the development of long-term release systems for parenteral administration (e.g., protein-loaded implants) [24], [207]–[209]. Liquid protein formulations or pre-filled syringes containing a freeze-dried protein which has to be reconstituted prior administration often require storage under refrigerated conditions at -20 to 8 °C to maintain the protein stability before administration [78].

Encapsulation of proteins within solid-state polymeric matrices can improve the thermal protein stability, may resulting in less stringent storage conditions (e.g., storage at room temperature) [209], [210]. The need of dry powder mixtures as starting material for the production of protein-loaded implants tends to be a major limitation of HME processing. However, the use of polymer powders as starting material in HME can be advantageous, since polymers as stabilizing excipients are not or difficult to be processed via SD or SFD either due to the rheological behavior of the spray solution that is strongly depended on the polymer and its concentration. Additionally, often no common solvent for protein and polymer is available [157]–[159]. Several authors report, that HME can be used as approach for the production of long-term protein delivery systems [24], [207], [208], [211]–[215], by embedding of the protein in dissolving or eroding polymer matrices, where the protein is slowly released by either diffusion or matrix erosion or a combination of erosion and diffusion [214]. At the same time the polymers are not only controlling the protein release but, contribute to an increased protein stability related to the solid state [207], [212]. Polymers can protect the thermodynamically stable folded structure of a protein after the melt extrusion process due to the immobilization of protein molecules in the solidified polymeric matrix (i.e., vitrification) [207], [216], [217].

A polymer of specific interest in combination with proteins is polyethylene glycol (PEG), a non-ionic, hydrophilic polymer. PEG is commonly used for liquid-liquid partitioning, precipitation of proteins, or protein stabilization in aqueous solutions. These applications make PEG by far the most widely used polymer in liquid protein formulations [218]. Recent studies suggest that stabilization of proteins in liquid-state can be achieved either by PEGylation, or addition of PEG-chains to proteins [21], [219], [220]. Covalently bonded to the protein PEG (physical PEGylation) increases half-life after parenteral application of a protein solution by size enlargement and subsequent slower renal elimination. The stabilization of insulin by PEGylation was successfully shown by shielding of the insulin monomeric structure, which is normally prone to fibrillation and aggregation [221]. Furthermore, several studies suggest that

long PEG-chains (e.g., PEG 20,000) present in a liquid formulation can stabilize proteins by interacting with the protein surface resulting in an effective volume that is inaccessible to solvent molecules in the solution (excluded volume effect). As a result, the unfolding rate of the protein is decelerated and thus PEG can consistently lead to an enhanced conformational protein stability and beneficial pharmacokinetic effects [222], [223]. It might be worth trying to extend the use of PEG as a matrix polymer for the solid-state stabilization of proteins. PEG would offer the possibility as model polymer due to its (i) low melting temperature (~60 °C, depending on the chain-length), (ii) hydrophilicity, and (iii) potential as protein stabilizer. Furthermore, higher molecular weight PEGs (also known as polyethylene oxide (PEO) depending on its molecular weight) offer an potential as matrix polymers for controlled release dosage forms and are commercially available in a broad variety of PEO grades and different molecular weights (e.g., 100,000, 300,000, 1,000,000) [219]. Another frequently used polymer for the production of long-term release systems is Poly-lactic-*co*-glycolic acid (PLGA). PLGA is composed of poly lactic acid (PLA) and poly glycolic acid (PGA) [224]. Due to the biodegradability and biocompatibility a surgically removing after protein delivery is not required. As the biodegradation rate of PLGA is depending on the molecular weight and the monomer ratio the degradation can be tailored and is reported to range from several weeks to several months. Higher content of PGA leads generally to faster biodegradation rates (e.g., 75:25 or 50:50 lactide to glycolide ratio results in biodegradation rates of less than 6 and 3 months, respectively). Moreover, PLGA is approved for clinical use in humans by the FDA [225]. EVA is a non-biodegradable polymer with an extended-release behavior of up to 2 years and can be used for the development of long-term releasing implants (Figure 5) [226]–[228]. The alteration of ethylene and vinyl acetate (VA) monomer ratios of EVA is used to control the release of several molecular weight drugs and can affect the crystallinity and thus the melt temperature of EVA [229]. The use of EVA in SD or SFD is limited as it is poorly soluble or even insoluble in frequently used solvents such as water, ethanol, methanol, n-butyl acetate, or mixtures thereof [19], [152], [227]. Fortunately, despite the limited EVA solubility in solvents like dichloromethane, it can be indeed easily used in HME processing to produce implantable sustained protein release systems due to the broad and low melting temperature of approximately 45 to 55 °C at 40 wt.-% VA and low melt viscosity of EVA [226], [227].

HME based development of implantable sustained protein release systems can be a promising alternative to repeated injections of liquid or solid protein formulations due

to a single administration of a protein-loaded implant [209], [217]. The main stress factors during hot-melt extrusion processes (i.e., elevated temperatures in combination with shear forces) potentially affect the protein integrity and consequently may cause protein degradation or activity loss and has to be considered during the entire process chain (Figure 6) [60], [230]. Whereas the production of ASDs containing small-molecule drugs is achieved at extrusion temperatures of 130 to 160 °C or higher, HME processing of protein-based drugs is limited to extrusion temperatures of less than 100 °C due to their fragile and thermolabile structure [24], [192].

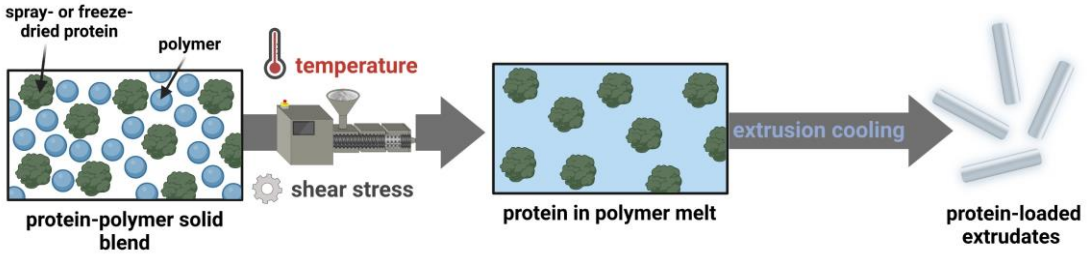

Figure 6 Schematic overview on HME processing for the production of protein-loaded implants; modified from **[209]**.

HME processing provides an embedding of high fraction of protein (i.e., > 40 % protein-load) into a polymer by vitrification compared to other formulation techniques.The use and availability of small-scale extruders is of crucial importance, as due to the cost of protein candidates, processing with commonly used 9- or 12-mm twin-screw extruders are not financially feasible [55]. Several studies have currently focused on the production of protein-loaded implants where model proteins and mAbs were embedded in polymeric or lipid-based matrices [24], [207], [208], [211], [212], [215], [231]–[233]. The numerous numbers of published works highlight the interest on using small-scale HME for the production of protein-loaded implants with improved protein stability, or long-term protein releasing behavior.

Cossé et al. [24] produced protein-loaded implants as sustained release systems by small-scale processing using 5- and 9-mm TSE. The HME process was downscaled to a small-scale 5-mm TSE (i.e., minimum batch size of 3 g), since the 9-mm TSE process required a minimum batch size of 10 g resulting in a high consumption of protein powder per batch [234]. The BSA-loaded implants based on PLGA as biodegradable polymer were characterized regarding their release properties and the *in vitro* release behavior of the embedded BSA. The study highlighted the feasibility of small-scale HME processing to obtain solid dispersions of a protein inside a

polymeric matrix providing sustained protein release. The sustained release of BSA from PLGA-based implants started after three weeks and was following after a low burst release phase. The work revealed that the incomplete release of BSA was depending on the interaction of PLGA degradation products such as mono- or oligomers and highlights that degradation properties of the polymeric carrier used are an essential factor to be considered in protein formulation development [24]. In conclusion, the protein release properties and protein stability during *in vitro* release from PLGA-based implants produced by HME are highly dependent on (i) excipients, (ii) protein loading, (iii) protein distribution, and (iv) protein surface properties [209]. Ghalanbor et al. [207] evaluated the suitability of HME processing for the manufacturing of protein-loaded PLGA implants and focused on the protein stability, burst release, and release completeness. They highlighted the great potential of HME for the production of protein-PLGA implants as the protein release from all implants achieved 100 % within 60 to 80 days maintaining nearly complete enzymatic activity of the formulated model protein lysozyme. Moreover, HME processing did not negatively affect the protein integrity. Furthermore, Ghalanbor et al. [211] used also BSA as model protein for the preparation of BSA-PLGA-implants by HME. The focus of this work was the investigation of potential mechanisms to explain the incomplete protein release over time. The release of BSA from PLGA-based matrix systems is often biphasic as an initial burst is followed by a slow and incomplete release. The initial burst release was avoided by 25 % BSA-load and by milling the protein prior extrusion. Consequently, the BSA release was increased up to 97 % by high-protein loads. The potential mechanism behind the incomplete release was explained by PLGA-protein interactions mediated by the free cysteine residues of the protein. This hypothesis was confirmed by the results of Cossé et al. [24] and further corroborated by previously published data of the working group [207] as the used lysozyme exhibits no free cysteine residue and lysozyme was completely released from the PLGA implants.

Stanković et al. [233] used novel, biodegradable phase-separated poly(ε-caprolactone-PEG)-*block*-poly(ε-caprolactone), [PCL-PEG]-*b*-[PCL]) multiblock copolymers with different block ratios and with a low melting temperature (49 to 55 °C) for the production of protein-loaded (e.g., goserelin, insulin, lysozyme, carbonic anhydrase, and albumin) implants by HME. Prior HME, the model proteins were spray-dried with inulin as stabilizer to obtain a protein powder of uniform particle size. The spray-dried protein powders were then incorporated into polymeric implants by

HME, whereby all proteins completely preserved their structural integrity as determined after extraction of the proteins from the polymeric implants. The work revealed, that the protein release rate increased with decreasing molecular weight of the proteins and with increasing the PEG content of the polymer [233].

Vollrath et al. [212], [213] introduced the production of solid lipid implants (SLI) containing 10 to 20 % either of a lyophilized mAb or a F_{ab}-fragment by small-scale TSE (5 mm) at 35 °C and 40 rpm. Protein release was observed as sustained over 120 days. The analytical investigation of the incubation media containing the released and concentrated proteins showed a monomer loss of up to 7 % for the mAb, and less than 5 % for the F_{ab}-fragment. FT-IR analysis revealed the formation of random coil structures towards the end of the release study for the mAb and no changes in secondary structure for the F_{ab}-fragment. The results underline the potential of SLIs as protein delivery system, especially where long-term release systems are absolutely required, for instance in the case of intraocular drug delivery [212], [213].

The works published so far are limited to the production of protein-loaded extrudates by small-scale HME and characterization of the implants in terms of protein stability, protein recovery, and protein release. A mechanistic understanding and investigation of how process parameters (e.g., type of extruder, feed-rate, residence time distribution) and process-related stress factors (thermomechanical stress profiles along the ram extruder or TSE barrel, or in the extruder die) affect protein stability, remain “black boxes”. A consistent feeding the powdered starting material is a critical step in HME as it enables a stable, reliable, and reproducible process. The used powdered starting material described in the literature was either manually fed into the small-scale extruders or the authors did not exactly mention how feeding was proceeded. Apart from these facts, the use of computational simulations to gain better HME process understanding and correlation of the simulation data with experimental results of protein stability was hitherto not considered.

2 AIMS AND SCOPE

Solid protein formulations for peroral, nasal or parenteral administration would significantly improve the therapeutic use, the compliance, and stability of protein-based drugs. The aim of this work was to develop, assess and apply innovative pharmaceutical stabilization and formulation techniques for protein drugs. A further objective was to assess the general suitability of small-scale melt extrusion approaches for the production of stable solid protein formulations. This thesis focused on hot-melt extrusion processing (ram and twin-screw extrusion) and vacuum compression molding as techniques for the production of solid protein-loaded extrudates or discs, respectively. The stabilization of model proteins and a peptide (i.e., lysozyme, BSA, human insulin, respectively) took place by embedding in dissolving or eroding polymer matrices (i.e., PEG 20,000, PLGA 50:50, EVA (40 % VA)). Although proteins in solid-state formulations exhibit an enhanced stability, the proteins can undergo denaturation, degradation, or aggregation during processing. Since a mechanistic formulation development strategy is based on an extensive knowledge of the physicochemical peptide and protein stability, appropriate analytical methods were applied to evaluate the process-related stability of proteins and the peptide in different formulations.

Specific objectives of the individual projects are described below.

Introduction of small-scale melt extrusion approaches for the production of highly-loaded solid protein-PEG formulations and investigation of process stress on protein stability

This project (chapter 3) aimed to evaluate the impact of process stress on the protein stability in highly-loaded solid protein-PEG extrudates produced by small-scale ram extrusion and TSE. The applied analytical methods should offer an accurate assessment of protein stability in extrudates, enabling the comparison of different melt extrusion formulations and process parameters (e.g., shear stress levels, screw configurations, residence times). Furthermore, the focus was to provide a fundamental basis for future work, including the evaluation of the use of other process techniques (e.g., vacuum compression molding), as well as the use of sustained release polymers (e.g., PLGA (release over several months, EVA (release up to 2 years), since conventional HME screening requires considerable amounts of material even at a small-scale level (> 2 g batch size).

Micro-scale Vacuum Compression Molding as a predictive screening tool of protein integrity for potential hot-melt extrusion processes

HME requires considerable amounts of material (protein powder) even at a small-scale level. The aim of this project, presented in chapter 4, was the introduction of vacuum compression molding (VCM) as a predictive screening tool of protein stability for potential HME processing. The focus was to identify appropriate polymeric matrices (e.g., PEG 20,000, PLGA 50:50, EVA (40 % VA)) prior to extrusion and evaluation of protein stability after thermal stress using only a few milligrams of protein powder. The findings were directly correlated with the results of protein-loaded extrudates prepared by ram extrusion or TSE, as described in chapter 3.

Highly protein-loaded melt extrudates produced by small-scale ram and twin-screw extrusion – evaluation of extrusion process design on protein stability by experimental and numerical approaches

The use of HME processing in protein formulation development is still in its early stages. One major drawback in small-scale extrusion (e.g., 5 mm TSE) has been identified to be a long residence time of up to 5 min, which subsequently results in an increased thermomechanical stress and a potentially negative impact on protein stability. It is therefore crucial to carefully balance the process parameters (e.g., feed-rate, screw design, screw speed, die geometry, L/D-ratio) in order to avoid spots of elevated shear and/or thermal stress along the process. The gap towards a mechanistic understanding of the interactions between process variables and quality attributes needs therefore to be filled via numeric simulation. This project (chapter 5) was designed to retrospectively include relevant extrusion process parameters to facilitate potential correlations of process parameters (e.g., screw configuration, screw speed, temperature profiles, and residence time distributions (RTD)) with experimental data on polymer, and protein characteristics (e.g., rheology, melting temperature shifts, protein recovery rates, and biological activity). The combination of experimental and numerical approaches should reveal a better understanding of HME process parameters (e.g., type of extruder, shear rate distribution, RTD) on protein integrity. The goal was to enable a fundamental and early starting point for the production of protein-loaded extrudates without negatively affecting the protein integrity and prior protein formulation development of long-term release systems by small-scale HME processing based on 1D and 3D computational simulation with experimental data.

3 IMPACT OF PROCESS STRESS ON PROTEIN STABILITY IN HIGHLY-LOADED SOLID PROTEIN/PEG FORMULATIONS FROM SMALL-SCALE MELT EXTRUSION

Katharina Dauer[1], Christian Werner[2], Dirk Lindenblatt[2], Karl G. Wagner[1,*]

[1] University of Bonn, Department of Pharmaceutics, Institute of Pharmacy, Bonn, Germany

[2] University of Cologne, Department of Chemistry, Institute of Biochemistry, Cologne, Germany

This part was published as

K. Dauer, C. Werner, D. Lindenblatt, and K.G. Wagner: Impact of process stress on protein stability in highly-loaded solid protein/PEG formulations from small-scale melt extrusion, International Journal of Pharmaceutics: X, Volume 5, 2022, 100154, DOI: 10.1016/j.ijpx.2022.100154

CONTRIBUTION

I designed the outline of the study, performed literature search, developed the analytical methods, produced the protein-loaded extrudates by ram and twin-screw-extrusion, analyzed the data, interpreted the analytical results, and finally wrote the manuscript.

SUMMARY

Introduction:

Since biopharmaceutics play a steadily increasing role in the medical treatment of especially severe diseases, the sector of developing protein-based therapeutics is similarly growing. These Biopharmaceutics are more complex and have to be administered mostly parenteral as liquid formulations compared to other drug products based on small-molecule drugs [4]. As protein-based therapeutics often exhibit a limited stability in liquid formulations, there is a growing interest in the development of solid protein formulations due to improved protein stability in the solid state (e.g., production of protein-loaded extrudates or implants) [22], [235]. Nowadays, melt extrusion processing can be used for the production of solid protein-loaded implants or for encapsulation of protein particles in extrudates with focus on solid-state protein stabilization. However, the formulation development process of many biopharmaceutics often wastes time and resources, and the amount of a peptide or protein candidate in early development is limited (i.e., a few milligrams). The major drawback of conventional hot-melt extrusion processing is the need of sufficient amounts of API and input material. Therefore, melt extrusion approaches on a small-scale level are of crucial importance, as, small-scale melt extrusion is accompanied with (i) processing small batch sizes (e.g., less than 2 g of a protein formulation), (ii) high yield, and (iii) short process times (e.g., shorter than 3 min for 2 g of a powdered protein formulation). We used small-scale (< 3 g) ram and twin-screw extrusion for the solid stabilization of proteins (lysozyme, BSA, and human insulin) in PEG-matrices. The impact of process stress on protein stability in highly-loaded solid protein/PEG formulations from small-scale melt extrusion was then investigated by several analytical methods. The aim was to provide characterization methods to assess process-related protein stability in highly-loaded protein extrudates as well as to distinguish between the impact of different small-scale melt extrusion processes (i.e., ram and TSE) and extrusion parameters (e.g., shear stress levels, screw configurations, residence times) on protein stability. Melt extrusion was considered for the production of protein-loaded extrudates in order to further enhance protein stability in solid-state formulations compared to the starting material, for improved storage and logistic conditions.

Materials and methods:

Powdered lysozyme, BSA, or human insulin (i.e., 40 %) were embedded in 60 % PEG 20,000 either by ram extrusion at 63 °C or 5-mm twin-screw extrusion at 63 °C using two different screw configurations (conveying screws, or screws with a single 90° kneading element). Protein stability after extrusion was systematically and analytically investigated using the following methods: (i) RP-HPLC for the analysis of degradation products and chemical protein stability, (ii) size exclusion chromatography (SEC) for monitoring the loss of protein monomers as an indication of aggregate formation or fragmentation, (iii) SEM-EDX for visual protein particle distribution over the cross section of protein-loaded extrudate, (iv) ss-DSC for the determination of polymer melting peaks and protein unfolding temperatures, (v) ss-FTIR for the conformational protein stability and secondary structure analysis, (vi) circular-dichroism spectroscopy for comparison the molecular conformation and secondary structure elements of protein powder before and after melt extrusion, (vii) biological activity assay (only for lysozyme), and (viii) thermal stress test for 28 days at 40 °C to assess the protein stability under thermal stress (accelerated conditions) applying the before mentioned analytical methods.

Results and discussion:

During melt extrusion mainly the stress factors heat exposure in combination with shear stress, are potentially affecting protein stability and consequently can lead to their degradation or inactivation. Within the current study, the analytical investigation and characterization of protein stability in highly-loaded protein extrudates was demonstrated. The applied analytical methods offered an accurate assessment of protein stability in highly-loaded protein PEG-extrudates produced by ram extrusion and TSE with regard to the main challenges, i.e., protein instability due to heat exposure and shear stress during extrusion. Lysozyme was implemented as a model protein and was completely recovered in its active form after extrusion. Differences seen between Lysozyme- and BSA- or human insulin-loaded extrudates indicated that melt extrusion could have an impact on the conformational stability. In particular, BSA and human insulin were more susceptible to heat exposure and shear stress compared to Lysozyme, where shear stress was the dominant parameter. Consequently, ram extrusion led to less conformational changes compared to TSE. Ram extrusion showed good protein particle distribution resulting in the preferred method to produce highly-loaded solid protein formulations.

4 MICRO-SCALE VACUUM COMPRESSION MOLDING AS A PREDICTIVE SCREENING TOOL OF PROTEIN INTEGRITY FOR POTENTIAL HOT-MELT EXTRUSION PROCESSES

Katharina Dauer[1], Karl G. Wagner[1,*]

[1] University of Bonn, Department of Pharmaceutics, Institute of Pharmacy, Bonn, Germany

This part was published as

K. Dauer and K.G. Wagner: Micro-Scale Vacuum Compression Molding as a Predictive Screening Tool of Protein Integrity for Potential Hot-Melt Extrusion Processes. Pharmaceutics 2023, 15, 723, DOI: 10.3390/pharmaceutics15030723

CONTRIBUTION

I designed the outline of the study, performed literature search, developed the analytical methods, produced the protein-loaded discs by vacuum-compression molding, analyzed the data, interpreted the analytical results, and finally wrote the manuscript.

SUMMARY

Introduction:

The formulation development process of many biologics often wastes time and resources, and the amount of a peptide or protein candidate in early development is limited (i.e., a few milligrams) [98]. These aspects also need to be considered when evaluating alternative formulations formulation strategies, and modes of administration. Solid biopharmaceutical formulations offer the potential for increased stability and underline the importance of alternative solid protein formulations. Hot-melt extrusion (HME) can be used for the production of solid protein formulations mainly for two reasons: increased protein stability in solid state and/or long-term release systems (e.g., protein-loaded implants). However, HME requires considerable amounts of material even at small-scale (> 2 g batch size). An early evaluation and predictive screening of composition and formulation process parameters on a micro-scale level is of crucial importance, as, due to the costs of proteins, conventional development programs are financially unfeasible. The aim is to enable a good and early starting point for the production of solid protein formulations without negatively affecting the protein stability and prior cost-intensive protein formulation development of long-term release systems. In this study, micro-scale vacuum compression molding (VCM) was introduced as a predictive screening tool of protein integrity and polymers by overcoming the major drawback of conventional HME screening by using a minimum quantity of API and material [236]. VCM (combination of vacuum and temperature) was used to prepare cylindrical discs composed of different protein-polymer mixtures in view of a potential as a predictive screening tool for protein solid-state stabilization in the selected polymers. VCM is a novel, fusion-based tool for the simple preparation of thermoplastic specimens starting from powders, where the molten samples are evacuated and compressed into a defined solid form without any air inclusions [237]. A fundamental formulation development strategy is based on an extensive knowledge of the physicochemical protein stability and thus the protein-loaded discs were investigated using appropriate analytical methods to evaluate the process-related protein stability. The protein stability of 20 % lysozyme, BSA, and human insulin embedded in 80 % PEG 20,000, PLGA, or EVA by VCM was investigated by DSC, FT-IR, and SEC. The results from the protein-loaded discs provided important insights into the solid-state stabilizing mechanisms of protein candidates and a good basis for the evaluation of VCM as a predictive screening tool for the preselection of appropriate polymeric matrices prior to extrusion. VCM was

successfully applied for a set of proteins and polymers, showing, in particular, a high potential for EVA as a polymeric matrix for solid-state stabilization of proteins and for the production of extended-release dosage forms. Stable protein-polymer mixtures with improved protein stability after VCM could be then introduced to a combination of thermal and shear stress by HME and further investigated with regard to their process-related protein stability.

Materials and methods:

Powdered lysozyme, BSA, or human insulin (i.e., 20 %) were embedded in 80 % PEG 20,000, PLGA (Resomer® RG502 H), or EVA (40 % VA) by VCM. Prior VCM, PEG 20,000 flakes were milled utilizing a high-shear mixer, whereas EVA granules were milled using a cryogenic mill. VCM was conducted using a VCM tool with a 5 mm diameter disc geometry. Approx. 15 mg of each blend was loaded into the VCM device and heated under vacuum for 6 or 12 min at a temperature of 65 °C for PEG 20,000, or 70 °C for PLGA, and EVA. Protein stability after VCM was systematically and analytically investigated using the following methods: (i) SEC for monitoring the loss of protein monomers as an indication of aggregate formation or fragmentation, (ii) ss-DSC for the determination of polymer melting peaks and protein unfolding temperatures, (iii) ss-FTIR for the conformational protein stability and secondary structure analysis. The produced protein-loaded 5 mm-discs were directly used after production in their final form and without further sample preparation for FT-IR and DSC analysis. For SEC analysis, the sample preparation of protein-loaded discs was depended on the used polymer. Samples (i.e., physical mixture and protein-loaded discs) containing PEG 20,000 as polymer were directly dissolved in the mobile phase used for SEC analysis. Proteins embedded in PLGA were extracted by the use of acetonitrile, whereas for EVA-containing samples, dichloromethane was used [227].

Results and discussion:

The native state of a protein molecule is its orderly folded and assembled form and determines its functionality. The most common stress that can cause a loss of protein structure or functionality is an exposure to heat during processing (i.e., thermally induced protein denaturation and/or unfolding). The systematic analysis of the protein-loaded discs provided important insights into the solid-state stabilizing mechanisms of protein candidates since an understanding of molecular interactions within the polymeric matrix can support the identification of most promising polymer

carriers. The unfolding temperatures of the used proteins and PEG 20,000 or PLGA determined by DSC were comparable with or lower than the unfolding temperature of the native proteins. However, the unfolding temperature of the proteins in the presence of EVA were not reduced or even higher compared to the native protein powder. The trend of a potential protein stabilizing effect of EVA as polymer was confirmed by FT-IR analysis. The first and second derivatives of FT-IR spectra of VCM discs containing 20 % lysozyme, BSA, or human insulin and 80 % EVA were comparable to the powdered proteins used to prepare the discs. Since the spectra were overlaying, there was no indication of protein denaturation or aggregation as a consequence of the exposure to an elevated temperature of 70 °C during VCM processing. Moreover, VCM processing was not the trigger for the formation of protein fragments or aggregates in the case of lysozyme- and BSA-loaded discs. Human insulin-loaded PEG discs prepared by VCM showed further peaks in front of the peak of native human insulin, indicating the formation of HMWS in the presence of PEG 20,000. Therefore, PEG 20,000 is not an appropriate polymer carrier, since interactions of human insulin molecules with hydrophilic PEG chains induced the alteration of the local insulin structure. This hypothesis was also confirmed by the results of human insulin-loaded extrudates prepared by ram extrusion or TSE, as described in Chapter 3. EVA presented high potential as a polymeric matrix for solid-state stabilization of proteins (e.g., lysozyme, BSA, and human insulin) or the production of protein-loaded implants with extended-release behavior.

5 HIGHLY PROTEIN-LOADED MELT EXTRUDATES PRODUCED BY SMALL-SCALE RAM AND TWIN-SCREW EXTRUSION - EVALUATION OF EXTRUSION PROCESS DESIGN ON PROTEIN STABILITY BY EXPERIMENTAL AND NUMERICAL APPROACHES

Katharina Dauer[1], Kevin Kayser[1], Felix Ellwanger[2], Achim Overbeck[3], Arno Kwade[3], Heike P. Karbstein[2], Karl G. Wagner[1,*]

[1] University of Bonn, Department of Pharmaceutics, Institute of Pharmacy, Bonn, Germany

[2] Institute of Process Engineering in Life Sciences, Food Process Engineering, Karlsruhe Institute of Technology, Karlsruhe, Germany

[3] Technische Universität Braunschweig, Institute for Particle Technology (iPAT), Braunschweig, Germany

This part was published as

K. Dauer, K. Kayser, F. Ellwanger, A. Overbeck, A. Kwade, H.P. Karbstein, and K.G. Wagner: Highly protein-loaded melt extrudates produced by small-scale ram and twin-screw extrusion - evaluation of extrusion process design on protein stability by experimental and numerical approaches, International Journal of Pharmaceutics: X, 2023, DOI: 10.1016/j.ijpx.2023.100196

CONTRIBUTION

I designed the outline of the study, performed literature search, developed the analytical methods, produced the protein-loaded extrudates by ram and twin-screw-extrusion, analyzed the data, interpreted the analytical results, and finally wrote the manuscript.

SUMMARY

Introduction:

In pharmaceutical industry, hot-melt extrusion (HME) is mainly used as continuous and robust manufacturing technology for the production of solid dosage forms (e.g., ASDs) [187]. In the last few years, the application of HME was expanded to biopharmaceutics and can be used for the production of long-term release systems for parenteral administration (e.g., protein-loaded implants) or for solid-state protein stabilization [211], [212]. However, conventional HME processing requires batch sizes of about 20-30 g, which result in substantial amounts of drug substance and development costs, respectively [192], [199]. The amount of protein drug candidates within early formulation development studies however, is often limited and thus small-scale HME is particularly relevant [55]. Small-scale HME ideally enables the processing of batch sizes below 3 g accompanied with high yields of the produced protein-loaded extrudate under short processing times (e.g., less than 3 min) [25]. We introduced small-scale ram extrusion and TSE for the production of solid protein PEG-formulations (lysozyme and BSA). However, during the residence time in the extruder the protein particles are exposed to thermomechanical stress, which can potentially affect protein stability [24], [186]. It is therefore crucial to carefully balance the process parameters (e.g., feed-rate, screw design, screw speed, die geometry, L/D-ratio) in order to avoid spots of elevated shear and/or thermal stress along the process. As melt temperature and pressure in small-scale extrusion is usually determined in the die only, information on the extent and location of above-mentioned hot spots along the process are easily missed. The gap towards a mechanistic understanding of the interactions between process variables and quality attributes needs therefore to be filled via numeric simulation [192], [238]–[240]. The extrusion process understanding and design can be challenging due to fundamental differences in how heat and shear stress is generated in extruders of differing types and the significant role thermomechanical stress generation plays in determining the final product attributes and protein integrity [241]. The aim of the study was to include all relevant extrusion process parameters to facilitate potential correlations of process parameters (e.g., screw configuration, screw speed, and residence time distributions (RTD)) with experimental data on polymer, and protein characteristics (e.g., rheology, melting temperature shifts, protein recovery rates, and biological activity).

Materials and methods:

Powdered lysozyme or BSA (i.e., 20, 40, or 60 %) were embedded in 80, 60, or 40 % PEG 20,000, respectively either by ram extrusion at 63 °C or 5-mm twin-screw extrusion at 63 °C using two different screw configurations (i.e., conveying screws, or screws with a single 90° kneading element) and screw speeds (i.e., 100, 150, or 200 rpm). The physical mixtures were fed into the TSE by using a powder belt conveyor at constantly kept feed-rates of 0.4, 0.6, 1.0, 1.4, and 2.0 g/min. A correlation of experimental and numerical approaches for the evaluation of extrusion process design (e.g., type of extruder, screw configuration and speed, mean residence time) on protein integrity was applied. The comparison of extrusion experiments was evaluated with the computations of the 1D and 3D simulation software Ludovic® and Ansys Polyflow®, respectively. Input parameters for 1D simulation of the MRTs were: (i) screw configuration, (ii) screw speed, (iii) temperatures of the segments, (iv) feed-rate, (v) thermal characteristics of the extruded mixture (i.e., heat capacity, density, thermal conductivity, melting temperature, and melt rheology data). The MRTs as a function of screw configuration, screw speed, different feed-rates, and protein-load were also experimental measured with a color tracer and calculated by using the camera system ExtruVis3 and correlated with simulated MRTs. As mechanical stress in the extrusion process may lead to damaging of the proteins, 3D software was used to characterize mechanical stress profiles during ram extrusion and TSE (i.e., shear rate distribution of the die and screw sections). The particle size distribution analysis and mechanical single crystal analysis of the used protein powder particles were used for the evaluation of applied thermomechanical stress and potential particle grinding during extrusion. Protein stability after extrusion was analytically investigated using the following methods: (i) RP-HPLC for the determination of protein recovery rates from protein-loaded extrudates and analysis of degradation products and chemical protein stability, (ii) SEM-EDX for visual protein particle distribution over the cross section of protein-loaded extrudates, (iii) ss-DSC for the determination of polymer melting peaks and protein unfolding temperatures, (iv) biological activity assay (only for lysozyme).

Results and discussion:

The extrusion process for embedding protein particles into a polymeric matrix (e.g., PEG 20,000) can be separated into two steps for both, the ram extruder and the TSE. A thermal and mechanical treatment of the mixture in the reservoir of the ram extruder

or in the screw section of the TSE takes place. While for the ram extruder melting and extruding, i.e., introducing mechanical stress, were applied sequentially, during TSE these processes were introduced simultaneously. The selected polymer PEG 20,000 is waxy and shows a very high viscosity below the melting temperature (not extrudable due to an extensive torque) and a very low viscosity above the melting temperature (not extrudable due to liquification). Due to the narrow extrusion process window of PEG 20,000 and as mechanical stress in the extrusion process may lead to damaging of the proteins the need of computational simulation for gaining insights into extrusion process design is of crucial importance. In regard of mechanical stress, 3D simulations revealed that the die area of both extruders is comparable. The highest shear rates were found close to the wall and gradually decreased towards the center of the die channel. For TSE the highest shear rates were present in the screw section and particularly in the gap between the screws and between the screw and the barrel. The simulation of maximum shear rates raised the expectation of particle grinding during extrusion, especially when TSE is used. MRTs determined by TSE experiments and 1D simulation (Ludovic®) were compared. However, the MRTs of the blends in the heated barrels were short (3 min and less than 80 sec, for ram extrusion and TSE, respectively) and thus did not lead to a dissolution or grinding of protein particles in the PEG-matrix. The experimental MRTs for the pure PEG and 20 % protein-polymer mixture were congruent with simulated data. In mixtures with 40 % or 60 % protein, the impact on melt rheology behavior and thus the MRT is no longer neglectable and was reliably predicted by Ludovic®. Ram extrusion facilitates sufficient dispersion of protein particles for all protein-loads (20-60 %). The distributive mixing effects of TSE were not necessary for the production of protein-loaded extrudates and TSE were thus not superior compared to ram extrusion. In contrast mechanical stress within ram extrusion was generated in the die only. Ram extrusion had the lowest impact on unfolding temperatures which is in agreement with the results of 3D simulation. That die-induced stress was higher for the ram than for the TSE die, still much lower than the screw induced stress. A protein-load effect on the unfolding temperature was observed for extrudates produced by TSE. The MRT in the kneading element was slightly increased, implying that protein particles were entrapped within the gaps of the kneading element, resulting to a more frequent stressing and an increase in temperature as a result of the increasing viscous dissipation. Interestingly a higher protein-load of 60 % was protective resulting in a less pronounced decrease of unfolding temperatures.

6 SUMMARY AND CONCLUSIONS

The extension of conventional HME processing to therapeutically relevant proteins and peptides has been largely limited by the amount of protein substance available for development studies. Therefore, two small-scale HME approaches for embedding solid protein particles in polymeric matrices were established. Applying ram extrusion and 5-mm TSE required batch sizes of minimal 1.0 g and 3.0 g powder, respectively. The starting material for HME processing is composed of a solid freeze- or spray-dried protein or peptide powder, polymer powder, and optionally other powdered additives or excipients. In this work, lysozyme, BSA, and human insulin powder were used as proteins and peptide, respectively. TSE is known as continuous manufacturing approach and thus required a steady feeding of the powdered material into the feeding zone of the extruder. In many works a controlled feeding process in small scale HME is neglected and performed manually with a spatula or is not even mentioned. In this work, the feeding of powdered starting material was controlled via a conveying belt into the extruder barrel of the 5-mm TSE enabling constant feed-rates during the entire process. The feed-rates were adapted for each type of protein powder and the respective protein-loads of 20, 40, and 60 % protein, as the particle morphology, residual moisture content and protein-load affected the consistency of the feed-rate. The average time for adjusting an optimal feed-rate required approximately half an hour. In contrast, a time- and material-consuming adjustment of the feed-rate is not required in the case of ram extrusion as no continuous feeding was involved. Starting material composed of spherical protein powder particles and an average particle size of less than 200 µm such as lysozyme or human insulin powder could be fed at very low feed-rates (0.2 and 0.4 g/min), whereas the feeding of mixtures containing huge, elongated BSA crystals (450 µm) required up to 10-fold higher feed-rates maintaining a consistent TSE process (i.e., 2.0 g/min). The extremely low feed-rates were achieved using a self-built feeder based on a conveying belt and a powder reservoir hovering at a distinct gap above the belt. A major drawback of the used small-scale 5 mm TSE, with a short barrel, was the missing possibility of active cooling in the feeding zone. The protein-polymer powder adheres to the wall of the feeding opening at the very beginning of the barrel and the polymer begins to melt. The process continuity is less stable due to an increased clogging of the feeding zone. In contrast, the barrel of the discontinuously operating ram extruder (8.25 cm^3) was filled with the entire batch of minimal 1.0 up to 8.0 g of powder depending on the density of the powder mixture. The powdered starting

material is filled in the vertically positioned ram extruder barrel with an active cooling possibility via air or water circulation in the feeding zone. A further advantage of the ram extruder was the very high yield of nearly 100 %, whereas TSE processing resulted in a yield of less than 80 % due to the dead volume between the extruder barrel and the screws as well as the die section. Another benefit of ram extrusion processing was the embedding of up to 80 % protein substance in a polymeric matrix, whereas the maximum achievable protein-load of TSE processing was 60 %, likely to the changes in viscoelastic properties of the melt, which prevented plastic flow through the die. However, when HME processes with higher throughputs are necessary, TSE offers ease scale-up whereas upscaling in ram extrusion is limited due to a not infinitely scalable inner volume of the ram extruder barrel. An increase in the inner volume results in an impaired heat flow and increased residence times due to a changed surface-volume ratio.

Despite all the limitations with regard to both applied HME processes, ram extrusion and TSE were successfully applied as protein solid-state stabilization approach and subsequently, for the perspective development of extended-release systems for parenteral administration (e.g., protein-loaded implants). A general issue of feeding freeze- or spray-dried proteins are the pronounced triboelectric charging which limits the accuracy of feeding and further processing like dispensing. HME processing were used for embedding of the highly potent and triboelectric charged protein particles in a solid matrix. Consequently, the solid-state stabilization of protein particles by HME provided a suitable intermediate step and eases the safe handling of the formulated proteins for subsequent processing or storage due to the drastically reduced triboelectric charging. However, HME processing of proteins was accompanied with stress factors, mainly elevated temperatures (< 75 °C) in combination with shear forces, that affected to various degrees the protein integrity. Hence, a fundamental understanding of extrusion processing by small-scale ram extrusion and TSE was essential as an early starting point for the production of stable protein-loaded extrudates.

Chemical degradation of a protein due to oxidation can occur during any stage of protein manufacturing, particularly when the protein is exposed to thermomechanical stress during processing. Chemical stability analysis of the extracted proteins by RP-HPLC showed that no oxidation or hydrolysis of the proteins occurred during ram extrusion or TSE. The physical protein stability after extrusion was investigated using various analytical methods. SEC was used to identify any process-induced protein

fragmentation or the formation of HMWS/protein aggregates. The thermomechanical stress applied to the proteins during HME processing did not result in the formation of protein fragments or protein aggregates in the case of lysozyme and BSA. Human insulin in combination with PEG 20,000 showed the formation of approximately 0.2 % HMWS. However, the formation of HMWS was independent of the extrusion process, since HMWS appeared also in the case of the unprocessed, starting material composed of human insulin and PEG 20,000 in a powder mixture. Human insulin molecules presumably interact with hydrophilic PEG 20,000 molecules likely due to a PEG-induced alteration of the local peptide structure. Despite intensive investigations, details about the initial triggers for insulin HMWS formation have remained elusive at the molecular level.

The reported unfolding temperatures for proteins in the solid state are predominately high, often above 200 °C and vary slightly according to the protein. In general, proteins do not show typical melting behavior, but rather a change in molecular conformation from a native to a denatured state at the unfolding temperature. DSC thermograms exhibited broad peaks designated as the protein unfolding temperatures, which is equivalent to the temperature where 50 % of the protein is in the unfolded state, i.e., not completely denatured. Ss-DSC analysis was successfully used for the selection of appropriate extrusion temperatures (60 to 65 °C) by means of the determined melting temperature of the designated polymer and by selecting an extrusion temperature that is far below the unfolding temperature of the used protein. Nevertheless, the most common stress that can cause a loss of protein structure is elevated temperature and designated as thermally induced protein denaturation (unfolding). In general, a significant decrease in the unfolding temperature of the protein reflects a decrease in the conformational protein stability. The protein-loaded extrudates were thus evaluated with respect to the thermal protein stability after extrusion. The ram extrusion process did not significantly affect the unfolding temperature of lysozyme. In general, ram extrusion had the lowest impact on protein unfolding temperatures, whereas TSE showed significantly reduced unfolding temperatures for 20 % and 40 % protein-load, especially in combination with screws containing 90° kneading elements. In conventional HME processing, the kneading elements of a screw play a decisive role in both melting the polymers and in enhancing dispersive as well as distributive mixing of the API-polymer mixture by introducing maximum shear stress at no conveying of material. Surprisingly, a protein-load effect on the unfolding temperature was observed for extrudates produced by TSE. A higher

protein-load of 60 % was protective resulting in a less pronounced decrease of unfolding temperatures. We hypothesize that the generated shear stress during TSE were distributed to a larger protein particle collective and thus, high protein-loads of > 50 % should be favored.

CD and FT-IR spectroscopy were used to compare the molecular conformation and secondary structure elements of protein powder before and after HME processing. The conformational stability of lysozyme and BSA was neither negatively affected by ram extrusion nor TSE without indication for denaturation (shifts or distortion of bands) or aggregation (intermolecular β-sheet formation) as a consequence of the thermomechanical stress during ram extrusion or TSE. However, BSA and human insulin were more susceptible to thermomechanical stress than lysozyme. A probable explanation for the observed differences in the FT-IR spectra of BSA-loaded extrudates and the unprocessed BSA reference may be the extrusion procedure, since thermomechanical stress can cause reversible changes in protein conformation and is associated with a reduction in the α-helical content and an increase in the random chain content. The secondary structure elements of BSA could be partially unfolded but still presenting a native-like secondary structure and thus no process-induced loss in functionality occurred. CD and FT-IR spectra of human insulin-loaded extrudates prepared by TSE showed clear shifts and changes in secondary structure elements. These changes indicated the transformation of α-helix content to β-sheets or a disordered structure which enhanced the tendency to aggregate. In particular, the α-helical structures were obviously affected by TSE with screws containing a kneading element due to higher shear stress and a longer residence time compared to non-modular conveying screws. The extent to which the functionality of human insulin was negatively affected by HME processing is challenging to assess, since no activity assays for insulin are available. The activity assay available for lysozyme revealed no loss in activity as the remaining activity was higher than 90 % after ram extrusion and TSE and highlights the extreme stability of lysozyme against thermomechanical stress. An accelerated thermal stability study (40 °C for 28 days) revealed that neither chemical degradation of the stored proteins embedded in PEG-matrices by ram extrusion or TSE, nor the formation of HMWS occurred. In the case of lysozyme and BSA the unfolding temperatures as well as the secondary structure elements were not negatively affected or shifted due to the thermal stress during storage. In contrast, the physical stability of human insulin was negatively affected during storage. However, the amount of formed HMWS was in the same magnitude

as the stored unprocessed human insulin powder. Therefore, HME processing was not the main driver for the observed physical instability.

Overall, ram extrusion had the lowest impact on the thermal stability (unfolding temperature) and conformational stability (secondary structure changes) of the extruded proteins compared to TSE due to lower shear stress. The aim of a homogenous embedding of protein powder particles in a polymeric matrix by HME without negatively affecting the protein stability was achieved.

The protein particle distribution over the cross section of extrudates was analyzed by SEM-EDX and coefficients of variance (CV) were used to describe the protein particle distribution quantitatively. Protein-loaded extrudates prepared by ram extrusion showed indeed up to 1.5-fold higher CVs compared to extrudates processed by TSE, but the protein recovery rates were still above 97.5 % depending on the size of the embedded protein particles. The barrel of the ram extruder does not contain any restrictive elements for mixing like the co-rotating screws of a TSE. However, a highly homogeneous protein particle distribution could be also achieved by ram extrusion especially when the size of protein particles was below 200 µm (d_{50}) as presented by lysozyme and human insulin. In contrast, the embedding of elongated BSA crystals with a very broad particle size distribution (d_{50} = 450 ± 70 µm) revealed CVs of 10.0 %, 7.5 %, and 6.3 % for BSA-loaded extrudates produced by ram extrusion, TSE with conveying screws, and TSE with a kneading screw element, respectively. Starting material composed of such huge and elongated particles would be generally homogenized (i.e., milling and sieving) before processing in terms of achieving a consistent particle morphology and size. In this work, the BSA crystals were intentionally not pretreated in order to investigate process-related effects on the particles like particle size reduction or dissolving. As both ram extrusion and TSE revealed homogeneously distributed protein particles over the cross section of the extrudates, the dispersive power of TSE revealed not to be necessary. Consequently, the ram extruder would be favored for the production of stable protein-loaded extrudates in small-scale. The images of the cross sections of protein-loaded extrudates showed also that the protein particles were solely embedded in the polymeric matrices without dissolution or particle size reduction in the polymer as the particle size of the used protein powders was identical for the starting material and particles detected in the cross section of extrudates. On protein folding, hydrophobic AAs get buried inside the protein such that they are shielded from the surrounding water, whereas hydrophilic AAs are positioned outside of the buried core. As the

solubility characteristics of a protein depend on process parameters, such as pH, ionic strength, mechanical forces, and temperature stress, we expected at least a partial dissolution of the protein particles in the hydrophilic, molten PEG. The MRT of the protein particles in the extruder was 3 min for the ram extruder and less than 1.5 min for the TSE process, dependent on protein-load and TSE process parameters. Obviously, MRT in combination with the high viscous melt obstructed the dissolution of protein particles. The protein particles acted as a neutral filler in the polymer matrix, resulting in a reduced amount of energy as viscous dissipation was increasing. Micro compression analysis of the pure protein powder particles showed that BSA crystals were more ductile and less fragile than solid lysozyme or human insulin particles as the values for breakage force and breakage displacement were 2-times lower for lysozyme and human insulin than for BSA. However, the mechanical stress generated during ram extrusion and TSE did not exceed the break limit of lysozyme, BSA, or the human insulin particles, which might be related to the elastic deformation properties of the protein particles compensating local shear stress peaks.

A mechanistic evaluation of the process parameters including various feed-rates, screw designs, screw speeds, die geometry, L/D-ratio, in order to avoid spots of elevated shear and/or thermal stress along the process is of crucial importance. The gap towards a mechanistic understanding of the interactions between process variables and CQAs were therefore filled via numerical simulation by using 1D and 3D simulation software Ludovic® and Ansys Polyflow®, respectively. A systematic adaption of numerical simulation, particularly to a scale as small as 5-mm TSE in comparison to ram extrusion, and a subsequent correlation to protein stability of dispersed protein particles within a molten polymer matrix was applied. Several extrusion process characteristics and material properties (e.g., heat capacity, density, melt rheology data) of the investigated polymer-protein mixtures were considered. As mechanical stress in the extrusion process may lead to damaging of the proteins, 3D software was used to characterize mechanical stress profiles during ram extrusion and TSE. Low shear rates were found in the reservoir of the ram extruder. In regard of mechanical stress, the die area of both extruders was comparable. For TSE the highest shear rates were present in the screw section and particularly in the gap between the screws and between the screw and the barrel. In comparison to ram extrusion, in a kneading or conveying element TSE extrusion a single protein particle in the molten polymer is exposed for 9.5 s or 7.4 s to a 4.5- to 5.5-fold higher shear stress, respectively. The MRT in the ram extruder was approximately 3 min and in the

TSE extruder either equipped with conveying screws or screws containing a 90° kneading element in the range of 18 s to 57 s, or 21 s to 68 s, respectively and dependent on the screw speed and feed-rate. Despite the 3-times higher MRT in the ram extruder, the overall introduced shear stress was lower compared to TSE as the stress was generated in the die only and for a very short time of 0.05 s. However, so far, no simple 1D simulation model is available for ram extrusion thus, 3D simulations were employed for crucial process steps or areas, respectively. As the die in the ram extrusion was identified as the most critical process area, this limitation is negligible. The increased shear rate for the kneading element in TSE can be attributed to different flow profiles resulting from the restriction of 90° kneading discs. In contrast to TSE, ram extrusion offers the potential to prepare highly-loaded solid protein formulations at high yield, higher protein-loads of up to 80 %, and at lower shear stress.

TSE strongly profits from both 1D and 3D simulations where 1D identifies critical process steps while 3D simulations boost the mechanistic understanding. Ludovic® proposes a global analysis of co-rotating TSE processes for describing the material behavior evolution along the process. Nonetheless, simulation via Ludovic® is expected to better converge with experimental data when using feed-rates higher than 0.1 kg/h and larger size TSE (e.g., 9-, 11-, or 12-mm) with better instrumentation spread over the entire extrusion process (e.g., multiple temperature, die pressure, and torque monitoring). A pressure instrumentation for the experimental determination of the pressure particularly in the die section, was neither available in the small-scale 5 mm TSE nor ram extrusion. Compared to the reliably simulated thermomechanical and temperature profiles and RTDs along the TSE barrel and the die and as torque could not adequately measured in the 5 mm TSE experiments, 1D simulation could not reveal pressure distribution, which would otherwise be standard. 1D simulation proved to be difficult and may involve a higher risk for wrong assumptions regarding the simulated RTDs and temperature profiles as we used very low feed-rates in the range of 0.2 to 2.0 g/min corresponding to 0.012 kg/h and 0.12 kg/h, respectively. The pressure would indeed be an excellent variable to validate the 3D simulations of the die section. Advanced instrumentation would facilitate improved model validation as pressure and temperature profiles could be correlated. In conclusion, the presented combined approach of small-scale extrusion and 1D and 3D numerical simulation enabled a good starting point for ram extrusion and TSE trials for the production of highly-loaded protein extrudates without

negatively affecting protein stability, protein recovery rates, and homogenous distributed protein particles.

Besides the application of numerical simulation approaches, VCM technology was successfully implemented as predictive screening tool of protein integrity. Even small-scale HME processing requires considerable amounts of material (> 2 g batch size). The focus of the applied VCM technology was to identify appropriate polymeric matrices and formulation compositions prior to HME processing and evaluation of protein stability after thermal stress using only a few milligrams of protein. The protein stability of lysozyme, BSA, and human insulin embedded in PEG 20,000, PLGA, or EVA by VCM was investigated by ss-DSC, ss-FT-IR, and SEC. The produced protein-loaded discs by VCM were directly used after production in their final form for ss-FT-IR and ss-DSC analysis without a further and complex sample preparation and thus accelerated the formulation screening studies significantly. The systematic analysis of the protein-loaded discs provided important insights into the solid-state stabilizing mechanisms of lysozyme, BSA, and human insulin. The formulation screening revealed that EVA shows a high potential as polymeric matrix carrier for solid-state stabilization of proteins, since the unfolding temperature of the proteins in the presence of EVA were not reduced but, even higher compared to the native protein powder. Since several studies highlight the potential of PEG as protein stabilizer mainly in liquid formulations, PEG 20,000 was selected in this work as matrix former for an intended solid-state stabilization of the model proteins. In particular, as the stabilization of insulin, which is known to be prone to fibrillation and aggregation, by PEGylation was successfully shown by shielding of the insulin monomeric structure, it was expected that embedding of human insulin in a PEG-matrix would offer a similar stabilizing effect. However, the formation of HMWS and thus strong interactions between human insulin molecules and PEG 20,000 were observed in all kinds of human insulin containing samples independent whether human insulin was co-processed with PEG or unprocessed. These highly unfavorable interactions between PEG 20,000 and human insulin were further confirmed by the polymer screening via VCM. As these interactions resulted in the formation of HMWS, PEG 20,000 cannot be recommended as polymeric matrix and protein stabilizer for human insulin formulations. This fact highlights also the need of suitable and appropriate screening tools for an early evaluation of favorable and unfavorable formulation compositions. Differences seen between the potential stabilizing effect of EVA and the destabilizing effect of PEG 20,000 could be due to the hydrophobic and hydrophilic nature of EVA

and PEG 20,000, respectively. PEG may bind to hydrophilic sites on the protein or peptide surface by inducing subtle unfolding while EVA may induce subtle compaction of the protein or peptide structure forced by repulsive interactions.

For an intensive analytical screening (n = 3) of a single formulation composition (protein-polymer-mixture) by SEC, RP-HPLC, ss-DSC, and ss-FT-IR spectroscopy, approximately 15 mg of protein substance was required (corresponding to 20 % protein-load). In comparison for the production of a single formulation composition by ram extrusion and TSE, 300 or 600 mg of protein substance are required. The amount of a peptide or protein candidate in early development is strictly limited to a few hundred milligrams and thus small-scale ram extrusion or TSE cannot be used for an extensive formulation screening to identify the best formulation conditions. VCM technology proved to be an appropriate screening tool for the investigation of potential protein solid-state stabilization for melt-based formulations at a micro-scale as well as for the evaluation of suitable polymers and excipients for further planned HME processing.

The use of HME for the development of implantable sustained protein release systems is a promising alternative to repeated injections of liquid or solid protein formulations due to a single administration of a protein-loaded implant. VCM technology is a particularly appropriate tool for screening the best polymer matrices, excipients, and thus formulation compositions in early stages of pre-development programs. Identified stable protein-polymer-excipient mixtures with improved protein stability after VCM could be then introduced to a combination of thermal and shear stress by HME and further investigated with regard to their process-related protein stability. Ram extrusion technology is particularly the best choice in pre-development studies for the production of protein-loaded implants based on the identified appropriate formulation composition by VCM. As both extruder designs revealed homogeneously distributed protein particles over the cross section of the extrudates for all protein-loads (20 to 60 %), the distributive power of TSE revealed not to be decisive and the dispersive power not high enough to affect the particle size. However, the limitation of ram extrusion is the missing ability of distributive mixing. Especially in the case of complex protein formulations composed of more than three ingredients ram extrusion could reach its limits resulting in less sufficient and homogenous protein particle distribution in the implant. In the case of complex protein formulation compositions, advanced development studies, or for the preparation of clinical samples, TSE technology should be applied to meet the required distributive

mixing for homogeneous protein distribution over the entire implant and for process scalability. The therapeutic and highly potent protein or mAb is released from the produced protein-loaded implant of various shape and size for an extended period of time and in a controlled manner and thus enhances the attractiveness for intraocular or intrathecal applications for the treatment of age-related macular degeneration, chronic uveitis, or neurodegenerative diseases such as amyotrophic lateral sclerosis, multiple sclerosis, Parkinson's disease, or Alzheimer's disease, respectively.

7 REFERENCES

[1] H. Kaplon, M. Muralidharan, Z. Schneider, und J. M. Reichert, „Antibodies to watch in 2020“, *mAbs*, Bd. 12, Nr. 1, S. 1703531, Jan. 2020, doi: 10.1080/19420862.2019.1703531.

[2] J. L. Lau und M. K. Dunn, „Therapeutic peptides: Historical perspectives, current development trends, and future directions“, *Bioorg. Med. Chem.*, Bd. 26, Nr. 10, S. 2700–2707, Juni 2018, doi: 10.1016/j.bmc.2017.06.052.

[3] R. Nongkhlaw, P. Patra, A. Chavrasiya, N. Jayabalan, und S. Dubey, „Biologics: Delivery options and formulation strategies“, in *Drug Delivery Aspects*, Elsevier, 2020, S. 115–155. doi: 10.1016/B978-0-12-821222-6.00006-3.

[4] V. Gervasi, R. Dall Agnol, S. Cullen, T. McCoy, S. Vucen, und A. Crean, „Parenteral protein formulations: An overview of approved products within the European Union“, *Eur. J. Pharm. Biopharm.*, Bd. 131, S. 8–24, Okt. 2018, doi: 10.1016/j.ejpb.2018.07.011.

[5] G. Walsh, „Biopharmaceutical benchmarks 2010“, *Nat. Biotechnol.*, Bd. 28, Nr. 9, 2010.

[6] S. S. Usmani *u. a.*, „THPdb: Database of FDA-approved peptide and protein therapeutics“, *PLOS ONE*, Bd. 12, Nr. 7, S. e0181748, Juli 2017, doi: 10.1371/journal.pone.0181748.

[7] U.S. Food and Drug Administration, „Fact Sheet: FDA at a Glance“. FDA, 17. August 2022. Zugegriffen: 2. Mai 2023. [Online]. Verfügbar unter: https://www.fda.gov/about-fda/fda-basics/fact-sheet-fda-glance

[8] B. Lücke, Jürgen Mathias, „Medizinische Biotechnologie in Deutschland 2023“, Boston Consulting Group, Juni 2023.

[9] M. van de Weert, L. Jorgensen, E. Horn Moeller, und S. Frokjaer, „Factors of importance for a successful delivery system for proteins“, *Expert Opin. Drug Deliv.*, Bd. 2, Nr. 6, S. 1029–1037, Nov. 2005, doi: 10.1517/17425247.2.6.1029.

[10] S. Frokjaer und D. E. Otzen, „Protein drug stability: a formulation challenge“, *Nat. Rev. Drug Discov.*, Bd. 4, Nr. 4, S. 298–306, Apr. 2005, doi: 10.1038/nrd1695.

[11] A. Kurz und J. Seifert, „Factors Influencing Proteolysis and Protein Utilization in the Intestine of Pigs: A Review“, *Animals*, Bd. 11, Nr. 12, S. 3551, Dez. 2021, doi: 10.3390/ani11123551.

[12] J. Renukuntla, A. D. Vadlapudi, A. Patel, S. H. S. Boddu, und A. K. Mitra, „Approaches for enhancing oral bioavailability of peptides and proteins“, *Int. J. Pharm.*, Bd. 447, Nr. 1–2, S. 75–93, Apr. 2013, doi: 10.1016/j.ijpharm.2013.02.030.

[13] A. Viehof, L. Javot, A. Béduneau, Y. Pellequer, und A. Lamprecht, „Oral insulin delivery in rats by nanoparticles prepared with non-toxic solvents“, *Int. J. Pharm.*, Bd. 443, Nr. 1–2, S. 169–174, Feb. 2013, doi: 10.1016/j.ijpharm.2013.01.017.

[14] H. O. Alpar, S. Somavarapu, K. N. Atuah, und V. W. Bramwell, „Biodegradable mucoadhesive particulates for nasal and pulmonary antigen and DNA delivery“,

Adv. Drug Deliv. Rev., Bd. 57, Nr. 3, S. 411–430, Jan. 2005, doi: 10.1016/j.addr.2004.09.004.

[15] U. B. Kompella und V. H. Lee, „Delivery systems for penetration enhancement of peptide and protein drugs: design considerations“, *Adv. Drug Deliv. Rev.*, Bd. 46, Nr. 1–3, S. 211–245, März 2001, doi: 10.1016/s0169-409x(00)00137-x.

[16] W. R. Gombotz und D. K. Pettit, „Biodegradable polymers for protein and peptide drug delivery“, *Bioconjug. Chem.*, Bd. 6, Nr. 4, S. 332–351, 1995, doi: 10.1021/bc00034a002.

[17] H.-C. Mahler, W. Friess, U. Grauschopf, und S. Kiese, „Protein aggregation: Pathways, induction factors and analysis“, *J. Pharm. Sci.*, Bd. 98, Nr. 9, S. 2909–2934, Sep. 2009, doi: 10.1002/jps.21566.

[18] P. S. Odegard und K. L. Capoccia, „Inhaled Insulin: Exubera“, *Ann. Pharmacother.*, Bd. 39, Nr. 5, S. 843–853, Mai 2005, doi: 10.1345/aph.1E522.

[19] J. T. Pinto *u. a.*, „Progress in spray-drying of protein pharmaceuticals: Literature analysis of trends in formulation and process attributes“, *Dry. Technol.*, Bd. 39, Nr. 11, S. 1415–1446, Aug. 2021, doi: 10.1080/07373937.2021.1903032.

[20] L. Heinemann, „The Failure of Exubera: Are We Beating a Dead Horse?“, *J. Diabetes Sci. Technol.*, Bd. 2, Nr. 3, S. 518–529, Mai 2008, doi: 10.1177/193229680800200325.

[21] W. Al-Azzam, E. A. Pastrana, und K. Griebenow, „Co-lyophilization of bovine serum albumin (BSA) with poly(ethylene glycol) improves efficiency of BSA encapsulation and stability in polyester microspheres by a solid-in-oil-in-oil technique“, S. 8.

[22] A. Rezvankhah, Z. Emam-Djomeh, und G. Askari, „Encapsulation and delivery of bioactive compounds using spray and freeze-drying techniques: A review“, *Dry. Technol.*, Bd. 38, Nr. 1–2, S. 235–258, Jan. 2020, doi: 10.1080/07373937.2019.1653906.

[23] R. J. Mehta, A. Gastaldelli, B. Balas, A. Ricotti, R. A. DeFronzo, und D. Tripathy, „Mechanism of Action of Inhaled Insulin on Whole Body Glucose Metabolism in Subjects with Type 2 Diabetes Mellitus“, *Int. J. Mol. Sci.*, Bd. 20, Nr. 17, S. 4230, Aug. 2019, doi: 10.3390/ijms20174230.

[24] A. Cossé, C. König, A. Lamprecht, und K. G. Wagner, „Hot Melt Extrusion for Sustained Protein Release: Matrix Erosion and In Vitro Release of PLGA-Based Implants“, *AAPS PharmSciTech*, Bd. 18, Nr. 1, S. 15–26, Jan. 2017, doi: 10.1208/s12249-016-0548-5.

[25] K. Dauer, C. Werner, D. Lindenblatt, und K. G. Wagner, „Impact of process stress on protein stability in highly-loaded solid protein/PEG formulations from small-scale melt extrusion“, *Int. J. Pharm. X*, S. 100154, Dez. 2022, doi: 10.1016/j.ijpx.2022.100154.

[26] Y. Y. Elsayed, T. Kühl, K. Dauer, A. Sayin, K. G. Wagner, und D. Imhof, „Bioanalytical Workflow for Qualitative and Quantitative Assessment of Hot-Melt Extruded Lysozyme Formulations“, *ACS Omega*, Bd. 7, Nr. 45, S. 40836–40843, Nov. 2022, doi: 10.1021/acsomega.2c03559.

[27] S. N. Eggerstedt, M. Dietzel, M. Sommerfeld, R. Süverkrüp, und A. Lamprecht, „Protein spheres prepared by drop jet freeze drying“, *Int. J. Pharm.*, Bd. 438, Nr. 1–2, S. 160–166, Nov. 2012, doi: 10.1016/j.ijpharm.2012.08.035.

[28] T. M. Serim, J. Kožák, A. Rautenberg, A. N. Özdemir, Y. Pellequer, und A. Lamprecht, „Spray Freeze Dried Lyospheres® for Nasal Administration of Insulin“, *Pharmaceutics*, Bd. 13, Nr. 6, S. 852, Juni 2021, doi: 10.3390/pharmaceutics13060852.

[29] T. Sanvictores und F. Farci, „Biochemistry, Primary Protein Structure“, in *StatPearls [Internet]*, StatPearls Publishing, 2022. Zugegriffen: 4. Mai 2023. [Online]. Verfügbar unter: https://www.ncbi.nlm.nih.gov/books/NBK564343/

[30] B. Alberts, A. Johnson, J. Lewis, M. Raff, K. Roberts, und P. Walter, „The Shape and Structure of Proteins“, in *Molecular Biology of the Cell. 4th edition*, Garland Science, 2002. Zugegriffen: 15. Mai 2023. [Online]. Verfügbar unter: https://www.ncbi.nlm.nih.gov/books/NBK26830/

[31] P. D. Sun, C. E. Foster, und J. C. Boyington, „Overview of Protein Structural and Functional Folds“, *Curr. Protoc. Protein Sci.*, Bd. 35, Nr. 1, Feb. 2004, doi: 10.1002/0471140864.ps1701s35.

[32] J. Jenkins und R. Pickersgill, „The architecture of parallel β-helices and related folds“, *Prog. Biophys. Mol. Biol.*, Bd. 77, Nr. 2, S. 111–175, Okt. 2001, doi: 10.1016/S0079-6107(01)00013-X.

[33] K. Kappel, I. Jarmoskaite, P. P. Vaidyanathan, W. J. Greenleaf, D. Herschlag, und R. Das, „Blind tests of RNA–protein binding affinity prediction“, *Proc. Natl. Acad. Sci. U. S. A.*, Bd. 116, Nr. 17, S. 8336–8341, Apr. 2019, doi: 10.1073/pnas.1819047116.

[34] M. Banach, L. Konieczny, und I. Roterman, „Secondary and Supersecondary Structure of Proteins in Light of the Structure of Hydrophobic Cores“, *Methods Mol. Biol. Clifton NJ*, Bd. 1958, S. 347–378, 2019, doi: 10.1007/978-1-4939-9161-7_19.

[35] P. P. Nakka, K. Li, und D. Forciniti, „Effect of Differences in the Primary Structure of the A-Chain on the Aggregation of Insulin Fragments“, *ACS Omega*, Bd. 3, Nr. 8, S. 9636–9647, Aug. 2018, doi: 10.1021/acsomega.8b00500.

[36] S.-G. Chang, K.-D. Choi, S.-H. Jang, und H.-C. Shin, „Role of disulfide bonds in the structure and activity of human insulin“, *Mol. Cells*, Bd. 16, Nr. 3, S. 323–330, Dez. 2003.

[37] K. Huus, S. Havelund, H. B. Olsen, M. van de Weert, und S. Frokjaer, „Thermal Dissociation and Unfolding of Insulin“, *Biochemistry*, Bd. 44, Nr. 33, S. 11171–11177, Aug. 2005, doi: 10.1021/bi0507940.

[38] Q. Hua und M. A. Weiss, „Mechanism of Insulin Fibrillation“, *J. Biol. Chem.*, Bd. 279, Nr. 20, S. 21449–21460, Mai 2004, doi: 10.1074/jbc.M314141200.

[39] L. Nielsen, S. Frokjaer, J. F. Carpenter, und J. Brange, „Studies of the structure of insulin fibrils by Fourier transform infrared (FTIR) spectroscopy and electron microscopy“, *J. Pharm. Sci.*, Bd. 90, Nr. 1, S. 29–37, Jan. 2001, doi: 10.1002/1520-6017(200101)90:1<29::aid-jps4>3.0.co;2-4.

[40] C. Kilo, N. Mezitis, R. Jain, J. Mersey, J. McGill, und P. Raskin, „Starting patients with type 2 diabetes on insulin therapy using once-daily injections of biphasic insulin aspart 70/30, biphasic human insulin 70/30, or NPH insulin in

combination with metformin“, *J. Diabetes Complications*, Bd. 17, Nr. 6, S. 307–313, Nov. 2003, doi: 10.1016/S1056-8727(03)00076-X.

[41] R. Shah, M. Patel, D. Maahs, und V. Shah, „Insulin delivery methods: Past, present and future“, *Int. J. Pharm. Investig.*, Bd. 6, Nr. 1, S. 1, 2016, doi: 10.4103/2230-973X.176456.

[42] G. Lesnierowski und J. Kijowski, „Lysozyme“, in *Bioactive Egg Compounds*, R. Huopalahti, R. López-Fandiño, M. Anton, und R. Schade, Hrsg., Berlin, Heidelberg: Springer Berlin Heidelberg, 2007, S. 33–42. doi: 10.1007/978-3-540-37885-3_6.

[43] P. Komorek, B. Jachimska, und I. Brand, „Adsorption of lysozyme on gold surfaces in the presence of an external electric potential“, *Bioelectrochemistry*, Bd. 142, S. 107946, Dez. 2021, doi: 10.1016/j.bioelechem.2021.107946.

[44] B. Gilquin, C. Guilbert, und D. Perahia, „Unfolding of hen egg lysozyme by molecular dynamics simulations at 300K: insight into the role of the interdomain interface“, *Proteins*, Bd. 41, Nr. 1, S. 58–74, Okt. 2000.

[45] C. Redfield und C. M. Dobson, „Sequential proton NMR assignments and secondary structure of hen egg white lysozyme in solution“, *Biochemistry*, Bd. 27, Nr. 1, S. 122–136, Jan. 1988, doi: 10.1021/bi00401a020.

[46] R. C. Davies, A. Neuberger, und B. M. Wilson, „The dependence of lysozyme activity on pH and ionic strength“, *Biochim. Biophys. Acta BBA - Enzymol.*, Bd. 178, Nr. 2, S. 294–305, Apr. 1969, doi: 10.1016/0005-2744(69)90397-0.

[47] M. F. Melzig und R. Helal, „Determination of lysozyme activity by a fluorescence technique in comparison with the classical turbidity assay“, *Phamazie*, Nr. 6, S. 415–419, Juni 2008, doi: 10.1691/ph.2008.7846.

[48] K. A. Majorek *u. a.*, „Structural and immunologic characterization of bovine, horse, and rabbit serum albumins“, *Mol. Immunol.*, Bd. 52, Nr. 3–4, S. 174–182, Okt. 2012, doi: 10.1016/j.molimm.2012.05.011.

[49] A. Jahanban-Esfahlan, A. Ostadrahimi, R. Jahanban-Esfahlan, L. Roufegarinejad, M. Tabibiazar, und R. Amarowicz, „Recent developments in the detection of bovine serum albumin“, *Int. J. Biol. Macromol.*, Bd. 138, S. 602–617, Okt. 2019, doi: 10.1016/j.ijbiomac.2019.07.096.

[50] D. Pangeni, C. Kapil, M. A. Jairajpuri, und P. Sen, „Inter-domain helix h10DOMI–h1DOMII is important in the molecular interaction of bovine serum albumin with curcumin: spectroscopic and computational analysis“, *Eur. Biophys. J.*, Bd. 44, Nr. 3, S. 139–148, Apr. 2015, doi: 10.1007/s00249-015-1009-x.

[51] R. Lu, W.-W. Li, A. Katzir, Y. Raichlin, H.-Q. Yu, und B. Mizaikoff, „Probing the secondary structure of bovine serum albumin during heat-induced denaturation using mid-infrared fiberoptic sensors“, *The Analyst*, Bd. 140, Nr. 3, S. 765–770, 2015, doi: 10.1039/C4AN01495B.

[52] D. Rout, S. Sharma, P. Agarwala, A. K. Upadhyaya, A. Sharma, und D. K. Sasmal, „Interaction of Ibuprofen with Partially Unfolded Bovine Serum Albumin in the Presence of Ionic Micelles and Oligosaccharides at Different λ_{ex} and pH: A Spectroscopic Analysis“, *ACS Omega*, Bd. 8, Nr. 3, S. 3114–3128, Jan. 2023, doi: 10.1021/acsomega.2c06447.

[53] L. R. S. Barbosa, M. G. Ortore, F. Spinozzi, P. Mariani, S. Bernstorff, und R. Itri, „The Importance of Protein-Protein Interactions on the pH-Induced

Conformational Changes of Bovine Serum Albumin: A Small-Angle X-Ray Scattering Study“, *Biophys. J.*, Bd. 98, Nr. 1, S. 147–157, Jan. 2010, doi: 10.1016/j.bpj.2009.09.056.

[54] F. Ameseder, R. Biehl, O. Holderer, D. Richter, und A. M. Stadler, „Localised contacts lead to nanosecond hinge motions in dimeric bovine serum albumin“, *Phys. Chem. Chem. Phys.*, Bd. 21, Nr. 34, S. 18477–18485, 2019, doi: 10.1039/C9CP01847F.

[55] K. Dauer, W. Kamm, K. G. Wagner, und S. Pfeiffer-Marek, „High-Throughput Screening for Colloidal Stability of Peptide Formulations Using Dynamic and Static Light Scattering“, *Mol Pharm.*, S. 17, 2021.

[56] W. Wang, „Instability, stabilization, and formulation of liquid protein pharmaceuticals“, *Int. J. Pharm.*, Bd. 185, Nr. 2, S. 129–188, Aug. 1999, doi: 10.1016/S0378-5173(99)00152-0.

[57] A. K. Banga, *Therapeutic Peptides and Proteins: Formulation, Processing, and Delivery Systems, Third Edition*, 0 Aufl. CRC Press, 2015. doi: 10.1201/b18392.

[58] T. Arakawa, Y. Kita, und J. F. Carpenter, „Protein–Solvent Interactions in Pharmaceutical Formulations“, *Pharm. Res.*, Bd. 08, Nr. 3, S. 285–291, 1991, doi: 10.1023/A:1015825027737.

[59] M. J. Pikal, „Mechanisms of protein stabilization in the solid state“, *J. Pharm. Sci.*, Bd. 98, Nr. 9, S. 23, 2009.

[60] M. C. Manning, D. K. Chou, B. M. Murphy, R. W. Payne, und D. S. Katayama, „Stability of Protein Pharmaceuticals: An Update“, *Pharm. Res.*, Bd. 27, Nr. 4, S. 544–575, Apr. 2010, doi: 10.1007/s11095-009-0045-6.

[61] M. E. Krause und E. Sahin, „Chemical and physical instabilities in manufacturing and storage of therapeutic proteins“, *Curr. Opin. Biotechnol.*, Bd. 60, S. 159–167, Dez. 2019, doi: 10.1016/j.copbio.2019.01.014.

[62] R. Krishnamurthy und M. Manning, „The Stability Factor: Importance in Formulation Development“, *Curr. Pharm. Biotechnol.*, Bd. 3, Nr. 4, S. 361–371, Dez. 2002, doi: 10.2174/1389201023378229.

[63] J. L. Cleland, M. F. Powell, und S. J. Shire, „The development of stable protein formulations: a close look at protein aggregation, deamidation, and oxidation“, *Crit. Rev. Ther. Drug Carrier Syst.*, Bd. 10, Nr. 4, S. 307–377, 1993.

[64] M. C. Manning, J. Liu, T. Li, und R. E. Holcomb, „Rational Design of Liquid Formulations of Proteins“, in *Advances in Protein Chemistry and Structural Biology*, Elsevier, 2018, S. 1–59. doi: 10.1016/bs.apcsb.2018.01.005.

[65] T. Geiger und S. Clarke, „Deamidation, isomerization, and racemization at asparaginyl and aspartyl residues in peptides. Succinimide-linked reactions that contribute to protein degradation.“, *J. Biol. Chem.*, Bd. 262, Nr. 2, S. 785–794, Jan. 1987, doi: 10.1016/S0021-9258(19)75855-4.

[66] M. Karimi *u. a.*, „Reactivity of disulfide bonds is markedly affected by structure and environment: implications for protein modification and stability“, *Sci. Rep.*, Bd. 6, Nr. 1, Art. Nr. 1, Dez. 2016, doi: 10.1038/srep38572.

[67] L. Jorgensen, S. Hostrup, E. H. Moeller, und H. Grohganz, „Recent trends in stabilising peptides and proteins in pharmaceutical formulation –

considerations in the choice of excipients“, *Expert Opin. Drug Deliv.*, Bd. 6, Nr. 11, S. 1219–1230, Nov. 2009, doi: 10.1517/17425240903199143.

[68] E. J. McNally, E. McNally, J. E. Hastedt, und J. E. Hastedt, Hrsg., *Protein Formulation and Delivery*, 0 Aufl. CRC Press, 2007. doi: 10.3109/9780849379529.

[69] C. J. Roberts, „Protein aggregation and its impact on product quality“, *Curr. Opin. Biotechnol.*, Bd. 30, S. 211–217, Dez. 2014, doi: 10.1016/j.copbio.2014.08.001.

[70] W. Wang, S. Nema, und D. Teagarden, „Protein aggregation—Pathways and influencing factors“, *Int. J. Pharm.*, Bd. 390, Nr. 2, S. 89–99, Mai 2010, doi: 10.1016/j.ijpharm.2010.02.025.

[71] S. Kiese, A. Papppenberger, W. Friess, und H.-C. Mahler, „Shaken, not stirred: Mechanical stress testing of an IgG1 antibody“, *J. Pharm. Sci.*, Bd. 97, Nr. 10, S. 4347–4366, 2008, doi: 10.1002/jps.21328.

[72] H.-C. Mahler und W. Jiskoot, *Analysis of aggregates and particles in protein pharmaceuticals*. Hoboken, N.J.: John Wiley & Sons, 2012.

[73] L. Nicoud, M. Lattuada, A. Yates, und M. Morbidelli, „Impact of aggregate formation on the viscosity of protein solutions“, *Soft Matter*, Bd. 11, Nr. 27, S. 5513–5522, 2015, doi: 10.1039/C5SM00513B.

[74] S. Amin, G. V. Barnett, J. A. Pathak, C. J. Roberts, und P. S. Sarangapani, „Protein aggregation, particle formation, characterization & rheology“, *Curr. Opin. Colloid Interface Sci.*, Bd. 19, Nr. 5, S. 438–449, Okt. 2014, doi: 10.1016/j.cocis.2014.10.002.

[75] W. G. Lilyestrom, S. Yadav, S. J. Shire, und T. M. Scherer, „Monoclonal Antibody Self-Association, Cluster Formation, and Rheology at High Concentrations“, *J. Phys. Chem. B*, Bd. 117, Nr. 21, S. 6373–6384, Mai 2013, doi: 10.1021/jp4008152.

[76] V. Burckbuchler, G. Mekhloufi, A. P. Giteau, J. L. Grossiord, S. Huille, und F. Agnely, „Rheological and syringeability properties of highly concentrated human polyclonal immunoglobulin solutions“, *Eur. J. Pharm. Biopharm.*, Bd. 76, Nr. 3, S. 351–356, Nov. 2010, doi: 10.1016/j.ejpb.2010.08.002.

[77] D. J. Houde, Hrsg., *Biophysical characterization of proteins in developing biopharmaceuticals*. Amsterdam: Elsevier, 2015.

[78] A. Sharma, D. Khamar, S. Cullen, A. Hayden, und H. Hughes, „Innovative Drying Technologies for Biopharmaceuticals“, *Int. J. Pharm.*, Bd. 609, S. 121115, Nov. 2021, doi: 10.1016/j.ijpharm.2021.121115.

[79] A. Blumlein und J. J. McManus, „Reversible and non-reversible thermal denaturation of lysozyme with varying pH at low ionic strength“, *Biochim. Biophys. Acta BBA - Proteins Proteomics*, Bd. 1834, Nr. 10, S. 2064–2070, Okt. 2013, doi: 10.1016/j.bbapap.2013.06.001.

[80] K. D. Ratanji, J. P. Derrick, R. J. Dearman, und I. Kimber, „Immunogenicity of therapeutic proteins: influence of aggregation“, *J. Immunotoxicol.*, Bd. 11, Nr. 2, S. 99–109, Juni 2014, doi: 10.3109/1547691X.2013.821564.

[81] D. J. A. Crommelin, A. Hawe, und W. Jiskoot, „Formulation of Biologics Including Biopharmaceutical Considerations“, in *Pharmaceutical Biotechnology*, D. J. A. Crommelin, R. D. Sindelar, und B. Meibohm, Hrsg.,

Cham: Springer International Publishing, 2019, S. 83–103. doi: 10.1007/978-3-030-00710-2_5.

[82] R. L. Remmele, S. Krishnan, und W. J. Callahan, „Development of Stable Lyophilized Protein Drug Products“, *Curr. Pharm. Biotechnol.*, Bd. 13, Nr. 3, S. 471–496, März 2012, doi: 10.2174/138920112799361990.

[83] H. Svilenov und G. Winter, „Rapid sample-saving biophysical characterisation and long-term storage stability of liquid interferon alpha2a formulations: Is there a correlation?“, *Int. J. Pharm.*, Bd. 562, S. 42–50, Mai 2019, doi: 10.1016/j.ijpharm.2019.03.025.

[84] N. Whitaker *u. a.*, „A Formulation Development Approach to Identify and Select Stable Ultra–High-Concentration Monoclonal Antibody Formulations With Reduced Viscosities“, *J. Pharm. Sci.*, Bd. 106, Nr. 11, S. 3230–3241, Nov. 2017, doi: 10.1016/j.xphs.2017.06.017.

[85] C. D. Ren *u. a.*, „Application of a High Throughput and Automated Workflow to Therapeutic Protein Formulation Development“, *J. Pharm. Sci.*, Bd. 110, Nr. 3, S. 1130–1141, März 2021, doi: 10.1016/j.xphs.2020.10.040.

[86] W. Jiskoot *u. a.*, „Protein Instability and Immunogenicity: Roadblocks to Clinical Application of Injectable Protein Delivery Systems for Sustained Release“, *J. Pharm. Sci.*, Bd. 101, Nr. 3, S. 946–954, März 2012, doi: 10.1002/jps.23018.

[87] A. van Maarschalkerweerd, G.-J. Wolbink, S. O. Stapel, W. Jiskoot, und A. Hawe, „Comparison of analytical methods to detect instability of etanercept during thermal stress testing“, *Eur. J. Pharm. Biopharm.*, Bd. 78, Nr. 2, S. 213–221, Juni 2011, doi: 10.1016/j.ejpb.2011.01.012.

[88] A. Hawe, M. Wiggenhorn, M. van de Weert, J. H. O. Garbe, H. Mahler, und W. Jiskoot, „Forced Degradation of Therapeutic Proteins“, *J. Pharm. Sci.*, Bd. 101, Nr. 3, S. 895–913, März 2012, doi: 10.1002/jps.22812.

[89] P. Manikwar *u. a.*, „Correlating excipient effects on conformational and storage stability of an IgG1 monoclonal antibody with local dynamics as measured by hydrogen/deuterium-exchange mass spectrometry“, *J. Pharm. Sci.*, Bd. 102, Nr. 7, S. 2136–2151, Juli 2013, doi: 10.1002/jps.23543.

[90] A. L. Daniels und T. W. Randolph, „Flow Microscopy Imaging Is Sensitive to Characteristics of Subvisible Particles in Peginesatide Formulations Associated With Severe Adverse Reactions“, *J. Pharm. Sci.*, Bd. 107, Nr. 5, S. 1313–1321, Mai 2018, doi: 10.1016/j.xphs.2018.01.015.

[91] I. Fawaz, S. Schaz, A. Boehrer, P. Garidel, und M. Blech, „Micro-flow imaging multi-instrument evaluation for sub-visible particle detection“, *Eur. J. Pharm. Biopharm.*, Bd. 185, S. 55–70, Apr. 2023, doi: 10.1016/j.ejpb.2023.01.017.

[92] F. Schleinzer, M. Strebl, M. Blech, und P. Garidel, „Backgrounded Membrane Imaging—A Valuable Alternative for Particle Detection of Biotherapeutics?“, *J. Pharm. Innov.*, Mai 2023, doi: 10.1007/s12247-023-09734-5.

[93] A. Bolje und S. Gobec, „Analytical Techniques for Structural Characterization of Proteins in Solid Pharmaceutical Forms: An Overview“, *Pharmaceutics*, Bd. 13, Nr. 4, S. 534, Apr. 2021, doi: 10.3390/pharmaceutics13040534.

[94] P. Manikwar *u. a.*, „Correlating Excipient Effects on Conformational and Storage Stability of an IgG1 Monoclonal Antibody with Local Dynamics as Measured by Hydrogen/Deuterium-Exchange Mass Spectrometry“, *J. Pharm. Sci.*, Bd. 102, Nr. 7, S. 2136–2151, Juli 2013, doi: 10.1002/jps.23543.

[95] H. Ma, C. Ó'Fágáin, und R. O'Kennedy, „Antibody stability: A key to performance - Analysis, influences and improvement", *Biochimie*, Bd. 177, S. 213–225, Okt. 2020, doi: 10.1016/j.biochi.2020.08.019.

[96] H. Goshima *u. a.*, „Addition of Monovalent Electrolytes to Improve Storage Stability of Freeze-Dried Protein Formulations", *J. Pharm. Sci.*, Bd. 105, Nr. 2, S. 530–541, Feb. 2016, doi: 10.1016/j.xphs.2015.10.004.

[97] W. Wang, „Advanced protein formulations: Protein Formulations", *Protein Sci.*, Bd. 24, Nr. 7, S. 1031–1039, Juli 2015, doi: 10.1002/pro.2684.

[98] K. Dauer, S. Pfeiffer-Marek, W. Kamm, und K. G. Wagner, „Microwell Plate-Based Dynamic Light Scattering as a High-Throughput Characterization Tool in Biopharmaceutical Development", *Pharmaceutics*, Bd. 13, Nr. 2, S. 172, Jan. 2021, doi: 10.3390/pharmaceutics13020172.

[99] N. Alt *u. a.*, „Determination of critical quality attributes for monoclonal antibodies using quality by design principles", *Biologicals*, Bd. 44, Nr. 5, S. 291–305, Sep. 2016, doi: 10.1016/j.biologicals.2016.06.005.

[100] M. J. Maltesen und M. van de Weert, „Drying methods for protein pharmaceuticals", *Drug Discov. Today Technol.*, Bd. 5, Nr. 2, S. e81–e88, Sep. 2008, doi: 10.1016/j.ddtec.2008.11.001.

[101] F. Emami, A. Vatanara, E. Park, und D. Na, „Drying Technologies for the Stability and Bioavailability of Biopharmaceuticals", *Pharmaceutics*, Bd. 10, Nr. 3, S. 131, Aug. 2018, doi: 10.3390/pharmaceutics10030131.

[102] K. Traub-Hoffmann, B. Furtmann, L. Laber, S. Helm, C. Geiger, und T. Bussemer, „Standardization of the Reconstitution Procedure of Protein Lyophilizates as a Key Parameter to Control Product Stability", *J. Pharm. Sci.*, Bd. 109, Nr. 1, S. 211–215, Jan. 2020, doi: 10.1016/j.xphs.2019.10.032.

[103] Y. Ionova und L. Wilson, „Biologic excipients: Importance of clinical awareness of inactive ingredients", *PLOS ONE*, Bd. 15, Nr. 6, S. e0235076, Juni 2020, doi: 10.1371/journal.pone.0235076.

[104] S. Pramanick, D. Singodia, und V. Chandel, „Excipient Selection In Parenteral Formulation Development", Bd. 45, Nr. 3, S. 14, 2013.

[105] E. T. Maggio, „Use of excipients to control aggregation in peptide and protein formulations.", *J. Excip. Food Chem.*, S. 10, Sep. 2010.

[106] H. Narayanan *u. a.*, „Design of Biopharmaceutical Formulations Accelerated by Machine Learning", *Mol. Pharm.*, Bd. 18, Nr. 10, S. 3843–3853, Okt. 2021, doi: 10.1021/acs.molpharmaceut.1c00469.

[107] S. Brudar und B. Hribar-Lee, „Effect of Buffer on Protein Stability in Aqueous Solutions: A Simple Protein Aggregation Model", *J. Phys. Chem. B*, Bd. 125, Nr. 10, S. 2504–2512, März 2021, doi: 10.1021/acs.jpcb.0c10339.

[108] T. J. Zbacnik *u. a.*, „Role of Buffers in Protein Formulations", *J. Pharm. Sci.*, Bd. 106, Nr. 3, S. 713–733, März 2017, doi: 10.1016/j.xphs.2016.11.014.

[109] V. Vagenende, M. G. S. Yap, und B. L. Trout, „Mechanisms of Protein Stabilization and Prevention of Protein Aggregation by Glycerol", *Biochemistry*, Bd. 48, Nr. 46, S. 11084–11096, Nov. 2009, doi: 10.1021/bi900649t.

[110] S. Ohtake, Y. Kita, und T. Arakawa, „Interactions of formulation excipients with proteins in solution and in the dried state", *Adv. Drug Deliv. Rev.*, Bd. 63, Nr. 13, S. 1053–1073, Okt. 2011, doi: 10.1016/j.addr.2011.06.011.

[111] R. C. Rowe, Hrsg., *Handbook of pharmaceutical excipients*, 6. ed. London: APhA, (PhP) Pharmaceutical Press, 2009.

[112] H.-C. Mahler und R. Mathäs, „Trends in Formulation and Drug Delivery for Antibodies“, in *Process Scale Purification of Antibodies*, John Wiley & Sons, Ltd, 2017, S. 673–697. doi: 10.1002/9781119126942.ch31.

[113] E. V. Brovč, J. Mravljak, R. Šink, und S. Pajk, „Rational design to biologics development: The polysorbates point of view“, *Int. J. Pharm.*, Bd. 581, S. 119285, Mai 2020, doi: 10.1016/j.ijpharm.2020.119285.

[114] A. J. Castañeda Ruiz *u. a.*, „Alternative Excipients for Protein Stabilization in Protein Therapeutics: Overcoming the Limitations of Polysorbates“, *Pharmaceutics*, Bd. 14, Nr. 12, S. 2575, Nov. 2022, doi: 10.3390/pharmaceutics14122575.

[115] M. Katakam, L. N. Bell, und A. K. Banga, „Effect of Surfactants on the Physical Stability of Recombinant Human Growth Hormone“, *J. Pharm. Sci.*, Bd. 84, Nr. 6, S. 713–716, Juni 1995, doi: 10.1002/jps.2600840609.

[116] T. Arakawa und Y. Kita, „Protection of Bovine Serum Albumin from Aggregation by Tween 80“, *J. Pharm. Sci.*, Bd. 89, Nr. 5, S. 646–651, Mai 2000, doi: 10.1002/(SICI)1520-6017(200005)89:5<646::AID-JPS10>3.0.CO;2-J.

[117] E. Y. Chi, S. Krishnan, T. W. Randolph, und J. F. Carpenter, „Physical Stability of Proteins in Aqueous Solution: Mechanism and Driving Forces in Nonnative Protein Aggregation“, *Pharm. Res.*, Bd. 20, Nr. 9, S. 1325–1336, 2003, doi: 10.1023/A:1025771421906.

[118] F. Begum und S. Amin, „Investigating the Influence of Polysorbate 20/80 and Polaxomer P188 on the Surface & Interfacial Properties of Bovine Serum Albumin and Lysozyme“, *Pharm. Res.*, Bd. 36, Nr. 7, S. 107, Mai 2019, doi: 10.1007/s11095-019-2631-6.

[119] L. Stroppel *u. a.*, „Antimicrobial Preservatives for Protein and Peptide Formulations: An Overview“, *Pharmaceutics*, Bd. 15, Nr. 2, S. 563, Feb. 2023, doi: 10.3390/pharmaceutics15020563.

[120] S. M. Singh, R. L. Hutchings, und K. M. G. Mallela, „Mechanisms of m-cresol-induced Protein Aggregation Studied Using a Model Protein Cytochrome c“, *J. Pharm. Sci.*, Bd. 100, Nr. 5, S. 1679–1689, Mai 2011, doi: 10.1002/jps.22426.

[121] T. Arakawa *u. a.*, „Suppression of protein interactions by arginine: A proposed mechanism of the arginine effects“, *Biophys. Chem.*, Bd. 127, Nr. 1, S. 1–8, Apr. 2007, doi: 10.1016/j.bpc.2006.12.007.

[122] N. A. Kim, S. Hada, R. Thapa, und S. H. Jeong, „Arginine as a protein stabilizer and destabilizer in liquid formulations“, *Int. J. Pharm.*, Bd. 513, Nr. 1–2, S. 26–37, Nov. 2016, doi: 10.1016/j.ijpharm.2016.09.003.

[123] C. Lange und R. Rudolph, „Suppression of Protein Aggregation by L-Arginine“, *Curr. Pharm. Biotechnol.*, Bd. 10, Nr. 4, S. 408–414, Juni 2009, doi: 10.2174/138920109788488851.

[124] D. Shukla und B. L. Trout, „Interaction of Arginine with Proteins and the Mechanism by Which It Inhibits Aggregation“, *J. Phys. Chem. B*, Bd. 114, Nr. 42, S. 13426–13438, Okt. 2010, doi: 10.1021/jp108399g.

[125] L. Platts, S. J. Darby, und R. J. Falconer, „Control of Globular Protein Thermal Stability in Aqueous Formulations by the Positively Charged Amino Acid

Excipients“, *J. Pharm. Sci.*, Bd. 105, Nr. 12, S. 3532–3536, Dez. 2016, doi: 10.1016/j.xphs.2016.09.013.

[126] S. Taneja und F. Ahmad, „Increased thermal stability of proteins in the presence of amino acids“, *Biochem. J.*, Bd. 303, Nr. 1, S. 147–153, Okt. 1994, doi: 10.1042/bj3030147.

[127] Z. Shahrokh, V. Sluzky, J. L. Cleland, S. J. Shire, und T. W. Randolph, Hrsg., *Therapeutic Protein and Peptide Formulation and Delivery*, Bd. 675. in ACS Symposium Series, vol. 675. Washington, DC: American Chemical Society, 1997. doi: 10.1021/bk-1997-0675.

[128] M. Zalar, H. L. Svilenov, und A. P. Golovanov, „Binding of excipients is a poor predictor for aggregation kinetics of biopharmaceutical proteins“, *Eur. J. Pharm. Biopharm.*, S. S0939641120300849, Apr. 2020, doi: 10.1016/j.ejpb.2020.04.002.

[129] Y. Chen, T. T. Mutukuri, N. E. Wilson, und Q. (Tony) Zhou, „Pharmaceutical protein solids: Drying technology, solid-state characterization and stability“, *Adv. Drug Deliv. Rev.*, Bd. 172, S. 211–233, Mai 2021, doi: 10.1016/j.addr.2021.02.016.

[130] L. W. Simpson, T. A. Good, und J. B. Leach, „Protein folding and assembly in confined environments: Implications for protein aggregation in hydrogels and tissues“, *Biotechnol. Adv.*, S. 107573, Juni 2020, doi: 10.1016/j.biotechadv.2020.107573.

[131] L. (Lucy) Chang *u. a.*, „Mechanism of protein stabilization by sugars during freeze-drying and storage: Native structure preservation, specific interaction, and/or immobilization in a glassy matrix?“, *J. Pharm. Sci.*, Bd. 94, Nr. 7, S. 1427–1444, Juli 2005, doi: 10.1002/jps.20364.

[132] R. Fang, W. Obeidat, M. J. Pikal, und R. H. Bogner, „Evaluation of Predictors of Protein Relative Stability Obtained by Solid-State Hydrogen/Deuterium Exchange Monitored by FTIR“, *Pharm. Res.*, Bd. 37, Nr. 9, S. 168, Sep. 2020, doi: 10.1007/s11095-020-02897-7.

[133] K. Schersch, O. Betz, P. Garidel, S. Muehlau, S. Bassarab, und G. Winter, „Systematic investigation of the effect of lyophilizate collapse on pharmaceutically relevant proteins III: Collapse during storage at elevated temperatures“, *Eur. J. Pharm. Biopharm.*, Bd. 85, Nr. 2, S. 240–252, Okt. 2013, doi: 10.1016/j.ejpb.2013.05.009.

[134] K. M. Forney-Stevens, R. H. Bogner, und M. J. Pikal, „Addition of Amino Acids to Further Stabilize Lyophilized Sucrose-Based Protein Formulations: I. Screening of 15 Amino Acids in Two Model Proteins“, *J. Pharm. Sci.*, Bd. 105, Nr. 2, S. 697–704, Feb. 2016, doi: 10.1002/jps.24655.

[135] N. Chieng, M. T. Cicerone, Q. Zhong, M. Liu, und M. J. Pikal, „Characterization of dynamics in complex lyophilized formulations: II. Analysis of density variations in terms of glass dynamics and comparisons with global mobility, fast dynamics, and Positron Annihilation Lifetime Spectroscopy (PALS)“, *Eur. J. Pharm. Biopharm.*, Bd. 85, Nr. 2, S. 197–206, Okt. 2013, doi: 10.1016/j.ejpb.2013.03.036.

[136] M. A. Mensink, „Solid state stabilization of proteins by sugars“, Rijksuniversiteit Groningen, Groningen, 2017.

[137] V. Saluja, J.-P. Amorij, J. C. Kapteyn, A. H. de Boer, H. W. Frijlink, und W. L. J. Hinrichs, „A comparison between spray drying and spray freeze drying to produce an influenza subunit vaccine powder for inhalation“, *J. Control. Release Off. J. Control. Release Soc.*, Bd. 144, Nr. 2, S. 127–133, Juni 2010, doi: 10.1016/j.jconrel.2010.02.025.

[138] J. Massant, „Formulating monoclonal antibodies as powders for reconstitution at high concentration using spray-drying_ Trehalose/amino acid combinations as reconstitution time reducing and stability improving formulations“, *Eur. J. Pharm. Biopharm.*, S. 12, 2020.

[139] S. Wanning, R. Süverkrüp, und A. Lamprecht, „Impact of excipient choice on the aerodynamic performance of inhalable spray-freeze-dried powders“, *Int. J. Pharm.*, Bd. 586, S. 119564, Aug. 2020, doi: 10.1016/j.ijpharm.2020.119564.

[140] A. H. Mohammad Zadeh, A. Rouholamini Najafabadi, A. Vatanara, H. Faghihi, und K. Gilani, „Effect of molecular weight and ratio of poly ethylene glycols' derivatives in combination with trehalose on stability of freeze-dried IgG“, *Drug Dev. Ind. Pharm.*, Bd. 43, Nr. 12, S. 1945–1951, Dez. 2017, doi: 10.1080/03639045.2017.1353520.

[141] M. A. Mensink, H. W. Frijlink, K. van der Voort Maarschalk, und W. L. J. Hinrichs, „How sugars protect proteins in the solid state and during drying (review): Mechanisms of stabilization in relation to stress conditions“, *Eur. J. Pharm. Biopharm.*, Bd. 114, S. 288–295, Mai 2017, doi: 10.1016/j.ejpb.2017.01.024.

[142] M. Adler, M. Unger, und G. Lee, „Surface composition of spray-dried particles of bovine serum albumin/trehalose/surfactant“, *Pharm. Res.*, Bd. 17, Nr. 7, S. 863–870, Juli 2000, doi: 10.1023/a:1007568511399.

[143] Y. F. Maa, P. A. Nguyen, und S. W. Hsu, „Spray-drying of air-liquid interface sensitive recombinant human growth hormone“, *J. Pharm. Sci.*, Bd. 87, Nr. 2, S. 152–159, Feb. 1998, doi: 10.1021/js970308x.

[144] M. Jalalipour, A. Rouholamini Najafabadi, H. Tajerzadeh, K. Gilani, und M. Barghi, „The effect of protein stabilizers on the physical state and aerosol performance of spray-dried albumin microparticles“, *J. Drug Deliv. Sci. Technol.*, Bd. 17, Nr. 2, S. 149–153, Jan. 2007, doi: 10.1016/S1773-2247(07)50023-7.

[145] J. C. K. Lo, H. W. Pan, und J. K. W. Lam, „Inhalable Protein Powder Prepared by Spray-Freeze-Drying Using Hydroxypropyl-β-Cyclodextrin as Excipient“, *Pharmaceutics*, Bd. 13, Nr. 5, S. 615, Apr. 2021, doi: 10.3390/pharmaceutics13050615.

[146] J. Dieplinger, J. T. Pinto, M. Dekner, G. Brachtl, und A. Paudel, „Impact of Different Saccharides on the In-Process Stability of a Protein Drug During Evaporative Drying: From Sessile Droplet Drying to Lab-Scale Spray Drying“, *Pharm. Res.*, Apr. 2023, doi: 10.1007/s11095-023-03498-w.

[147] T. Sou, M. P. McIntosh, L. M. Kaminskas, R. J. Prankerd, und D. A. V. Morton, „Designing a Multicomponent Spray-Dried Formulation Platform for Pulmonary Delivery of Biomacromolecules: The Effect of Polymers on the Formation of an Amorphous Matrix for Glassy State Stabilization of Biomacromolecules“, *Dry. Technol.*, Bd. 31, Nr. 13–14, S. 1451–1458, Okt. 2013, doi: 10.1080/07373937.2013.788019.

[148] J. F. Carpenter, S. J. Prestrelski, und T. Arakawa, „Separation of freezing- and drying-induced denaturation of lyophilized proteins using stress-specific stabilization. I. Enzyme activity and calorimetric studies“, *Arch. Biochem. Biophys.*, Bd. 303, Nr. 2, S. 456–464, Juni 1993, doi: 10.1006/abbi.1993.1309.

[149] M. T. Cicerone, M. J. Pikal, und K. K. Qian, „Stabilization of proteins in solid form“, *Adv. Drug Deliv. Rev.*, Bd. 93, S. 14–24, Okt. 2015, doi: 10.1016/j.addr.2015.05.006.

[150] S. Farinha *u. a.*, „Spray Freeze Drying of Biologics: A Review and Applications for Inhalation Delivery“, *Pharm. Res.*, Dez. 2022, doi: 10.1007/s11095-022-03442-4.

[151] L. Chen, T. Okuda, X.-Y. Lu, und H.-K. Chan, „Amorphous powders for inhalation drug delivery“, *Adv. Drug Deliv. Rev.*, Bd. 100, S. 102–115, Mai 2016, doi: 10.1016/j.addr.2016.01.002.

[152] S. Ji *u. a.*, „Investigation of factors affecting the stability of lysozyme spray dried from ethanol-water solutions“, *Int. J. Pharm.*, Bd. 534, Nr. 1–2, S. 263–271, Dez. 2017, doi: 10.1016/j.ijpharm.2017.10.021.

[153] A. Ziaee *u. a.*, „A rational approach towards spray drying of biopharmaceuticals: The case of lysozyme“, *Powder Technol.*, Bd. 366, S. 206–215, Apr. 2020, doi: 10.1016/j.powtec.2020.02.057.

[154] K. Ståhl, M. Claesson, P. Lilliehorn, H. Lindén, und K. Bäckström, „The effect of process variables on the degradation and physical properties of spray dried insulin intended for inhalation“, *Int. J. Pharm.*, Bd. 233, Nr. 1–2, S. 227–237, Feb. 2002, doi: 10.1016/S0378-5173(01)00945-0.

[155] S. Schüle, W. Frieß, K. Bechtold-Peters, und P. Garidel, „Conformational analysis of protein secondary structure during spray-drying of antibody/mannitol formulations“, *Eur. J. Pharm. Biopharm.*, Bd. 65, Nr. 1, S. 1–9, Jan. 2007, doi: 10.1016/j.ejpb.2006.08.014.

[156] H. Faghihi, A. Vatanara, A. R. Najafabadi, V. Ramezani, und K. Gilani, „The use of amino acids to prepare physically and conformationally stable spray-dried IgG with enhanced aerosol performance“, *Int. J. Pharm.*, Bd. 466, Nr. 1–2, S. 163–171, Mai 2014, doi: 10.1016/j.ijpharm.2014.03.020.

[157] G. Assegehegn, E. Brito-de la Fuente, J. M. Franco, und C. Gallegos, „An Experimental-Based Approach to Construct the Process Design Space of a Freeze-Drying Process: An Effective Tool to Design an Optimum and Robust Freeze-Drying Process for Pharmaceuticals“, *J. Pharm. Sci.*, Bd. 109, Nr. 1, S. 785–796, Jan. 2020, doi: 10.1016/j.xphs.2019.07.001.

[158] M. C. Heller, J. F. Carpenter, und T. W. Randolph, „Manipulation of Lyophilization-Induced Phase Separation: Implications For Pharmaceutical Proteins“, *Biotechnol. Prog.*, Bd. 13, Nr. 5, S. 590–596, Okt. 1997, doi: 10.1021/bp970081b.

[159] A. Al-Hussein und H. Gieseler, „The Effect of Mannitol Crystallization in Mannitol–Sucrose systems on LDH Stability during Freeze-Drying“, *J. Pharm. Sci.*, Bd. 101, Nr. 7, S. 2534–2544, Juli 2012, doi: 10.1002/jps.23173.

[160] S. Telikepalli *u. a.*, „Characterization of the Physical Stability of a Lyophilized IgG1 mAb after Accelerated Shipping-Like Stress“, *J. Pharm. Sci.*, Bd. 104, Nr. 2, S. 495–507, Feb. 2015, doi: 10.1002/jps.24242.

[161] V. Kumar, V. K. Sharma, und D. S. Kalonia, „In situ precipitation and vacuum drying of interferon alpha-2a: development of a single-step process for obtaining dry, stable protein formulation“, *Int. J. Pharm.*, Bd. 366, Nr. 1–2, S. 88–98, Jan. 2009, doi: 10.1016/j.ijpharm.2008.09.001.

[162] D. Nowak und E. Jakubczyk, „The Freeze-Drying of Foods—The Characteristic of the Process Course and the Effect of Its Parameters on the Physical Properties of Food Materials“, *Foods*, Bd. 9, Nr. 10, S. 1488, Okt. 2020, doi: 10.3390/foods9101488.

[163] S. S. Kulkarni, R. Suryanarayanan, J. V. Rinella, und R. H. Bogner, „Mechanisms by which crystalline mannitol improves the reconstitution time of high concentration lyophilized protein formulations“, *Eur. J. Pharm. Biopharm.*, Bd. 131, S. 70–81, Okt. 2018, doi: 10.1016/j.ejpb.2018.07.022.

[164] „<1> Injections., USP 37-NF32“, The United States Pharmecopeia.

[165] W. Cao *u. a.*, „Rational design of lyophilized high concentration protein formulations-mitigating the challenge of slow reconstitution with multidisciplinary strategies“, *Eur. J. Pharm. Biopharm.*, Bd. 85, Nr. 2, S. 287–293, Okt. 2013, doi: 10.1016/j.ejpb.2013.05.001.

[166] X. Tang und M. J. Pikal, „Design of freeze-drying processes for pharmaceuticals: practical advice“, *Pharm. Res.*, Bd. 21, Nr. 2, S. 191–200, Feb. 2004, doi: 10.1023/b:pham.0000016234.73023.75.

[167] M. J. Pikal und S. Shah, „The collapse temperature in freeze drying: Dependence on measurement methodology and rate of water removal from the glassy phase“, *Int. J. Pharm.*, Bd. 62, Nr. 2, S. 165–186, Juli 1990, doi: 10.1016/0378-5173(90)90231-R.

[168] F. Fonseca, S. Passot, O. Cunin, und M. Marin, „Collapse Temperature of Freeze-Dried Lactobacillus bulgaricusSuspensions and Protective Media“, *Biotechnol. Prog.*, Bd. 20, Nr. 1, S. 229–238, Sep. 2008, doi: 10.1021/bp034136n.

[169] C. Haeuser, P. Goldbach, J. Huwyler, W. Friess, und A. Allmendinger, „Be Aggressive! Amorphous Excipients Enabling Single-Step Freeze-Drying of Monoclonal Antibody Formulations“, *Pharmaceutics*, Bd. 11, Nr. 11, S. 616, Nov. 2019, doi: 10.3390/pharmaceutics11110616.

[170] V. R. Koganti *u. a.*, „Investigation of Design Space for Freeze-Drying: Use of Modeling for Primary Drying Segment of a Freeze-Drying Cycle“, *AAPS PharmSciTech*, Bd. 12, Nr. 3, S. 854–861, Sep. 2011, doi: 10.1208/s12249-011-9645-7.

[171] K. Schersch, O. Betz, P. Garidel, S. Muehlau, S. Bassarab, und G. Winter, „Systematic investigation of the effect of lyophilizate collapse on pharmaceutically relevant proteins I: Stability after freeze-drying“, *J. Pharm. Sci.*, Bd. 99, Nr. 5, S. 2256–2278, Mai 2010, doi: 10.1002/jps.22000.

[172] K. Schersch, O. Betz, P. Garidel, S. Muehlau, S. Bassarab, und G. Winter, „Systematic Investigation of the Effect of Lyophilizate Collapse on Pharmaceutically Relevant Proteins, Part 2: Stability During Storage at Elevated Temperatures“, *J. Pharm. Sci.*, Bd. 101, Nr. 7, S. 2288–2306, Juli 2012, doi: 10.1002/jps.23121.

[173] S. Groël, T. Menzen, und G. Winter, „Calorimetric Investigation of the Relaxation Phenomena in Amorphous Lyophilized Solids“, *Pharmaceutics*, Bd. 13, Nr. 10, S. 1735, Okt. 2021, doi: 10.3390/pharmaceutics13101735.

[174] R. E. Johnson, M. E. Oldroyd, S. S. Ahmed, H. Gieseler, und L. M. Lewis, „Use of manometric temperature measurements (MTM) to characterize the freeze-drying behavior of amorphous protein formulations“, *J. Pharm. Sci.*, Bd. 99, Nr. 6, S. 2863–2873, Juni 2010, doi: 10.1002/jps.22031.

[175] B.-H. Peters, F. Molnár, und J. Ketolainen, „Structural attributes of model protein formulations prepared by rapid freeze-drying cycles in a microscale heating stage“, *Eur. J. Pharm. Biopharm.*, Bd. 87, Nr. 2, S. 347–356, Juli 2014, doi: 10.1016/j.ejpb.2014.02.016.

[176] S. S. Wang, Y. (Susie) Yan, und K. Ho, „US FDA-approved therapeutic antibodies with high-concentration formulation: summaries and perspectives“, *Antib. Ther.*, Bd. 4, Nr. 4, S. 262–272, Nov. 2021, doi: 10.1093/abt/tbab027.

[177] M. E. Ali und A. Lamprecht, „Spray freeze drying as an alternative technique for lyophilization of polymeric and lipid-based nanoparticles“, *Int. J. Pharm.*, Bd. 516, Nr. 1–2, S. 170–177, Jan. 2017, doi: 10.1016/j.ijpharm.2016.11.023.

[178] S. Wanning, R. Süverkrüp, und A. Lamprecht, „Pharmaceutical spray freeze drying“, *Int. J. Pharm.*, Bd. 488, Nr. 1–2, S. 136–153, Juli 2015, doi: 10.1016/j.ijpharm.2015.04.053.

[179] Y. Maa, P. Nguyen, T. Sweeney, S. J. Shire, und C. C. Hsu, „Protein Inhalation Powders: Spray Drying vs Spray Freeze Drying“, *Pharm. Res.*, Bd. 16, Nr. 2, S. 249–254, 1999, doi: 10.1023/A:1018828425184.

[180] R. J. Garmise, H. F. Staats, und A. J. Hickey, „Novel dry powder preparations of whole inactivated influenza virus for nasal vaccination“, *AAPS PharmSciTech*, Bd. 8, Nr. 4, S. 2–10, Okt. 2007, doi: 10.1208/pt0804081.

[181] S. Wanning, R. Süverkrüp, und A. Lamprecht, „Jet-vortex spray freeze drying for the production of inhalable lyophilisate powders“, *Eur. J. Pharm. Sci.*, Bd. 96, S. 1–7, Jan. 2017, doi: 10.1016/j.ejps.2016.08.062.

[182] F. Emami *u. a.*, „Effect of amino acids on the stability of spray freeze-dried immunoglobulin G in sugar-based matrices“, *Eur. J. Pharm. Sci.*, Bd. 119, S. 39–48, Juli 2018, doi: 10.1016/j.ejps.2018.04.013.

[183] H. R. Costantino *u. a.*, „Protein spray freeze drying. 2. Effect of formulation variables on particle size and stability“, *J. Pharm. Sci.*, Bd. 91, Nr. 2, S. 388–395, Feb. 2002, doi: 10.1002/jps.10059.

[184] N. Poursina, A. Vatanara, M. R. Rouini, K. Gilani, und A. R. Najafabadi, „The effect of excipients on the stability and aerosol performance of salmon calcitonin dry powder inhalers prepared via the spray freeze drying process“, *Acta Pharm. Zagreb Croat.*, Bd. 66, Nr. 2, S. 207–218, Juni 2016, doi: 10.1515/acph-2016-0012.

[185] M. A. Repka, S. Majumdar, S. Kumar Battu, R. Srirangam, und S. B. Upadhye, „Applications of hot-melt extrusion for drug delivery“, *Expert Opin. Drug Deliv.*, Bd. 5, Nr. 12, S. 1357–1376, Dez. 2008, doi: 10.1517/17425240802583421.

[186] H. Patil, R. V. Tiwari, und M. A. Repka, „Hot-Melt Extrusion: from Theory to Application in Pharmaceutical Formulation“, *AAPS PharmSciTech*, Bd. 17, Nr. 1, S. 20–42, Feb. 2016, doi: 10.1208/s12249-015-0360-7.

[187] M. M. Crowley *u. a.*, „Pharmaceutical Applications of Hot-Melt Extrusion: Part I“, *Drug Dev. Ind. Pharm.*, Bd. 33, Nr. 9, S. 909–926, Jan. 2007, doi: 10.1080/03639040701498759.

[188] M. Wilson, M. A. Williams, D. S. Jones, und G. P. Andrews, „Hot-melt extrusion technology and pharmaceutical application“, *Ther. Deliv.*, Bd. 3, Nr. 6, S. 787–797, Juni 2012, doi: 10.4155/tde.12.26.

[189] D. E. Zecevic, R. C. Evans, K. Paulsen, und K. G. Wagner, „From benchtop to pilot scale–experimental study and computational assessment of a hot-melt extrusion scale-up of a solid dispersion of dipyridamole and copovidone“, *Int. J. Pharm.*, Bd. 537, Nr. 1–2, S. 132–139, Feb. 2018, doi: 10.1016/j.ijpharm.2017.12.033.

[190] V. L. Bravo, A. N. Hrymak, und J. D. Wright, „Numerical simulation of pressure and velocity profiles in kneading elements of a co-rotating twin screw extruder“, *Polym. Eng. Sci.*, Bd. 40, Nr. 2, S. 525–541, Feb. 2000, doi: 10.1002/pen.11184.

[191] R. C. Evans, „Application of Sensitive API-Based Indicators and Numerical Simulation Tools to Advance Hot-Melt Extrusion Process Understanding“.

[192] D. E. Zecevic und K. G. Wagner, „Rational Development of Solid Dispersions via Hot-Melt Extrusion Using Screening, Material Characterization, and Numeric Simulation Tools“, *J. Pharm. Sci.*, Bd. 102, Nr. 7, S. 2297–2310, Juli 2013, doi: 10.1002/jps.23592.

[193] M. A. Repka *u. a.*, „Pharmaceutical Applications of Hot-Melt Extrusion: Part II“, *Drug Dev. Ind. Pharm.*, Bd. 33, Nr. 10, S. 1043–1057, Jan. 2007, doi: 10.1080/03639040701525627.

[194] U. W. Gedde, M. S. Hedenqvist, M. Hakkarainen, F. Nilsson, und O. Das, „Processing of Polymeric Materials“, in *Applied Polymer Science*, U. W. Gedde, M. S. Hedenqvist, M. Hakkarainen, F. Nilsson, und O. Das, Hrsg., Cham: Springer International Publishing, 2021, S. 453–487. doi: 10.1007/978-3-030-68472-3_8.

[195] M. Gajda, K. P. Nartowski, J. Pluta, und B. Karolewicz, „The role of the polymer matrix in solvent-free hot melt extrusion continuous process for mechanochemical synthesis of pharmaceutical cocrystal“, *Eur. J. Pharm. Biopharm.*, Bd. 131, S. 48–59, Okt. 2018, doi: 10.1016/j.ejpb.2018.07.002.

[196] S. Madan und S. Madan, „Hot melt extrusion and its pharmaceutical applications“, *Asian J. Pharm. Sci.*, Bd. 7, Nr. 2, S. 123–133, 2012.

[197] F. J. Simons und K. G. Wagner, „Modeling, design and manufacture of innovative floating gastroretentive drug delivery systems based on hot-melt extruded tubes“, *Eur. J. Pharm. Biopharm.*, Bd. 137, S. 196–208, Apr. 2019, doi: 10.1016/j.ejpb.2019.02.022.

[198] S. Prodduturi, R. V. Manek, W. M. Kolling, S. P. Stodghill, und M. A. Repka, „Solid-State Stability and Characterization of Hot-Melt Extruded Poly(ethylene oxide) Films“, *J. Pharm. Sci.*, Bd. 94, Nr. 10, S. 2232–2245, Okt. 2005, doi: 10.1002/jps.20437.

[199] J. Jiang, A. Lu, X. Ma, D. Ouyang, und R. O. Williams, „The applications of machine learning to predict the forming of chemically stable amorphous solid dispersions prepared by hot-melt extrusion“, *Int. J. Pharm. X*, Bd. 5, S. 100164, Dez. 2023, doi: 10.1016/j.ijpx.2023.100164.

[200] F. P. Pons-Faudoa, A. Ballerini, J. Sakamoto, und A. Grattoni, „Advanced implantable drug delivery technologies: transforming the clinical landscape of therapeutics for chronic diseases“, *Biomed. Microdevices*, Bd. 21, Nr. 2, S. 47, Juni 2019, doi: 10.1007/s10544-019-0389-6.

[201] C. J. F. Bertens, M. Gijs, F. J. H. M. Van Den Biggelaar, und R. M. M. A. Nuijts, „Topical drug delivery devices: A review“, *Exp. Eye Res.*, Bd. 168, S. 149–160, März 2018, doi: 10.1016/j.exer.2018.01.010.

[202] M. A. Fischer, „Implanon: a new contraceptive implant“, *J. Obstet. Gynecol. Neonatal Nurs. JOGNN*, Bd. 37, Nr. 3, S. 361–368, 2008, doi: 10.1111/j.1552-6909.2008.00247.x.

[203] Walter LEGER, Klaus Nickisch, Ze'ev Shaked, Karin Eggenreich, Simone EDER, und Andreas WITSCHNIGG, „Targeted delivery of progestins and estrogens via vaginal ring devices for fertility control and hrt products“, 31. Oktober 2019

[204] I. Lete, M. C. Cuesta, J. M. Marín, und S. Guerra, „Vaginal health in contraceptive vaginal ring users - A review“, *Eur. J. Contracept. Reprod. Health Care Off. J. Eur. Soc. Contracept.*, Bd. 18, Nr. 4, S. 234–241, Aug. 2013, doi: 10.3109/13625187.2013.801954.

[205] K. Malcolm, Fetherston, McCoy, Boyd, und Major, „Vaginal rings for delivery of HIV microbicides“, *Int. J. Womens Health*, S. 595, Nov. 2012, doi: 10.2147/IJWH.S36282.

[206] F. Rafiei *u. a.*, „Development of Hormonal Intravaginal Rings: Technology and Challenges“, *Geburtshilfe Frauenheilkd.*, Bd. 81, Nr. 07, S. 789–806, Juli 2021, doi: 10.1055/a-1369-9395.

[207] Z. Ghalanbor, M. Körber, und R. Bodmeier, „Improved Lysozyme Stability and Release Properties of Poly(lactide-co-glycolide) Implants Prepared by Hot-Melt Extrusion“, *Pharm. Res.*, Bd. 27, Nr. 2, S. 371–379, Feb. 2010, doi: 10.1007/s11095-009-0033-x.

[208] M. Stanković *u. a.*, „Low temperature extruded implants based on novel hydrophilic multiblock copolymer for long-term protein delivery“, *Eur. J. Pharm. Sci.*, Bd. 49, Nr. 4, S. 578–587, Juli 2013, doi: 10.1016/j.ejps.2013.05.011.

[209] P. W. Lee und J. K. Pokorski, „Poly(lactic-co-glycolic acid) devices: Production and applications for sustained protein delivery“, *Wiley Interdiscip. Rev. Nanomed. Nanobiotechnol.*, Bd. 10, Nr. 5, S. e1516, Sep. 2018, doi: 10.1002/wnan.1516.

[210] M. Morlock, H. Koll, G. Winter, und T. Kissel, „Microencapsulation of rh-erythropoietin, using biodegradable poly(d,l-lactide-co-glycolide): protein stability and the effects of stabilizing excipients“, *Eur. J. Pharm. Biopharm.*, Bd. 43, Nr. 1, S. 29–36, Jan. 1997, doi: 10.1016/S0939-6411(96)00017-3.

[211] Z. Ghalanbor, M. Körber, und R. Bodmeier, „Protein release from poly(lactide-co-glycolide) implants prepared by hot-melt extrusion: Thioester formation as a reason for incomplete release“, *Int. J. Pharm.*, Bd. 438, Nr. 1–2, S. 302–306, Nov. 2012, doi: 10.1016/j.ijpharm.2012.09.015.

[212] M. Vollrath, J. Engert, und G. Winter, „Long-term release and stability of pharmaceutical proteins delivered from solid lipid implants“, *Eur. J. Pharm. Biopharm.*, Bd. 117, S. 244–255, Aug. 2017, doi: 10.1016/j.ejpb.2017.04.017.

[213] M. Vollrath, J. Engert, und G. Winter, „New insights into process understanding of solid lipid extrusion (SLE) of extruded lipid implants for sustained protein delivery“, *Eur. J. Pharm. Biopharm.*, Bd. 130, S. 11–21, Sep. 2018, doi: 10.1016/j.ejpb.2018.06.016.

[214] R. Vaishya, V. Khurana, S. Patel, und A. K. Mitra, „Long-term delivery of protein therapeutics“, *Expert Opin. Drug Deliv.*, Bd. 12, Nr. 3, S. 415–440, März 2015, doi: 10.1517/17425247.2015.961420.

[215] M. Stanković, H. W. Frijlink, und W. L. J. Hinrichs, „Polymeric formulations for drug release prepared by hot melt extrusion: application and characterization“, *Drug Discov. Today*, Bd. 20, Nr. 7, S. 812–823, Juli 2015, doi: 10.1016/j.drudis.2015.01.012.

[216] S. L. Lee, A. E. Hafeman, P. G. Debenedetti, B. A. Pethica, und D. J. Moore, „Solid-State Stabilization of α-Chymotrypsin and Catalase with Carbohydrates“, *Ind. Eng. Chem. Res.*, Bd. 45, Nr. 14, S. 5134–5147, Juli 2006, doi: 10.1021/ie0513503.

[217] Y. Zheng und J. K. Pokorski, „Hot melt extrusion: An emerging manufacturing method for slow and sustained protein delivery“, *WIREs Nanomedicine Nanobiotechnology*, Bd. 13, Nr. 5, Sep. 2021, doi: 10.1002/wnan.1712.

[218] O. Annunziata, N. Asherie, A. Lomakin, J. Pande, O. Ogun, und G. B. Benedek, „Effect of polyethylene glycol on the liquid–liquid phase transition in aqueous protein solutions“, *Proc. Natl. Acad. Sci.*, Bd. 99, Nr. 22, S. 14165–14170, Okt. 2002, doi: 10.1073/pnas.212507199.

[219] O. Cantin, F. Siepmann, J. F. Willart, F. Danede, J. Siepmann, und Y. Karrout, „PEO hot melt extrudates for controlled drug delivery: Importance of the type of drug and loading“, *J. Drug Deliv. Sci. Technol.*, Bd. 61, S. 102238, Feb. 2021, doi: 10.1016/j.jddst.2020.102238.

[220] B.-M. Chen, T.-L. Cheng, und S. R. Roffler, „Polyethylene Glycol Immunogenicity: Theoretical, Clinical, and Practical Aspects of Anti-Polyethylene Glycol Antibodies“, *ACS Nano*, Bd. 15, Nr. 9, S. 14022–14048, Sep. 2021, doi: 10.1021/acsnano.1c05922.

[221] F. Mastrotto *u. a.*, „Physical PEGylation to Prevent Insulin Fibrillation“, *J. Pharm. Sci.*, Bd. 109, Nr. 1, S. 900–910, Jan. 2020, doi: 10.1016/j.xphs.2019.10.020.

[222] S.-H. Chao, S. S. Matthews, R. Paxman, A. Aksimentiev, M. Gruebele, und J. L. Price, „Two Structural Scenarios for Protein Stabilization by PEG“, *J. Phys. Chem. B*, Bd. 118, Nr. 28, S. 8388–8395, Juli 2014, doi: 10.1021/jp502234s.

[223] B. K. Pandey *u. a.*, „Impact of Site-Specific PEGylation on the Conformational Stability and Folding Rate of the Pin WW Domain Depends Strongly on PEG Oligomer Length“, *Bioconjug. Chem.*, Bd. 24, Nr. 5, S. 796–802, Mai 2013, doi: 10.1021/bc3006122.

[224] A. Pandey und D. Jain, „Poly Lactic-Co-Glycolic Acid (PLGA) Copolymer and Its Pharmaceutical Application“, in *Handbook of Polymers for Pharmaceutical Technologies*, 2015, S. 151–172. doi: 10.1002/9781119041412.ch6.

[225] P. Gentile, V. Chiono, I. Carmagnola, und P. Hatton, „An Overview of Poly(lactic-co-glycolic) Acid (PLGA)-Based Biomaterials for Bone Tissue Engineering“, *Int. J. Mol. Sci.*, Bd. 15, Nr. 3, S. 3640–3659, Feb. 2014, doi: 10.3390/ijms15033640.

[226] C. Schneider, R. Langer, D. Loveday, und D. Hair, „Applications of ethylene vinyl acetate copolymers (EVA) in drug delivery systems“, *J. Controlled Release*, Bd. 262, S. 284–295, Sep. 2017, doi: 10.1016/j.jconrel.2017.08.004.

[227] R. Langer, L. Brown, und E. Edelman, „[30] Controlled release and magnetically modulated release systems for macromolecules“, in *Methods in Enzymology*, Elsevier, 1985, S. 399–422. doi: 10.1016/S0076-6879(85)12032-X.

[228] L. R. Brown, C. L. Wei, und R. Langer, „In Vivo and In Vitro Release of Macromolecules from Polymeric Drug Delivery Systems“, *J. Pharm. Sci.*, Bd. 72, Nr. 10, S. 1181–1185, Okt. 1983, doi: 10.1002/jps.2600721019.

[229] V. P. Shastri, „Non-degradable biocompatible polymers in medicine: past, present and future“, *Curr. Pharm. Biotechnol.*, Bd. 4, Nr. 5, S. 331–337, Okt. 2003, doi: 10.2174/1389201033489694.

[230] M. C. Lai und E. M. Topp, „Solid-state chemical stability of proteins and peptides“, *J. Pharm. Sci.*, Bd. 88, Nr. 5, S. 489–500, Mai 1999, doi: 10.1021/js980374e.

[231] M.-P. Even, S. Bobbala, B. Gibson, S. Hook, G. Winter, und J. Engert, „Twin-screw extruded lipid implants containing TRP2 peptide for tumour therapy“, *Eur. J. Pharm. Biopharm.*, Bd. 114, S. 79–87, Mai 2017, doi: 10.1016/j.ejpb.2016.12.033.

[232] G. Sax und G. Winter, „Mechanistic studies on the release of lysozyme from twin-screw extruded lipid implants“, *J. Controlled Release*, Bd. 163, Nr. 2, S. 187–194, Okt. 2012, doi: 10.1016/j.jconrel.2012.08.025.

[233] M. Stanković, J. Tomar, C. Hiemstra, R. Steendam, H. W. Frijlink, und W. L. J. Hinrichs, „Tailored protein release from biodegradable poly(ε-caprolactone-PEG)-b-poly(ε-caprolactone) multiblock-copolymer implants“, *Eur. J. Pharm. Biopharm.*, Bd. 87, Nr. 2, S. 329–337, Juli 2014, doi: 10.1016/j.ejpb.2014.02.012.

[234] Cossé, Anne, „Development of polymeric implants for the long-term release of proteins“.

[235] W. Al-Azzam, E. A. Pastrana, und K. Griebenow, „Co-lyophilization of bovine serum albumin (BSA) with poly(ethylene glycol) improves efficiency of BSA encapsulation and stability in polyester microspheres by a solid-in-oil-in-oil technique“, *Biotechnol. Lett.*, Bd. 24, Nr. 16, S. 1367–1374, Aug. 2002, doi: 10.1023/A:1019881505734.

[236] G. Shadambikar *u. a.*, „Vacuum Compression Molding as a Screening Tool to Investigate Carrier Suitability for Hot-Melt Extrusion Formulations“, *Pharmaceutics*, Bd. 12, Nr. 11, S. 1019, Okt. 2020, doi: 10.3390/pharmaceutics12111019.

[237] D. Treffer, A. Troiss, und J. Khinast, „A novel tool to standardize rheology testing of molten polymers for pharmaceutical applications“, *Int. J. Pharm.*, Bd. 495, Nr. 1, S. 474–481, Nov. 2015, doi: 10.1016/j.ijpharm.2015.09.001.

[238] E. S. Bochmann, K. E. Steffens, A. Gryczke, und K. G. Wagner, „Numerical simulation of hot-melt extrusion processes for amorphous solid dispersions using model-based melt viscosity“, *Eur. J. Pharm. Biopharm.*, Bd. 124, S. 34–42, März 2018, doi: 10.1016/j.ejpb.2017.12.001.

[239] M. A. Emin, P. Wittek, und Y. Schwegler, „Numerical analysis of thermal and mechanical stress profile during the extrusion processing of plasticized starch by non-isothermal flow simulation“, *J. Food Eng.*, Bd. 294, S. 110407, Apr. 2021, doi: 10.1016/j.jfoodeng.2020.110407.

[240] M. A. Emin und H. P. Schuchmann, „Droplet breakup and coalescence in a twin-screw extrusion processing of starch based matrix“, *J. Food Eng.*, Bd. 116, Nr. 1, S. 118–129, Mai 2013, doi: 10.1016/j.jfoodeng.2012.12.010.

[241] M. A. Emin und H. P. Schuchmann, „Analysis of the dispersive mixing efficiency in a twin-screw extrusion processing of starch based matrix“, *J. Food Eng.*, Bd. 115, Nr. 1, S. 132–143, März 2013, doi: 10.1016/j.jfoodeng.2012.10.008.

FURTHER INFORMATION ON ASSISTANCE RECEIVED AND RESOURCES USED

General:

This research was funded by the German Research Foundation (DFG) within the research project “SPP 1934 DiSPBiotech” (project number: 273937032).

The Institute of Applied Physics of the University of Bonn designed and produced ram extruder components.

Figures in the introduction section were created with BioRender.com.

Sanofi-Aventis Deutschland GmbH provided human insulin for the studies via a material transfer agreement of 5 August 2020. All publications containing data on human insulin (Chapter 3 and Chapter 4) were released prior publication by the legal department of Sanofi-Aventis Deutschland GmbH.

Chapter 3: Impact of process stress on protein stability in highly-loaded solid protein/PEG formulations from small-scale melt extrusion

Christian Werner and Dirk Lindenblatt (University of Cologne) performed circular-dichroism spectroscopy and analyzed the CD data of the provided protein-loaded extrudates. Prof. Dr. Karl Wagner supervised the research. All co-authors contributed to writing the manuscript. The 5-mm TSE ZE5 of Sanofi-Aventis Deutschland GmbH in Frankfurt was used during a visiting research fellowship for the production of protein-loaded extrudates. The legal department of Sanofi-Aventis Deutschland GmbH released the manuscript prior publication.

Chapter 4: Micro-Scale Vacuum Compression Molding as a predictive screening tool of protein integrity for potential Hot-Melt Extrusion processes

Prof. Dr. Karl Wagner supervised the research. The legal department of Sanofi-Aventis Deutschland GmbH released the manuscript prior publication.

Chapter 5: Highly protein-loaded melt extrudates produced by small-scale ram and twin-screw extrusion - evaluation of extrusion process design on protein integrity by experimental and numerical approaches

Kevin Kayser developed the rheological methodology and conducted partly rheological experiments including data analysis. Felix Ellwanger performed 3D isothermal simulation of the die sections and the screw section of extruders by ANSYS POLYFLOW® software, analyzed and interpreted the obtained data. Achim Overbeck conducted the mechanical single crystal analysis of provided protein powders and analyzed the data. Prof. Dr. Arno Kwade, Prof. Dr. Heike P. Karbstein, and Prof. Dr. Karl Wagner supervised the research. All co-authors contributed to writing the manuscript. The 5-mm TSE ZE5 of Sanofi-Aventis Deutschland GmbH in Frankfurt was used during a visiting research fellowship for the production of protein-loaded extrudates.

APPENDIX

Full-text publications and supplementary materials.

3 IMPACT OF PROCESS STRESS ON PROTEIN STABILITY IN HIGHLY-LOADED SOLID PROTEIN/PEG FORMULATIONS FROM SMALL-SCALE MELT EXTRUSION

Katharina Dauer[1], Christian Werner[2], Dirk Lindenblatt[2], Karl G. Wagner[1,*]

[1] University of Bonn, Department of Pharmaceutics, Institute of Pharmacy, Bonn, Germany

[2] University of Cologne, Department of Chemistry, Institute of Biochemistry, Cologne, Germany

This part was published as

K. Dauer, C. Werner, D. Lindenblatt, and K.G. Wagner: Impact of process stress on protein stability in highly-loaded solid protein/PEG formulations from small-scale melt extrusion, International Journal of Pharmaceutics: X, Volume 5, 2022, 100154, DOI: 10.1016/j.ijpx.2022.100154

3.1 Graphical Abstract

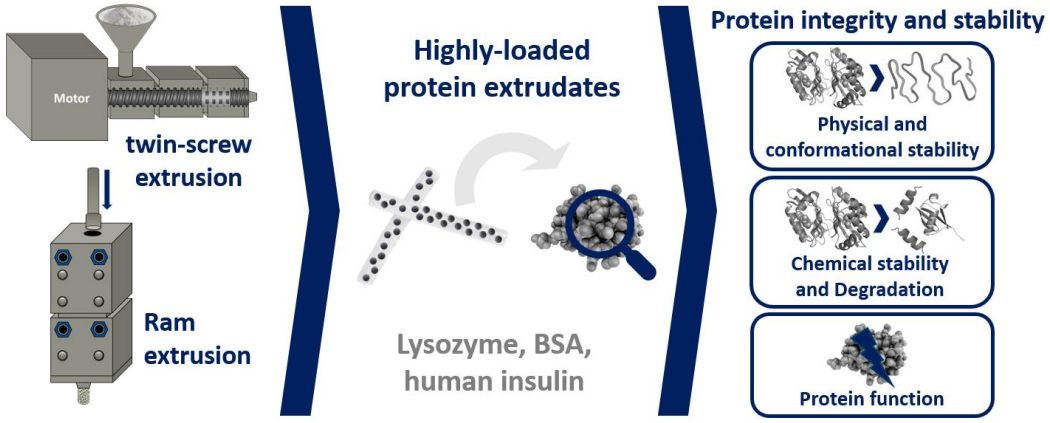

3.2 Abstract

As protein-based therapeutics often exhibit a limited stability in liquid formulations, there is a growing interest in the development of solid protein formulations due to improved protein stability in the solid state. We used small-scale (< 3 g) ram and twin-screw extrusion for the solid stabilization of proteins (Lysozyme, BSA, and human insulin) in PEG-matrices. Protein stability after extrusion was systematically investigated using ss-DSC, ss-FTIR, CD spectroscopy, SEM-EDX, SEC, RP-HPLC, and in case of Lysozyme an activity assay. The applied analytical methods offered an accurate assessment of protein stability in extrudates, enabling the comparison of different melt extrusion formulations and process parameters (e.g., shear stress levels, screw configurations, residence times). Lysozyme was implemented as a model protein and was completely recovered in its active form after extrusion. Differences seen between Lysozyme- and BSA- or human insulin-loaded extrudates indicated that melt extrusion could have an impact on the conformational stability. In particular, BSA and human insulin were more susceptible to heat exposure and shear stress compared to Lysozyme, where shear stress was the dominant parameter. Consequently, ram extrusion led to less conformational changes compared to TSE. Ram extrusion showed good protein particle distribution resulting in the preferred method to prepare highly-loaded solid protein formulations.

3.3 Keywords

hot-melt extrusion, protein stability, solid-state characterization, small-scale

3.4 INTRODUCTION

Since biopharmaceutics play a steadily increasing role in the medical treatment of especially severe diseases, the sector of developing protein-based therapeutics is similarly growing. Biopharmaceutics are more complex and have to be administered mostly parenteral as liquid formulations compared to other drug products based on small-molecule drugs [1]. However, the demand of liquid formulations for application is in contradiction to an often limited chemical and physical stability in liquid state (e.g., formation of aggregates) which is considered as major challenge for the successful development and lifecycle of a biopharmaceutical drug product (e.g., manufacturing, formulation development, processing, storage, and shipping) [2],[3]. The formation of protein aggregates in liquid formulations can lead to an increased immunogenicity, viscosity, and injection force. Further aggregation leads to countable sub-visible or visible particles, which are both not accepted by the authorities [2],[4–7]. Most of the analytical methods applied during protein formulation development studies focus on the investigation and characterization of proteins in solution or lyophilized proteins after their reconstitution. Analytical characterization methods for liquid protein formulations include: (i) RP HPLC for the analysis of degradation products and chemical stability, (ii) size exclusion chromatography (SEC) for monitoring the loss of protein monomers as an indication of aggregate formation, (iii) circular dichroism (CD) and nuclear magnetic resonance (NMR) to probe conformational stability and (iv) light scattering methods for estimating the colloidal stability of protein formulations and monitoring the appearance of sub-visible particles [8–12].

In contrast, solid formulations of proteins offer the potential of increased stability [13],[14]. Proteins are commonly freeze-dried to overcome the instability issues that may occur in liquid protein formulations. Thus, there is a growing interest in the development of other solid protein formulations (e.g., protein-loaded extrudates or implants) as well as encapsulation procedures that employ dehydrated protein powders due to improved protein stability in the solid state. During lyophilization, proteins are molecularly dispersed primarily in an amorphous excipient matrix resulting in an increased stability [15]. Nowadays, there is an increasing awareness to use melt extrusion processing for the preparation of solid protein-loaded implants or encapsulation of protein particles in extrudates with focus on solid-state protein stabilization. Melt extrusion is used in pharmaceutical industry as continuous and robust manufacturing tool for the preparation of solid dosage forms. Melt extrusion (i) can result in the embedment of drugs in polymeric matrices, (ii) is a solvent-free (e.g.,

organic solvents) technique, and (iii) does not require additional excipients such as surfactants or cryoprotectants [16],[17]. Melt extrusion processing is also applied for the embedding of drug particles or drug crystals at high drug loadings (up to 80 %) as well as for the preparation of amorphous solid dispersions, where the drug is dispersed on a molecular level in a polymeric carrier [18–20]. Additionally, small-scale melt extrusion is accompanied with (i) processing small batch sizes (e.g., less than 2 g of a protein formulation), (ii) high yield, and (iii) short process times (e.g., shorter than 3 minutes for 2 g of a powdered protein formulation). The major drawbacks of commonly used techniques such as spray- or freeze-drying to formulate or encapsulate proteins in solid-state are mostly (i) the use of low-concentrated protein solutions resulting in a limited powder yield, (ii) relatively long processing times, (iii) the need of disaccharides or surfactants in the aqueous solution to prevent protein aggregation or inactivation, and (iv) the limited process scalability [21–24]. Furthermore, the use of polymers as stabilizing excipients is not or difficult to be processed via spray-drying due to the rheological behavior of the spray solution and is strongly depended on the polymer used. Phase separation of polymers or the crystallization of other excipients and formulation components during spray-drying may lead to denaturation or the formation of protein aggregation [23],[25],[26]. However, the spray solution rheology depends not only on the polymer but also on the solvent system and their interaction, and thus determines the sprayability [27]. On the other hand, during freeze-drying, the formulations which contain amorphous saccharides (e.g., sucrose), are prone to collapse upon the primary drying step and the collapse is unfavorable and often negatively affects the storage stability of proteins [28]. In contrast, in melt extrusion processing, the polymers can be easily used to embed proteins in a polymeric matrix without dissolution of the protein particles in the polymer for solid-state stabilization, however, dry protein powders are required for melt extrusion processing. In this case, the protein particles act as fillers resulting in a reduced amount of energy required for the viscous dissipation during melt extrusion processing [29]. Polymers can ensure the thermodynamically stable folded structure of a protein during the melt extrusion process due to the immobilization of protein molecules in the polymeric matrix, which is critical for a successful protein formulation development [30–32]. Furthermore, by melt extrusions processing a high fraction of protein can be embed into a polymeric matrix resulting in high-drug loads (i.e., > 40 % protein) compared to other formulation techniques. Another benefit of hot-melt extruded solid protein formulations compared to lyophilized proteins is the reduced

static electricity. Often, the static electricity of lyophilized protein powder is so severe that it is impossible to handle it safely (e.g., weighed-in inaccurately, problems during sample preparation for analytical investigation).

However, during melt extrusion processing protein exposure to elevated temperatures and shear stress can potentially cause unfolding and degradation, leading to irreversible aggregation and/or a loss of functionality and is also a factor that should not be underestimated. Especially, information on an intensive assessment of protein stability in solid formulations prepared by melt extrusion processes and the impact of process stress is not as widely reported. In this study, we focused on the characterization of highly-loaded protein extrudates (i.e., 40 % protein content) prepared by ram extrusion and twin-screw extrusion (TSE) with regard to the main challenges, i.e., protein instability due to heat exposure [33] and shear stress during extrusion [34]. The aim was the implementation of a sensitive characterization pathway of protein stability in highly-loaded solid protein/PEG formulations. Lysozyme, bovine serum albumin (BSA), and human insulin were chosen as (model) proteins and peptide, respectively and were embedded in polyethylene glycol (PEG) 20,000-matrices. PEG is a hydrophilic polymer and next to an increasing half-life of the protein also used as potential protein stabilizer by addition of PEG-chains to proteins (PEG-ylation) or co-processing with PEG [35–37]. Furthermore, several studies suggest that long PEG-chains (e.g., PEG 20,000) can stabilize proteins by interacting with the protein surface or by the formation of the excluded volume effect to decelerate the unfolding rate of the protein [38],[39]. Furthermore, higher molecular weight PEG (also known as polyethylene oxide (PEO) depending on its molecular weight) offers a potential as matrix polymer for controlled release dosage forms and is commercially available in a broad variety of PEO grades and different molecular weights (e.g., 100,000, 300,000, 1,000,000) [36]. We selected PEG 20,000 as model polymer due to its (i) low melting temperature (~ 60 °C, depending on the chain-length), (ii) hydrophilicity and (iii) potential as protein stabilizer. Due to the hydrophilic character of PEG 20,000, we favored a solely embedment and dispersion of the protein particles in the polymeric matrix without dissolution of the protein particles in the polymer. Furthermore, the hydrophilicity of PEG enormously simplified the sample preparation and thus the analytical investigations. More specific, the development and implementation of a complex protein extraction protocol was not necessary. Lysozyme is a commonly used model protein in pharmaceutical and biological research [30],[40–42] and was used for the implementation of analytical procedures

in the sense of a negative control. The protein stability and integrity of Lysozyme, BSA and human insulin after melt extrusion was systematically investigated using (i) RP HPLC (chemical stability and protein concentration), (ii) SEC (protein fragment and aggregation analysis), (iii) SEM-EDX (protein particle distribution), (iv) DSC (protein's unfolding temperature), (v) FTIR and CD spectroscopy (conformational stability), and (vi) activity assay. We provide characterization methods to assess process-related protein stability in highly-loaded protein extrudates as well as to distinguish between the impact of different small-scale melt extrusion processes (i.e., ram and TSE) and extrusion parameters (e.g., shear stress levels, screw configurations, residence times) on protein stability. We considered melt extrusion for the production of protein-loaded extrudates in order to further enhance their stability in solid-state formulations compared to the starting material, for improved storage and logistic conditions. Another perspective would be the production of protein-loaded implants with sustained release profile. The proposed characterization pathway for proteins processed via small-scale melt extrusion proved to be a powerful tool to assess the formulation stability in PEG matrices and potentially other excipients like PEO, lipids, poloxamers, Poly Lactic-co-Glycolic Acid (PLGA), and Ethylene-vinyl acetate (EVA) [30],[43–50]. The two latter would subsequently lead to the development of long releasing implants and will be discussed in future works [46],[51]. Furthermore, the implemented methods should be expanded to or combined with other formulation and stabilization techniques (e.g., vacuum compression molding, a combination of spray-drying and melt extrusion) in order to study process-related effects on protein stability.

3.5 MATERIALS AND METHODS

3.5.1 MATERIALS

Lysozyme from chicken egg-white, lyophilized powder (Cat. No. L6876, d_{50} = 137 µm) was obtained from AppliChem (AppliChem GmbH, Darmstadt, Germany). Bovine serum albumin (BSA) (d_{50} = 505 µm), sodium chloride, di-sodium hydrogen phosphate dihydrate, sodium dihydrogen phosphate dihydrate, acetonitrile and trifluoroacetic acid (HPLC gradient grade) were purchased from Merck (Merck KGaA, Darmstadt, Germany). Human insulin (d_{50} = 141 µm) was kindly donated by Sanofi-Aventis Deutschland GmbH (Frankfurt, Germany). Polyethylene glycol 20,000 was obtained from Carl Roth (Carl Roth GmbH & Co. KG, Karlsruhe, Germany).

3.5.2 METHODS

3.5.2.1 PREPARATION OF PROTEIN-LOADED PEG-EXTRUDATES BY RAM AND TWIN-SCREW EXTRUSION

PEG 20,000 flakes were milled utilizing a high-shear mixer (Krups Mixette type 210, Krups, Frankfurt am Main, Germany) and passed through a 650 µm sieve to remove larger particles. For the preparation of protein-loaded extrudates, a physical mixture (3 g) composed of 60 % PEG 20,000 and 40 % protein powder (Lysozyme, BSA, or human insulin) were blended for 10 min at 50 rpm using a turbula mixer (Willy A. Bachofen AG, Muttenz, Switzerland). The physical mixtures of PEG 20,000 and protein powder (Table 1) were either ram extruded (lower shear stress) or hot melt extruded by using TSE (higher shear stress). We used a self-built ram extruder for the preparation of protein-loaded extrudates with lower shear stress (Figure 1). A barrel of 10 cm length and an inner cylindrical hole of 10 mm diameter consisted of three heating zones and was equipped with a cylindrical die (diameter 1 mm). Extrudates were prepared by feeding 3 g of the physical mixture into the 10 mm hole of the ram extruder. The temperature of the upper segment (filling-zone) was set to 58 °C, and the following two segments were set to 63 °C. The mixture was heated for three minutes and the molten blends were subsequently extruded through the 1 mm-die by a driving piston with a speed of 1 mm/s. TSE was performed using a 5 mm co-rotating twin-screw extruder ZE 5 (Three-Tec GmbH, Seon, Switzerland) with a functional length of 15:1 L/D and two heating zones, equipped with a 1 mm die and either a conveying screw configuration, or a screw configuration with a single

kneading element, which are presented in Figure 2. The physical mixtures (3 g) were fed into the extruder by using a powder belt conveyor (GUF-P Mini AD / 475 / 75, mk Technology Group, Troisdorf, Germany) at constantly kept feeding rates of 0.4 g/min or 0.8 g/min ± 5 % for Lysozyme, human insulin, or BSA, respectively (Table 1).

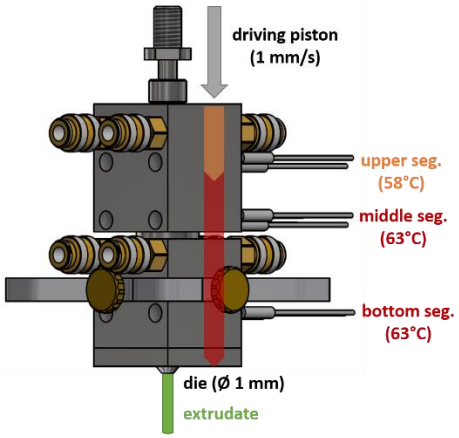

Figure 1 Self-built ram extruder. Barrel (10 cm length, inner cylindrical hole Ø = 10 mm) consisted of three heating zones and a cylindrical die (Ø = 1 mm). Upper temperature segment (filling-zone): 58 °C, middle segments were set to 63 °C. The mixture was heated for three minutes and the molten blends were subsequently extruded through the 1 mm-die by a driving piston with a speed of 1 mm/s.

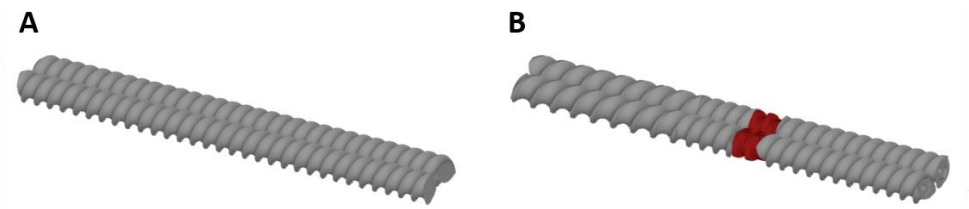

Figure 2 Screw configurations of the 5 mm TSE with: **A** conveying elements (5 mm pitch), **B** a single kneading element (7.5, 5 mm pitch, 90° kneading element (red), 5 mm pitch); Segment 1 (ambient temperature), segment 2 (63 °C), and segment 3 (60 °C).

Table 1 Overview of the compositions and prepared protein-loaded extrudates by ram or twin-screw extrusion with applied process parameters; the physical mixtures were prepared in a turbula mixer at a frequency of 50 rpm for 10 min.; for ram extrusion the physical mixture was heated for 3 min. at 63 °C and extruded with a piston speed of 1 mm/s through a 1 mm-die; for TSE the physical mixture was constantly fed (0.4 or 0.8 g/min.) into the heated barrel (63-60 °C) and extruded through a 1 mm-die, screw speed was 150 rpm.

Formulation	***Protein***	***Components (%)***		***Preparation method***	***Process parameters***
		Protein	**PEG 20,000**		
Lysozyme reference	LYS	100	0	-	
Physical mixture	LYS	40	60	Turbula mixer	10 min, 50 rpm
LR40	LYS	40	60	Ram extrusion	3 min, 63°C, 1 mm/s, 1 mm
LC40	LYS	40	60	TSE (conveying)	0.4 g/min., 150 rpm, 63-
LK40	LYS	40	60	TSE (kneading)	60°C, 1 mm

BSA reference	BSA	100	0	-	
Physical mixture	BSA	40	60	Turbula mixer	10 min, 50 rpm
BR40	BSA	40	60	Ram extrusion	3 min, 63°C, 1 mm/s, 1 mm
BC40	BSA	40	60	TSE (conveying)	0.8 g/min., 150 rpm, 63-
BK40	BSA	40	60	TSE (kneading)	60°C, 1 mm
Human insulin reference	IH	100	0	-	
Physical mixture	IH	40	60	Turbula mixer	10 min, 50 rpm
IHR40	IH	40	60	Ram extrusion	3 min, 63°C, 1 mm/s, 1 mm
IHC40	IH	40	60	TSE (conveying)	0.4 g/min., 150 rpm, 63-
IHK40	IH	40	60	TSE (kneading)	60°C, 1 mm

3.5.2.2 CHEMICAL STABILITY AND PROTEIN CONCENTRATION IN EXTRUDATES

Chemical stability and protein concentration in extrudates were determined by HPLC (Agilent 1100 Series equipped with, quaternary pump, diode array and multiple wavelength detector (DAD), Agilent Technologies, Waldbronn, Germany)) using a C18 reversed phase column (NUCLEOSIL 120-3, C18, 5 µm, 125x4 mm). Protein-loaded PEG-extrudates were dissolved in Milli-Q® water and properly mixed for the extraction of protein (n = 3). 1.5 mL of the supernatant was used for analysis. The solvent system consisted of water/acetonitrile/trifluoroacetic acid (A: 100/0/0.1, B: 0/100/0.1, V/V). A linear gradient method was applied (0-5-7 min 5-95-5 %B) at a flow rate of 1 mL/min for 7 min and a column temperature of 30 °C. Samples (10 µL) were injected, and chromatograms obtained with an UV-detector were quantified at 280 nm.

3.5.2.3 SIZE-EXCLUSION CHROMATOGRAPHY

SEC was performed with a Superdex 75 Increase 10/300 GL column, 10 × 300 mm (Cytiva, Marlborough, MA, USA), where the mobile phase was 50 mM pH 7.0 phosphate buffer containing 400 mM sodium chloride at a flow rate of 0.8 mL/min and a column temperature of 30 °C. Samples were prepared as triplicates by dissolving the protein powder, physical mixture, or protein-loaded extrudates in the mobile phase with a target concentration of 3 mg/mL protein. Human insulin containing samples were pre-dissolved in 0.05 M hydrochloric acid aqueous solution and then diluted with the mobile phase. The UV detector (SPD-40 UV Detector, Shimadzu, Japan) wavelength was 214 nm. Sample vials were cooled at 15 °C in the autosampler. 20 µL of each sample was injected and potential aggregate and/or fragment formation after

processing was analyzed in comparison with a chromatogram of the freshly prepared protein powder and physical mixture samples.

3.5.2.4 SCANNING ELECTRON MICROSCOPY COUPLED WITH ENERGY-DISPERSIVE X-RAY SPECTROSCOPY (SEM-EDX) AND IMAGE ANALYSIS OF SEM-EDX-MAPS

A scanning electron microscope (SU 3500, Hitachi High Technologies, Krefeld, Germany), equipped with a backscattered electron detector (BSE) was used to investigate the morphology of the surfaces and cross sections of the prepared protein-loaded extrudates. BSE images were collected at an acceleration voltage of 5 kV at a variable pressure mode of 30 Pa. The cut extrudates were placed on an aluminum stub and sputtered with a thin platinum layer (Sputter Coater, Cressington Scientific Instruments, Watford, England). The elemental distributions were investigated by SEM combined with an energy-dispersive X-ray detector (EDX) (EDAX Element-C2B, Ametek, Weiterstadt, Germany). Protein distribution was examined by elemental mapping of the cross sections of extrudates for the characteristic X-ray peak of nitrogen. The percentage of detected nitrogen was evaluated by the TEAM software (Version 4.4.1, Ametek, Weiterstadt, Germany). Image analysis of SEM/EDX-maps was used to parameterize the distribution of the protein particles in the PEG-matrix. The percentage of the area with protein was calculated using image editing software ImageJ (ImageJ 1.53q, National Institutes of Health, USA). The coefficient of variation (CV) of the average protein particle area (nitrogen signal in green) was calculated. This relative protein particle area variation (calculated as CV in %) was taken as a descriptor for the protein particle distribution. Low levels in CV indicate a homogenous protein particle distribution, whereas high levels would represent a high variation of protein particle distribution, i.e., an inhomogenous particle distribution [52]. For every formulation, three extrudate cross sections (Ø = 1 mm) were analyzed in total for mean value and standard deviation calculation of this distribution value.

3.5.2.5 SOLID-STATE DIFFERENTIAL SCANNING CALORIMETRY (SS-DSC)

DSC studies of protein powder, physical mixture and extrudates were performed with a DSC 2 (Mettler Toledo, Gießen, Germany) equipped with an auto sampler, nitrogen cooling and nitrogen as purge gas (30 mL/min). The system was calibrated with indium and zinc standards. At least three samples of ~10 mg were accurately weighed in 40 µL aluminum crucibles with a pierced lid. DSC scans were recorded from 25 °C to 230 °C using a heating rate of 10 K/min. STAR^e software (Mettler Toledo, Gießen, Germany) was employed for acquiring thermograms. Thermograms were normalized

for sample weight and the peak minimum was designated as unfolding temperature of the protein.

3.5.2.6 SOLID-STATE FOURIER TRANSFORM INFRARED SPECTROSCOPY (SS-FTIR)

ss-FTIR spectra were generated with a Spectrum Two™ FT-IR spectrophotometer equipped with an UATR accessory (PerkinElmer Inc., Waltham, USA). The measured samples included protein powders, physical mixtures and extrudates. Protein-loaded extrudates were milled with a mortar and pestle prior measurement. A tight pressure clamp with a flat tip ensured a good contact between the sample and the reflection diamond crystal. Each sample was measured as triplicate. The spectra were recorded against an air background between 4000-400 cm^{-1} with an average of four scans and a resolution of 4 cm^{-1}. Data were collected in the absorption mode. First and second derivative analysis was performed with GraphPad PRISM Software (San Diego, CA, USA). The secondary structure elements (i.e., β-sheet structure, α-helix, β-turn, or unordered structures) were considered in the amide-I region (1700-1600 cm^{-1}) of the protein.

3.5.2.7 CIRCULAR-DICHROISM SPECTROSCOPY

In order to analyze the secondary structure of the proteins, Far-UV-CD was exploited. Firstly, samples of pure proteins serving as reference samples were diluted to a concentration of 0.4 mg/mL in pure water (BSA and Lysozyme) or 0.5 % formic acid in pure water (Insulin human) as insulin turned out to be only poorly soluble at a neutral pH. Following this, 40 % protein extrudates were diluted to concentrations ranging from 0.4 mg/mL to 1.0 mg/mL of the respective extrudate (0.16 mg/mL protein to 0.4 mg/mL protein) with pure water (BSA and Lysozyme samples) or with 0.5 % (v/v) formic acid in pure water (human insulin samples). In addition, a solution containing 0.6 mg/mL PEG 20,000, resembling the PEG 20,000 concentrations from the protein extrudate samples was prepared in pure water and in 0.5 % formic acid in pure water. The CD spectra were recorded using a spectropolarimeter (J-715, Jasco Corp., Japan) by scanning the sample from 195 to 260 nm at 20 °C using a 0.1 cm quartz cuvette. Bandwidth, sensitivity, and scanning speed was set at 0.5 or 1.0 nm, 100 mdeg and 100 nm/min, respectively. Three spectra were recorded with each spectrum being the average of three scans. Initially, datasets were recorded of the respective solvents lacking of the respective protein component and of the PEG only containing solutions. They were used for subtraction of the solvent, respectively PEG

20,000 background from the actual protein containing spectra in the Jasco spectra manager software. After subtraction, these spectra were smoothed using the preset values in the Jasco spectra manager software.

3.5.2.8 BIOLOGICAL ACTIVITY OF LYSOZYME

Lysozyme activity was determined by a fluorescence-based assay (EnzChek® Lysozyme Assay Kit, Molecular Probes Europe BV, Leiden, The Netherlands) using a suspension of *Micrococcus lysodeikticus* labeled with fluorescein. The assay determines the Lysozyme activity on labeled cell walls of *Micrococcus lysodeikticus*. The fluorescence increase was measured using a microplate reader with a fluorescein filter and OptiPlate™-96 F microwell plates (VICTOR3™ Multilabel Plate Reader; 96-Well plates black, PerkinElmer Life and Analytical Sciences, Shelton, USA). Preparation of DQ Lysozyme substrate stock suspension, Lysozyme standard curve, as well as the procedure were conducted according to the manufacturer's protocol. The reaction mixtures were incubated at 37 °C for 30 min, protected from light. The fluorescence intensity of each reaction in a microwell plate was measured at 494 nm (absorption maximum) and 518 nm (emission maximum). The fluorescence values obtained from the control without enzyme were subtracted.

3.5.2.9 ACCELERATED THERMAL STRESS TEST

To assess the protein stability under thermal stress (accelerated conditions) protein-loaded PEG-extrudates and protein powder (reference) were stored at 40 °C for 28 days. Briefly, protein-loaded PEG-extrudates and protein powder (Lysozyme, BSA, and human insulin) were stored in an upright orientation (Eppendorf LoBind, 0.5 mL, Eppendorf, Hamburg, Germany) at 40 ± 1 °C (Thermocabinet BE400, Memmert GmbH & Co. KG, Schwabach, Germany) for 28 days. After 28 days of storage, the samples were analyzed by (i) RP HPLC (chemical stability and protein concentration), (ii) SEC (protein fragment and aggregation analysis), (iii) DSC (protein's unfolding temperature), (iv) FTIR spectroscopy (conformational stability), and (v) activity assay (only for Lysozyme).

3.5.2.10 STATISTICAL ANALYSIS

Statistical analysis and testing for statistical significance was carried out using GraphPad PRISM Software (San Diego, CA, USA).

3.6 RESULTS AND DISCUSSION

During melt extrusion mainly the stress factors heat exposure in combination with shear stress, are potentially affecting protein stability and consequently can lead to their degradation or inactivation. Within the current study, the analytical investigation and characterization of protein stability in highly-loaded protein extrudates was demonstrated. The stability of Lysozyme, BSA, and human insulin after ram extrusion and TSE at low temperatures (< 70 °C) was evaluated by RP-HPLC (chemical stability and protein concentration), SEC (protein fragment and aggregation analysis), SEM-EDX (protein particle distribution over extrudate cross section), DSC (unfolding temperature of the proteins), CD and FTIR spectroscopy (conformational stability), and in case of Lysozyme biological activity (Lysozyme activity assay).

3.6.1 CHEMICAL PROTEIN STABILITY AND PROTEIN CONCENTRATION IN EXTRUDATES

Chemical degradation of a protein due to oxidation can occur during any stage of protein production, purification, formulation and storage and any protein that contains Histidine, Methionine, Cysteine, Tyrosine and Tryptophan amino acids is susceptible to oxidation [34]. The degradation behavior (i.e., appearance of chemically and structurally modified degradation products) of Lysozyme, BSA, and human insulin after melt extrusion was monitored by RP-HPLC. Chemical stability analysis of the extracted proteins by RP-HPLC showed that no oxidation or hydrolysis of the proteins occurred during ram extrusion or TSE at 63 °C. The protein content in extrudates was also analyzed by RP-HPLC and compared to the theoretical or target protein concentration (Figure 3). The theoretical protein concentration resulted from the weighed amounts (40 % protein powder and 60 % PEG 20,000) of the components to prepare the respective physical mixture. The actual protein concentration was measured by RP-HPLC as mentioned before. The protein concentration in ram extrudates showed the highest deviation of target and actual protein concentration (Δc = difference between target and actual concentration) compared to extrudates prepared by TSE and was 1.9, 1.5, and 2.5 % for Lysozyme-, BSA-, and human insulin-loaded extrudates, respectively. TSE with conveying screw configuration showed the lowest deviation in protein content Δc = 0.3, 0.8, and 1.5 % for Lysozyme, BSA, and human insulin, respectively) and hit the target concentration closest. The results also highlight, that the use of conveying screws was satisfactory in terms of homogenous protein particle distribution and the use of a single kneading element did

not improve the distribution and was thus not superior. In contrast to ram extrusion, TSE uses co-rotating screws to press the molten material through a cylindrical die. Once the physical powder mixture has passed through the feed system to the screws, it is conveyed by the turning motion of the screws along the extruder barrel, which introduces mixing and heat into the material through both external heaters and friction between the screws, barrel and within the material (viscous dissipation).

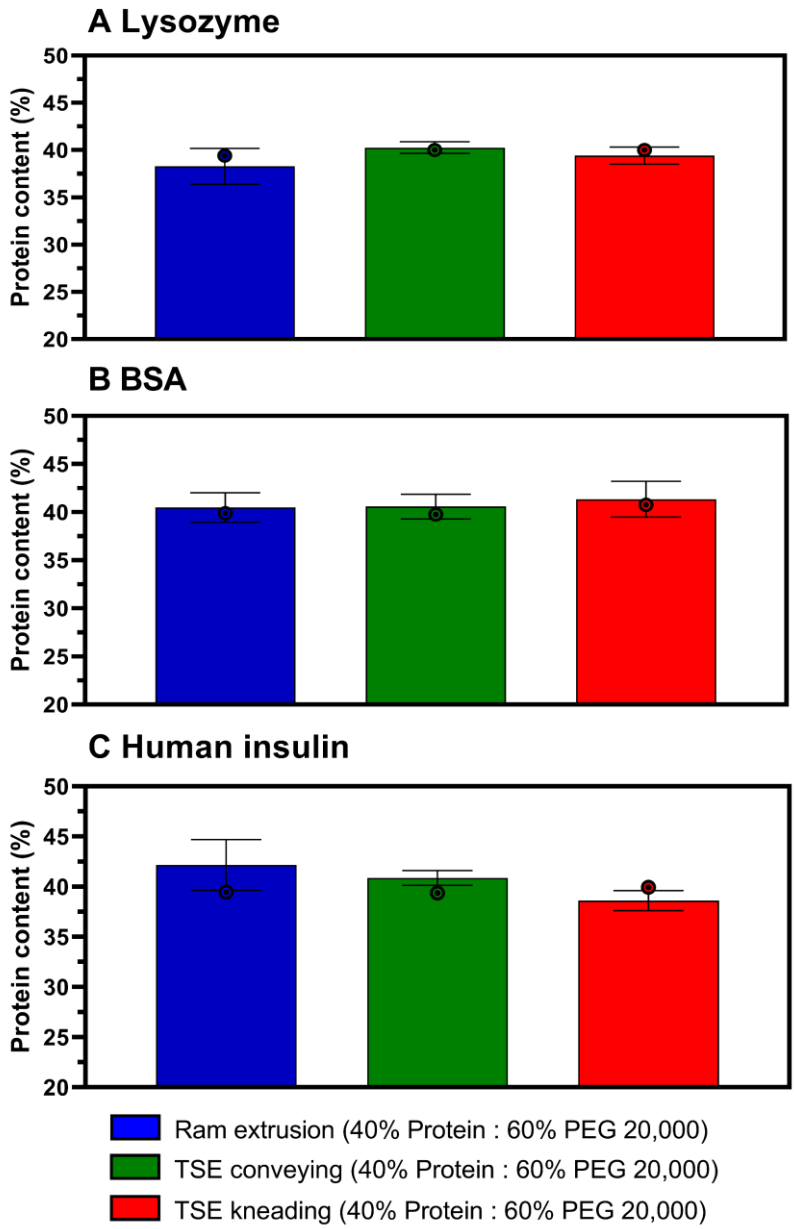

Figure 1 Protein concentration in 40 % protein-loaded extrudates (n = 3) prepared by ram extrusion (blue) or TSE with only conveying screw configuration (green), or screws containing a single 90° kneading element (red), at 63 °C; **A** Lysozyme-loaded extrudates, **B** BSA-loaded extrudates, and **C** human insulin-loaded extrudates; bars represent the measured protein concentration; error bars represent the standard deviation of three measurements for the protein content by RP-HPLC; the dots show the target protein concentration based on the protein concentration of the processed physical mixture.

3.6.2 FRAGMENT AND PROTEIN AGGREGATION ANALYSIS

Protein denaturation can occur and lead to aggregation and formation of high molecular weight species (HMWS). When the protein is denatured (partially or completely), more hydrophobic parts of the molecule are exposed, as well as a higher flexibility of the whole protein molecule [15]. However, proteins in solid-state formulations can tend to aggregate without any detectable change in secondary structure and are therefore indistinguishable from native protein species using techniques such as FTIR spectroscopy [53]. SEC is a commonly used method for the detection of protein aggregation and fragment formation. The aggregation behavior of Lysozyme, BSA, and human insulin after melt extrusion was monitored and HMWS or fragments were separated from monomeric derivatives. SEC revealed, that extrusion did not trigger the formation of protein fragments or protein aggregates in the case of Lysozyme and BSA. Lysozyme was only present as a monomer after dissolving the extrudates in eluent. Native BSA occurred as a mixture of monomers and dimers, however the ratio of these species was not negatively affected by ram extrusion or TSE. Native human insulin appeared as a species at a retention time of 21 min. A second small peak in front of the peak of native human insulin appeared in combination with PEG 20,000. This second population indicated the formation of HMWS in the presence of PEG 20,000. However, the amount of HMWS was < 0.2 % compared to the monomer species of human insulin. Furthermore, the formation of the HMWS was independent of the extrusion process, since HMWS appeared also in the case of the unprocessed, physical mixture composed of 40 % human insulin and 60 % PEG 20,000. This observation highlighted that human insulin molecules interacted with hydrophilic PEG 20,000 molecules may be due to a PEG-induced alteration of the local peptide structure. Recent studies suggest that stabilization of a protein by PEG is dependent on the protein size and its sequence and is thus not generally transferable [38]. As these interactions are unfavorable, we cannot recommend PEG 20,000 as polymeric matrix and protein stabilizer for human insulin formulations.

3.6.3 PROTEIN PARTICLE DISTRIBUTION OVER THE CROSS SECTIONS OF EXTRUDATES

Protein particle distribution was analyzed by SEM-EDX. Images of the cross section of extrudates produced at 63 °C using ram extrusion or TSE were compared. The cross-section cut of the extrudates prepared by ram extrusion (Figure 4) showed no

pores or cracks inside of the extrudates, whereas the extrudates prepared by TSE showed only few pores (Figure 4). Elemental mapping of the protein's nitrogen atoms showed a homogenous distribution of protein particles in extrudates prepared by ram extrusion and TSE at 63 °C. Furthermore, the protein particles were solely embedded in the hydrophilic matrix of PEG 20,000 and not shredded or dissolved during ram extrusion or TSE (Figure 4). Moseson et al. (2022) discuss the dependence of the residence time during hot melt extrusion and the dissolution rate of drug crystals in the molten polymer. The crystal model drugs showed a significant residual crystallinity for short residence times (2 min.), indicating a low crystal dissolution rate [54]. During our TSE experiments, the residence times were < 1 min assuming that the time for dissolving and dissolution rate of protein powder particles in molten PEG 20,000 was extremely small. The shown particle morphology of embedded protein particles compared to the used protein powder particles (right column of Figure 4) confirmed the hypothesis of a solely embedment in the hydrophilic matrix of PEG 20,000 without dissolving or recrystallization of the protein particles during melt extrusion processing. The protein particles probably act as filler material resulting in a reduced amount of energy required for the viscous dissipation during melt extrusion processing. Coefficients of variance were used to describe the protein particle distribution over the cross section of extrudates quantitatively. Protein-loaded extrudates prepared by ram extrusion showed the highest CV (3.58, 10.07, and 12.39 % for Lysozyme, BSA, and human insulin, respectively) compared to extrudates processed by TSE (conveying screw configuration: 3.31, 7.48, and 6.59 %; kneading screw configuration: 0.41, 6.33, and 8.41 % for Lysozyme, BSA, and human insulin, respectively) and is thus associated with a less homogenous particle distribution. During ram extrusion the molten blend is forced through the die with the aid of a driving piston. The barrel of the ram extruder does not contain any restrictive elements for mixing like the co-rotating screws of a twin-screw extruder. However, the homogeneity depends on the initial particle size and distribution of the protein particles. In general, the small lysozyme particles resulted in low CV at all processing variants. Ram extrusion provided also homogenously distributed protein-loaded extrudates when small-sized protein particles (< 200 µm) with a narrow particle distribution will be used. In contrast to TSE, ram extrusion offers the potential to prepare highly-loaded solid protein formulations at high yield, high drug load and at low shear stress.

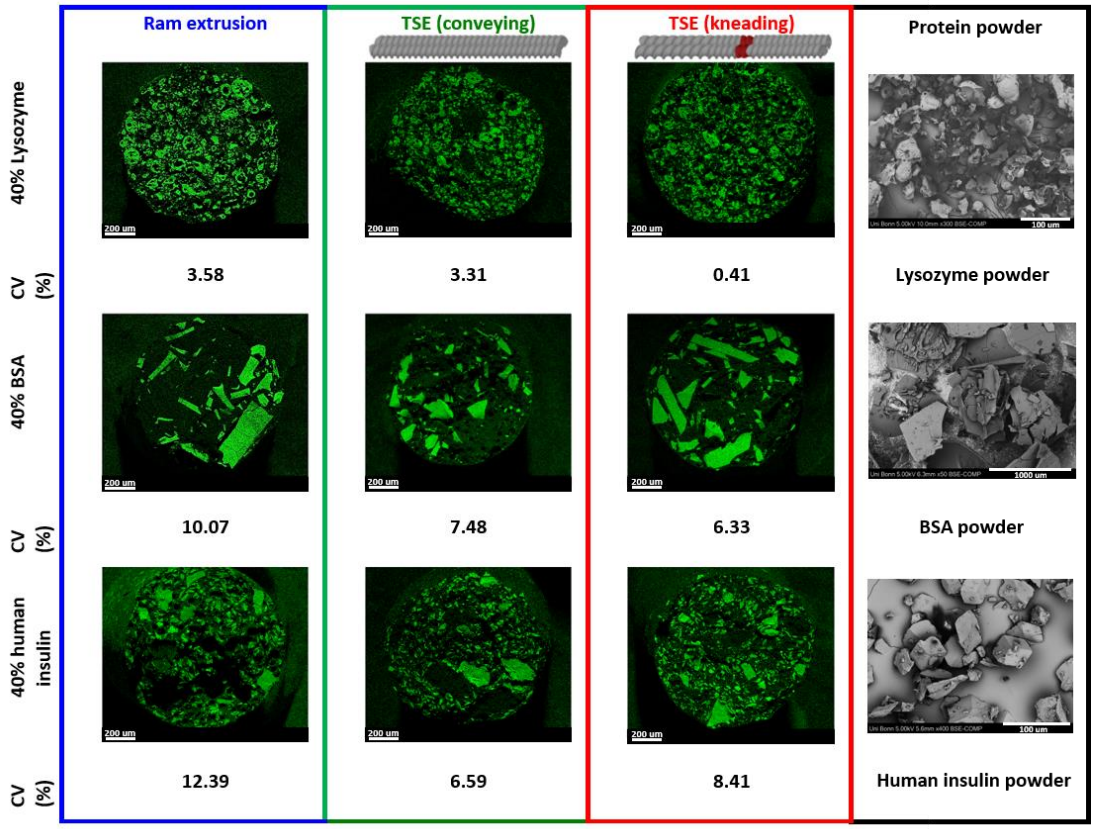

Figure 4 Protein particle distribution of Lysozyme, BSA, human insulin illustrated with EDX-SEM elemental mapping of nitrogen (green spots) on cross section of 40 % protein-loaded extrudates prepared by ram (blue) or TSE with only conveying screw configuration (green), or screws containing a single 90° kneading element (red), at 63 °C; and coefficients of variation (%) of the image analyses of SEM-EDX-maps. The scale bar corresponds to 200 µm. SEM-images of the used protein powder (black) are shown on the right column.

3.6.4 UNFOLDING TEMPERATURE

The globular structure of proteins is referred to as the native state. Unfolding and denaturation is mostly accompanied by a loss of that globular structure or the loss of secondary or tertiary structures that most proteins adopt. Consequently, upon unfolding or denaturation, the protein structure changes its physical state, but maintaining the chemical composition [34]. Proteins do not melt, but they change their molecular conformation from a native to a denatured state at the unfolding temperature. DSC was used to measure the protein unfolding temperature in solid-state (midpoint being denoted as the T_m value) [30]. At T_m the attractive intra-molecular forces were overcome, which preserve their native state. The reported denaturation temperatures for proteins in the solid-state are predominately high and often above 200 °C [30]. DSC thermograms exhibited broad peaks designated as unfolding temperatures (T_m) of 204.7 °C, 218.2 °C, and 213.1 °C for native Lysozyme,

BSA, and human insulin, respectively (Figure 5). Moreover, Figure 5 shows that the unprocessed proteins unfolded and a peak was detected at their apparent denaturation temperatures, which varied according to the protein [30],[40],[41],[55],[56]. In general, an increasing unfolding temperature reflects an increase in conformational protein stability. The physical mixtures composed of 40 % protein powder and 60 % PEG 20,000, showed reduced unfolding temperatures for all the used proteins compared to the reference samples may be due to the formation of an eutectic mixture. This observation was confirmed by DSC scans of physical mixtures composed of 20, 40, and 60 % BSA (Supplementary Information, Figure S1). The unfolding temperature of BSA was reduced in the presence of PEG 20,000, and depending on the amount of polymer (80, 60, and 40 % PEG 20,000, ranking order: 216.3, 217.3, and 218.6 °C, respectively). Presumably the most common stress that can cause a loss of protein structure is elevated temperature and designated as thermally induced protein denaturation (unfolding). The presence of a melting peak > 200 °C in the DSC scan can indicate conservation of protein conformation after extrusion at 63 °C. Lysozyme showed a significantly reduced unfolding temperature after TSE with conveying screws (202.1 °C) and a screw configuration containing a single kneading element (201.8°C) at 63 °C. The ram extrusion process did not affect the unfolding temperature (203.9 °C) of Lysozyme significantly. For BSA and human insulin the applied formulation processes significantly affected the unfolding temperature towards lower temperatures compared to the reference samples. However, the total reduction of unfolding temperatures compared to the reference samples were < 1.5 °C and < 4.5 °C for BSA- and human insulin-containing extrudates, respectively. DSC was also used to evaluate extrusion processing and effects of the used extrusion process on the thermal stability of proteins. Ram extrusion resulted in the lowest, whereas TSE with a kneading screw element led to the largest reduction of unfolding temperatures of Lysozyme, BSA, and human insulin. The thermal unfolding mechanisms of Lysozyme, BSA, and human insulin include the appearance of a single melting peak. The proteins exhibit an irreversible unfolding mechanism [55] as was seen in the second DSC scan, since the single peak of the first scan was completely disappeared (data not shown).

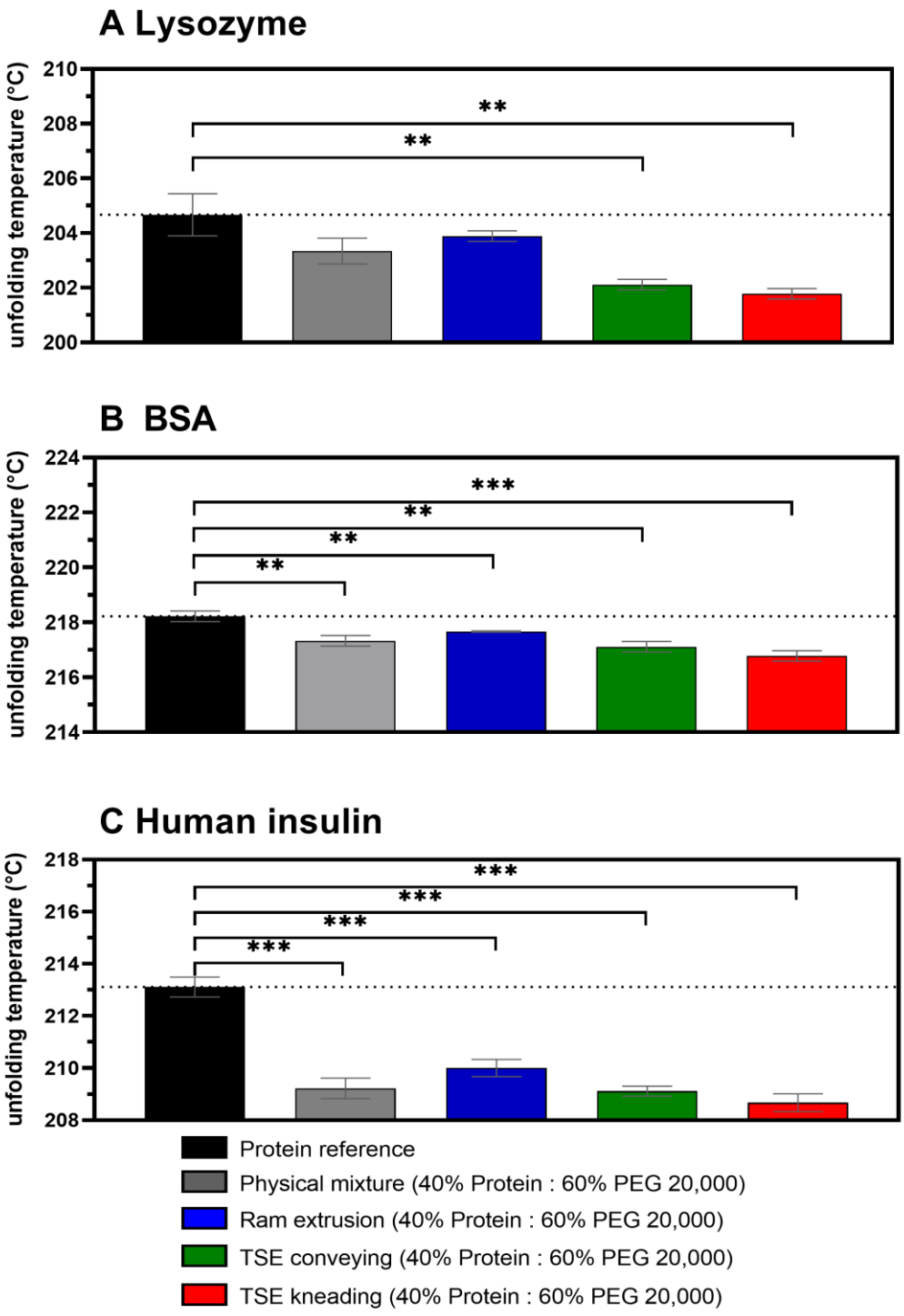

Figure 5 Unfolding temperature of protein powders (black), physical mixtures (gray), and 40 % protein-loaded extrudates prepared by ram extrusion (blue) or TSE with only conveying screw configuration (green), or screws containing a single 90° kneading element (red), at 63 °C; **A** Lysozyme-loaded extrudates, **B** BSA-loaded extrudates, and **C** human insulin-loaded extrudates; the dotted line shows the unfolding temperature of the unprocessed protein (reference). Error bars represent the standard deviation of three measurements for the unfolding temperature by DSC; unpaired *t*-test (two-sample assuming equal variances) was used and statistical significance was depicted by asterisks (*): * $p < 0.05$, ** $p < 0.01$, *** $p < 0.001$, **** $p < 0.0001$.

3.6.5 CONFORMATIONAL STABILITY AND SECONDARY STRUCTURE ANALYSIS

CD and FTIR spectroscopy were used to compare the molecular conformation and secondary structure elements of protein powder before and after melt extrusion. The secondary structure information of powdered Lysozyme, BSA, and human insulin was used as a reference (Figure 6). The model protein Lysozyme is a small globular protein having a molecular weight of 14.4 kDa, five helical regions, five regions of beta sheet, a large amount of random coil and beta turns.35 The secondary structure elements of Lysozyme as obtained from the Protein Data Bank mainly include α-helices (34 % – 42 %). and β-sheets (7 % – 12 %) [42],[57]. The native Lysozyme spectrum showed two minima around 206 and 220 nm, representing the main features of α-helical secondary structure. The conformational stability of Lysozyme in PEG-extrudates was confirmed by CD and FTIR spectroscopy. The conformational stability of Lysozyme was not negatively affected by ram extrusion or TSE. The spectra of extrudates containing 40 % Lysozyme and prepared by ram extrusion or TSE were comparable to the native Lysozyme powder used to prepare the physical mixture and thus the extrudates (Figure 6A). There was also no indication for denaturation (shifts or distortion of bands) or aggregation (intermolecular β-sheet formation) as a consequence of the heat exposure and shear stress during ram extrusion or TSE at 63 °C. Previous studies using CD and FTIR spectroscopy have reported the secondary structure of BSA (M_w = 66.5 kDa). These studies showed that the α-helical content of BSA ranges from 52 % to 68 % also containing 10 % turns, but no β-sheets [58–60]. The CD spectra of all BSA samples were mostly overlapping, however in the FTIR spectra some shifts are shown. A probable explanation for the observed differences in the FTIR spectra at 1652 cm^{-1} may be the extrusion procedure, since extrusion (thermal and shear stress) can cause reversible changes in protein conformation and is associated with a reduction in the α-helical content and an increase in the random chain content [61],[62]. Human insulin was also studied for changes in its secondary structure as a result of temperature and shear stress during extrusion processing. Human insulin (M_w = 5.8 kDa) is a peptide and composed of two peptide chains (A- and B-chain) including three α-helices and a short β-sheet segment (Figure 6B) [63]. CD spectra of human insulin-loaded extrudates prepared by TSE showed clear shifts and changes in secondary structure elements. The shifts were also confirmed by the FTIR spectra (second derivative). The second derivative spectra of the Amide I band suggested a red-shift of the bands around 1650-1665 cm^{-1}, assigned to turns and β-sheet, which can be caused by small loosening

of the turn structures. These changes indicated the transformation of α-helix content to β-sheets or a disordered structure which enhances the tendency to aggregate. In particular, the band at 1652 cm^{-1} which corresponds to α helical structures [61], was obviously affected by TSE with screws containing a kneading element due to higher shear stress and residence time. As can be seen in the CD and FTIR spectra, ram extrusion had the lowest impact on secondary structure changes of human insulin (Figure 6C).

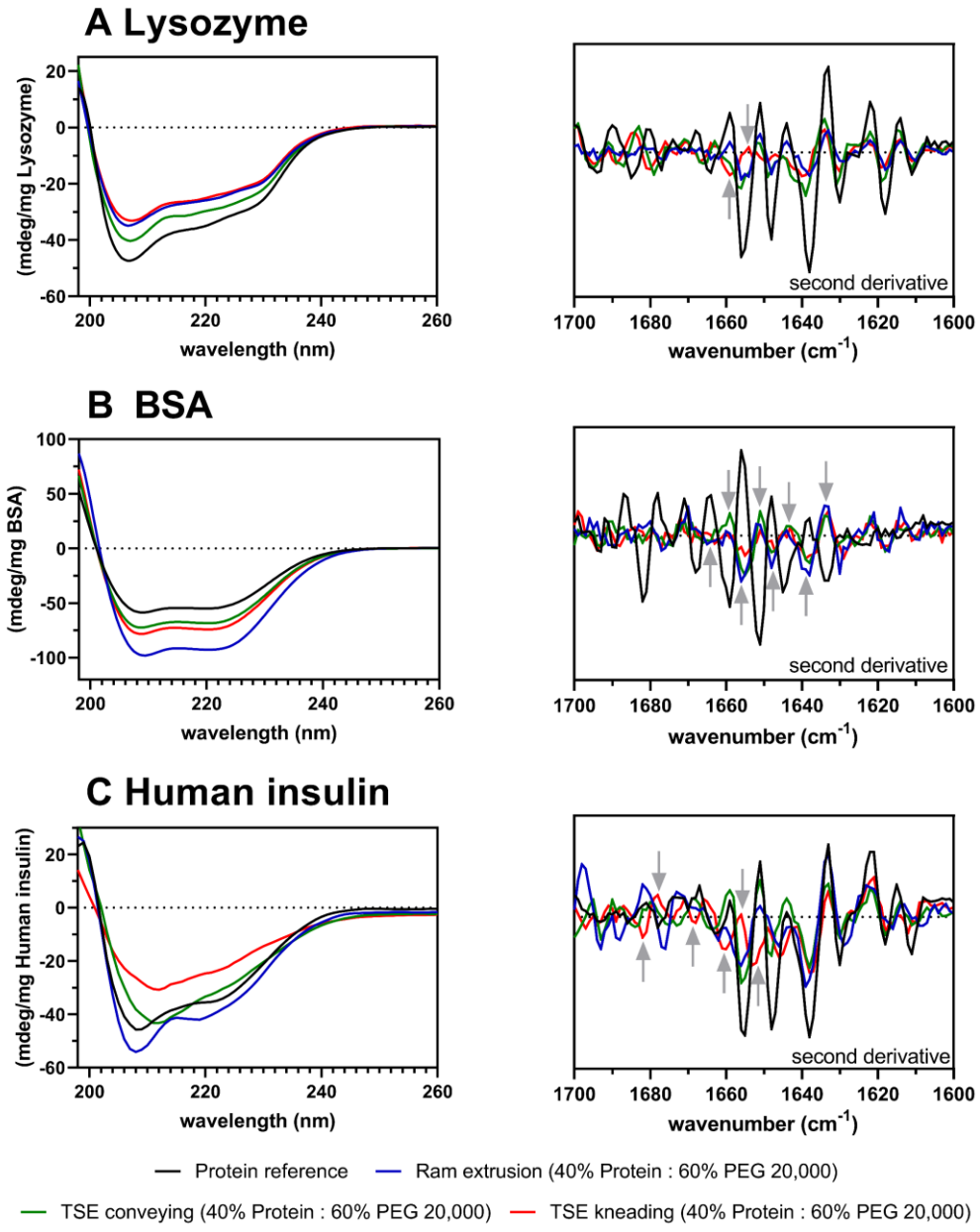

Figure 6 Left: CD spectra of **A** Lysozyme, **B** BSA, and **C** human insulin (protein reference samples in black) in aqueous solution and 40 % protein-loaded extrudates after reconstitution at 20 °C; initial ellipticity values were corrected by the respective amount of protein weighed in for the measured solution; right: Second derivative of FTIR spectra in the Amide I region (1600-1700 cm^{-1}) of protein

powder (black), and 40 % protein-loaded extrudates prepared by ram extrusion (blue) or TSE with only conveying screw configuration (green), or screws containing a single 90° kneading element (red), at 63 °C; gray arrows highlight changes in secondary structure elements.

3.6.6 PROTEIN STABILITY AFTER ACCELERATED THERMAL STRESS

An accelerated thermal stability study was applied to obtain protein stability data. At the end of the storage period, the samples (unstressed protein powder as reference, protein powder and protein-loaded extrudates stored at 40 °C for 28 days) were analyzed by HPLC, SEC, DSC, and FTIR spectroscopy. Lysozyme containing PEG-extrudates were additionally tested for a potential loss of biological activity (refer to section 3.7.7). Chemical degradation of the protein after storage at 40 °C was investigated by HPLC. The results showed that no oxidation or hydrolysis of the proteins occurred after storage. Protein denaturation, protein aggregation or formation of HMWS are also potential events occurring during thermal storage of protein formulations. The aggregation behavior of Lysozyme, BSA, and human insulin after storage was monitored and HMWS or fragments were separated from monomeric derivatives by SEC. Results showed, that the thermal storage of Lysozyme-loaded extrudates did not result in the formation of protein aggregates. Lysozyme was only present as a monomer after dissolving the extrudates in eluent (Figure 7A). Native BSA occurred as a mixture of monomers and dimers (Figure 7B). The BSA-containing samples (i.e., BSA powder, and BSA-loaded extrudates) stored at 40 °C showed a small shoulder of the dimeric peak assuming that trimers were present in the samples. BSA trimers occurred also in the stored BSA powder and thus the impact of melt extrusion processing was not the driver for the formation of trimers. Native human insulin showed a single peak at a retention time of 21 min. (Figure 7C). A second small peak in front of the peak of native human insulin appeared after storage at 40 °C. This second population indicated the formation of HMWS due to thermal stress during storage over 28 days. However, the amount of formed HMWS was in the same magnitude as the stored unprocessed human insulin powder.

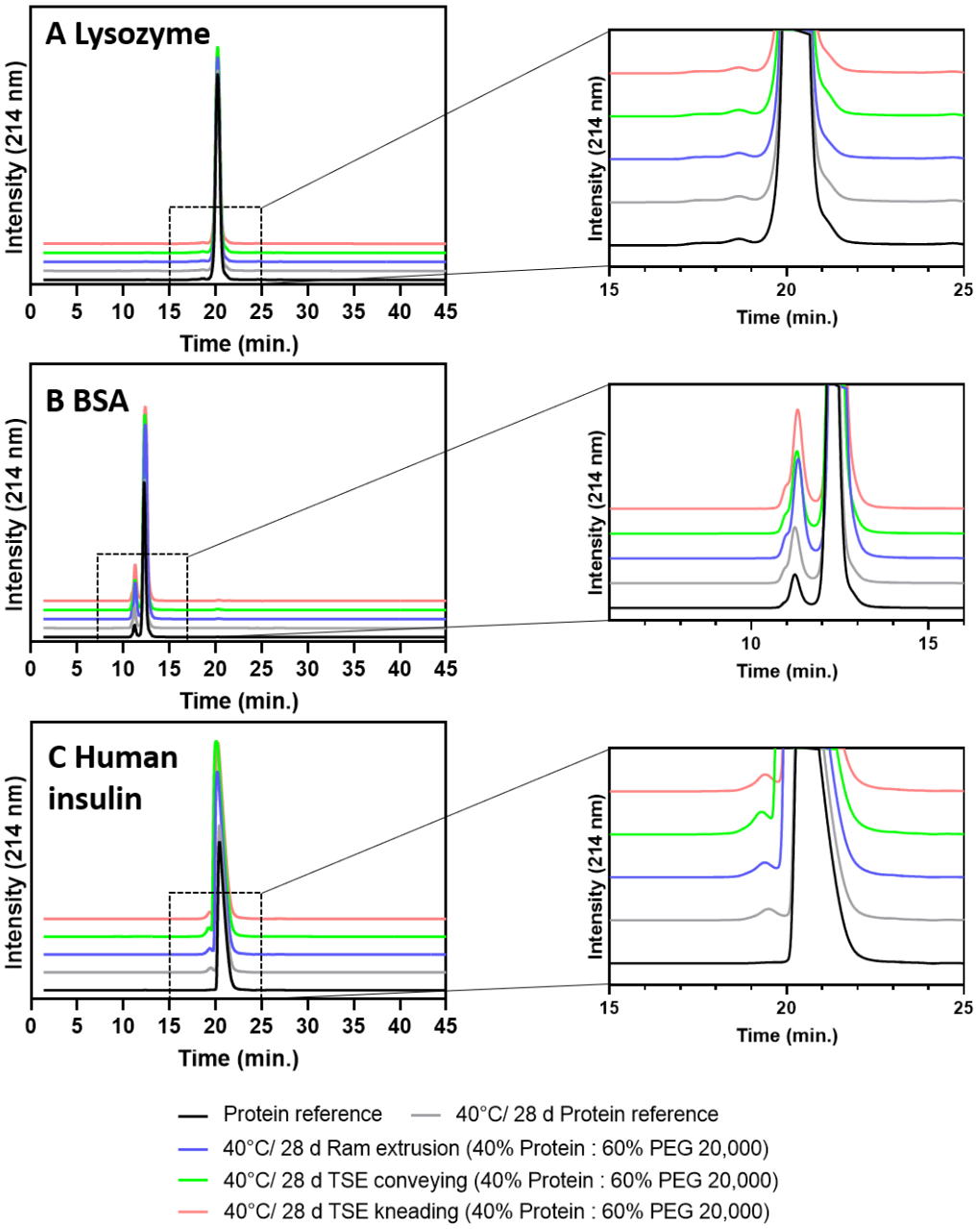

Figure 7 Chromatograms of SEC analysis after an accelerated stability study at 40 °C for 28 days. Protein powders (initial: black, after 28 days at 40 °C: gray), and 40 % protein-loaded extrudates prepared by ram extrusion (blue) or TSE with only conveying screw configuration (green), or screws containing a single 90° kneading element (red), at 63 °C; **A** Lysozyme-loaded extrudates, **B** BSA-loaded extrudates, and **C** human insulin-loaded extrudates. Right: Magnified areas of the peak of interest.

Protein unfolding and denaturation is mostly accompanied by a loss of the specific globular protein structure or the loss of secondary or tertiary structure elements. DSC was used to measure the protein unfolding temperature in solid-state (Figure 8). In the case of Lysozyme, the unfolding temperature as well as the secondary structure elements were not negatively affected or shifted due to thermal stress (i.e., 28 days at 40 °C) (Figure 8A). The unfolding temperature of BSA samples was also not

significantly reduced. The FTIR spectra (second derivative) of the unprocessed, stored BSA powder showed shifts in secondary structure elements. The shifts in the amide I region of BSA-loaded extrudates were comparable to the unprocessed, stored BSA powder, indicating that melt extrusion processing did not cause these modifications. The stability of the unprocessed and stored human insulin powder was significantly affected by thermal stress (Figure 8C) resulting in a reduced unfolding temperature and shifts in secondary structure elements compared to the reference. The secondary structure and unfolding temperature of human insulin was less affected in extrudates produced by ram extrusion or TSE during storage at 40 °C.

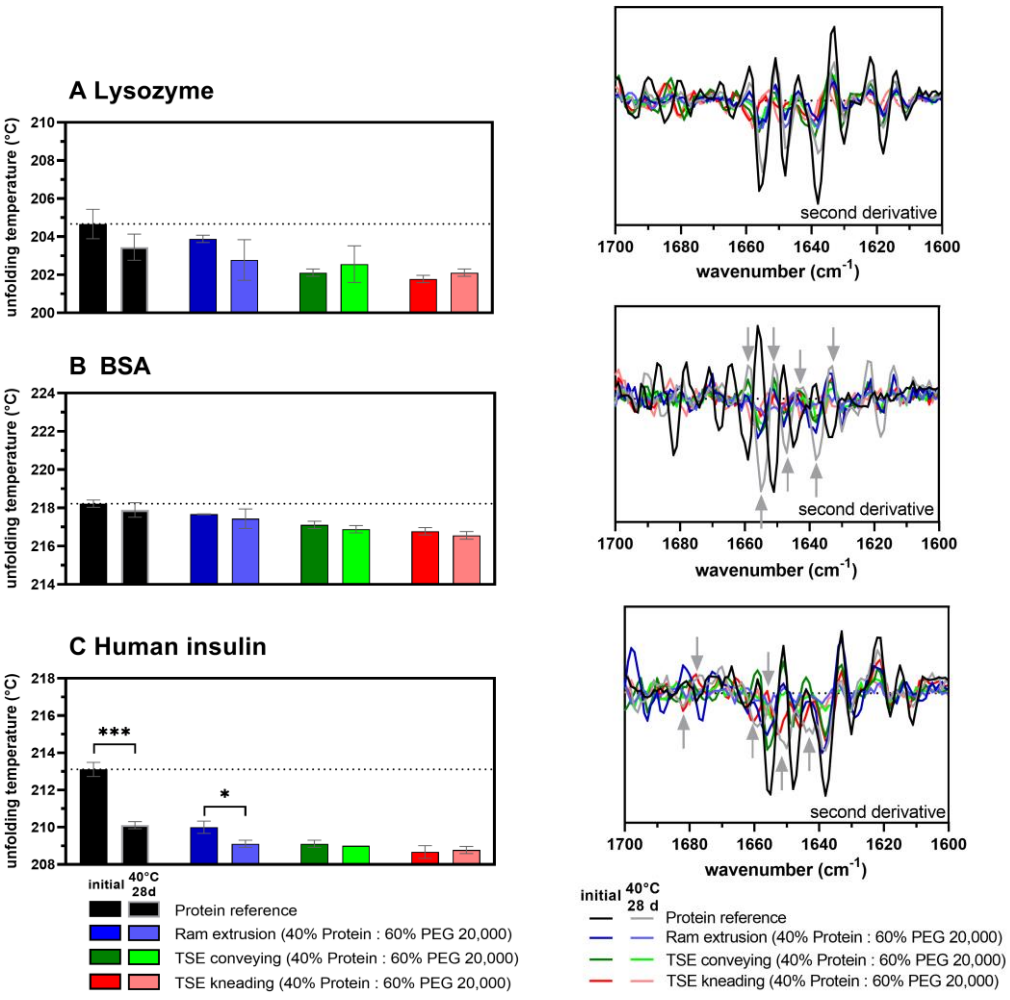

Figure 8 Results of accelerated thermal stability study at 40 °C for 28 days. Left: Unfolding temperature of protein powder references (black), and 40 % protein-loaded extrudates prepared by ram extrusion (blue) or TSE with only conveying screw configuration (green), or screws containing a single 90° kneading element (red), at 63 °C determined by DSC; **A** Lysozyme-loaded extrudates, **B** BSA-loaded extrudates, and **C** human insulin-loaded extrudates; the dotted line shows the melting unfolding temperature of the unprocessed protein (reference). Bars with gray border color represents the unfolding temperatures after an accelerated storage stability study at 40 °C for 28 days. Error bars represent the standard deviation of three measurements for the melting unfolding temperature by DSC; unpaired *t*-test

(two-sample assuming equal variances) was used and statistical significance was depicted by asterisks (*): * $p < 0.05$, ** $p < 0.01$, *** $p < 0.001$, **** $p < 0.0001$. Right: Second derivative of FTIR spectra in the Amide I region (1600-1700 cm^{-1}) of protein powder reference (black and gray), and 40 % protein-loaded extrudates prepared by ram extrusion (blue) or TSE with only conveying screw configuration (green), or screws containing a single 90° kneading element (red), at 63 °C; gray arrows highlight changes in secondary structure elements.

3.6.7 BIOLOGICAL LYSOZYME ACTIVITY AFTER EXTRUSION

Therapeutic proteins can rapidly denature and lose their function due to applied stresses during processing. Despite Lysozyme is known as one of the most stable proteins, it is an accepted model for investigating the relationship between protein structure and biological function. I.e., if a process results in a significant loss in activity of Lysozyme this process would disqualify itself for processing of other (model) proteins. The biological activity of Lysozyme was investigated immediately after ram extrusion and TSE at 63 °C and an accelerated thermal stress test at 40 °C for 28 days (refer to section 3.6). Lysozyme embedded in melt extrudates by ram extrusion or TSE at 63 °C and after the accelerated stress test maintained full enzymatic activity when compared to an unprocessed or initial sample (*t*-test: $p < 0.05$) as expected (Figure 9). The assay showed a satisfactory activity of Lysozyme after ram extrusion and TSE and highlights the extreme stability of Lysozyme against heat exposure and shear stress. This observation was confirmed by the results of other applied analytical methods in our study (i.e., RP-HPLC, SEC, DSC, CD and FTIR spectroscopy) and a prior conducted SDS-PAGE analysis of the Lysozyme-loaded extrudates by Elsayed et al. (2022) [64]. Here, the Lysozyme-loaded PEG-extrudates analyzed by one dimensional SDS-PAGE at reducing and nonreducing conditions showed always a clear single band for the samples between 10 and 15 kDa (~14 kDa) without indication of impurities or degradation products of Lysozyme after melt extrusion processing.

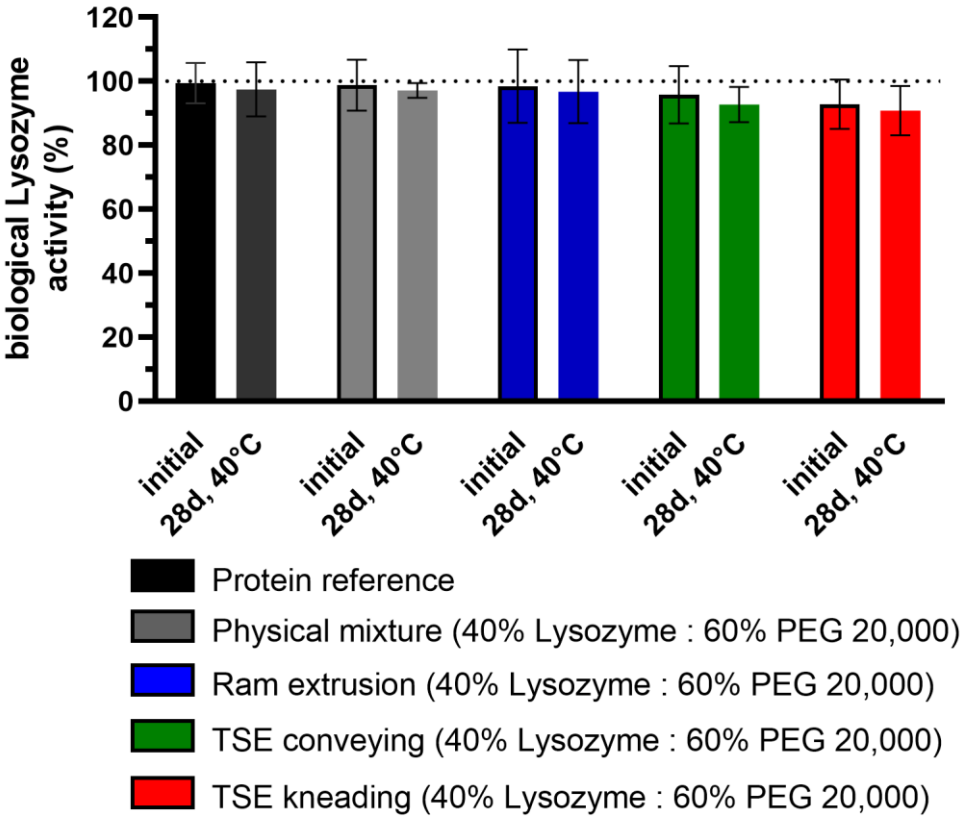

Figure 9 Biological activity of Lysozyme powder (black), the physical mixture (gray), and 40 % Lysozyme-loaded extrudates prepared by ram extrusion (blue) or TSE with only conveying screw configuration (green), or screws containing a single 90° kneading element (red), at 63 °C; initial: samples were immediately analyzed after melt extrusion processing; Bars without border represent the biological activity of Lysozyme of samples stored at 40 °C for 28 days; Error bars represent the standard deviation of three measurements.

3.7 CONCLUSION

In this study, we addressed the investigation of highly-loaded protein PEG-extrudates prepared by ram extrusion and TSE with regard to the main challenges, i.e., protein instability due to heat exposure and shear stress during extrusion. The applied methods, including (i) RP-HPLC (chemical stability and protein concentration), (ii) SEC (protein fragment and aggregation analysis), (iii) SEM-EDX (protein particle distribution), (iv) DSC (protein's unfolding temperature), (v) FTIR and CD spectroscopy (conformational stability), and (vi) activity assay, enabled the successful characterization of protein stability in extrudates (mg-scale) and proved to be very useful techniques to study process-related effects on protein stability and changes in model proteins induced by melt extrusion processing. PEG 20,000 was introduced as a first and simple polymer model due to its low processing temperature (< 70 °C) and hydrophilicity (i.e., simplifying the sample preparation and analytical investigations of protein-loaded extrudates). This study also offers the potential to compare different melt extrusion processes (i.e., ram extrusion vs. TSE (conveying) vs. TSE (kneading)) and extrusion parameters (e.g., shear stress levels, screw configurations, residence times). PEG 20,000 was used as a model polymer to embed and stabilize the proteins by interacting with the protein to decelerate the unfolding rate of the embed proteins. We showed the successful and homogenous embedment of proteins in PEG 20,000 matrices without dissolution of the protein particles in the polymer for solid-state stabilization. Nearly complete recovery of active Lysozyme illustrated that ram extrusion and TSE did not negatively affect the protein integrity. However, differences seen between Lysozyme- and BSA- or human insulin-loaded extrudates indicated that melt extrusion processing could have an impact on the conformational stability. In particular, BSA and human insulin were more susceptible to shear stress compared to Lysozyme. Consequently, ram extrusion led to less conformational changes compared to TSE due to lower shear stress. The use of conveying screws in TSE was satisfactory in terms of homogenous protein particle distribution and the use of a single kneading element did not improve the distribution. Ram extrusion showed also a good protein particle distribution and is especially for small-sized protein particles (< 200 µm) the preferred method to prepare highly-loaded solid protein formulations (i.e., satisfactory protein particle distribution accompanied with lower shear stress compared to TSE). As the results showed unfavorable interactions between PEG chains and human insulin molecules, the hydrophilic PEG is not the appropriate polymeric matrix for embedding human insulin and the stabilizing potential of PEG did

not apply in this case. This study proposes the implementation of a sensitive characterization pathway of protein stability and investigation of the impact of process-related stress on protein stability in highly-loaded solid protein/PEG formulations from small-scale melt extrusion. Melt extrusion processing for solid-state embedment and stabilization of Lysozyme, BSA, and human insulin in PEG-matrices was neither superior nor inferior immediately after processing or an accelerated storage stability study. However, the study highlighted that melt extrusion processing offers the potential for the production of polymer-based protein embeddings in general, e.g., sustained protein release formulations. The applied workflow provides a fundamental basis for future work, including the evaluation of the use of other process techniques (e.g., vacuum compression molding or a combination of spray-drying and melt extrusion), as well as the use of sustained release polymers (e.g., PEO (release over several weeks) PLGA (release over several months, EVA (release up to 2 years) or other excipients (e.g., pH-modifier, surfactants, plasticizer).

3.8 RESEARCH FUNDING

This work was supported by the German Research Foundation (DFG SPP1934, project number: 273937032).

3.9 ACKNOWLEDGEMENTS

The authors thank the German Research Foundation (DFG) for the financial support within the priority program 1934 DiSPBiotech. We kindly thank Sanofi-Aventis Deutschland GmbH for providing human insulin and the use of the 5 mm twin-screw extruder. We thank W. Graf and his team from the Institute of Applied Physics for the production of ram extruder components.

3.10 REFERENCES

[1] V. Gervasi, R. Dall Agnol, S. Cullen, T. McCoy, S. Vucen, und A. Crean, „Parenteral protein formulations: An overview of approved products within the European Union“, Eur. J. Pharm. Biopharm., Bd. 131, S. 8–24, Okt. 2018, doi: 10.1016/j.ejpb.2018.07.011.

[2] H.-C. Mahler, W. Friess, U. Grauschopf, und S. Kiese, „Protein aggregation: Pathways, induction factors and analysis“, J. Pharm. Sci., Bd. 98, Nr. 9, S. 2909–2934, Sep. 2009, doi: 10.1002/jps.21566.

[3] C. J. Roberts, „Protein aggregation and its impact on product quality“, Curr. Opin. Biotechnol., Bd. 30, S. 211–217, Dez. 2014, doi: 10.1016/j.copbio.2014.08.001.

[4] K. D. Ratanji, J. P. Derrick, R. J. Dearman, und I. Kimber, „Immunogenicity of therapeutic proteins: Influence of aggregation“, J Immunotoxicol, S. 11.

[5] W. Jiskoot u. a., „Protein Instability and Immunogenicity: Roadblocks to Clinical Application of Injectable Protein Delivery Systems for Sustained Release“, J. Pharm. Sci., Bd. 101, Nr. 3, S. 946–954, März 2012, doi: 10.1002/jps.23018.

[6] N. B. Pham und W. S. Meng, „Protein Aggregation and Immunogenicity of Biotherapeutics“, Int. J. Pharm., S. 119523, Juni 2020, doi: 10.1016/j.ijpharm.2020.119523.

[7] I. Fischer, A. Schmidt, A. Bryant, und A. Besheer, „Calculation of injection forces for highly concentrated protein solutions“, Int. J. Pharm., Bd. 493, Nr. 1–2, S. 70–74, Sep. 2015, doi: 10.1016/j.ijpharm.2015.07.054.

[8] M. A. H. Capelle, R. Gurny, und T. Arvinte, „High throughput screening of protein formulation stability: Practical considerations“, Eur. J. Pharm. Biopharm., Bd. 65, Nr. 2, S. 131–148, Feb. 2007, doi: 10.1016/j.ejpb.2006.09.009.

[9] R. Chaudhuri, Y. Cheng, C. R. Middaugh, und D. B. Volkin, „High-Throughput Biophysical Analysis of Protein Therapeutics to Examine Interrelationships Between Aggregate Formation and Conformational Stability“, AAPS J., Bd. 16, Nr. 1, S. 48–64, Jan. 2014, doi: 10.1208/s12248-013-9539-6.

[10] K. Dauer, W. Kamm, K. G. Wagner, und S. Pfeiffer-Marek, „High-Throughput Screening for Colloidal Stability of Peptide Formulations Using Dynamic and Static Light Scattering“, Mol Pharm., S. 17, 2021.

[11] A. Bhirde, B. V. Chikkaveeraiah, R. Venna, R. Carley, K. Brorson, und C. Agarabi, „High Performance Size Exclusion Chromatography and High-Throughput Dynamic Light Scattering as Orthogonal Methods to Screen for Aggregation and Stability of Monoclonal Antibody Drug Products“, J. Pharm. Sci., Bd. 109, Nr. 11, S. 3330–3339, Nov. 2020, doi: 10.1016/j.xphs.2020.08.013.

[12] H. Ma, C. Ó'Fágáin, und R. O'Kennedy, „Antibody stability: A key to performance - Analysis, influences and improvement“, Biochimie, Bd. 177, S. 213–225, Okt. 2020, doi: 10.1016/j.biochi.2020.08.019.

[13] W. Al-Azzam, E. A. Pastrana, und K. Griebenow, „Co-lyophilization of bovine serum albumin (BSA) with poly(ethylene glycol) improves efficiency of BSA encapsulation and stability in polyester microspheres by a solid-in-oil-in-oil technique“, S. 8.

[14] A. Rezvankhah, Z. Emam-Djomeh, und G. Askari, „Encapsulation and delivery of bioactive compounds using spray and freeze-drying techniques: A review“, Dry. Technol., Bd. 38, Nr. 1–2, S. 235–258, Jan. 2020, doi: 10.1080/07373937.2019.1653906.

[15] M. Gajda, K. P. Nartowski, J. Pluta, und B. Karolewicz, „The role of the polymer matrix in solvent-free hot melt extrusion continuous process for mechanochemical synthesis of pharmaceutical cocrystal“, Eur. J. Pharm. Biopharm., Bd. 131, S. 48–59, Okt. 2018, doi: 10.1016/j.ejpb.2018.07.002.

[16] S. Madan und S. Madan, „Hot melt extrusion and its pharmaceutical applications“, Asian J. Pharm. Sci., S. 11, 2012.

[17] A. Butreddy, K. Y. Janga, S. Ajjarapu, S. Sarabu, und N. Dudhipala, „Instability of therapeutic proteins — An overview of stresses, stabilization mechanisms and analytical techniques involved in lyophilized proteins“, Int. J. Biol. Macromol., S. S0141813020351242, Dez. 2020, doi: 10.1016/j.ijbiomac.2020.11.188.

[18] G. Assegehegn, E. Brito-de la Fuente, J. M. Franco, und C. Gallegos, „The Importance of Understanding the Freezing Step and Its Impact on Freeze-Drying Process Performance“, J. Pharm. Sci., Bd. 108, Nr. 4, S. 1378–1395, Apr. 2019, doi: 10.1016/j.xphs.2018.11.039.

[19] G. Assegehegn, E. Brito-de la Fuente, J. M. Franco, und C. Gallegos, „An Experimental-Based Approach to Construct the Process Design Space of a Freeze-Drying Process: An Effective Tool to Design an Optimum and Robust Freeze-Drying Process for Pharmaceuticals“, J. Pharm. Sci., Bd. 109, Nr. 1, S. 785–796, Jan. 2020, doi: 10.1016/j.xphs.2019.07.001.

[20] J. C. Kasper, M. J. Pikal, und W. Friess, „Investigations on Polyplex Stability During the Freezing Step of Lyophilization Using Controlled Ice Nucleation—The Importance of Residence Time in the Low-Viscosity Fluid State“, J. Pharm. Sci., Bd. 102, Nr. 3, S. 929–946, März 2013, doi: 10.1002/jps.23419.

[21] M. C. Heller, J. F. Carpenter, und T. W. Randolph, „Manipulation of Lyophilization-Induced Phase Separation: Implications For Pharmaceutical Proteins“, Biotechnol. Prog., Bd. 13, Nr. 5, S. 590–596, Okt. 1997, doi: 10.1021/bp970081b.

[22] A. Al-Hussein und H. Gieseler, „The Effect of Mannitol Crystallization in Mannitol–Sucrose systems on LDH Stability during Freeze-Drying“, J. Pharm. Sci., Bd. 101, Nr. 7, S. 2534–2544, Juli 2012, doi: 10.1002/jps.23173.

[23] T. Porfirio, F. J. Galindo-Rosales, L. Campo-Deaño, J. Vicente, und V. Semião, „Rheological characterization of polymeric solutions used in spray drying process“, Eur. J. Pharm. Sci., S. 105650, Dez. 2020, doi: 10.1016/j.ejps.2020.105650.

[24] C. Haeuser, P. Goldbach, J. Huwyler, W. Friess, und A. Allmendinger, „Be Aggressive! Amorphous Excipients Enabling Single-Step Freeze-Drying of Monoclonal Antibody Formulations“, Pharmaceutics, Bd. 11, Nr. 11, S. 616, Nov. 2019, doi: 10.3390/pharmaceutics11110616.

[25] Z. Ghalanbor, M. Körber, und R. Bodmeier, „Improved Lysozyme Stability and Release Properties of Poly(lactide-co-glycolide) Implants Prepared by Hot-Melt Extrusion“, Pharm. Res., Bd. 27, Nr. 2, S. 371–379, Feb. 2010, doi: 10.1007/s11095-009-0033-x.

[26] S. L. Lee, A. E. Hafeman, P. G. Debenedetti, B. A. Pethica, und D. J. Moore, „Solid-State Stabilization of α-Chymotrypsin and Catalase with Carbohydrates“, Ind. Eng. Chem. Res., Bd. 45, Nr. 14, S. 5134–5147, Juli 2006, doi: 10.1021/ie0513503.

[27] Y. Zheng und J. K. Pokorski, „Hot melt extrusion: An emerging manufacturing method for slow and sustained protein delivery“, WIREs Nanomedicine Nanobiotechnology, Bd. 13, Nr. 5, Sep. 2021, doi: 10.1002/wnan.1712.

[28] M. C. Lai und E. M. Topp, „Solid-state chemical stability of proteins and peptides“, J. Pharm. Sci., Bd. 88, Nr. 5, S. 489–500, Mai 1999, doi: 10.1021/js980374e.

[29] M. C. Manning, D. K. Chou, B. M. Murphy, R. W. Payne, und D. S. Katayama, „Stability of Protein Pharmaceuticals: An Update“, Pharm. Res., Bd. 27, Nr. 4, S. 544–575, Apr. 2010, doi: 10.1007/s11095-009-0045-6.

[30] O. Cantin, F. Siepmann, J. F. Willart, F. Danede, J. Siepmann, und Y. Karrout, „PEO hot melt extrudates for controlled drug delivery: Importance of the type of drug and loading“, J. Drug Deliv. Sci. Technol., Bd. 61, S. 102238, Feb. 2021, doi: 10.1016/j.jddst.2020.102238.

[31] S.-H. Chao, S. S. Matthews, R. Paxman, A. Aksimentiev, M. Gruebele, und J. L. Price, „Two Structural Scenarios for Protein Stabilization by PEG“, J. Phys. Chem. B, Bd. 118, Nr. 28, S. 8388–8395, Juli 2014, doi: 10.1021/jp502234s.

[32] B. K. Pandey u. a., „Impact of Site-Specific PEGylation on the Conformational Stability and Folding Rate of the Pin WW Domain Depends Strongly on PEG Oligomer Length“, Bioconjug. Chem., Bd. 24, Nr. 5, S. 796–802, Mai 2013, doi: 10.1021/bc3006122.

[33] M. A. Mohammad, I. M. Grimsey, und R. T. Forbes, „Mapping the solid-state properties of crystalline lysozyme during pharmaceutical unit-operations“, J. Pharm. Biomed. Anal., S. 8, 2015.

[34] A. A. Elkordy, R. T. Forbes, und B. W. Barry, „Integrity of crystalline lysozyme exceeds that of a spray-dried form“, Int. J. Pharm., Bd. 247, Nr. 1–2, S. 79–90, Okt. 2002, doi: 10.1016/S0378-5173(02)00379-4.

[35] L. Sheng, J. Wang, M. Huang, Q. Xu, und M. Ma, „The changes of secondary structures and properties of lysozyme along with the egg storage“, Int. J. Biol. Macromol., Bd. 92, S. 600–606, Nov. 2016, doi: 10.1016/j.ijbiomac.2016.07.068.

[36] P. Zarrintaj u. a., „Poloxamer: A versatile tri-block copolymer for biomedical applications“, Acta Biomater., S. S1742706120302257, Mai 2020, doi: 10.1016/j.actbio.2020.04.028.

[37] M. C. Hamoudi-Ben Yelles, V. Tran Tan, F. Danede, J. F. Willart, und J. Siepmann, „PLGA implants: How Poloxamer/PEO addition slows down or accelerates polymer degradation and drug release“, J. Controlled Release, Bd. 253, S. 19–29, Mai 2017, doi: 10.1016/j.jconrel.2017.03.009.

[38] Z. Ghalanbor, M. Körber, und R. Bodmeier, „Protein release from poly(lactide-co-glycolide) implants prepared by hot-melt extrusion: Thioester formation as a reason for incomplete release“, Int. J. Pharm., Bd. 438, Nr. 1–2, S. 302–306, Nov. 2012, doi: 10.1016/j.ijpharm.2012.09.015.

[39] A. Cossé, C. König, A. Lamprecht, und K. G. Wagner, „Hot Melt Extrusion for Sustained Protein Release: Matrix Erosion and In Vitro Release of PLGA-Based Implants“, AAPS PharmSciTech, Bd. 18, Nr. 1, S. 15–26, Jan. 2017, doi: 10.1208/s12249-016-0548-5.

[40] M.-P. Even, S. Bobbala, B. Gibson, S. Hook, G. Winter, und J. Engert, „Twin-screw extruded lipid implants containing TRP2 peptide for tumour therapy“, Eur. J. Pharm. Biopharm., Bd. 114, S. 79–87, Mai 2017, doi: 10.1016/j.ejpb.2016.12.033.

[41] M. Stanković, H. W. Frijlink, und W. L. J. Hinrichs, „Polymeric formulations for drug release prepared by hot melt extrusion: application and characterization“, Drug Discov. Today, Bd. 20, Nr. 7, S. 812–823, Juli 2015, doi: 10.1016/j.drudis.2015.01.012.

[42] M. Stanković u. a., „Low temperature extruded implants based on novel hydrophilic multiblock copolymer for long-term protein delivery“, Eur. J. Pharm. Sci., Bd. 49, Nr. 4, S. 578–587, Juli 2013, doi: 10.1016/j.ejps.2013.05.011.

[43] M. Vollrath, J. Engert, und G. Winter, „Long-term release and stability of pharmaceutical proteins delivered from solid lipid implants“, Eur. J. Pharm. Biopharm., Bd. 117, S. 244–255, Aug. 2017, doi: 10.1016/j.ejpb.2017.04.017.

[44] J. Buske, C. König, S. Bassarab, A. Lamprecht, S. Mühlau, und K. G. Wagner, „Influence of PEG in PEG–PLGA microspheres on particle properties and protein release“, Eur. J. Pharm. Biopharm., Bd. 81, Nr. 1, S. 57–63, Mai 2012, doi: 10.1016/j.ejpb.2012.01.009.

[45] M. E. Ali und A. Lamprecht, „Spray freeze drying as an alternative technique for lyophilization of polymeric and lipid-based nanoparticles“, Int. J. Pharm., Bd. 516, Nr. 1–2, S. 170–177, Jan. 2017, doi: 10.1016/j.ijpharm.2016.11.023.

[46] K. E. Steffens, M. B. Brenner, M. U. Hartig, M. Monschke, und K. G. Wagner, „Melt granulation: A comparison of granules produced via high-shear mixing and twin-screw granulation“, Int. J. Pharm., Bd. 591, S. 119941, Dez. 2020, doi: 10.1016/j.ijpharm.2020.119941.

[47] W. Wang, S. Nema, und D. Teagarden, „Protein aggregation—Pathways and influencing factors“, Int. J. Pharm., Bd. 390, Nr. 2, S. 89–99, Mai 2010, doi: 10.1016/j.ijpharm.2010.02.025.

[48] K. Griebenow und A. M. Klibanov, „Lyophilization-induced reversible changes in the secondary structure of proteins.“, Proc. Natl. Acad. Sci., Bd. 92, Nr. 24, S. 10969–10976, Nov. 1995, doi: 10.1073/pnas.92.24.10969.

[49] D. E. Moseson u. a., „Optimization of Amorphization Kinetics during Hot Melt Extrusion by Particle Engineering: An Experimental and Computational Study“, Cryst. Growth Des., Bd. 22, Nr. 1, S. 821–841, Jan. 2022, doi: 10.1021/acs.cgd.1c01306.

[50] M. A. Mohammad, „Effect of mechanical denaturation on surface free energy of protein powders“, S. 8, 2016.

[51] L. Han u. a., „Insulin-Loaded pH-Sensitive Hyaluronic Acid Nanoparticles Enhance Transcellular Delivery“, AAPS PharmSciTech, Bd. 13, Nr. 3, S. 836–845, Sep. 2012, doi: 10.1208/s12249-012-9807-2.

[52] F. H. White, „Studies on Secondary Structure in Chicken Egg-White Lysozyme after Reductive Cleavage of Disulfide Bonds“, S. 7.

[53] Y. Chen u. a., „Understanding the Impact of Protein–Excipient Interactions on Physical Stability of Spray-Dried Protein Solids“, Mol. Pharm., Bd. 18, Nr. 7, S. 2657–2668, Juli 2021, doi: 10.1021/acs.molpharmaceut.1c00189.

[54] S. Servagent-Noinville, M. Revault, H. Quiquampoix, und M.-H. Baron, „Conformational Changes of Bovine Serum Albumin Induced by Adsorption on Different Clay Surfaces: FTIR Analysis“, J. Colloid Interface Sci., Bd. 221, Nr. 2, S. 273–283, Jan. 2000, doi: 10.1006/jcis.1999.6576.

[55] R. Lu, W.-W. Li, A. Katzir, Y. Raichlin, H.-Q. Yu, und B. Mizaikoff, „Probing the secondary structure of bovine serum albumin during heat-induced denaturation using mid-infrared fiberoptic sensors“, The Analyst, Bd. 140, Nr. 3, S. 765–770, 2015, doi: 10.1039/C4AN01495B.

[56] A. Bolje und S. Gobec, „Analytical Techniques for Structural Characterization of Proteins in Solid Pharmaceutical Forms: An Overview“, Pharmaceutics, Bd. 13, Nr. 4, S. 534, Apr. 2021, doi: 10.3390/pharmaceutics13040534.

[57] K. Bagińska, J. Makowska, W. Wiczk, F. Kasprzykowski, und L. ChmurzyńSKI, „Conformational studies of alanine-rich peptide using CD and FTIR spectroscopy“, J. Pept. Sci., Bd. 14, Nr. 3, S. 283–289, März 2008, doi: 10.1002/psc.923.

[58] E. Ciszak, J. M. Beals, B. H. Frank, J. C. Baker, N. D. Carter, und G. D. Smith, „Role of C-terminal B-chain residues in insulin assembly: the structure of hexameric LysB28ProB29-human insulin“, Structure, Bd. 3, Nr. 6, S. 615–622, Juni 1995, doi: 10.1016/S0969-2126(01)00195-2.

3.11 SUPPLEMENTARY DATA

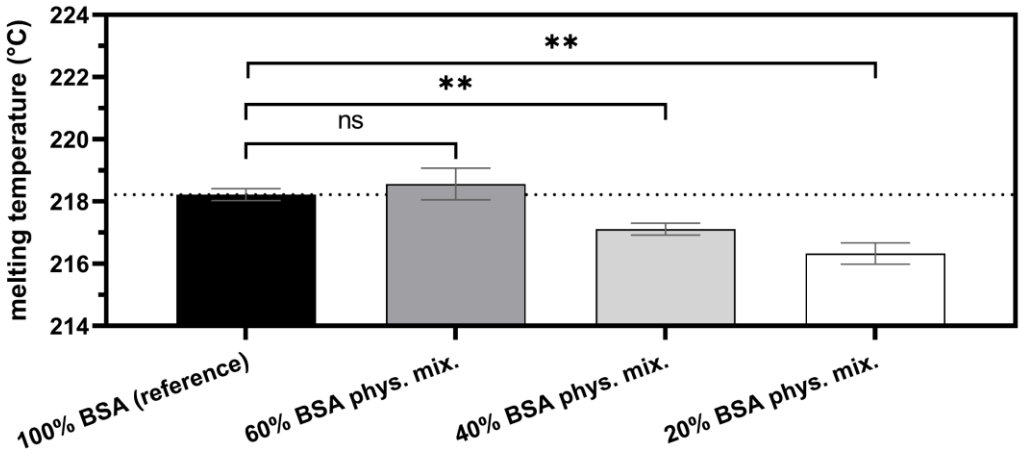

Figure S1 Melting temperature of BSA reference (100 % BSA) and physical mixtures (60, 40, and 20 % BSA and 40, 60, and 80 % PEG 20,000, respectively), the dotted line shows the melting temperature of the unprocessed protein (reference). Error bars represent the standard deviation of three measurements for the melting temperature by DSC. Unpaired *t*-test (two-sample assuming equal variances) was used and statistical significance was depicted by asterisks (*): * $p < 0.05$, ** $p < 0.01$, *** $p < 0.001$, **** $p < 0.0001$.

4 MICRO-SCALE VACUUM COMPRESSION MOLDING AS A PREDICTIVE SCREENING TOOL OF PROTEIN INTEGRITY FOR POTENTIAL HOT-MELT EXTRUSION PROCESSES

Katharina Dauer[1], Karl G. Wagner[1,*]

[1] University of Bonn, Department of Pharmaceutics, Institute of Pharmacy, Bonn, Germany

This part was published as

K. Dauer and K.G. Wagner: Micro-Scale Vacuum Compression Molding as a Predictive Screening Tool of Protein Integrity for Potential Hot-Melt Extrusion Processes. Pharmaceutics 2023, 15, 723, DOI: 10.3390/pharmaceutics15030723

4.1 Graphical Abstract

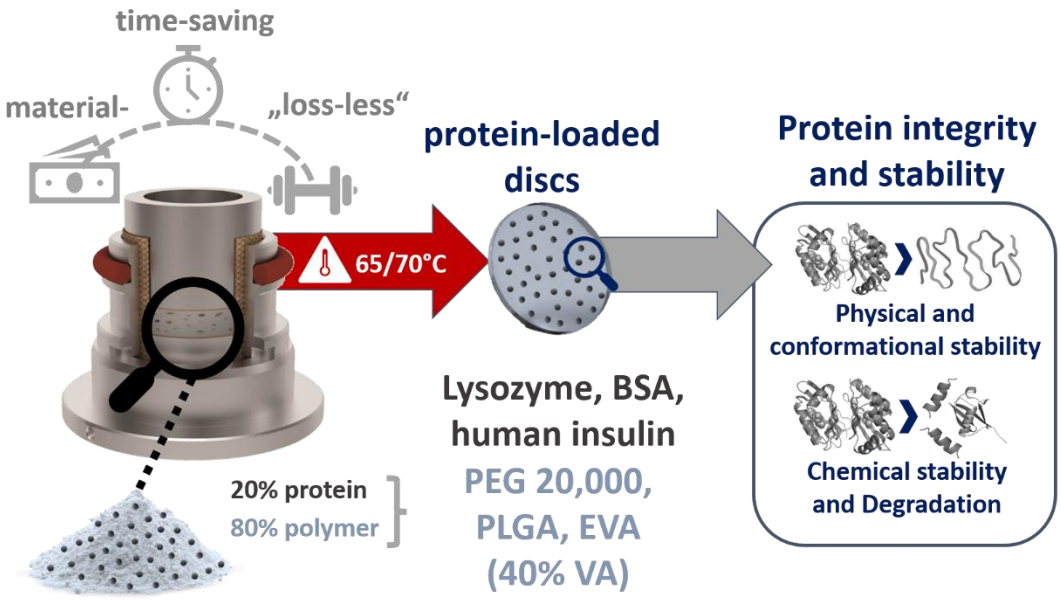

4.2 Abstract

Hot-melt extrusion (HME) is used for the production of solid protein formulations mainly for two reasons: increased protein stability in solid state and/or long-term release systems (e.g., protein-loaded implants). However, HME requires considerable amounts of material even at small-scale (> 2 g batch size). In this study, we introduced vacuum compression molding (VCM) as a predictive screening tool of protein stability for potential HME processing. The focus was to identify appropriate polymeric matrices prior to extrusion and evaluation of protein stability after thermal stress using only a few milligrams of protein. The protein stability of lysozyme, BSA, and human insulin embedded in PEG 20,000, PLGA, or EVA by VCM was investigated by DSC, FT-IR, and SEC. The results from the protein-loaded discs provided important insights into the solid-state stabilizing mechanisms of protein candidates. We demonstrated the successful application of VCM for a set of proteins and polymers, showing, in particular, a high potential for EVA as a polymeric matrix for solid-state stabilization of proteins and the production of extended-release dosage forms. Stable protein-polymer mixtures with sufficient protein stability after VCM could be then introduced to a combination of thermal and shear stress by HME and further investigated with regard to their process-related protein stability.

4.3 KEYWORDS

Vacuum compression molding, screening tool, formulation development, protein stability, protein characterization, biopharmaceuticals, solid-state stability

4.4 INTRODUCTION

The global biopharmaceutical sector is growing, and is developing innovative medicines that address a wide range of therapies for severe diseases and other human-related needs [1,2]. Moreover, the formulation development process of many biologics often wastes time and resources, and the amount of a peptide or protein candidate in early development is limited (i.e., a few milligrams) [3]. These aspects also need to be considered when evaluating alternative formulations, formulation strategies, and modes of administration. In particular, solid biopharmaceutics for peroral, nasal, or parenteral administration would significantly expand or improve the therapeutic use and the compliance of protein-based drugs [4,5,6]. Furthermore, solid protein and peptide formulations offer the potential for increased stability and underline the importance of alternative solid protein formulations (e.g., protein-loaded extrudates or implants). In addition to protein stability issues, an early evaluation and predictive screening of composition and formulation process parameters on a micro-scale level is of crucial importance, as, due to the costs of proteins, conventional development programs are financially unfeasible. The aim is to enable a good and early starting point for the production of solid protein formulations with sufficient protein stability and prior cost-intensive protein formulation development of long-term release systems. The stabilization of proteins can be achieved by embedding the protein or peptide powder in eroding or dissolving polymer matrices by scalable formulation technologies such as hot-melt extrusion (HME), freeze-drying (FD), or spray-freeze drying (SFD) [7,8,9]. HME was introduced with increasing awareness in several works as a manufacturing tool for the production of solid protein formulations, for instance, as a solid-state stabilization approach or for the development of long-term release systems for parenteral administration (e.g., protein-loaded implants) [8,10,11,12]. The use of HME provides a variety of motives for the formulation of long-term delivery systems: (i) no use of organic solvents, (ii) high drug loadings in polymeric matrices are feasible, (iii) simple scale-up, and (iv) use of additional excipients such as surfactants are not mandatory [13,14]. Different types of polymers can be simply used to embed proteins or peptides in a matrix for solid-state stabilization and optimizing the protein release behavior by HME processing [8,10].

Furthermore, the used polymers can ensure the stable folded structure of a protein or peptide during the HME process due to an immobilization of active biomolecules in the polymeric matrix [15,16]. However, during HME, the protein and peptide molecules are exposed to a combination of temperature and shear stress (designated as thermomechanical stress). Both can affect or initiate an unfolding of the protein or its degradation, resulting in an irreversible aggregation accompanied by a potential loss of protein functionality [15]. In a previously described study, we presented a sensitive characterization pathway of protein stability focused on the characterization of protein-loaded extrudates at a high drug load (i.e., > 40 %) prepared by ram extrusion and twin-screw extrusion (TSE). Here, changes in protein stability affected by thermomechanical stress during the extrusion process were investigated [10]. Although small-scale HME leads to high yields of an extruded powder mixture, the process is still associated with a moderate material input (i.e., > 2 g of the powdered protein-polymer mixture) and material loss (e.g., < 0.5 g of the protein-polymer mixture due to gaps between the rotating screws in TSE processing). Additionally, innovative formulation and screening tools in micro-scale (mg-scale) are highly desirable especially in the early phase of formulation development. Furthermore, a fundamental formulation development strategy is based on an extensive knowledge of the physicochemical peptide and protein stability accompanied with appropriate analytical methods to evaluate the process-related stability of active biomolecules in different formulations. This study proposes the implementation of micro-scale vacuum compression molding (VCM) as a predictive screening tool of protein integrity and polymers by overcoming the major drawback of conventional HME screening by using a minimum quantity of API and material. VCM was introduced by Treffer et al. [17] and is a novel, fusion-based tool for the simple preparation of thermoplastic specimens starting from powders, where the molten samples are evacuated and compressed into a defined solid form (e.g., cylindrical discs or implants) without any air inclusions or voids [17]. Additionally, the design of the VCM tool reduces the preparation time of the samples compared to HME processing, which requires time for assembling of extruder components, adjusting constant feeding rates, and cleaning [17]. Drug-loaded implants are one of the promising solid dosage forms for parenteral extended release [15,18]. However, the design of such implants for sustained release of proteins is a complex challenge, achieving protein solid-state stabilization in combination with a micro-scale screening tool, which is predictive for further HME processing. We used three polymer model systems covering a broad

range of different properties: (i) polyethylene glycol (PEG) 20,000 is a hydrophilic and immediate release polymer, (ii) poly lactic-co-glycolic acid (PLGA) is a biodegradable sustained-release polymer, providing a drug release over several months, and (iii) ethylene-vinyl acetate (EVA) as non-biodegradable polymer with an extended-release behavior of up to 2 years. Various peptides/proteins (i.e., lysozyme, bovine serum albumin (BSA), and human insulin) were used as drug models. VCM (combination of vacuum and temperature) was used to prepare cylindrical discs composed of different protein-polymer mixtures in view of a potential as a predictive screening tool for protein solid-state stabilization in the selected polymers. The processability via VCM varied according to the used polymer: the process temperature for PEG 20,000 samples was 65 °C, whereas the samples based on PLGA 50:50 and EVA (40 % VA) were produced at 70 °C. In order to study the temperature-dependent stress, the process times were selected as 6 or 12 min to obtain homogenous discs. In view of protein analysis, a combination of analytical methods, i.e., SEC (protein fragment and aggregation analysis), DSC (unfolding temperature of the protein), and FT-IR spectroscopy (conformational stability) is reported and information provided on the protein stability of the formulated and screened proteins by VCM. The applied procedure provides a good basis for the evaluation of VCM as a predictive screening tool for the preselection of appropriate polymeric matrices prior to extrusion and evaluation of protein integrity after thermal stress. On the one hand, if the process of VCM negatively affected the protein stability in protein-polymer mixtures, this combination would disqualify itself for further processing by HME. On the other hand, stable protein-polymer mixtures with sufficient protein stability after VCM could then be introduced to a combination of thermal and shear stress by HME and further investigated with regard to their process-related protein stability.

4.5 MATERIALS AND METHODS

4.5.1 MATERIALS

Human insulin was kindly donated by Sanofi Deutschland GmbH (Frankfurt am Main, Germany). Lysozyme from chicken egg-white, lyophilized powder (Cat. No. L6876) was obtained from AppliChem (AppliChem GmbH, Darmstadt, Germany). Bovine serum albumin (BSA), sodium chloride, disodium hydrogen phosphate dihydrate, sodium dihydrogen phosphate dihydrate, acetonitrile, and dichloromethane were purchased from Merck (Merck KGaA, Darmstadt, Germany). PLGA (Resomer® RG502 H) was purchased from Evonik (Evonik Nutrition & Care GmbH, Darmstadt, Germany). Polyethylene glycol (PEG) 20,000 was obtained from Carl Roth (Karlsruhe, Germany). Poly(ethylene/vinyl acetate) (EVA; 60:40 (wt)) granules were purchased from Polysciences (Polysciences Inc., Warrington, PA, USA). All chemicals were of analytical grade or equivalent purity.

4.5.2 METHODS

4.5.2.1 PREPARATION OF PHYSICAL MIXTURES AND SAMPLE DISCS BY VCM

PEG 20,000 flakes were milled utilizing a high-shear mixer (Krups Mixette type 210, Krups, Frankfurt am Main, Germany). EVA granules were milled using a cryogenic mill (6775 Freezer/Mill® Cryogenic Grinder, SPEX SamplePrep LLC, Metuchen, NJ, USA). The EVA granules were loaded into the sample holder and placed in the grinding chamber, which maintains cryogenic temperatures due to continuous immersion in liquid nitrogen. EVA granules were pre-cooled for 10 min and then milled through 3 grinding cycles (10 cycles per second) at 2 min each with 2 min intercool time. For the preparation of protein-loaded discs, a physical mixture composed of polymer and 20 % protein powder was manually blended with a spatula. The physical mixtures of polymer and protein powder were then vacuum compression molded. VCM was conducted using a VCM tool (MeltPrep GmbH, Graz, Austria) with a 5 mm diameter disc geometry. Approx. 15 mg of each blend was loaded into the VCM device and heated under vacuum [17] for 6 or 12 min at a temperature of 65 °C for PEG 20,000, or 70 °C for PLGA, and EVA (Table 1).

Table 1. Overview of the compositions and prepared protein-loaded discs by VCM.

Formulation	***Components (%)***		***Preparation method***	***Process parameters***
	Protein	**Polymer**		
LYS reference	100% Lysozyme			
LYS PEG PM	20% Lysozyme	80% PEG 20,000	Phys. mix.	
LYS PEG VCM 6	20% Lysozyme	80% PEG 20,000	VCM	6 min. at 65°C
LYS PEG VCM 12	20% Lysozyme	80% PEG 20,000	VCM	12 min. at 65°C
LYS PLGA PM	20% Lysozyme	80% PLGA	Phys. mix.	
LYS PLGA VCM 6	20% Lysozyme	80% PLGA	VCM	6 min. at 70°C
LYS PLGA VCM 12	20% Lysozyme	80% PLGA	VCM	12 min. at 70°C
LYS EVA PM	20% Lysozyme	80% EVA	Phys. mix.	
LYS EVA VCM 6	20% Lysozyme	80% EVA	VCM	6 min. at 70°C
LYS EVA VCM 12	20% Lysozyme	80% EVA	VCM	12 min. at 70°C
BSA reference	100% BSA			
BSA PEG PM	20% BSA	80% PEG 20,000	Phys. mix.	
BSA PEG VCM 6	20% BSA	80% PEG 20,000	VCM	6 min. at 65°C
BSA PEG VCM 12	20% BSA	80% PEG 20,000	VCM	12 min. at 65°C
BSA PLGA PM	20% BSA	80% PLGA	Phys. mix.	
BSA PLGA VCM 6	20% BSA	80% PLGA	VCM	6 min. at 70°C
BSA PLGA VCM 12	20% BSA	80% PLGA	VCM	12 min. at 70°C
BSA EVA PM	20% BSA	80% EVA	Phys. mix.	
BSA EVA VCM 6	20% BSA	80% EVA	VCM	6 min. at 70°C
BSA EVA VCM 12	20% BSA	80% EVA	VCM	12 min. at 70°C
IHU reference	100% Human Insulin			
IHU PEG PM	20% Human Insulin	80% PEG 20,000	Phys. mix.	
IHU PEG VCM 6	20% Human Insulin	80% PEG 20,000	VCM	6 min. at 65°C
IHU PEG VCM 12	20% Human Insulin	80% PEG 20,000	VCM	12 min. at 65°C
IHU PLGA PM	20% Human Insulin	80% PLGA	Phys. mix.	
IHU PLGA VCM 6	20% Human Insulin	80% PLGA	VCM	6 min. at 70°C
IHU PLGA VCM 12	20% Human Insulin	80% PLGA	VCM	12 min. at 70°C
IHU EVA PM	20% Human Insulin	80% EVA	Phys. mix.	
IHU EVA VCM 6	20% Human Insulin	80% EVA	VCM	6 min. at 70°C
IHU EVA VCM 12	20% Human Insulin	80% EVA	VCM	12 min. at 70°C

4.5.2.2 SAMPLE PREPARATION FOR SEC ANALYSIS (PROTEIN EXTRACTION PROCEDURES)

Samples (i.e., physical mixture and protein-loaded discs) containing PEG 20,000 as polymer were dissolved in the mobile phase (50 mM pH 7.0 phosphate buffer, 400 mM sodium chloride) for SEC analysis (refer to Section 4.5.4.) corresponding to a final

protein concentration of 4 mg/mL. For PLGA-containing samples, the physical mixture or protein-loaded disc was dissolved in acetonitrile. As described in the literature, proteins can be precipitated in acetonitrile without degradation of the protein structure [19]. Three cycles of protein precipitation and removal of acetonitrile by pipetting off the supernatant and evaporation of residual acetonitrile were applied to separate proteins (insoluble) from the polymer matrix (soluble). Then, 4 mg of extracted, dried proteins were pre-dissolved in 500 µL Milli-Q® water (i.e., lysozyme and BSA) and diluted with 500 µL mobile phase to a target concentration of 4 mg/mL protein. Extracted human insulin was an exception, as the human insulin was firstly pre-dissolved in 0.1 M HCl and then further dissolved with the mobile phase, resulting in a final peptide concentration of 4 mg/mL. Proteins embedded in EVA were extracted by the use of dichloromethane, as described by Langer et al. [20]. The physical mixture or protein-loaded EVA discs were dissolved in dichloromethane, resulting in a precipitation of the proteins. Dichloromethane was then covered by a layer of Milli-Q® water or 0.1 M hydrochloride acid in order to dissolve the precipitated proteins (lysozyme and BSA, or human insulin, respectively) by solvent extraction method. The extracted protein was collected by pipetting 500 µL of the supernatant and diluted with 500 µL of the mobile phase (corresponding to a final protein concentration of 4 mg/mL). All samples were prepared as triplicates and directly filtered into HPLC vials by syringeless filtration (Mini-UniPrep, 0.20 µm PTFE, Whatman, Cytiva, Marlborough, MA, USA) and then analyzed using the SEC method.

4.5.2.3 SIZE-EXCLUSION CHROMATOGRAPHY (SEC)

Size-exclusion chromatography was performed with a Superdex 75 Increase 10/300 GL column, 10 × 300 mm (Cytiva, Marlborough, MA, USA), where the mobile phase was 50 mM pH 7.0 phosphate buffer containing 400 mM sodium chloride (isocratic) at a flow rate of 0.8 mL/min (LC-20AT, Shimadzu, Kyoto, Japan) and a column temperature of 30 °C (CTO-10AC VP, Shimadzu, Kyoto, Japan). Samples were prepared as triplicates by extracting and dissolving the samples (i.e., pure protein (reference sample 1), the physical mixture (reference sample 2), or the protein-loaded disc (VCM)) according to Section 4.5.3. Samples vials were cooled at 5 °C in the autosampler (SIL-A10, Shimadzu, Kyoto, Japan). Then, 10 µL of each sample was injected and potential aggregate and/or fragment formation after VCM was analyzed in comparison with a chromatogram of the freshly prepared reference solutions. The

UV detection (SPD-40 UV Detector, Shimadzu, Kyoto, Japan) wavelength was 214 nm.

4.5.2.4 DIFFERENTIAL SCANNING CALORIMETRY (DSC)

DSC studies of protein powder, physical mixture, and protein-loaded discs were performed with a DSC 2 (Mettler Toledo, Gießen, Germany) equipped with an autosampler, nitrogen cooling, and nitrogen as purge gas (30 mL/min). At least three samples of ~15 mg were accurately weighed in 40 µL aluminum crucibles with a pierced lid. DSC scans were recorded from 25 °C to 230 °C using a heating rate of 10 K/min STAR^e software (Mettler Toledo, Gießen, Germany) was employed for acquiring thermograms.

4.5.2.5 FOURIER-TRANSFORM INFRARED SPECTROSCOPY (FT-IR)

FT-IR spectra were generated with a Spectrum Two^{TM} FT-IR spectrophotometer equipped with a UATR accessory (PerkinElmer, Inc., Waltham, MA, USA). A tight pressure clamp with a flat tip ensured a good contact between the sample and the reflection diamond crystal. Each sample (i.e., protein powder, physical mixture, protein-loaded discs) was measured as triplicate. The spectra were recorded against an air background between 4000 and 400 cm^{-1} with an average of four scans and a resolution of 4 cm^{-1}. Data were collected in the absorption mode. First and second derivative analysis of the amide-I region (1600–1700 cm^{-1}) were performed with GraphPad Prism v. 8.0.2 (GraphPad Software, La Jolla, CA, USA).

4.5.2.6 STATISTICAL ANALYSIS

Statistical analysis and testing for statistical significance were carried out using GraphPad PRISM Software (San Diego, La Jolla, CA, USA). An unpaired *t*-test (two-sample assuming equal variances) was used for the evaluation of statistical significance.

4.6 RESULTS AND DISCUSSION

4.6.1 UNFOLDING TEMPERATURE OF PROTEINS BY DSC

he native state of a protein is its orderly folded and assembled form and determines its functionality. However, this intact structure can be altered by heat, shear stress, chemicals, or denaturants. The most common stress that can cause a loss of protein structure or functionality is an exposure to heat during processing (i.e., thermally induced protein denaturation and/or unfolding). In the case of temperature-dependent unfolding, the protein structure is lost due to elevated temperatures or a longer exposition at a high temperature [15]. We used DSC for analyzing the protein unfolding temperature in solid-state after VCM and compared it to unprocessed samples. DSC presented unfolding temperatures of native lysozyme, BSA, and human insulin as 204.7 °C, 218.2 °C, and 213.1 °C, respectively (Figure 1), which served as reference values [10]. The DSC thermograms of protein powder, pure polymers, physical mixtures composed of 20 % protein powder and 80 % polymer, and 20 % protein-loaded discs are shown in the Supplementary Materials (Figures S1-S3). In general, the occurrence or preservation of a peak in the DSC thermogram can indicate the conservation of protein conformation after VCM, and an increasing unfolding temperature of the proteins after processing even reflects an increase in conformational protein stability. The unfolding temperatures of the physical mixtures composed of 20 % protein powder and 80 % PEG 20,000 or 80 % PLGA were comparable with or lower than the unfolding temperature of the native proteins. However, the unfolding temperature of the proteins in the presence of EVA were not reduced or even higher compared to the native protein powder. The residence time of the molten protein-polymer mixture in the VCM tool is even higher compared to HME (e.g., mean residence time: 1 to 3 min), but 6 min was the minimum residence time for complete melting during VCM processing. The longer residence times present the worst-case scenario for when VCM should be used as a predictive screening tool for the evaluation of protein integrity for potential HME processing. VCM for 6 min highlights an optimum processing time since the unfolding temperatures of the proteins were not negatively affected compared to the unprocessed protein-polymer powder mixtures. The embedding of 20 % lysozyme or BSA in 80 % EVA showed a significantly increased unfolding temperature of the protein compared to the native protein powder as well as to the unprocessed physical mixture. The results indicate a potential protein stabilizing effect of EVA as polymeric matrix. Moreover, in the case

of human insulin, the unfolding temperature was least negatively affected by embedding in EVA. The two-fold processing time of 12 min was not favorable since the unfolding temperatures were reduced compared to the 6 min processing time.

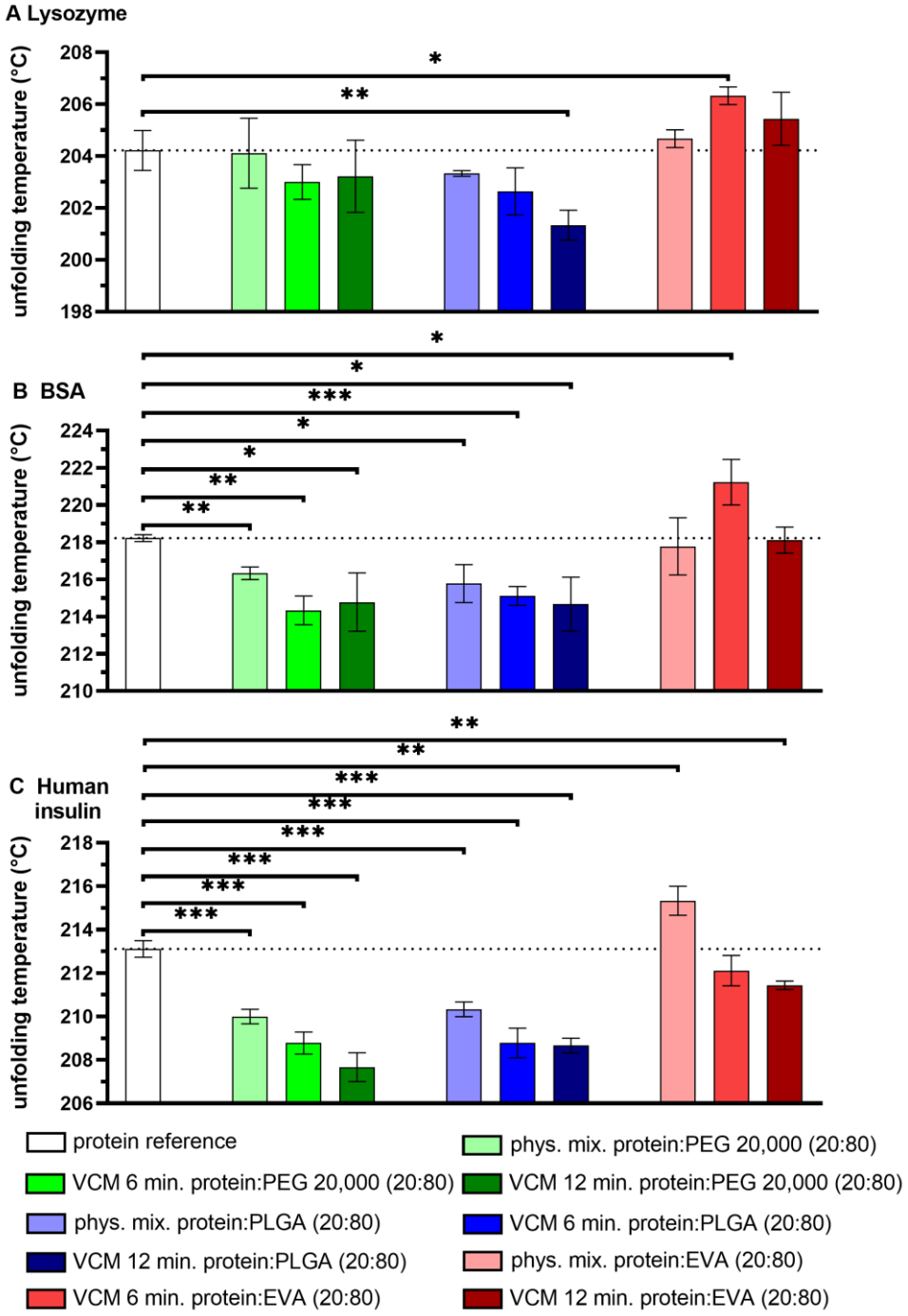

Figure 1 Unfolding temperature of protein powders (white), physical mixtures, and 20 % protein-loaded (**A:** lysozyme, **B:** BSA, **C:** human insulin) discs with the polymers: PEG 20,000 (green) at 65 °C, PLGA (blue) at 70 °C, or EVA (red) at 70 °C prepared by VCM in 6 or 12 min.; the dotted line represents the unfolding temperature of the respective unprocessed protein (reference sample); error bars represent the standard deviation of three measurements; statistical significance is depicted by asterisks (*): * $p < 0.05$, ** $p < 0.01$, *** $p < 0.001$.

4.6.2 SECONDARY STRUCTURE ANALYSIS AND CONFORMATIONAL PROTEIN STABILITY BY FT-IR SPECTROSCOPY

FT-IR spectroscopy was applied for comparison of the molecular protein conformation and secondary structure elements of protein powder (i.e., lysozyme, BSA, and human insulin) before and after VCM processing. The secondary structure information of the native protein powders served as a reference (Figure 2). The trend of a potential protein stabilizing effect of EVA as polymer was confirmed by FT-IR analysis. One benefit of the use of 5 mm discs was the extremely simplified analytical investigation, as the produced specimens showed a high reproducibility, were free of air inclusions, and could be directly used after production in their final form and without further sample preparation for FT-IR and DSC analysis. The first and second derivatives of spectra of VCM discs containing 20 % lysozyme, BSA, or human insulin and 80 % EVA were comparable to the powdered proteins used to prepare the discs. Since the spectra were overlaying, there was no indication of protein denaturation or aggregation as a consequence of the exposure to an elevated temperature of 70 °C for 6 or 12 min and vacuum during VCM processing. An exception was the formulation composed of 20 % human insulin and 80 % EVA processed for 12 min. Here, the spectrum was shifted compared to the reference spectra, indicating that alpha-helical structures might be disrupted due to the longer processing time at 70 °C. The use of PLGA as a polymer matrix showed no inferior effect on protein stability and was comparable to the performance of PEG 20,000. In the case of human insulin-loaded PLGA and PEG 20,000 discs, the process of VCM led to slight changes in secondary structure elements independent of the applied processing times. As discussed in a previous work, the conformational stability of lysozyme was not negatively affected by HME processing [10]. The FT-IR spectra of lysozyme-loaded PEG-extrudates produced by ram extrusion or twin-screw extrusion (TSE), as described by Dauer et al. [10], were comparable to the native lysozyme powder used to prepare the physical mixture and thus the extrudates. In contrast, the FT-IR spectra of BSA- and human insulin-loaded PEG extrudates produced by TSE showed clear shifts, when screws with a kneading element were used. The kneading element results in higher shear stress and longer residence times, to which the protein particles during processing are exposed. In particular, BSA and human insulin showed a higher susceptibility to thermal and shear stress compared to lysozyme [10]. The results of this study highlight the suitability of VCM as a screening tool for protein stability prior to HME as it follows the same trend regarding DSC and FT-IR analysis.

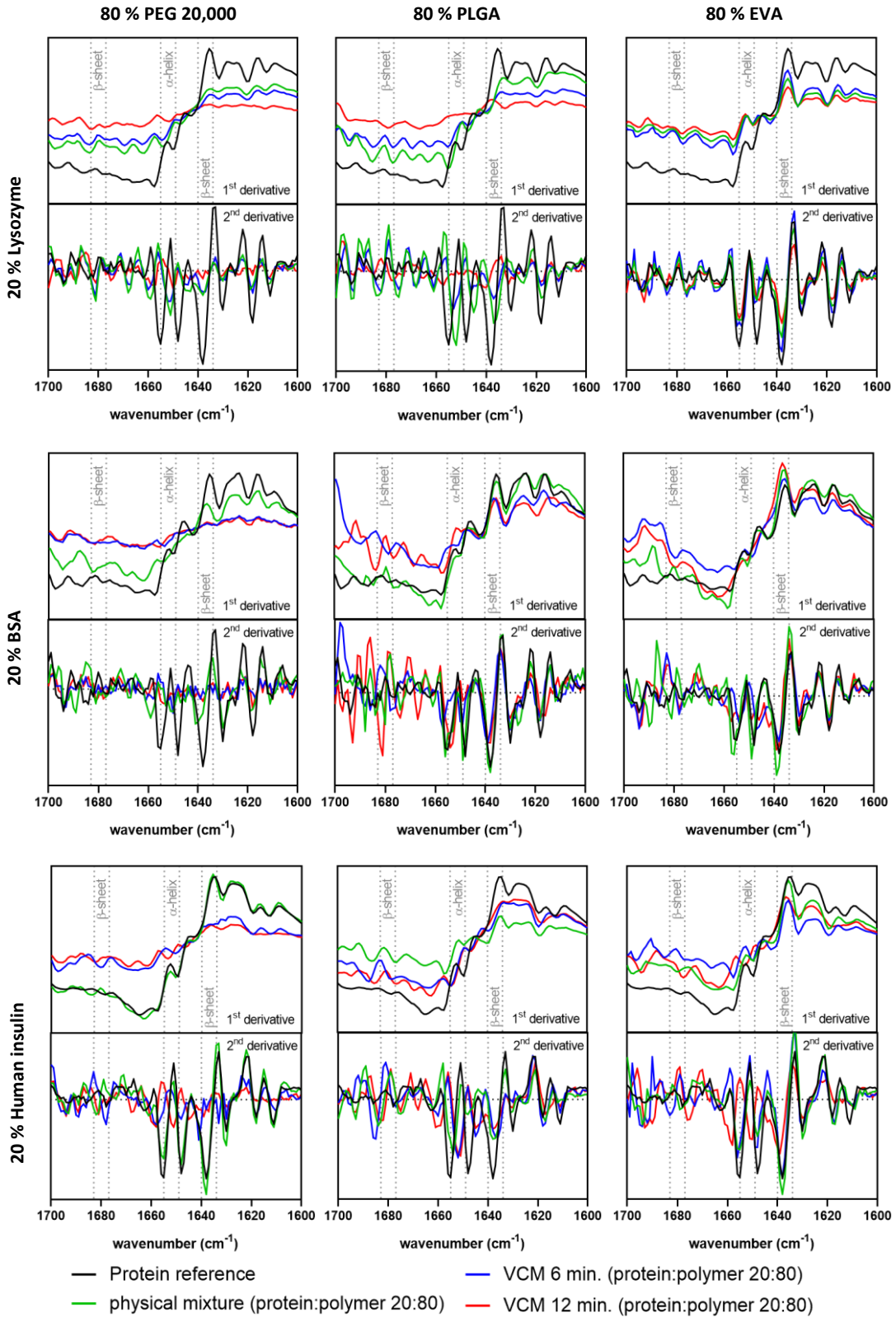

Figure 2 FT-IR spectra (first and second derivative) in the amide-I region (1600–1700 cm^{-1}) of the respective protein powder (black); physical mixture composed of 20 % protein powder and 80 % polymer (green); and 20 % protein-loaded (**A:** lysozyme, **B:** BSA, **C:** human insulin) discs with the polymers: PEG 20,000 at 65 °C, PLGA at 70 °C, or EVA at 70 °C prepared by VCM in 6 min (blue) or 12 min (red); dotted gray lines highlight secondary structure elements such as α-helices and β-sheets.

4.6.3 PROCESS-INDUCED FORMATION OF PROTEIN AGGREGATES OR FRAGMENTS BY SEC

Although proteins in solid-state formulations exhibit an enhanced stability, the processed proteins can undergo denaturation, degradation, or aggregation without any detectable change in their secondary structure. Consequently, structural changes of proteins cannot be distinguished from native protein species using methods such as FT-IR spectroscopy [21]. Therefore, thermal-induced protein denaturation or aggregation was investigated by SEC. The potential formation aggregation of lysozyme, BSA, and human insulin after VCM for 6 or 12 min was monitored and high-molecular weight species (HMWS)/protein aggregates or fragments were separated from native protein species. VCM processing was not the trigger for the formation of protein fragments or aggregates in the case of lysozyme- and BSA-loaded discs (Supplementary Materials: Figures S4 and S5, respectively). Lysozyme was only present as a monomer after dissolving the discs composed of 20 % lysozyme and 80 % PEG 20,000 in eluent, or after extraction of lysozyme from PLGA- or EVA-based discs dissolved in eluent (refer to Supplementary Materials, Figure S4). The used unprocessed and native BSA was a mixture of monomers and dimers [10]. Alteration in the ratio of monomer to dimer, or the occurrence of trimers or oligomers indicates process-related effects on BSA structure. However, the monomer-to-dimer ratio of BSA was not negatively affected by VCM (refer to Supplementary Materials, Figure S5). Native human insulin appeared as a species at a retention time of 20 min (Figure 3) and is in good agreement with previously published data [10]. Human insulin-loaded PEG discs prepared by VCM showed further peaks in front of the peak of native human insulin, indicating the formation of HMWS in the presence of PEG 20,000. With increasing process time from 6 to 12 min, the amount of HMWS was also increased. Additionally, the monomeric peak of human insulin was shifted and divided into several, non-baseline-separated small peaks. However, the formation of the HMWS was not process-related and independent of the VCM process. This is corroborated by the fact that HMWS of human insulin occurred also in the unprocessed, physical mixture (20 % human insulin, 80 % PEG 20,000). Therefore, PEG 20,000 is not an appropriate polymer carrier, since interactions of human insulin molecules with hydrophilic PEG chains induced the alteration of the local insulin structure [22]. This hypothesis is also confirmed by the results of human insulin-loaded extrudates prepared by ram extrusion or TSE, as described previously [10]. Human insulin-loaded PLGA discs showed a series of small peaks after the

monomeric peak. Whether this observation is a polymer-, temperature-, or vacuum-related effect has to be further evaluated by an extrusion experiment. The inference is that it is a vacuum-related effect of VCM processing, since the peak areas of human insulin from PLGA discs prepared in 6 or 12 min were of the same magnitude. Human insulin extracted from EVA discs prepared in 6 or 12 min showed only a single peak at a retention time of 20 min, confirming the potential of EVA for the production of solid protein-loaded long-term release dosage forms with sufficient protein stability.

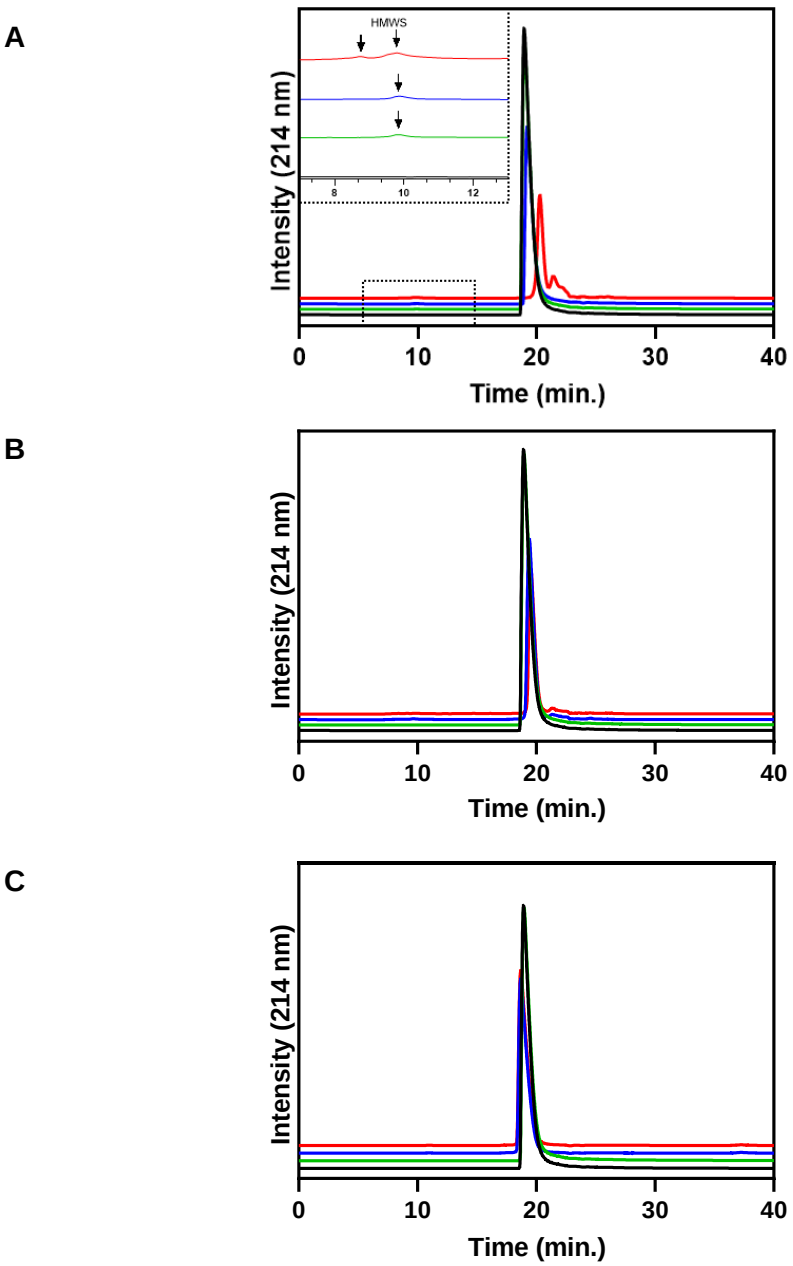

Figure 3 Chromatograms of SEC analysis; human insulin powder (initial: black), physical mixture composed of 20 % human insulin and 80 % polymer (green); and 20 % human insulin-loaded discs with the polymers: **A:** PEG 20,000 at 65 °C; **B:** PLGA at 70 °C; **C:** EVA at 70 °C prepared by VCM in 6 min (blue) or 12 min (red); insert: magnified area of HMWS (arrows).

4.7 CONCLUSIONS

In this study, VCM proved to be an appropriate screening tool for the investigation of potential protein solid-state stabilization for melt-based formulations at a micro-scale as well as for the evaluation of suitable polymers and excipients for further planned HME processing. The protein-loaded discs were directly used after production in their final form for FT-IR and DSC analysis and without a further and complex sample preparation. The systematic analysis of the protein-loaded discs prepared by VCM provided important insights into the solid-state stabilizing mechanisms of protein candidates since an understanding of molecular interactions within the polymeric matrix can support the identification of most promising polymer carriers. DSC analysis proved to be a useful method for a first and rapid screening of appropriate polymers for the embedding of proteins. One benefit of using VCM as an early screening tool is to identify potential interactions between protein candidates and test polymers provoked by thermal stress during processing. Presenting short sample preparation times and flexibility regarding the manufacturing of different specimens, VCM can be used as predictive and early screening tool for extruded formulations, especially on a micro-scale level. Furthermore, VCM exploits small quantities of material and offers a “loss-less” method compared to HME, thus preventing the waste of expensive API and material in early formulation development and screening. EVA presented high potential as a polymeric matrix for solid-state stabilization of proteins (e.g., lysozyme, BSA, and human insulin) or the production of protein-loaded implants with extended-release behavior. When comparing the used polymers, EVA demonstrated better results among all selected polymers. Identified, stable protein-polymer mixtures with sufficient protein stability after VCM would then, in a next step, be introduced to a combination of thermal and shear stress by HME processing and further investigated with regard to their process-related protein stability.

4.8 RESEARCH FUNDING

This research was funded by the German Research Foundation (DFG SPP1934, project number: 273937032).

4.9 ACKNOWLEDGEMENTS

The authors would like to thank the German Research Foundation (DFG) for financial support in the research project SPP 1934 DiSPBiotech. We thank Sanofi-Aventis Deutschland GmbH for providing human insulin for our study.

4.10 REFERENCES

[1] X. Lyu u. a., „The global landscape of approved antibody therapies“, Antib. Ther., Bd. 5, Nr. 4, S. 233–257, Okt. 2022, doi: 10.1093/abt/tbac021.

[2] V. Gervasi, R. Dall Agnol, S. Cullen, T. McCoy, S. Vucen, und A. Crean, „Parenteral protein formulations: An overview of approved products within the European Union“, Eur. J. Pharm. Biopharm., Bd. 131, S. 8–24, Okt. 2018, doi: 10.1016/j.ejpb.2018.07.011.

[3] K. Dauer, S. Pfeiffer-Marek, W. Kamm, und K. G. Wagner, „Microwell Plate-Based Dynamic Light Scattering as a High-Throughput Characterization Tool in Biopharmaceutical Development“, Pharmaceutics, Bd. 13, Nr. 2, S. 172, Jan. 2021, doi: 10.3390/pharmaceutics13020172.

[4] A. M. Privalova, N. V. Gulyaeva, und T. V. Bukreeva, „Intranasal administration: a prospective drug delivery route to the brain“, Neurochem. J., Bd. 6, Nr. 2, S. 77–88, Apr. 2012, doi: 10.1134/S1819712412020080.

[5] J. Shaji und V. Patole, „Protein and Peptide Drug Delivery: Oral Approaches“, Indian J. Pharm. Sci., Bd. 70, Nr. 3, S. 269–277, 2008, doi: 10.4103/0250-474X.42967.

[6] S. Türker, E. Onur, und Y. Ozer, „Nasal route and drug delivery systems“, Pharm. World Sci. PWS, Bd. 26, Nr. 3, S. 137–142, Juni 2004, doi: 10.1023/b:phar.0000026823.82950.ff.

[7] K. B. Preston und T. W. Randolph, „Stability of lyophilized and spray dried vaccine formulations“, Adv. Drug Deliv. Rev., Bd. 171, S. 50–61, Apr. 2021, doi: 10.1016/j.addr.2021.01.016.

[8] A. Cossé, C. König, A. Lamprecht, und K. G. Wagner, „Hot Melt Extrusion for Sustained Protein Release: Matrix Erosion and In Vitro Release of PLGA-Based Implants“, AAPS PharmSciTech, Bd. 18, Nr. 1, S. 15–26, Jan. 2017, doi: 10.1208/s12249-016-0548-5.

[9] M. B. Adali, A. A. Barresi, G. Boccardo, und R. Pisano, „Spray Freeze-Drying as a Solution to Continuous Manufacturing of Pharmaceutical Products in Bulk“, Processes, Bd. 8, Nr. 6, S. 709, Juni 2020, doi: 10.3390/pr8060709.

[10] K. Dauer, C. Werner, D. Lindenblatt, und K. G. Wagner, „Impact of process stress on protein stability in highly-loaded solid protein/PEG formulations from small-scale melt extrusion“, Int. J. Pharm. X, S. 100154, Dez. 2022, doi: 10.1016/j.ijpx.2022.100154.

[11] M. Stanković, H. W. Frijlink, und W. L. J. Hinrichs, „Polymeric formulations for drug release prepared by hot melt extrusion: application and characterization“, Drug Discov. Today, Bd. 20, Nr. 7, S. 812–823, Juli 2015, doi: 10.1016/j.drudis.2015.01.012.

[12] M. Stanković u. a., „Low temperature extruded implants based on novel hydrophilic multiblock copolymer for long-term protein delivery“, Eur. J. Pharm. Sci., Bd. 49, Nr. 4, S. 578–587, Juli 2013, doi: 10.1016/j.ejps.2013.05.011.

[13] Madan, S.M.S. Hot melt extrusion and its pharmaceutical applications. Asian J. Pharm. Sci. 2012, 7, 123–133.

[14] M. Gajda, K. P. Nartowski, J. Pluta, und B. Karolewicz, „The role of the polymer matrix in solvent-free hot melt extrusion continuous process for mechanochemical synthesis of pharmaceutical cocrystal“, Eur. J. Pharm. Biopharm., Bd. 131, S. 48–59, Okt. 2018, doi: 10.1016/j.ejpb.2018.07.002.

[15] Z. Ghalanbor, M. Körber, und R. Bodmeier, „Improved Lysozyme Stability and Release Properties of Poly(lactide-co-glycolide) Implants Prepared by Hot-Melt Extrusion“, Pharm. Res., Bd. 27, Nr. 2, S. 371–379, Feb. 2010, doi: 10.1007/s11095-009-0033-x.

[16] S. L. Lee, A. E. Hafeman, P. G. Debenedetti, B. A. Pethica, und D. J. Moore, „Solid-State Stabilization of α-Chymotrypsin and Catalase with Carbohydrates“, Ind. Eng. Chem. Res., Bd. 45, Nr. 14, S. 5134–5147, Juli 2006, doi: 10.1021/ie0513503.

[17] D. Treffer, A. Troiss, und J. Khinast, „A novel tool to standardize rheology testing of molten polymers for pharmaceutical applications“, Int. J. Pharm., Bd. 495, Nr. 1, S. 474–481, Nov. 2015, doi: 10.1016/j.ijpharm.2015.09.001.

[18] P. Agarwal und I. D. Rupenthal, „Injectable implants for the sustained release of protein and peptide drugs“, Drug Discov. Today, Bd. 18, Nr. 7–8, S. 337–349, Apr. 2013, doi: 10.1016/j.drudis.2013.01.013.

[19] R. L. Gundry u. a., „Preparation of Proteins and Peptides for Mass Spectrometry Analysis in a Bottom-Up Proteomics Workflow“, Curr. Protoc. Mol. Biol., S. mb1025s88, Okt. 2009, doi: 10.1002/0471142727.mb1025s88.

[20] R. Langer, L. Brown, und E. Edelman, „[30] Controlled release and magnetically modulated release systems for macromolecules“, in Methods in Enzymology, Bd. 112, Elsevier, 1985, S. 399–422. doi: 10.1016/S0076-6879(85)12032-X.

[21] K. Griebenow und A. M. Klibanov, „Lyophilization-induced reversible changes in the secondary structure of proteins.“, Proc. Natl. Acad. Sci., Bd. 92, Nr. 24, S. 10969–10976, Nov. 1995, doi: 10.1073/pnas.92.24.10969.

[22] S.-H. Chao, S. S. Matthews, R. Paxman, A. Aksimentiev, M. Gruebele, und J. L. Price, „Two Structural Scenarios for Protein Stabilization by PEG“, J. Phys. Chem. B, Bd. 118, Nr. 28, S. 8388–8395, Juli 2014, doi: 10.1021/jp502234s.

4.11 SUPPLEMENTARY DATA

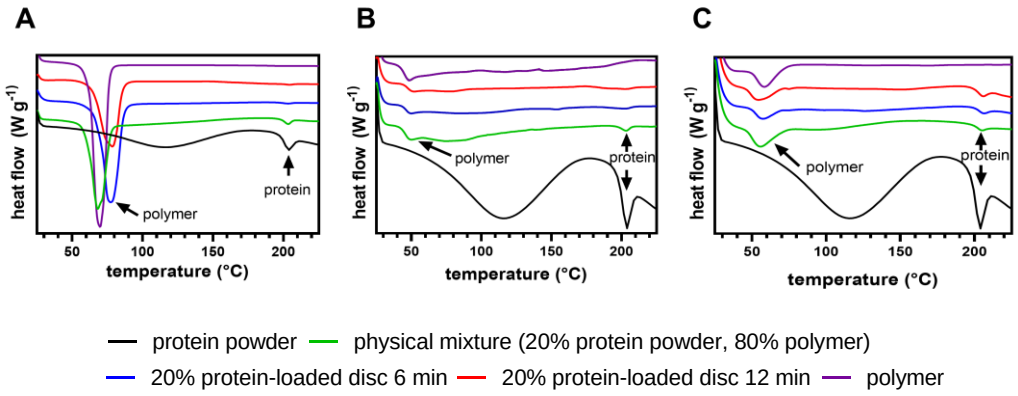

Figure S1 DSC thermograms (25 to 230 °C) of lysozyme powder (black), polymers (purple) (**A:** PEG 20,000, **B:** PLGA, and **C:** EVA), physical mixture composed of 20 % lysozyme powder and 80 % polymer (green), and 20 % lysozyme-loaded disc produced by VCM in 6 min (blue) or 12 min (red).

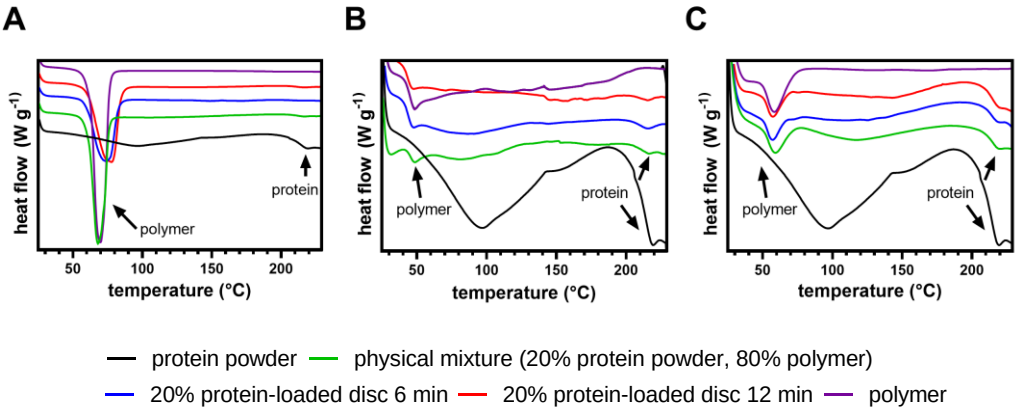

Figure S2 DSC thermograms (25 to 230 °C) of BSA powder (black), polymers (purple) (**A:** PEG 20,000, **B:** PLGA, and **C:** EVA), physical mixture composed of 20 % BSA powder and 80 % polymer (green), and 20 % BSA-loaded disc produced by VCM in 6 min (blue) or 12 min (red).

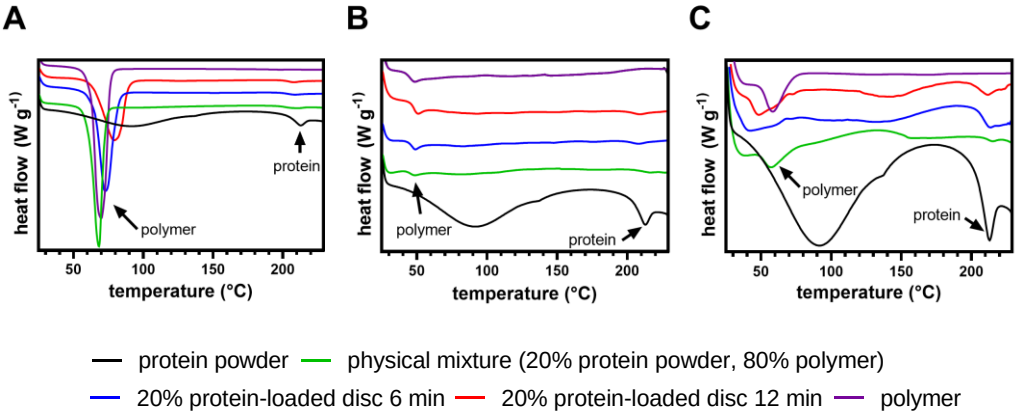

Figure S3 DSC thermograms (25 to 230 °C) of human insulin powder (black), polymers (purple) (**A**: PEG 20,000, **B**: PLGA, and **C**: EVA), physical mixture composed of 20 % human insulin powder and 80 % polymer (green), and 20 % human insulin-loaded disc produced by VCM in 6 min (blue) or 12 min (red).

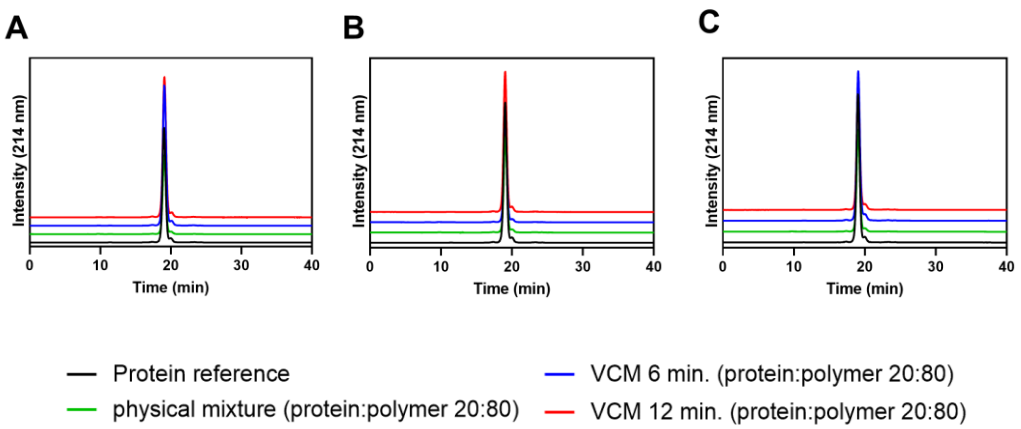

Figure S4 Chromatograms of SEC analysis; lysozyme powder (initial: black), physical mixture composed of 20 % lysozyme and 80 % polymer (green); and 20 % lysozyme-loaded discs with the polymers: **A:** PEG 20,000 at 65 °C; **B:** PLGA at 70 °C; **C**: EVA at 70 °C prepared by VCM in 6 min (blue) or 12 min (red).

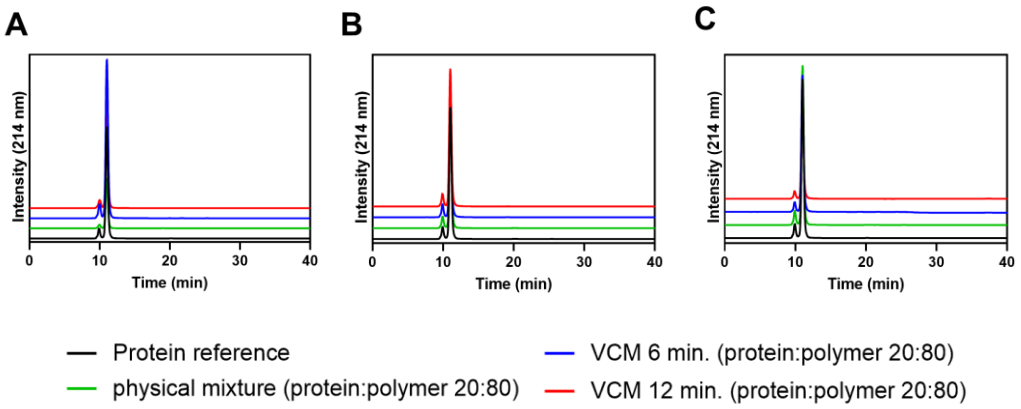

Figure S5 Chromatograms of SEC analysis; BSA powder (initial: black), physical mixture composed of 20 % BSA and 80 % polymer (green); and 20 % BSA-loaded discs with the polymers: **A:** PEG 20,000 at 65 °C; **B:** PLGA at 70 °C; **C**: EVA at 70 °C prepared by VCM in 6 min (blue) or 12 min (red).

5 HIGHLY PROTEIN-LOADED MELT EXTRUDATES PRODUCED BY SMALL-SCALE RAM AND TWIN-SCREW EXTRUSION - EVALUATION OF EXTRUSION PROCESS DESIGN ON PROTEIN STABILITY BY EXPERIMENTAL AND NUMERICAL APPROACHES

Katharina Dauer[1], Kevin Kayser[1], Felix Ellwanger[2], Achim Overbeck[3], Arno Kwade[3], Heike P. Karbstein[2], Karl G. Wagner[1,*]

[1] University of Bonn, Department of Pharmaceutics, Institute of Pharmacy, Bonn, Germany

[2] Institute of Process Engineering in Life Sciences, Food Process Engineering, Karlsruhe Institute of Technology, Karlsruhe, Germany

[3] Technische Universität Braunschweig, Institute for Particle Technology (iPAT), Braunschweig, Germany

This part was published as

K. Dauer, K. Kayser, F. Ellwanger, A. Overbeck, A. Kwade, H.P. Karbstein, and K.G. Wagner: Highly protein-loaded melt extrudates produced by small-scale ram and twin-screw extrusion - evaluation of extrusion process design on protein stability by experimental and numerical approaches, International Journal of Pharmaceutics: X, 2023, DOI: 10.1016/j.ijpx.2023.100196

5.1 GRAPHICAL ABSTRACT

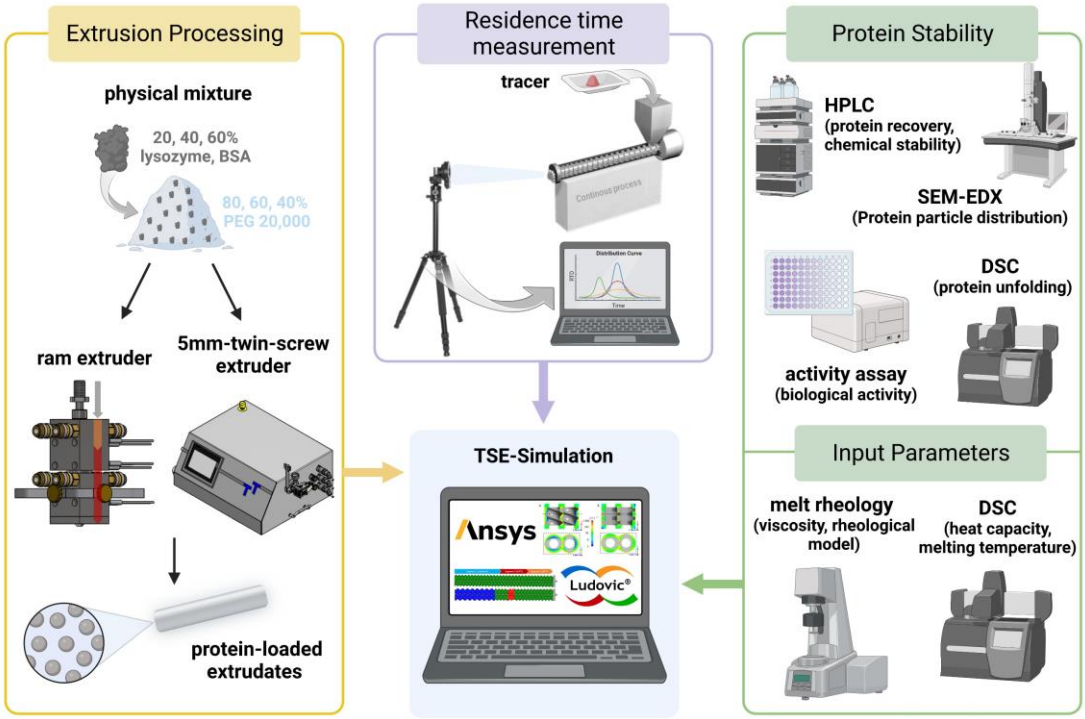

5.2 ABSTRACT

Understanding of generation, extent and location of thermomechanical stress in small-scale (< 3 g) ram and twin-screw melt-extrusion is crucial for mechanistic correlations to the stability of protein particles (lysozyme and BSA) in PEG-matrices. The aim of the study was to apply and correlate experimental and numerical approaches (1D and 3D) for the evaluation of extrusion process design on protein stability. The simulation of thermomechanical stress during extrusion raised the expectation of protein degradation and protein particle grinding during extrusion, especially when TSE was used. This was confirmed by experimental data on protein stability. Ram extrusion had the lowest impact on protein unfolding temperatures, whereas TSE showed significantly reduced unfolding temperatures, especially in combination with kneading elements containing screws. In TSE, the mechanical stress in the screws always exceeded the shear stress in the die, while mechanical stress within ram extrusion was generated in the die, only. As both extruder designs revealed homogeneously distributed protein particles over the cross section of the extrudates for all protein-loads (20-60 %), the dispersive power of TSE revealed not to be decisive. Consequently, the ram extruder would be favored for the production of stable protein-loaded extrudates in small scale.

5.3 KEYWORDS

Hot-melt extrusion, protein formulation, solid-state stability, computational fluid dynamics, numerical simulation

5.4 INTRODUCTION

The biopharmaceutical sector has grown rapidly over the last two decades [1]. However, compared to small-molecule based drug products, biopharmaceuticals are more complex and have to be parenterally administered mostly as liquid formulation [2]. One of the challenges is that many protein-based drugs are not stable in liquid formulations. Therefore the solid state is preferred for a wide range of used protein-based drugs for biopharmaceutical development [3], [4]. Physical and chemical stability of protein-based drugs is considered as bottleneck for a successful biopharmaceutical development. Even in the solid state, protein degradation can occur during the whole life cycle of a protein formulation [4], [5]. As the thermal stability of a protein depends on the relation between the degree of protein degradation and process-related stress applied the unfolding behavior of a protein is commonly studied.

Lyophilization and spray-drying are the mainly used techniques to convert biopharmaceutical formulations from an aqueous to a solid-state formulation providing improved stability during storage [6]–[10].

In pharmaceutical industry, hot melt extrusion (HME) is mainly used as continuous and robust manufacturing technology for the production of solid dosage forms [11]. In the last few years, the application of HME was expanded to biopharmaceutics and can be used for the production of long-term release systems for parenteral administration (e.g., protein-loaded implants) or for solid-state protein stabilization by embedding proteins in polymeric carriers [12]–[14].

In early formulation development, 9- or 12-mm co-rotating twin-screw extruders (TSE) are frequently used for the production of amorphous solid dispersions (ASD) mainly resulting in a solubility enhancement of poorly water-soluble drugs, but still require batch sizes of about 20-30 g, which result in substantial amounts of drug substance and development costs, respectively [15], [16]. The amount of protein-based drug candidates within early formulation development studies however, is often limited and thus small-scale HME is particularly relevant [17]. Small-scale HME such as ram extrusion and TSE ideally enables the processing of batch sizes below 3 g

accompanied with high yields of the produced protein-loaded extrudate under short processing times of less than 3 min [18]. The aim is a homogenous embedding of protein powder particles in a polymeric matrix by HME without negatively affecting the protein stability. The embedding of protein drugs in polymeric or lipid-based matrices by HME approaches at a small-scale level has been described in previously published works. Ghalanbor et al. assessed the feasibility of HME for preparing lysozyme-PLGA-implants and showed a complete recovery of active lysozyme from PLGA implants [12], whereas Cossé et al. used 5- and 9-mm mini-scale twin screw extruders for the preparation of BSA-PLGA-implants. A special focus was paid to the erosion properties and the in vitro release of the embedded BSA [19]. Another working group introduced the production of solid lipid implants (SLI) containing 10 to 20 % either of a lyophilized mAb or a fab-fragment by small-scale TSE (5 mm) at 35 °C and 40 rpm. The analytical investigations revealed a process-related impact on the physical protein stability as there were a loss in the monomer content of both the mAb and the f_{ab}-fragment and changes in secondary structure elements of the mAb [14]. The use of novel, biodegradable phase-separated poly(ε-caprolactone-PEG)-*block*-poly(*ε*-caprolactone), [PCL-PEG]-*b*-[PCL]) multiblock copolymers with different block ratios and with a low melting temperature (49 to 55 °C) for the production of protein-loaded implants was successfully shown by Stanković et al. The spray-dried protein powders goserelin, insulin, lysozyme, carbonic anhydrase, and albumin were incorporated into the polymers, whereby all proteins completely preserved their structural integrity as determined after extraction of the proteins from the polymeric implants [20], [21].

The works published so far are limited only to the production of protein-loaded extrudates by small-scale HME and characterization of the implants in terms of protein stability, protein recovery, and protein release. A mechanistic understanding and investigation of how process parameters such as type of extruder, feed-rate, residence time distribution, and process-related stress factors (thermomechanical stress profiles along the ram extruder or TSE barrel, or in the extruder die) affect protein stability, remain “black boxes”. Apart from that, the use of computational simulations to gain better HME process understanding and correlation of the simulation data with experimental results of protein stability was hitherto not considered.

One major issue in small-scale extrusion, especially when 5 mm TSE are used, has been identified to be a long residence time of up to 5 min, which subsequently results in an increased thermomechanical stress and a potentially negative impact on protein

stability [19], [22]. It is therefore crucial to carefully balance the process parameters: (i) Feed-rate, (ii) screw design, (iii) screw speed, (iv) die geometry, and (v) L/D-ratio, in order to avoid spots of elevated shear and/or thermal stress along the process. As melt temperature and pressure in small-scale extrusion is usually determined in the die only, information on the extent and location of above-mentioned hot spots along the process are easily missed. The gap towards a mechanistic understanding of the interactions between process variables and quality attributes needs therefore to be filled via numeric simulation [16], [23]–[25]. The present study evaluates ram extrusion and TSE as small-scale extrusion designs to produce protein-loaded extrudates. During ram extrusion, a powder mixture is loaded into a heated barrel where a piston is forced down onto the molten material [18]. The main shear stress generated during ram extrusion is found as the reservoir of the ram extruder is tapered into the die section. On the contrary, a TSE provides the opportunity of dispersive and distributive mixing [26], [27]. The powdered starting material is fed into the feed zone and transported to the subsequent zones by the turning motion of the screw along the barrel under pre-heating [28]. This process of conveying introduces mixing and heat into the material through both external heaters and viscous heat dissipation [11]. In the die zone head pressure is developed, which is determined by several factors: (i) the molten blend viscosity, (ii) the flow rate of the molten blend, and (iii) the die temperature [29]. TSE provides a continuous system with much better mixing, shorter residence times, ease of material feeding, high kneading (distributive) and dispersion capacities as injection molding or ram extrusion [26].

For our study, we used the hydrophilic polymer polyethylene glycol (PEG) 20,000 and the two model proteins lysozyme and bovine serum albumin (BSA) for the production of protein-loaded extrudates by ram extrusion and TSE. PEG 20,000 was selected as challenging polymer, since it exhibits a complex crystallization and melting behavior [30] and thus a narrow extrusion process window. Due to the low melting temperature of PEG 20,000, it enables extrusion at a temperature of below 65 °C, which in combination with a short residence time can minimize the risk of heat-induced protein degradation during HME processing. PEG 20,000 is waxy and shows a very high viscosity below the melting temperature (not extrudable due to an extensive torque) and a very low viscosity above the melting temperature (not extrudable due to liquification). Additionally, the screw configuration including conveying screws, and screws with a single 90° kneading element as well as the screw speed influence the resulting mechanical stress on polymer and protein particles [31]. The present work

aimed to include relevant extrusion process parameters such as: (i) screw configuration, (ii) screw speed, and (iii) residence time distributions (RTD) to facilitate potential correlations of the parameters with experimental data on polymer, and protein characteristics: (i) rheology, (ii) melting temperature shifts, (iii) protein recovery rates, and (iv) biological activity). Comparison of extrusion experiments were evaluated with the computations of the 1D and 3D simulation software Ludovic® and Ansys Polyflow®, respectively. The goal was to enable a fundamental and early starting point for the production of protein-loaded extrudates with sufficient protein stability and prior protein formulation development of long-term release systems by small-scale HME processing.

5.5 MATERIALS AND METHODS

5.5.1 MATERIALS

Lysozyme from chicken egg-white (Cat. No. L6876) was obtained from AppliChem GmbH (Darmstadt, Germany). Polyethylene glycol (PEG) 20,000 was obtained from Carl Roth (Karlsruhe, Germany). Bovine serum albumin (BSA) was purchased from Merck KGaA (Darmstadt, Germany). All chemicals were of analytical grade or equivalent purity.

5.5.2 METHODS

5.5.2.1 PREPARATION OF PHYSICAL MIXTURES AND PROTEIN-LOADED EXTRUDATES BY SMALL-SCALE RAM AND TWIN-SCREW EXTRUSION (5 MM)

PEG 20,000 flakes were milled in 3 cycles of 30 s utilizing a high-shear mixer at a fixed shear rate (Krups Mixette type 210, Krups, Frankfurt am Main, Germany) and passed through a 650 µm sieve to remove larger particles. For the preparation of protein-loaded extrudates, a physical mixture composed of polymer and 20, 40, or 60 % w/w either of lysozyme or BSA powder was blended for 10 min at 50 rpm using a turbula mixer (Willy A. Bachofen AG, Muttenz, Switzerland). The physical mixtures of PEG 20,000 and protein powder (Table 1) were either ram extruded or hot melt extruded by using twin-screw extrusion (TSE).

A self-built ram extruder was used for the preparation of protein-loaded extrudates with lower shear stress as previously described by [18]. A barrel of 10 cm length and an inner hole of 10 mm diameter consisted of three heating zones and was equipped with a cylindrical die (diameter 1 mm, length 7 mm). Extrudates were prepared by feeding 3 g of the physical mixture into the 10 mm hole of the ram extruder. The temperature of the first segment (filling-zone) was set to 58 °C, and the other two segments were set to 63 °C. The mixture was molten for three minutes and the blends were then extruded through the die by a driving piston with a speed of 1 mm/s.

TSE was performed using a 5 mm co-rotating twin-screw extruder (ZE 5, Three-Tec GmbH, Seon, Switzerland) with a length to diameter ratio (L/D) of 15:1 and two heating zones. The outlet of the extruder was equipped with a 1 mm die and either a conveying screw configuration, or a screw configuration with a single kneading element were used, which are presented in Figure 1. The physical mixtures were fed into the extruder by using a powder belt conveyor (GUF-P Mini AD / 475 / 75, mk

Technology Group, Troisdorf, Germany) at constantly kept feed-rates of 0.4, and 0.8, or 2.0 g/min ± 5 % for lysozyme- and BSA-composed mixtures (Table 1), respectively. The screw speed was set to 100, 150, or 200 rpm. Extrudates were collected in the steady-state of the extrusion process and the amount of extruded formulations was 1.5 to 3.0 g depending on the feed-rates and process parameters.

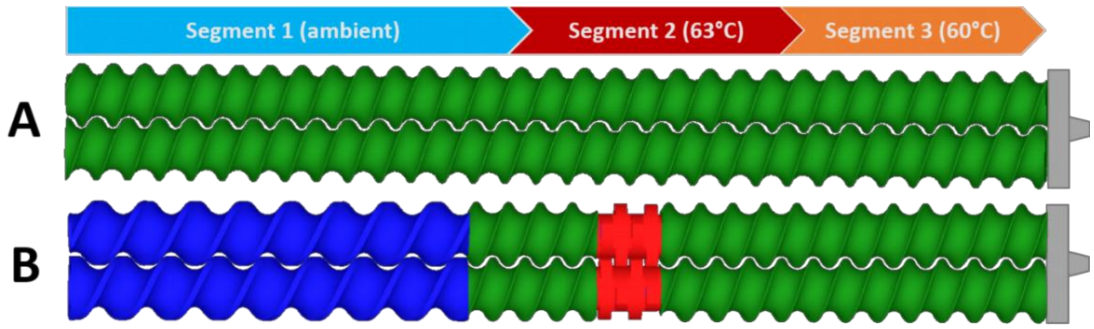

Figure 1 Screw configurations of the 5 mm twin-screw extruder with: **A** only conveying elements, **B** a single kneading element; 5 mm pitch (green), 7.5 mm pitch (blue), 90° kneading element (red); Segment 1 (ambient temperature), segment 2 (63 °C), and segment 3 (60 °C).

Table 1 Overview of the compositions and prepared protein-loaded extrudates by ram or twin-screw extrusion

Formulation	***Protein***	***Components (%)***		***Preparation method***
		Protein	**PEG 20,000**	
LR20	Lysozyme	20	80	Ram extrusion
LR40	Lysozyme	40	60	Ram extrusion
LR60	Lysozyme	60	40	Ram extrusion
BR20	BSA	20	80	Ram extrusion
BR40	BSA	40	60	Ram extrusion
BR60	BSA	60	40	Ram extrusion
LC20	Lysozyme	20	80	TSE (conveying)
LC40	Lysozyme	40	60	TSE (conveying)
LC60	Lysozyme	60	40	TSE (conveying)
BC20	BSA	20	80	TSE (conveying)
BC40	BSA	40	60	TSE (conveying)
BC60	BSA	60	40	TSE (conveying)
LK20	Lysozyme	20	80	TSE (kneading)
LK40	Lysozyme	40	60	TSE (kneading)

LK60	Lysozyme	60	40	TSE (kneading)
BK20	BSA	20	80	TSE (kneading)
BK40	BSA	40	60	TSE (kneading)
BK60	BSA	60	40	TSE (kneading)

5.5.2.2 RESIDENCE TIME DISTRIBUTION (RTD)

For TSE trials a 5 mm twin-screw extruder (ZE 5, Three-Tec GmbH, Seon, Switzerland) was used with two different screw configurations (Figure 1). PEG 20,000 powder was extruded at 60 and 63 °C at five different feed-rates of 0.4, 0.6, 1.0, 1.4, or 2.0 g/min. The screw speed was set to 100 or 200 rpm. In order to investigate a potential effect of protein concentration on residence time, MRT measurements of powder blends composed of PEG 20,000 and 0, 20, 40, or 60 % protein at a fixed feed-rate of 0.6 g/min were also performed. Mean residence times (MRTs) were measured with iron oxide as dye tracer (Sicovit® Red 30 E 172, BASF SE, Ludwigshafen, Germany) and calculated by using a camera system (ExtruVis3, ExtruVis, Riedstadt, Germany).

5.5.2.3 PARTICLE SIZE DISTRIBUTION ANALYSIS OF PROTEIN POWDER

Protein powder were analyzed in terms of particle size distribution and particle shape via dynamic image analysis (DIA) (Camsizer® X2, Retsch Technology, Haan, Germany). The continuous minimum diameter ($d_{xc\ min}$) of the analyzed particles was used for the particle size determination (n = 4).

5.5.2.4 MECHANICAL SINGLE CRYSTAL ANALYSIS

For mechanical analysis, single crystal compression tests were performed using a TiboIndenter Hysitron (Ti900, Bruker Minneapolis MN, USA) equipped with a 100 µm diameter diamond flatpunch probe. The protein crystals were dispersed on a flat sapphire substrate so that the average distance between them was greater than 200 µm to ensure individual loading. BSA crystals were sieved with a 125 µm mesh sieve prior to sample preparation.

The size of each crystal was determined prior to each loading with the calibrated instrument optics by determining the longest axis of the project surface and the length approximately perpendicular to it. The load function was displacement controlled to a maximum of 10 µm for Lysozyme and 20 µm for BSA crystals at a displacement rate

of 1 µm·s^{-1}. Compression tests were performed in ambient air at a temperature of 22 °C and humidity between 45 and 60 %. After each compression test, the flat punch probe was cleaned of any crystal debris. The force-displacement curves obtained in this way were analyzed for fracture events, which appear as discontinuities with a clear drop in force. The breaking force and breaking displacement were read from the first breaking event in each case.

5.5.2.5 SCANNING ELECTRON MICROSCOPY COUPLED WITH ENERGY-DISPERSIVE X-RAY SPECTROSCOPY (SEM-EDX)

A scanning electron microscope (SU 3500, Hitachi High Technologies, Krefeld, Germany), equipped with a backscattered electron detector (BSE) was used to investigate the morphology of the surfaces and cross sections of the prepared extrudates. BSE images were collected at an acceleration voltage of 5 kV at a variable pressure mode of 30 Pa. The cut extrudates were placed on an aluminum stub. Samples were sputtered with a thin platin layer (Sputter Coater, Cressington Scientific Instruments, Watford, England). Protein particle distribution was examined by elemental mapping of the cross sections of extrudates for the characteristic X-ray peak of nitrogen. The elemental distributions were investigated by SEM combined with an energy-dispersive X-ray detector (EDX) (EDAX Element-C2B, Ametek, Weiterstadt, Germany). The percentage of detected nitrogen was evaluated by the TEAM software (Version 4.4.1, Ametek, Weiterstadt, Germany).

5.5.2.6 DETERMINATION OF PROTEIN CONCENTRATION AND RECOVERY RATE BY RP-HPLC

Protein concentration in extrudates was determined by HPLC (LC20AT Solvent Delivery Pump, CBM-40lite system controller, SIL-10AF Autosampler, CTO-10A column oven, Shimadzu, Kyoto, Japan) using a C18 reversed phase column (NUCLEOSIL 120-3, C18, 5 µm, 125x4 mm, MACHEREY-NAGEL GmbH & Co. KG, Düren, Germany). Approximately 50 mg of the extrudates were accurately weighed and dissolved in Milli-Q® water (n = 3). Samples vials were cooled at 5 °C in the autosampler and 10 µL of each sample was injected. The solvent system consisted of water/acetonitrile/trifluoroacetic acid (A: 100/0/0.1, B: 0/100/0.1, V/V). A linear gradient method was applied (0–5–7 min 5–95–5 %B) at a flow rate of 1 mL/min for 7 min and a column temperature of 30 °C. Chromatograms were obtained using an UV-detector (SPD-40 UV Detector, Shimadzu, Japan) at 220 nm.

5.5.2.7 VACUUM COMPRESSION MOLDING (VCM)

Samples for rheological and DSC measurements were prepared with a VCM tool (MeltPrep GmbH, Graz, Austria) as described by [32]. In brief, a setup with a diameter of 20 mm (500 mg) and 5 mm (20 mg) for rheological and DSC measurements was used, respectively. PEG 20,000 and mixtures were molded at 65 °C for 5 min.

5.5.2.8 MELT RHEOLOGY

An oscillatory, small amplitude (SAOS) rheometer (HAAKE MARS III, Thermo Scientific, Karlsruhe, Germany) equipped with a roughened plate-plate geometry (d = 20 mm) was used. All experiments were conducted in controlled deformation AutoStrain (CDAuto-Strain) mode after equilibration of the samples for 5 min at the starting temperature with a gap height of 1.2 mm. PEG 20,000 and PEG 20,000-BSA mixtures containing 20, 40, or 60 % w/w BSA were measured using the following parameters: amplitude 0.0018 % at 1.0 – 10.0 Hz for the temperatures 62.8, 63.5, 64.0, 64.5 and 65.0 °C. The amplitude of each blend and plain PEG 20,000 was determined to be in the linear viscoelastic range (LVR) by amplitudes sweeps. A horizontal time-temperature superposition (TTS) was conducted where feasible resulting in master curves shifted to 64.0 °C [33]. The resulting master curve(s) were fitted to the power law fit:

$$\eta^* = \mathrm{K} \cdot \gamma^{\mathrm{n}} \tag{1}$$

where K is the consistency Index (Pa·s), γ is the shear rate (s^{-1}) and n is the power law index. Subsequently, to allow simulations an expression of temperature dependency is necessary. Therefore, temperature sweeps with an underlying heating rate of 0.2 °C/min were conducted to allow the determination of the Arrhenius activation energy of flow (E_A) employing the following equations (2) and (3):

$$|\boldsymbol{\eta}^*| = \mathbf{A} \cdot \mathbf{e}^{\frac{-\mathbf{E_A}}{\mathbf{R} \cdot \mathbf{T}}} \tag{2}$$

$$\ln|\eta^*| = \mathrm{A} - \frac{\mathrm{E_A}}{\mathrm{R}} \cdot \frac{1}{\mathrm{T}} \tag{3}$$

where $|\eta^*|$ is the measured complex viscosity (Pa·s), A is the pre-exponential factor, R is the gas constant (8.314 $J \cdot K^{-1} \cdot mol^{-1}$), T is the respective temperature (K) and E_A is the slope of the resulting plot.

5.5.2.9 DIFFERENTIAL SCANNING CALORIMETRY (DSC)

DSC studies of PEG 20,000, protein powder, and protein-loaded extrudates were performed with a DSC 2 (Mettler Toledo, Gießen, Germany) equipped with an auto sampler, nitrogen cooling and nitrogen as purge gas (30 mL/min). The system was calibrated with indium and zinc standards. Extrudates were milled with a mortar and pestle. At least three samples of ~10 mg were accurately weighed in 40 µL aluminum crucibles with a pierced lid. DSC scans were recorded from 25 °C to 230 °C using a heating rate of 10 °C/min. STAR^e software (Mettler Toledo, Gießen, Germany) was employed for acquiring thermograms. Thermograms were normalized for sample weight. The heat capacity (input parameter for simulation) of PEG 20,000, pure BSA and Lysozyme, and protein-PEG 20,000 mixtures were determined using a multi-frequency temperature modulation (TOPEM® mode) with an underlying heating rate of 2 °C/min, a pulse height of 1 °C, from 25 °C to 100 °C and a constant nitrogen purge (30 mL/min).

5.5.2.10 BIOLOGICAL ACTIVITY OF LYSOZYME AFTER EXTRUSION

Lysozyme activity was determined by a fluorescence-based assay (EnzChek® Lysozyme Assay Kit, Molecular Probes Europe BV, Leiden, The Netherlands) using a suspension of *Micrococcus lysodeikticus* labeled with fluorescein. The assay determines the lysozyme activity on the cell walls of *Micrococcus lysodeikticus*, which are labeled to such a degree that fluorescence is quenched. The fluorescence increase was measured using a microplate reader with a fluorescein filter and OptiPlateTM-96 F microwell plates (VICTOR3™ Multilabel Plate Reader; 96-Well plates black, PerkinElmer Life and Analytical Sciences, Shelton, Germany). Preparation of DQ Lysozyme substrate stock suspension, lysozyme standard curve, as well as the procedure were conducted according to the manufacturer's protocol. The reaction mixtures were incubated at 37 °C for 30 min, protected from light. The fluorescence intensity of each reaction in a microwell plate was measured at 494 nm (absorption maximum) and 518 nm (emission maximum). The fluorescence values obtained from the control without enzyme were subtracted.

5.5.2.11 SIMULATION OF MEAN RESIDENCE TIME

The one-dimensional (1D) simulation software Ludovic® V6.0 PharmaEdition (Sciences Computers Consultants, Saint Etienne, France) was used for computing thermo-mechanical analysis. This approach allows the calculation of various

parameters along the screw profile (e.g., temperature, residence time, etc.). The model assumes non-isothermal flow conditions and an instantaneous melting prior to the first restrictive screw element. Due to the unknown filling ratio of a starve-fed extruder, the computation starts at the die and proceeds backwards in an iterative procedure until the final product temperature is achieved. Input parameters were: (i) screw configuration, (ii) screw speed, (iii) temperatures of the segments, (iv) feed-rate, (v) thermal characteristics of the extruded mixture (i.e., heat capacity, density, thermal conductivity: 0.16 W/m·K, melting temperature, and melt rheology data).

5.5.2.12 3D ISOTHERMAL SIMULATION OF THE DIE SECTIONS AND THE SCREW SECTION

The calculation of the numerical equations was performed with the commercial software Ansys Polyflow® by Ansys Inc. (Canonsburg, PA, USA). The software is specifically suitable for HME processing and provides a finite element method solver for highly viscous media. Simulations were performed on a cluster server, computing one node with 32 Intel Xeon Gold 6230 processors and 70 GB of Random-Acess Memory.

The geometric dimensions of the simulated dies correspond to the dimensions of the dies of the ram extruder and TSE used in experiments. To reduce the computational effort, the geometries were quartered and calculated with symmetry planes. A mesh independence study resulted in computational meshes with 162,000 elements for the ram extruder die and 347,850 elements for the TSE die. A three-dimensional overview of the geometries and according meshes can be found in the Supplementary Material (Figure S1-S3). The boundary conditions for the ram extruder were chosen as 1 mm/s normal velocity at the inflow, outflow conditions at the outlet, 1 mm/s normal velocity at the reservoir wall, zero velocity condition at the conical die inlet wall and the die wall. The boundary conditions for the TSE die were chosen as 0.15 g/min mass flow rate inlet at the inflow, outflow conditions at the outlet and zero velocity at all walls.

In order to simulate the rotating screw elements of the TSE, the mesh superposition technique was used [34]. A detailed description of the application of the technique used on TSE can be found in a recent work [24]. The geometric dimensions of the simulated screw elements correspond to the conveying element (5 mm pitch) and the 90° kneading element shown in Figure 1. A mesh independence study resulted in computational meshes with 245,000 elements for the barrel, 206,984 elements for each conveying element, and 237,711 elements for each kneading element. A three-dimensional overview of the geometries and according meshes can be found in the

Supplementary Material (Figure S1-S3). The boundary conditions were chosen as 0.6 g/min mass flow rate inlet at the inflow, outflow conditions at the outlet, zero velocity at the outer barrel walls, screw elements and inner barrel walls rotate with 200 rpm. While wall slip can occur at high shear rates in the extrusion process, it was neglected for the simulations for simplicity. Accordingly, the no slip condition was assumed at the surface of the barrel and the rotating screw. Due to its symmetry, only half a revolution of the screw elements was simulated in 60-time steps.

Energy equation and gravity acceleration were neglected. Linear velocities and linear pressure were chosen for interpolation settings. Iterations on the viscosity were performed with a Picard scheme. The material parameters used for the simulations correspond to the 100 % PEG batch of the extrusion trials. The density of the material was set as 1200 kg/m³. The viscosity was described using a power law fit according to section 5.5.2.8. The fitted model is given in equation (4):

$$\eta(\dot{\gamma}) = 2{,}887{,}070 \cdot \dot{\gamma}^{-0.6783}\ Pa \cdot s \qquad (4)$$

To further analyze the simulation results, particle tracking analysis were performed. Therefore, 2000 mass- and volume less, non-interacting particles were randomly distributed at the inflow. Based on the velocity field solved, particles move through the domain where each point of the trajectories and its corresponding values were tracked and recorded.

5.5.2.13 STATISTICAL ANALYSIS

Statistical analysis and testing for statistical significance were carried out using Prism (GraphPad Software Inc., La Jolla, USA).

5.6 RESULTS

5.6.1 PROTEIN CONTENT IN EXTRUDATES AND PROTEIN PARTICLE DISTRIBUTION OVER THE CROSS SECTION OF EXTRUDATES

The particle size distribution analysis of the used protein powder particles for the preparation of highly-loaded protein-extrudates showed a narrow particle size distribution for lysozyme (d_{50} = 133 ± 7 µm), whereas BSA (d_{50} = 444 ± 70 µm) showed a very broad particle size distribution (Figure 2).

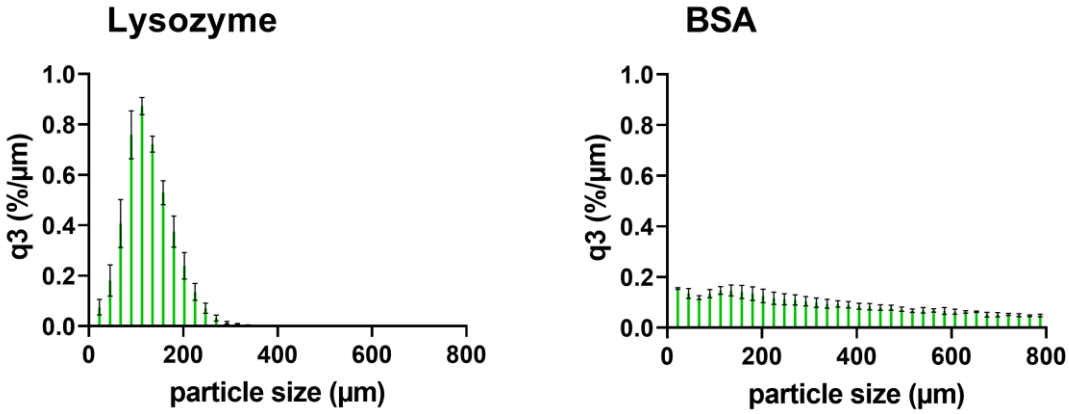

Figure 2 Particle size distribution of protein powder (lysozyme and BSA); q3 is the cumulative distribution referred to the percentage (%) of particles below that micron size (µm); error bars represent the standard deviation of four measurements by DIA.

The degree of protein powder particle embedding in the polymeric matrix and protein particle distribution over the cross section of extrudates produced by ram extrusion or TSE was analyzed by SEM-EDX (Figure 3). The surface of the extrudates prepared by TSE appeared smoother compared to extrudates produced by ram extrusion. The cross-section cut of the extrudates prepared by ram extrusion showed no pores or cracks inside of the extrudates, whereas the extrudates prepared by TSE showed only few pores. Elemental mapping of the cross sections showed an overall homogeneous distribution of protein particles in extrudates prepared by ram extrusion and TSE. Furthermore, the protein particles were only dispersed in the PEG- matrix and were not dissolved or notably grinded during extrusion. The protein recovery rate determined by HPLC was over 97 % for all extruded samples.

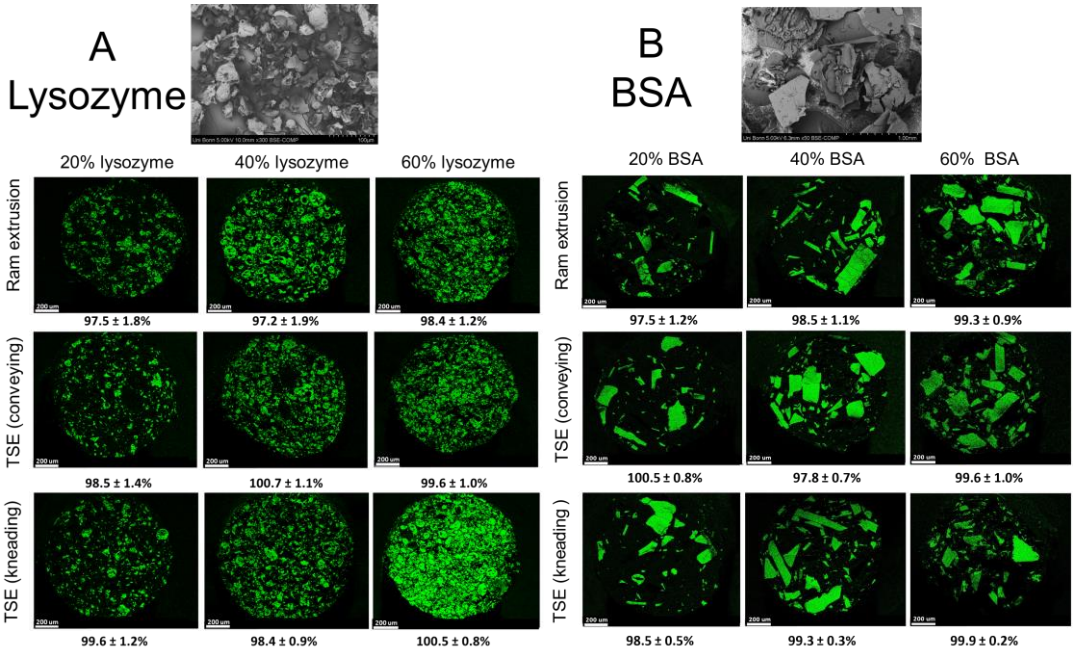

Figure 3 SEM-images of the used protein powder; protein particle distribution by SEM-EDX and elemental mapping of nitrogen (green spots) on cross section of 20, 40, and 60 % protein-loaded extrudates (**A** lysozyme and **B** BSA) prepared by ram or twin-screw extrusion (screw speed: 150 rpm) at 63 °C and protein recovery rates determined by RP-HPLC (n = 3) below the SEM-EDX-images. The scale bar of SEM-images corresponds to 200 µm.

5.6.2 MECHANICAL SINGLE CRYSTAL ANALYSIS

The mechanical properties of the protein crystals were determined using micro compression experiments. Figure 4A shows a representative force-displacement curve for lysozyme (grey) and BSA with a significant fracture event. For lysozyme, 46 crystals were examined, 44 of which showed one or more breakage events. For BSA, 28 crystals were tested, of which 13 showed an evaluable breakage event. If more than one fracture event occurred, only the first one was evaluated, as the number and size of the particles for the following loading is unknown.

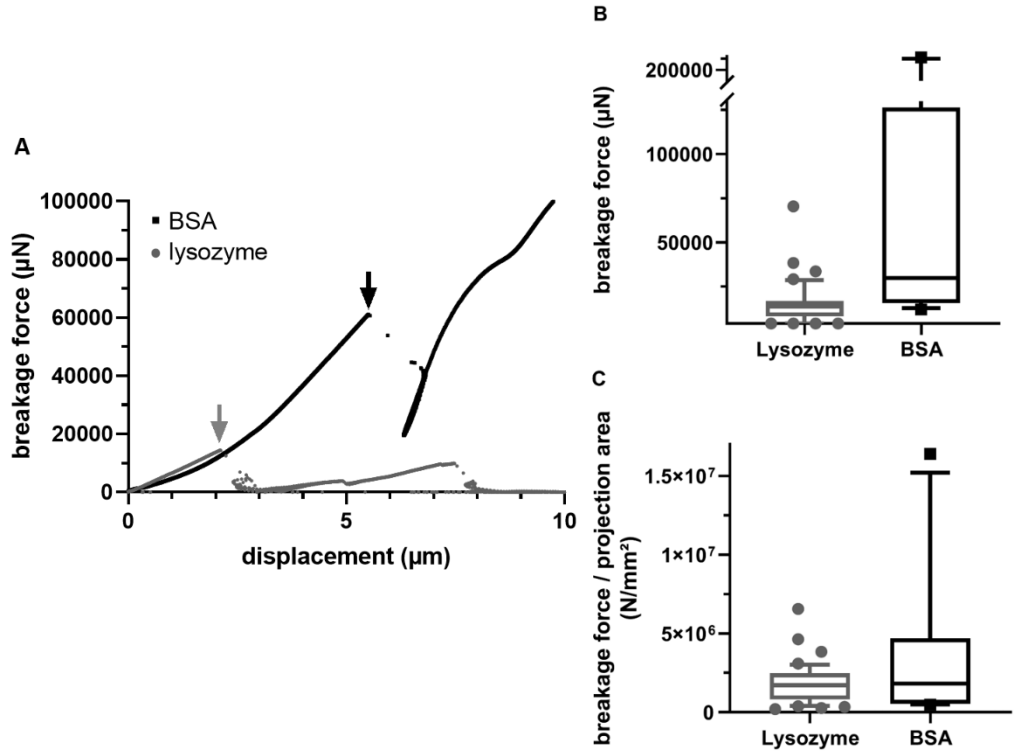

Figure 4 A Representative force - displacement data for the compression of lysozyme (gray) and BSA (black) crystals, each with a significant breakage event (arrows). Box plot representation of **B** breakage force and **C** breakage force/ projection area for lysozyme (gray) and BSA (black); horizontal line in the center of the box indicates the median, whiskers are drawn to the 90th and 10th percentiles of the data set.

Figure 4 B and C summarizes the micro-compression results. The values for breakage force and breakage displacement were significantly lower for lysozyme than for BSA. However, BSA with an average particle size of 94 µm was also coarser than lysozyme with an average particle size of 52 µm for the crystals examined by micro-compression. However, the fracture force for BSA was twice that of lysozyme in relation to the projected area. This ratio, which is similar to a fracture stress, tends to be a size independent material parameter. For comparison, compression tests of native lysozyme crystals in mother liquid are mentioned by [35], who determined a mean bursting force of only 238.3 ± 124.5 µN for a comparable particle size (48.7 ± 1.6 µm), which corresponds to a fracture stress of about 3.2 · 104 N/mm². Therefore, the dried crystals used in this work are comparatively stable.

5.6.3 UNFOLDING TEMPERATURE

Unfolding temperatures of lysozyme and BSA in protein-loaded extrudates produced by ram extrusion and TSE were determined by DSC (Figure 5). The reported unfolding temperatures of the protein powders served as references and were compared to the

produced protein-loaded extrudates. Lysozyme- and BSA-loaded extrudates (20, 40, and 60 % protein-load) prepared by ram extrusion showed no significantly reduced unfolding temperatures compared to the unprocessed neat protein powder. Processing of 40 % lysozyme by TSE at 100, 150, and 200 rpm screw speed and at a constant feed-rate of 0.4 g/min shifted the unfolding temperature towards lower temperatures whereas the unfolding temperatures of 60 % lysozyme-loaded extrudates were not significantly reduced and were independent of the applied screw speed. The unfolding temperatures of 60 % BSA-loaded extrudates were not reduced neither when produced by ram extrusion nor by TSE. 40 % BSA-loaded extrudates prepared by TSE with conveying or kneading screw configuration showed significantly reduced unfolding temperatures.

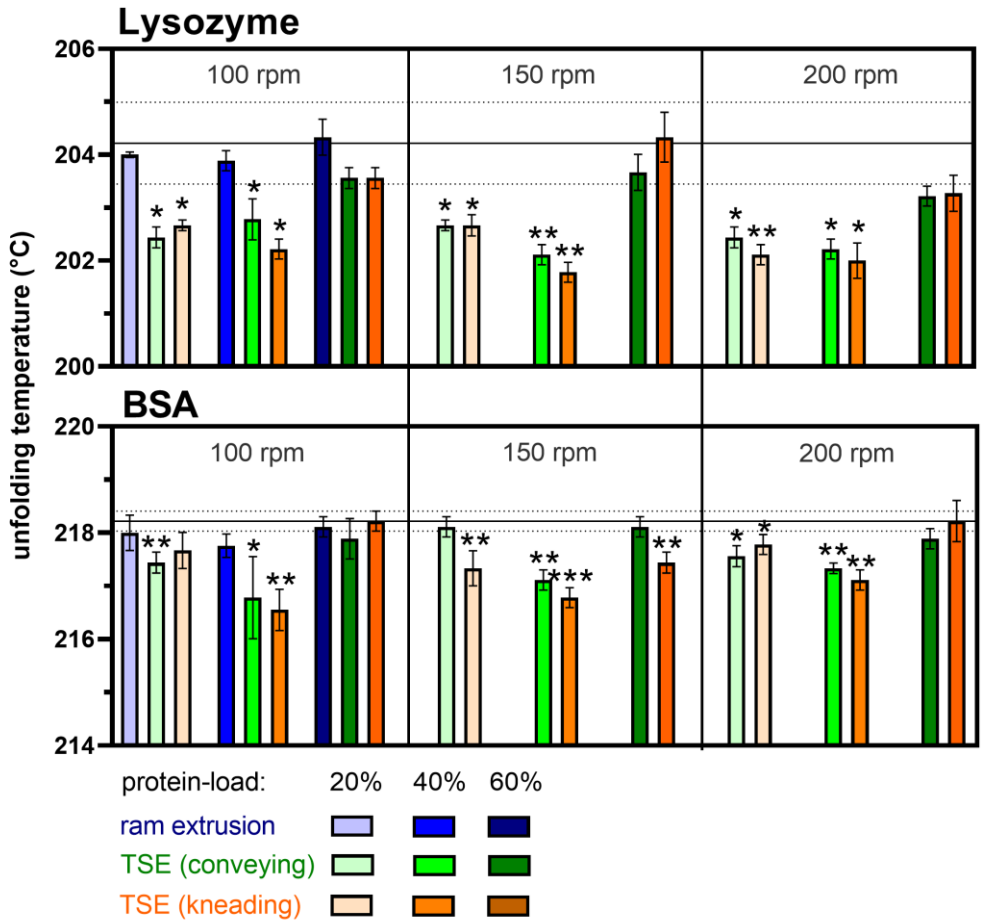

Figure 5 Unfolding temperatures of 20, 40, and 60 % protein-loaded (lysozyme and BSA) extrudates prepared by ram extrusion (blue) or TSE with only conveying screw configuration (green), or screws containing a single 90° kneading element (orange) at 100, 150, or 200 rpm screw speed, at 63 °C; error bars represent the standard deviation of three measurements for the unfolding temperature by DSC; the line shows the melting temperature of the unprocessed protein (reference) and the dotted lines represent the

standard deviation (n = 3); statistical significance is compared to the reference and depicted by asterisks (*): * $p < 0.05$, ** $p < 0.01$, *** $p < 0.001$.

5.6.4 LYSOZYME ACTIVITY AFTER EXTRUSION

The biological activity of lysozyme in 40 % lysozyme-loaded extrudates was investigated immediately after ram extrusion and TSE with conveying and kneading screw configuration, at 100, 150, and 200 rpm and at 63 °C. The activity of lysozyme embedded in melt extrudates by ram extrusion or TSE was higher than 90 % and thus maintained the full biological activity when compared to the activity of the unprocessed lysozyme powder, which was 99.86 ± 5.29 % (*t*-test: $p < 0.05$) (Figure 6).

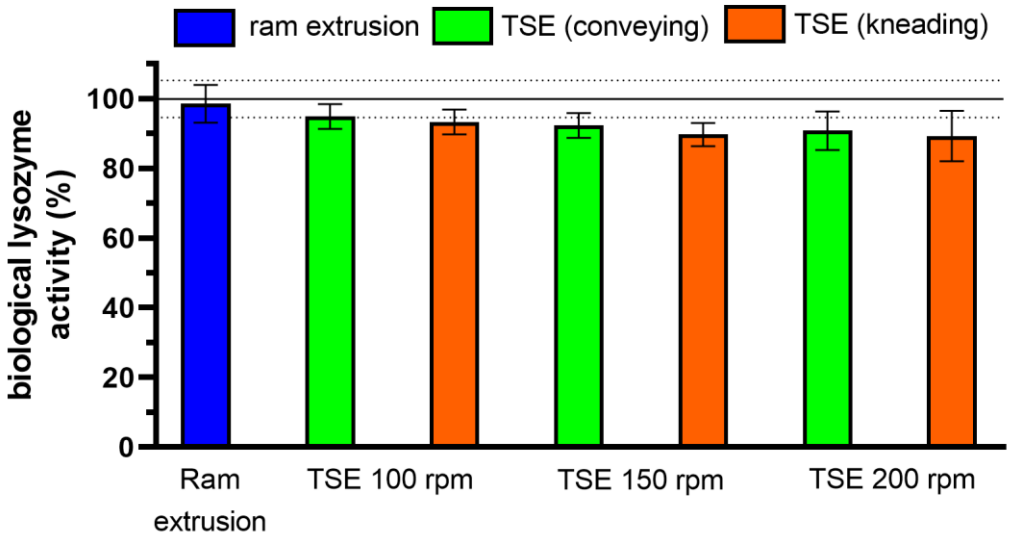

Figure 6 Biological activity of lysozyme of 40 % lysozyme-loaded extrudates prepared by ram extrusion (blue) or TSE with only conveying screw configuration (green), or screws containing a single 90° kneading element (orange), at 63 °C and 100, 150, and 200 rpm screw speed; samples (n = 3) were immediately analyzed after extrusion processing; error bars represent the standard deviation of three measurements; the line shows the biological activity of the unprocessed lysozyme (reference) and the dotted lines represent the standard deviation (99.86 ± 5.29 %).

5.6.5 RESIDENCE TIME DISTRIBUTION

In order to receive information about the residence time distribution of the material within the extrusion barrel in dependence of feed-rate, screw configuration, and screw speed, MRT measurements were performed.

Figure 7 shows the determined MRT by an experimental and simulative approach for five feed-rates, two screw configurations and varying screw speed. For the simulation of MRT by Ludovic®, melt rheology data were key input parameters (refer to Supplementary Material, Figures S4-6). The experimental MRT for a feed-rate of

0.4 g/min was found at 57.0 ± 0.2 s at 100 rpm and 47.4 ± 1.7 s at 200 rpm, with a comparably broad distribution using the conveying screw configuration, whereas simulation revealed MRTs of 67.1 s at 100 rpm and 63.3 s at 200 rpm. The experimental MRT measurements using the screw configuration with a single kneading element at a feed-rate of 0.4 g/min resulted in 68.3 ± 6.2 s at 100 rpm and 58.5 ± 1.1 s at 200 rpm. The simulated MRTs at a feed-rate of 0.4 g/min were found at 71.3 s and 68.1 s at 100 rpm and 200 rpm, respectively.

MRTs for 2.0 g/min at 100 and 200 rpm were found at 29.3 ± 1.0 s and 18.3 ± 0.5 s for the conveying screw configuration, and 33.4 ± 1.2 s and 21.6 ± 0.9 s for the kneading screw configuration, respectively. The MRTs obtained by simulation were 21.9 s and 19.2 s for the conveying screw configuration at 100 and 200 rpm, respectively, whereas the MRT data for the kneading screws were 21.9 s at 100 rpm and 19.8 s at 200 rpm. Higher feed-rates resulted in more narrow residence time distributions (data not shown). The simulation accuracy of MRTs was higher at increasing feed-rates. For feed rates of 1.0 g/min and higher the simulated MRTs were within the experimental MRTs including their standard deviations. The smallest deviations between experimental and simulated MRT were found for the conveying and kneading screw configuration at a screw speed of 200 rpm.

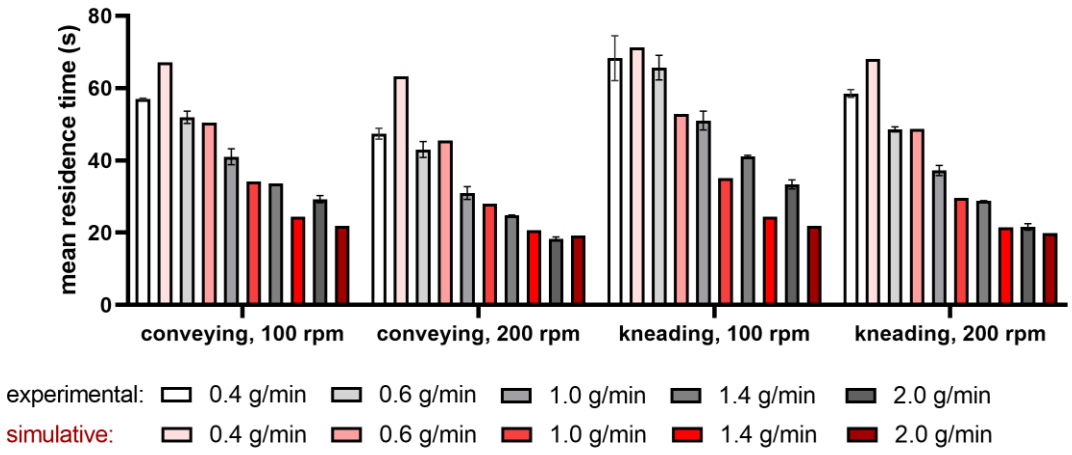

Figure 7 Mean residence time as a function of screw configuration (conveying, kneading; screw speed: 100 and 200 rpm); 100 % PEG 20,000 was fed into the extruder at five different feed-rates (0.4, 0.6, 1.0, 1.4, and 2.0 g/min); error bars represent the standard deviation of three MRT measurements.

Figure 8 shows the MRT data obtained by experiments or simulations as a function of protein concentration at a fixed feed-rate of 0.6 g/min. For the conveying screw configuration, the MRT decreased with increasing protein concentration as 0 % compared to 60 % protein-load showed a decrease in the experimental and simulated MRT of 11.9 s at 100 rpm and 6.2 s at 200 rpm and 12.9 s at 100 rpm and 12.0 s at

200 rpm, respectively. For the screw configuration containing a single kneading element, the MRT was slightly increased with increasing protein concentration. For the mixture containing 60 % protein MRT was prolonged compared to 0 % protein load about 6.6 s at 100 rpm and 9.4 s at 200 rpm, while simulation of the MRTs at 100 and 200 rpm revealed an increase of 4.8 s and 7.3 s, respectively.

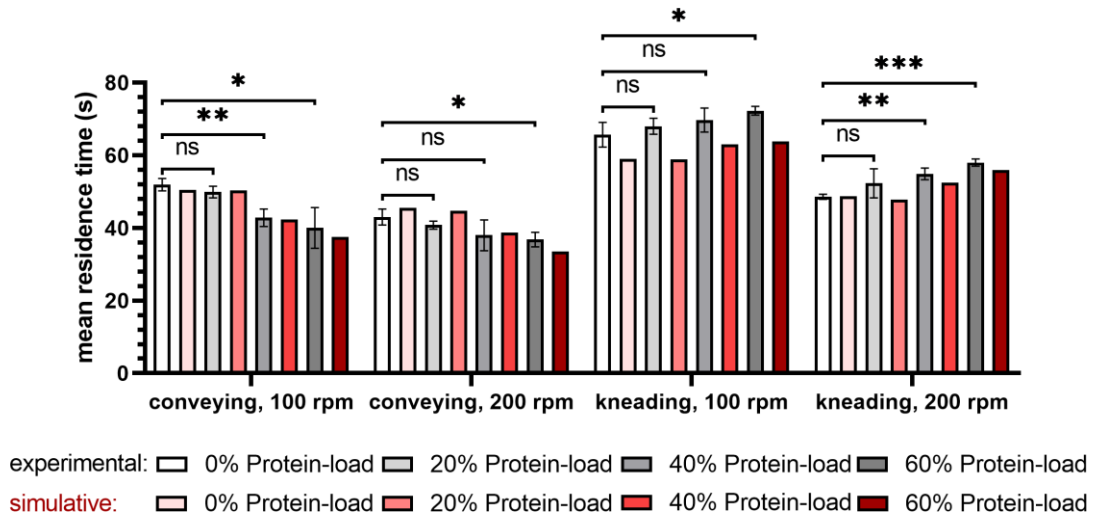

Figure 8 Mean residence time as a function of screw configuration (conveying, kneading; screw speed: 100 and 200 rpm) and protein-load (0, 20, 40, and 60 % protein-PEG 20,000 mixtures) at a feed-rate of 0.6 g/min; simulated MRT is displayed in gray color; experimental MRT is displayed in red color; error bars represent the standard deviation of three MRT measurements; unpaired *t*-test (two-sample assuming equal variances) was used and statistical significance was depicted by asterisks (*) for MRT. ns = not significant, significant differences are indicated by asterisks: *, $p < 0.05$, **, $p < 0.01$ and, ***, $p < 0.001$.

5.6.6 MECHANICAL STRESS HISTORY IN EXTRUSION PROCESSING

Figure 9 shows color plots of the shear rate distribution in the dies of the ram extruder and the TSE. Low shear rates were found in the reservoir of the ram extruder. As the capillary narrows in the direction of flow, the flow is accelerated, resulting in increasing shear rates. In the area of the smallest radius, shear rates up to 1,500 s^{-1} were observed. In this area the shear rate increased over the radius of the die and reached its maximum at the wall. Likewise, the highest shear rate was also achieved in the area of the smallest radius for the TSE with values up to 150 s^{-1}. The shear rate profile is similar to the ram extruder, but with values 10-times lower.

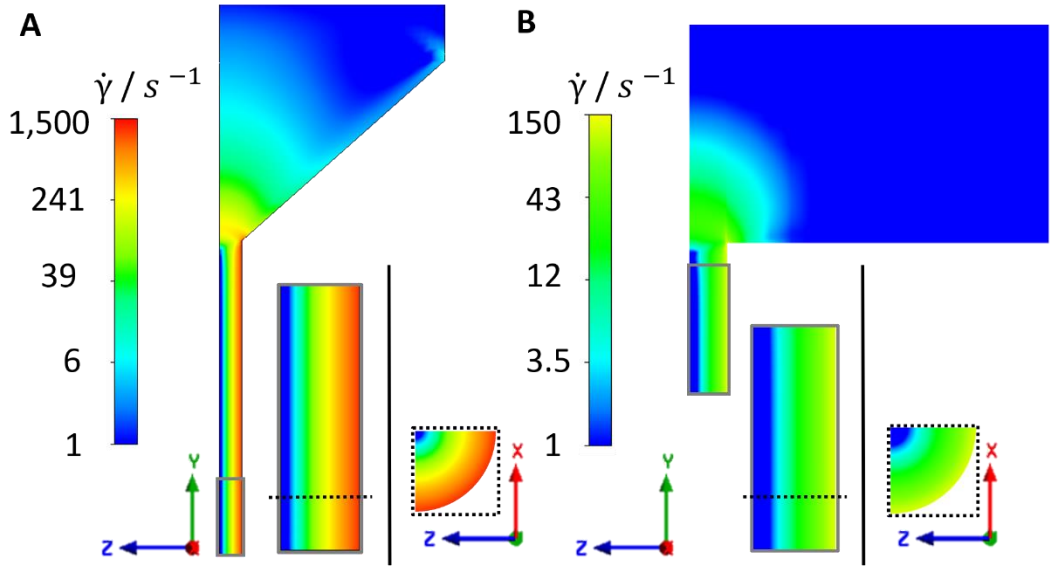

Figure 9 Color plots of the shear rate distribution of **A** ram extruder die **B** twin-screw extruder die

The shear rate distribution of a fully filled screw section of the TSE is shown for a pair of conveying elements and kneading elements in Figure 10. For both type of elements, the highest shear rates were observed in the gap between the screw tip and the barrel wall as well as in the gap between the rotating elements. The maximum shear rates were similar for both element types with values up to 1,500 s^{-1}. For the kneading element, the shear rates were higher than 30 s^{-1} in the whole area, whereas for the conveying elements in the channel also low shear rates were found.

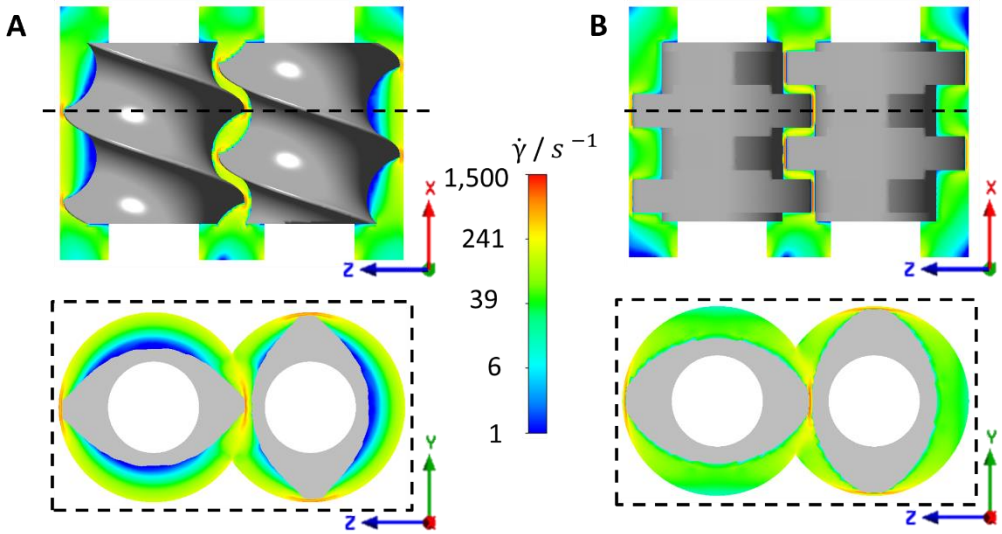

Figure 10 Color plots of the shear rate distribution of **A** TSE conveying elements (5 mm pitch) die **B** TSE 90° kneading elements

Although the color plots of the different geometries provided information about the shear rate distribution, it was not possible to conclude about the mechanical stress experienced by the material in these sections. Therefore, particle tracking analyses were performed with the solved velocity fields and particle trajectories were obtained. The maximum shear rate and residence time were calculated for each trajectory and cumulative distributions were created. Figure 11 shows the cumulative distributions of the maximum experienced shear rate and the residence time distribution for the different dies and screw elements. As expected, the material experienced higher shear rates in the screw section than in the die section for both screw configurations and in comparison to the shear stress in the ram extruder die. The median ($Q_{0,50}$) was found at 237 s^{-1} for the ram extruder die, 46 s^{-1} for the TSE die, 1,295 s^{-1} for the conveying elements, and 1,040 s^{-1} for the kneading elements.

Regarding the residence time distribution, it can be observed that particles remained longer in the die of the TSE than in the ram extruder die. However, the residence times were shorter than in the simulated screw elements. Comparing the screw elements, a slightly longer residence time of the particles in the kneading block were observed, although the volume which passed the kneading block was similar and the mass flow constant, respectively. The median (Q0,50) was found at 0.05 s for the ram die, 0.16 s for the TSE die, 7.4 s for the conveying elements, and 9.4 s for the kneading elements.

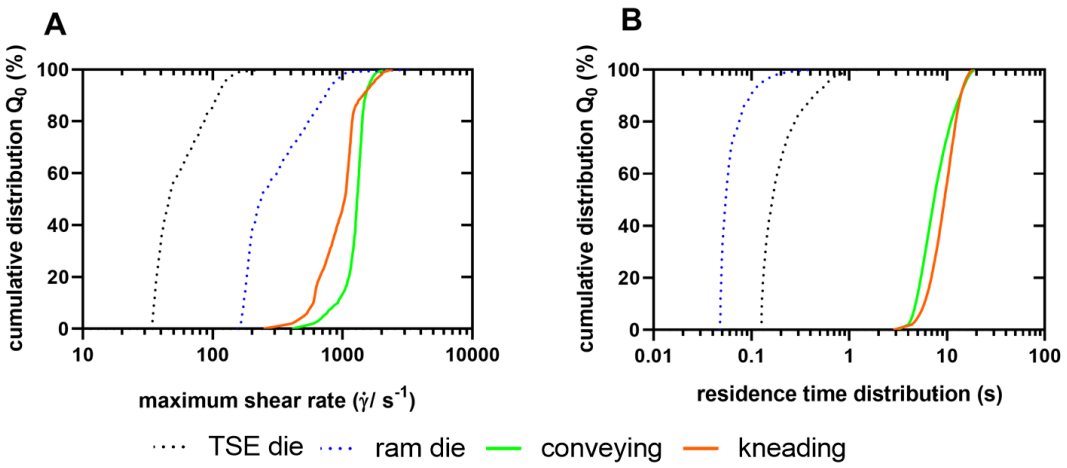

Figure 11 A Cumulative number distribution of the maximum shear rate along the particles tracked for the TSE die, the ram die, the conveying elements and the kneading elements **B** Residence time distribution along the particles tracked for the twin-screw extruder die (area of smallest radius only), the ram extruder die (area of smallest radius only), the conveying elements and the kneading elements.

5.7 DISCUSSION

While for the ram extruder melting and extruding, i.e., introducing mechanical stress, were applied sequentially, these processes were introduced simultaneously during TSE and thermomechanical stress was certainly present for the unmolten and molten material during TSE processing. Monitoring and characterization of the magnitude and duration of the generated thermomechanical stress is often not feasible and highlights the need of computational simulation for gaining insights into small-scale HME processing including temperature profiles, mechanical stress distributions, and RTDs. The particle tracking approach utilized describes infinitesimally small, massless particles moving through the resolved flow fields. Accordingly, the motion of actual protein particles was only partially replicated.

In regard of mechanical stress, the die area of both extruders was comparable and the highest shear rates were found close to the wall, gradually decreasing towards the center of the die channel. Particles dispersed in the PEG-melt passing the die rather in the center, subsequently experienced a lower shear stress compared to those closer to the wall. For TSE the highest shear rates were present in the screw section and particularly in the gap between the screws and the gap between screw and barrel. The increased shear rate for the kneading element can be attributed to different flow profiles resulting from the restriction of 90° kneading discs.

The MRTs of the blends in the heated barrels were short, namely 3 min and less than 80 s, for ram extrusion and TSE, respectively, and thus did not lead to a dissolution of protein particles but rather a solely dispersing of protein particles in the PEG-matrix. In this study, lysozyme and BSA particles could be regarded as fillers during extrusion, since the particle size of the used protein powders was identical for the starting material and particles determined in the cross section of extrudates. Ram extrusion facilitated sufficient dispersion of protein particles for protein-loads in the range of 20 to 60 %. Consequently, the distributive mixing power of TSE was not necessary for the production of protein-loaded extrudates and TSE was thus not superior in particle distribution compared to ram extrusion. The simulation of maximum shear rates raised the expectation of particle size reduction during extrusion, especially when TSE was used. Micro compression analysis showed that BSA crystals were more ductile and less fragile than solid lysozyme particles (Figure 4). However, the mechanical stress generated during ram extrusion and TSE was not high enough to break either the lysozyme or the BSA particles. Since the protein particles showed also an elastic deformation behavior, a compensation of local shear stress peaks during extrusion

could be possible [36], [37]. However, a correlation of the simulated mechanical stress with the micro compression analysis could not be established in this study, as more advanced approaches would be needed, such as coupling CFD simulations with DEM simulations [38].

Ram extrusion had the lowest impact on unfolding temperatures as the main mechanical stress was generated only in the die for less than 1 s as confirmed by the results of 3D simulation. The ram extrusion process had unexceptionally no negative effect on the unfolding temperatures of lysozyme and BSA in the various extrudates compared to the unprocessed proteins and were also independent of the protein-load. As experimental and simulated data revealed, ram extrusion provides a gentle approach for the production of protein-loaded extrudates.

In contrast, a protein-load effect on the unfolding temperature was observed for extrudates produced by TSE. Interestingly a higher protein-load of 60 % was protective resulting in a less pronounced decrease of unfolding temperatures. According to a correlation of the unfolding temperatures with the simulated temperature profiles along the TSE process and MRTs, we hypothesize that the generated shear stress during TSE were distributed to a larger protein particle collective and thus, protein-loads higher than 50 % should be favored for the embedding of a thermally stable protein. For a better understanding of TSE processing, MRTs determined by TSE experiments and 1D simulation (Ludovic®) were compared. The experimental MRTs for the pure PEG and 20 % protein-polymer mixture were congruent with simulated data (Figure 7). In mixtures with 40 % or 60 % protein, the impact on melt rheology behavior (Figures S4-6) and thus the MRT is no longer neglectable and was reliably predicted by Ludovic®. The MRT in the kneading element was slightly increased, implying that protein particles were entrapped within the gaps of the kneading element, resulting in an increased viscous dissipation (see Figure S7). This is confirmed by the results of unfolding temperatures and provides an important correlation for the evaluation of extrusion process design on protein stability. The shorter simulated MRTs for the screws comprising the kneading element at 100 rpm might resulted in a deviation between the apparent melt viscosity in the experiment compared to the anticipated melt viscosity of 1D simulation (Figure 8). As the simulation anticipates a molten continuum to begin with, in reality this condition needs to be established within the first part of the extrusion process. 1D simulation revealed that the highest temperature of the molten blend was achieved by entering in the die zone (Figure S7). At 100 rpm the contribution of the introduced viscous

dissipation to the overall melt energy was lower compared to 200 rpm (peak temperatures: 75.6 °C and 78.1 °C, respectively). As the kneading elements have no conveying functionality the mass will pile up in front of the element. As the condition of being molten in reality would have been reached later at 100 rpm, this was likely the reason of the more pronounced deviation of experimental and simulated MRTs using segmented screws at low screw speed.

Compared to the reliably simulated thermomechanical and temperature profiles and RTDs along the TSE barrel and the die and as torque could not adequately measured in the 5 mm TSE experiments, 1D simulation could not reveal pressure distribution, which would otherwise be standard. For an increased simulation accuracy, improved instrumentation especially for pressure and melt temperatures along the entire process length would be necessary. Especially, the pressure would indeed be an excellent variable to validate the 3D simulations of the die section. Advanced instrumentation would facilitate improved model validation as pressure and temperature profiles could be correlated. Unfortunately, such advanced instrumentation was not available for the applied extruders and will be part of further studies. Additionally, some simplifications during simulation might have added to a higher variance, such as isothermal conditions, no wall slippage and no viscosity transition from waxy condition into melt. Subsequently, the simulated pressure values are likely to be higher than in an experiment. Therefore, simulations were primarily intended to compare geometries and to improve process understanding for the appropriate selection of protein-related process and formulation demands.

5.8 CONCLUSIONS

A fundamental and early starting point for the production of highly protein-loaded extrudates with sufficient protein stability and enabling an understanding of extrusion processing prior protein formulation development of potential long-term release systems by small-scale extrusion processing was provided. A mechanistic understanding and investigation of how process parameters such as type of extruder, feed-rate, RTD, and process-related stress factors (thermomechanical stress profiles along the ram extruder or TSE barrel, or in the extruder die) affect protein stability, was hitherto not considered in the literature. In our study, several extrusion process characteristics and material properties such as heat capacity, density, melt rheology data of the investigated polymer-protein mixtures have been considered as input parameters for 1D and 3D simulations. The combination of experimental and numerical approaches resulted in a better understanding of HME process parameters including mainly the type of extruder, and residence time distribution on protein stability with a special focus on thermal protein stability and a potential process-induced loss in lysozyme activity. The 1D and 3D simulation software Ludovic® and Ansys Polyflow®, respectively proved to be valuable tools for the evaluation of extrusion process design and provided important insights into extrusion processing optimization and potential scale-up challenges at a small-scale level as critical process steps and locations of thermomechanical stress hot spots along the process were identified. This approach supports also a rationale to identify appropriate extrusion process conditions for the production of highly protein-loaded extrudates and to define in perspective the best protein-polymer compositions. In particular, ram extrusion was identified as favored method for the production of stable protein-loaded extrudates, since the thermomechanical stress was low and still a homogenous distribution of protein particles over the cross section was achieved. However, so far, no simple 1D simulation model is available for ram extrusion thus, 3D simulations had to be employed for crucial process steps or areas, respectively. As the die in the ram extrusion was identified as the most critical process area, this limitation is negligible. In contrast, TSE strongly profits from both 1D and 3D simulations where 1D identifies critical process steps while 3D simulations boost the mechanistic understanding. Nonetheless simulation via Ludovic® is expected to better converge with experimental data when using higher feed-rates and larger size 9-, 11-, or 12-mm TSE with better instrumentation spread over the entire extrusion process (e.g., multiple temperature, die pressure, and torque monitoring). The present procedure enables a good starting

point for ram extrusion and TSE trials for the production of highly-loaded protein extrudates with sufficient protein stability, protein recovery rates and homogenous distributed protein particles.

5.9 RESEARCH FUNDING

This research was funded by the German Research Foundation (DFG SPP1934, project number: 273937032).

5.10 ACKNOWLEDGEMENTS

The authors would like to thank the “Deutsche Forschungsgemeinschaft (DFG)” for financial support in the research project SPP 1934 DiSPBiotech. We thank W. Graf and his team from the Institute of Applied Physics for the production of ram extruder components. The authors acknowledge support by the state of Baden-Württemberg through bwHPC.

5.11 REFERENCES

[1] A. C. Martins, M. Y. Oshiro, F. Albericio, B. G. de la Torre, G. J. V. Pereira, und R. V. Gonzaga, „Trends and Perspectives of Biological Drug Approvals by the FDA: A Review from 2015 to 2021“, Biomedicines, Bd. 10, Nr. 9, S. 2325, Sep. 2022, doi: 10.3390/biomedicines10092325.

[2] Z. Antosova, M. Mackova, V. Kral, und T. Macek, „Therapeutic application of peptides and proteins: parenteral forever?“, Trends Biotechnol., Bd. 27, Nr. 11, S. 628–635, Nov. 2009, doi: 10.1016/j.tibtech.2009.07.009.

[3] M. C. Lai und E. M. Topp, „Solid-state chemical stability of proteins and peptides“, J. Pharm. Sci., Bd. 88, Nr. 5, S. 489–500, Mai 1999, doi: 10.1021/js980374e.

[4] M. J. Pikal, „Mechanisms of protein stabilization in the solid state“, J. Pharm. Sci., Bd. 98, Nr. 9, S. 23, 2009.

[5] M. C. Manning, D. K. Chou, B. M. Murphy, R. W. Payne, und D. S. Katayama, „Stability of Protein Pharmaceuticals: An Update“, Pharm. Res., Bd. 27, Nr. 4, S. 544–575, Apr. 2010, doi: 10.1007/s11095-009-0045-6.

[6] A. Sharma, D. Khamar, S. Cullen, A. Hayden, und H. Hughes, „Innovative Drying Technologies for Biopharmaceuticals“, Int. J. Pharm., Bd. 609, S. 121115, Nov. 2021, doi: 10.1016/j.ijpharm.2021.121115.

[7] J. Massant, „Formulating monoclonal antibodies as powders for reconstitution at high concentration using spray-drying_ Trehalose/amino acid combinations

as reconstitution time reducing and stability improving formulations“, Eur. J. Pharm. Biopharm., S. 12, 2020.

[8] J. Horn, J. Schanda, und W. Friess, „Impact of fast and conservative freeze-drying on product quality of protein-mannitol-sucrose-glycerol lyophilizates“, Eur. J. Pharm. Biopharm., Bd. 127, S. 342–354, Juni 2018, doi: 10.1016/j.ejpb.2018.03.003.

[9] S. K. Pansare und S. M. Patel, „Lyophilization Process Design and Development: A Single-Step Drying Approach“, J. Pharm. Sci., Bd. 108, Nr. 4, S. 1423–1433, Apr. 2019, doi: 10.1016/j.xphs.2018.11.021.

[10] S. Schüle, W. Frieß, K. Bechtold-Peters, und P. Garidel, „Conformational analysis of protein secondary structure during spray-drying of antibody/mannitol formulations“, Eur. J. Pharm. Biopharm., Bd. 65, Nr. 1, S. 1–9, Jan. 2007, doi: 10.1016/j.ejpb.2006.08.014.

[11] M. M. Crowley u. a., „Pharmaceutical Applications of Hot-Melt Extrusion: Part I“, Drug Dev. Ind. Pharm., Bd. 33, Nr. 9, S. 909–926, Jan. 2007, doi: 10.1080/03639040701498759.

[12] Z. Ghalanbor, M. Körber, und R. Bodmeier, „Improved Lysozyme Stability and Release Properties of Poly(lactide-co-glycolide) Implants Prepared by Hot-Melt Extrusion“, Pharm. Res., Bd. 27, Nr. 2, S. 371–379, Feb. 2010, doi: 10.1007/s11095-009-0033-x.

[13] Z. Ghalanbor, M. Körber, und R. Bodmeier, „Protein release from poly(lactide-co-glycolide) implants prepared by hot-melt extrusion: Thioester formation as a reason for incomplete release“, Int. J. Pharm., Bd. 438, Nr. 1–2, S. 302–306, Nov. 2012, doi: 10.1016/j.ijpharm.2012.09.015.

[14] M. Vollrath, J. Engert, und G. Winter, „Long-term release and stability of pharmaceutical proteins delivered from solid lipid implants“, Eur. J. Pharm. Biopharm., Bd. 117, S. 244–255, Aug. 2017, doi: 10.1016/j.ejpb.2017.04.017.

[15] J. Jiang, A. Lu, X. Ma, D. Ouyang, und R. O. Williams, „The applications of machine learning to predict the forming of chemically stable amorphous solid dispersions prepared by hot-melt extrusion“, Int. J. Pharm. X, Bd. 5, S. 100164, Dez. 2023, doi: 10.1016/j.ijpx.2023.100164.

[16] D. E. Zecevic und K. G. Wagner, „Rational Development of Solid Dispersions via Hot-Melt Extrusion Using Screening, Material Characterization, and Numeric Simulation Tools“, J. Pharm. Sci., Bd. 102, Nr. 7, S. 2297–2310, Juli 2013, doi: 10.1002/jps.23592.

[17] K. Dauer, W. Kamm, K. G. Wagner, und S. Pfeiffer-Marek, „High-Throughput Screening for Colloidal Stability of Peptide Formulations Using Dynamic and Static Light Scattering“, Mol Pharm., S. 17, 2021.

[18] K. Dauer, C. Werner, D. Lindenblatt, und K. G. Wagner, „Impact of process stress on protein stability in highly-loaded solid protein/PEG formulations from small-scale melt extrusion“, Int. J. Pharm. X, S. 100154, Dez. 2022, doi: 10.1016/j.ijpx.2022.100154.

[19] A. Cossé, C. König, A. Lamprecht, und K. G. Wagner, „Hot Melt Extrusion for Sustained Protein Release: Matrix Erosion and In Vitro Release of PLGA-Based Implants“, AAPS PharmSciTech, Bd. 18, Nr. 1, S. 15–26, Jan. 2017, doi: 10.1208/s12249-016-0548-5.

[20] M. Stanković, H. W. Frijlink, und W. L. J. Hinrichs, „Polymeric formulations for drug release prepared by hot melt extrusion: application and characterization“, Drug Discov. Today, Bd. 20, Nr. 7, S. 812–823, Juli 2015, doi: 10.1016/j.drudis.2015.01.012.

[21] M. Stanković u. a., „Low temperature extruded implants based on novel hydrophilic multiblock copolymer for long-term protein delivery“, Eur. J. Pharm. Sci., Bd. 49, Nr. 4, S. 578–587, Juli 2013, doi: 10.1016/j.ejps.2013.05.011.

[22] H. Patil, R. V. Tiwari, und M. A. Repka, „Hot-Melt Extrusion: from Theory to Application in Pharmaceutical Formulation“, AAPS PharmSciTech, Bd. 17, Nr. 1, S. 20–42, Feb. 2016, doi: 10.1208/s12249-015-0360-7.

[23] E. S. Bochmann, K. E. Steffens, A. Gryczke, und K. G. Wagner, „Numerical simulation of hot-melt extrusion processes for amorphous solid dispersions using model-based melt viscosity“, Eur. J. Pharm. Biopharm., Bd. 124, S. 34–42, März 2018, doi: 10.1016/j.ejpb.2017.12.001.

[24] M. A. Emin, P. Wittek, und Y. Schwegler, „Numerical analysis of thermal and mechanical stress profile during the extrusion processing of plasticized starch by non-isothermal flow simulation“, J. Food Eng., Bd. 294, S. 110407, Apr. 2021, doi: 10.1016/j.jfoodeng.2020.110407.

[25] M. A. Emin und H. P. Schuchmann, „Droplet breakup and coalescence in a twin-screw extrusion processing of starch based matrix“, J. Food Eng., Bd. 116, Nr. 1, S. 118–129, Mai 2013, doi: 10.1016/j.jfoodeng.2012.12.010.

[26] M. Wilson, M. A. Williams, D. S. Jones, und G. P. Andrews, „Hot-melt extrusion technology and pharmaceutical application“, Ther. Deliv., Bd. 3, Nr. 6, S. 787–797, Juni 2012, doi: 10.4155/tde.12.26.

[27] D. E. Zecevic, R. C. Evans, K. Paulsen, und K. G. Wagner, „From benchtop to pilot scale–experimental study and computational assessment of a hot-melt extrusion scale-up of a solid dispersion of dipyridamole and copovidone“, Int. J. Pharm., Bd. 537, Nr. 1–2, S. 132–139, Feb. 2018, doi: 10.1016/j.ijpharm.2017.12.033.

[28] V. L. Bravo, A. N. Hrymak, und J. D. Wright, „Numerical simulation of pressure and velocity profiles in kneading elements of a co-rotating twin screw extruder“, Polym. Eng. Sci., Bd. 40, Nr. 2, S. 525–541, Feb. 2000, doi: 10.1002/pen.11184.

[29] U. W. Gedde, M. S. Hedenqvist, M. Hakkarainen, F. Nilsson, und O. Das, „Processing of Polymeric Materials“, in Applied Polymer Science, U. W. Gedde, M. S. Hedenqvist, M. Hakkarainen, F. Nilsson, und O. Das, Hrsg., Cham: Springer International Publishing, 2021, S. 453–487. doi: 10.1007/978-3-030-68472-3_8.

[30] R. Paberit u. a., „Cycling Stability of Poly(ethylene glycol) of Six Molecular Weights: Influence of Thermal Conditions for Energy Applications“, ACS Appl. Energy Mater., Bd. 3, Nr. 11, S. 10578–10589, Nov. 2020, doi: 10.1021/acsaem.0c01621.

[31] M. A. Emin und H. P. Schuchmann, „Analysis of the dispersive mixing efficiency in a twin-screw extrusion processing of starch based matrix“, J. Food Eng., Bd. 115, Nr. 1, S. 132–143, März 2013, doi: 10.1016/j.jfoodeng.2012.10.008.

[32] D. Treffer, A. Troiss, und J. Khinast, „A novel tool to standardize rheology testing of molten polymers for pharmaceutical applications“, Int. J. Pharm., Bd. 495, Nr. 1, S. 474–481, Nov. 2015, doi: 10.1016/j.ijpharm.2015.09.001.

[33] P. Hajikarimi und F. Moghadas Nejad, „Time–temperature superposition“, in Applications of Viscoelasticity, Elsevier, 2021, S. 83–105. doi: 10.1016/B978-0-12-821210-3.00006-1.

[34] T. Avalosse, „Numerical simulation of distributive mixing in 3-D flows“, Macromol. Symp., Bd. 112, Nr. 1, S. 91–98, 1996, doi: 10.1002/masy.19961120114.

[35] B. Cornehl, A. Overbeck, A. Schwab, J.-P. Büser, A. Kwade, und H. Nirschl, „Breakage of lysozyme crystals due to compressive stresses during cake filtration“, Chem. Eng. Sci., Bd. 111, S. 324–334, Mai 2014, doi: 10.1016/j.ces.2014.02.016.

[36] M. Kubiak, M. Staar, I. Kampen, A. Schallmey, und C. Schilde, „The Depth-Dependent Mechanical Behavior of Anisotropic Native and Cross-Linked HheG Enzyme Crystals“, Crystals, Bd. 11, Nr. 7, Art. Nr. 7, Juli 2021, doi: 10.3390/cryst11070718.

[37] R. Suzuki, M. Tachibana, H. Koizumi, und K. Kojima, „Direct observation of stress-induced dislocations in protein crystals by synchrotron X-ray topography“, Acta Mater., Bd. 156, S. 479–485, Sep. 2018, doi: 10.1016/j.actamat.2018.06.018.

[38] G. Frungieri, G. Boccardo, A. Buffo, D. Marchisio, H. A. Karimi-Varzaneh, und M. Vanni, „A CFD-DEM approach to study the breakup of fractal agglomerates in an internal mixer“, Can. J. Chem. Eng., Bd. 98, Nr. 9, S. 1880–1892, Sep. 2020, doi: 10.1002/cjce.23773.

5.12 SUPPLEMENTARY DATA

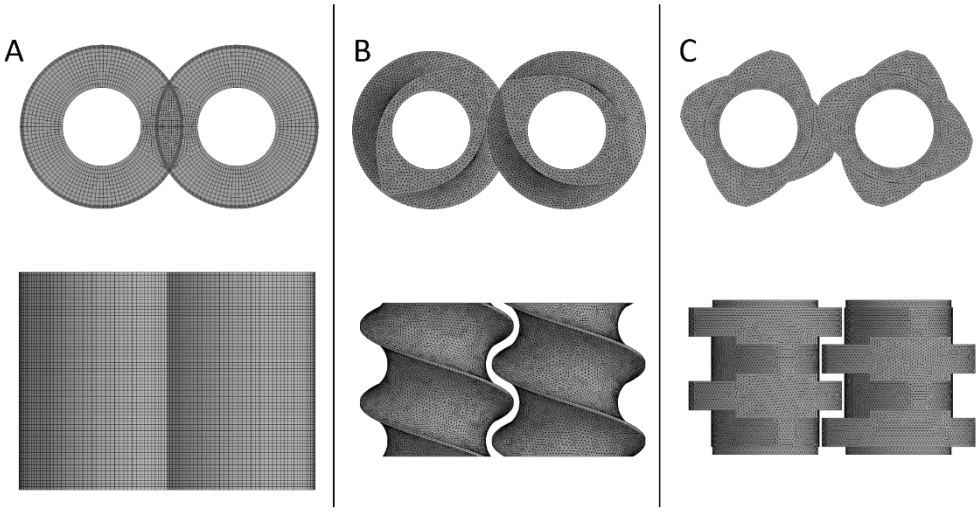

Figure S1 Geometry and computational mesh of the TSE for **A** barrel **B** 5 mm pitch conveying elements and **C** 90° kneading elements.

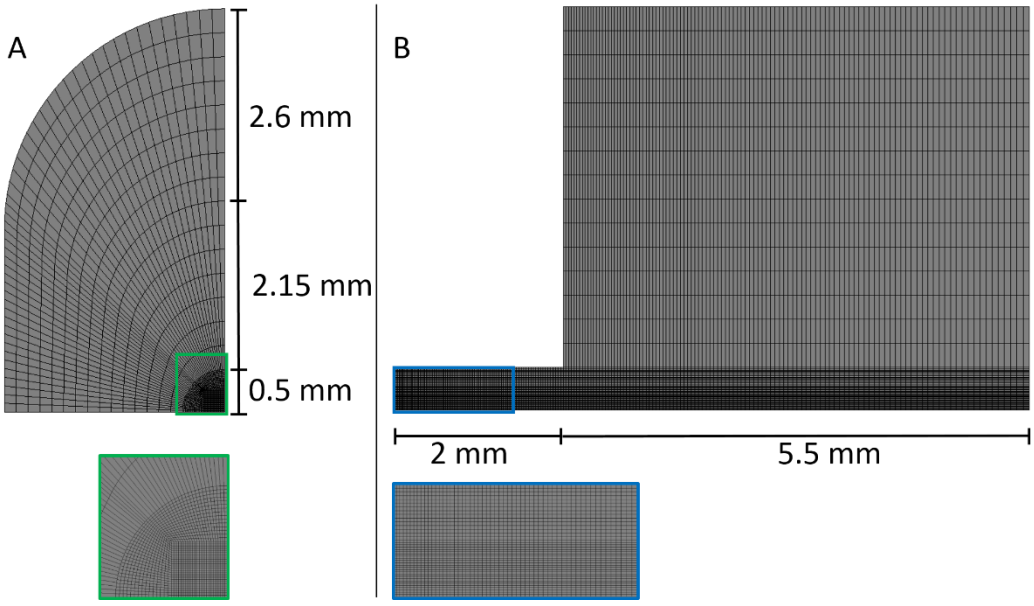

Figure S2 Geometry and computational mesh of the TSE die for **A** front view and **B** side view of a plane of symmetry.

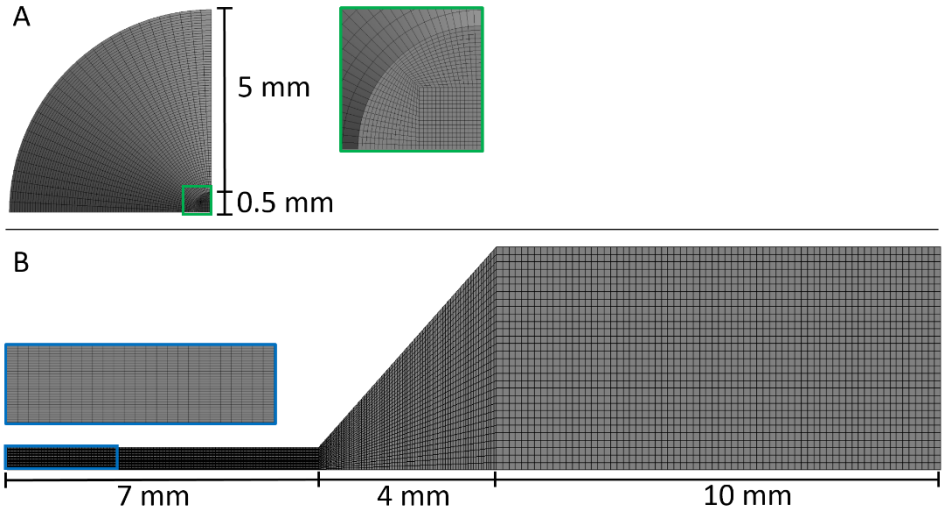

Figure S3 Geometry and computational mesh of the ram extruder die for **A** front view and **B** side view of a plane of symmetry.

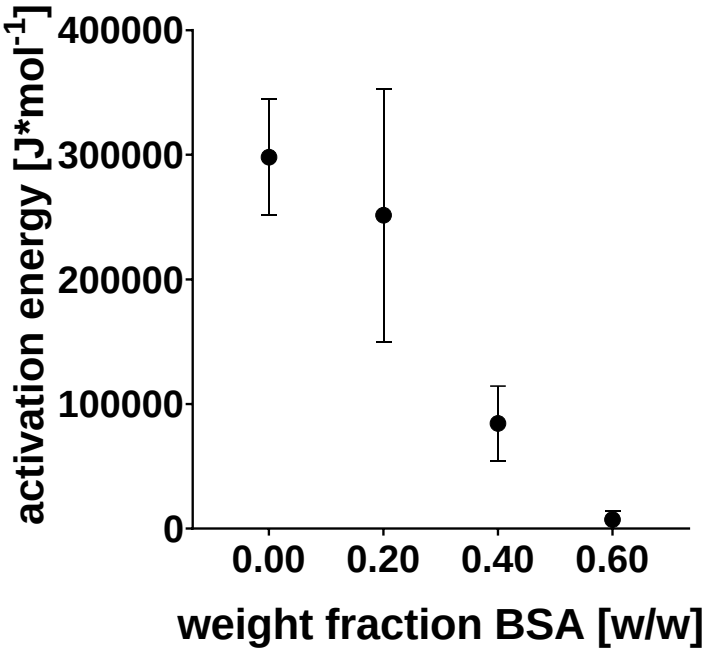

Figure S4 Comparison of the activation energy of flow of plain PEG 20,000 and mixtures containing BSA.

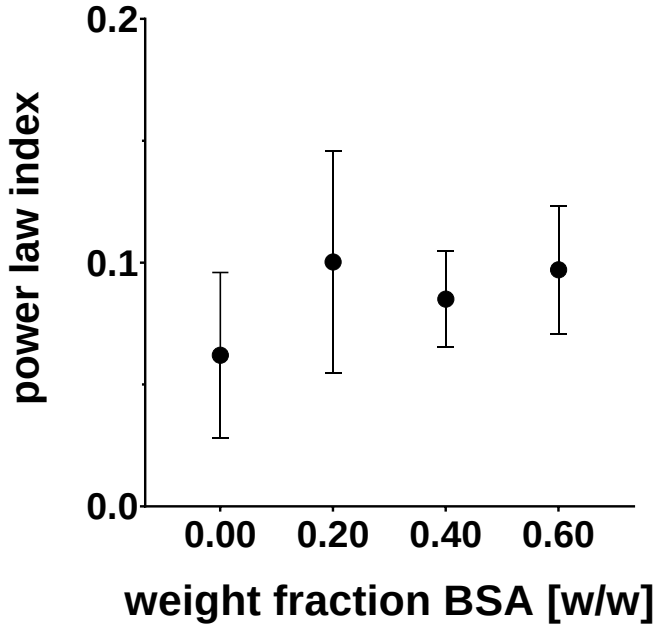

Figure S5 Comparison of power law index derived from utilizing the power law fit for the respective master curves of plain PEG 20,000 and mixtures containing BSA. The master curves were employed with a reference temperature of 64.0 °C.

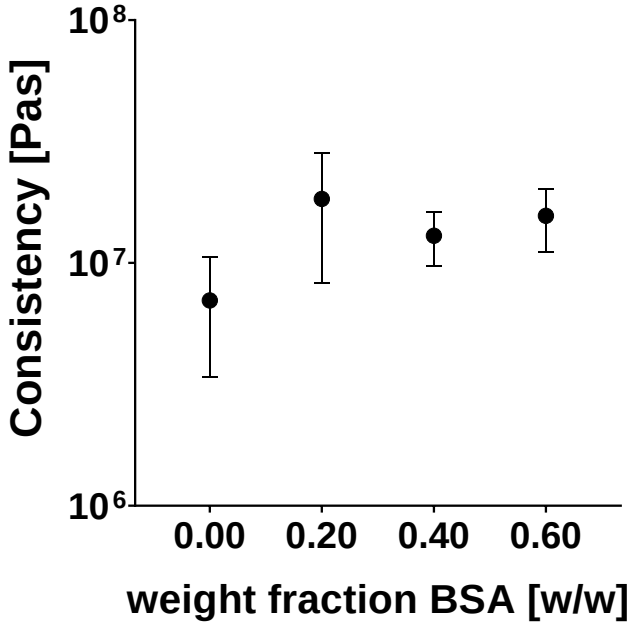

Figure S6 Comparison of the consistency derived from utilizing the power law fit for the respective master curves of plain PEG 20,000 and mixtures containing BSA. The master curves were employed with a reference temperature of 64.0 °C.

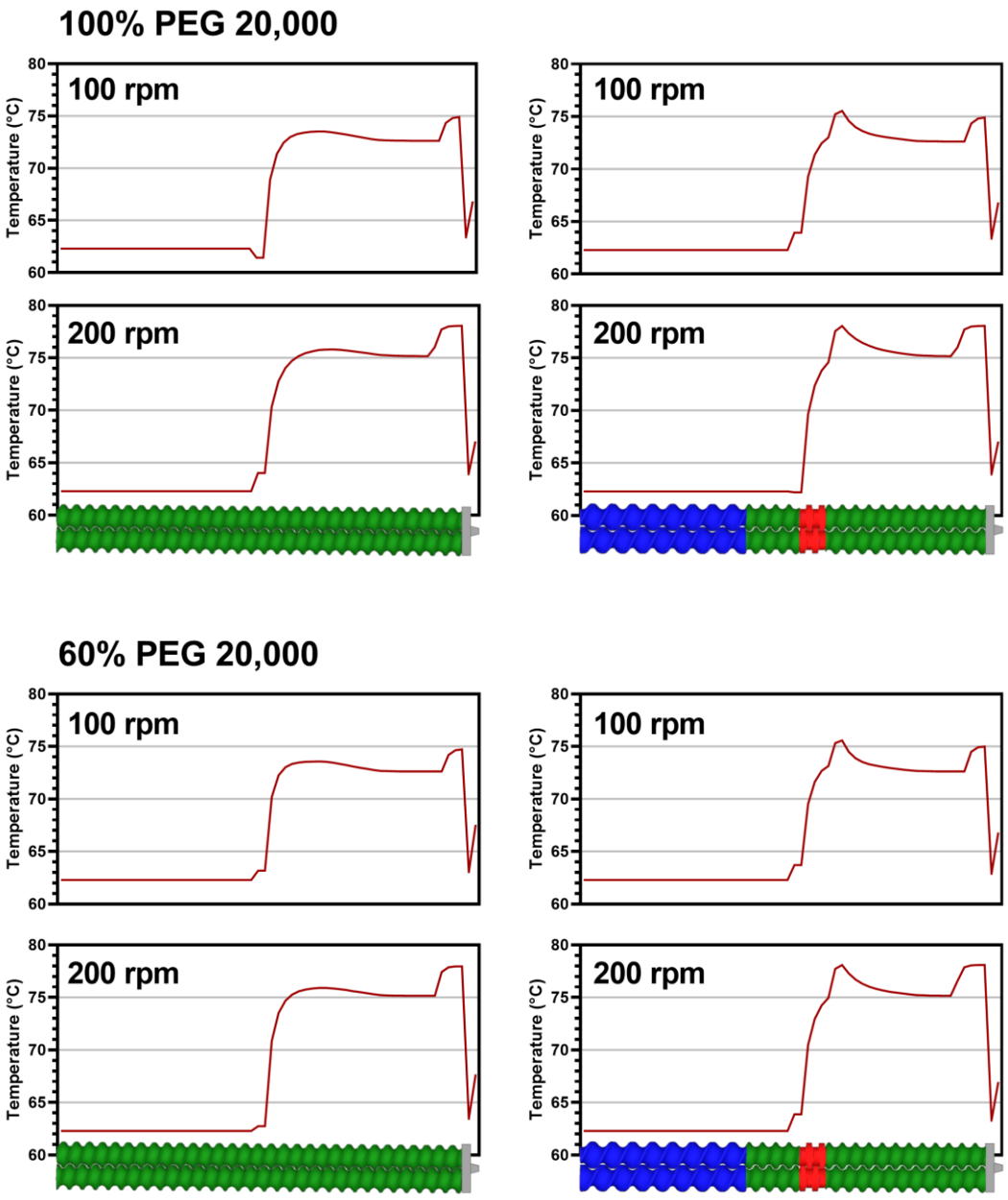

Figure S7 Exemplary presentation of simulated melt temperature of simulations based on input parameters along the extrusion process. The example shows the simulation of 100 % PEG 20,000 (top) and 60 % PEG 20,000/ 40 % BSA (bottom) with conveying screw configuration (left) and screws containing a single 90° kneading element (red) (right) at 100 and 200 rpm screw speed with a feed-rate of 0.6 g/min.